Regulation of the Ryanodine Receptor Calcium Release Channel by FK506-Binding Protein

by

Gerard Peter Ahern

A thesis for the degree of Doctor of Philosophy at

The Australian National University

April 3rd, 1996

Statement

All of the work presented in this thesis was performed by the author unless otherwise stated in the text. SR vesicles were prepared by Suzie Pace and Joan Stivala under the direction of Dr Pauline Junankar, who also performed the Western blots and densitometry. Patch clamp experiments using autaptic neurons were performed with the assistance of Dr Louis Premkumar in the laboratory of Professor Peter Gage.

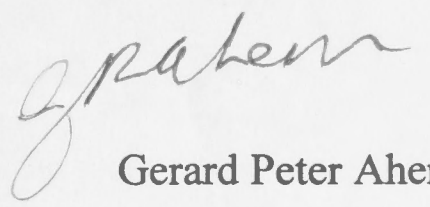

Gerard Peter Ahern

Division of Neuroscience

John Curtin School of Medical Research

Australian National University

April 3rd, 1996

Acknowledgments

I would like to thank my supervisor Angela Dulhunty for her advice and encouragement. I am very grateful to Pauline Junankar for her assistance with the FKBP12 studies and helpful discussions. Thanks to Derek Laver, particularly for quality advice on analysis.

To the girls, Suzie Pace, Joan Stivala and Linda Roden who did all the grisly bits that I avoided, my delicate sensibilities say thank you.

Thanks also to Louis Premkumar, for his enthusiasm with the patch clamp studies; Michael Smith for excellent computer support; Kevin for being a Kiwi, and all the other staff and students at JCSMR who were helpful and even the ones who were not so helpful...

Abstract

The single channel properties of the ryanodine receptor were studied by fusion of terminal cisternae vesicles into planar lipid bilayers. The role of the immunophilin, FKBP12, in regulating RyR channel activity was investigated.

1. Native RyR channels displayed a characteristic large conductance of ~ 500 pS in symmetric 250 mM Cs^+ and sensitivity to *cis* [Ca^{2+}], adenine nucleotides, ryanodine and ruthenium red.

2. The macrolide immunosuppressants, FK506 and rapamycin increased the open probability of RyR channels with 10^{-9} - 10^{-3} M *cis* Ca^{2+} and irreversibly stabilised submaximal conductance states. The results were consistent with FK506/rapamycin removal of FKBP12 from the RyR.

3. RyRs, incorporated from terminal cisternae vesicles stripped of FKBP12, by pre-treatment with rapamycin, displayed prominent subconductance states at ~ 0.25, 0.5 and 0.75 fractions of the maximum conductance. "FKBP12-stripped" RyRs retained sensitivity to Ca^{2+}, adenine nucleotides, ryanodine and ruthenium red, except that their sensitivity to Ca^{2+}-activation was increased ~ 10-fold and their sensitivity to Ca^{2+}-inhibition decreased ~ 10-fold, compared with native channels. Subconductance states in FKBP12-stripped channels were observed at similar fractions of the maximum conductance before and after ryanodine modification. Implications of the multiple conductance states in terms of channel structure are discussed.

4. FKBP12-stripped RyRs were reversibly activated by rapamycin. Structurally related macrolides, ivermectin and midecamycin increased the open probability of native RyRs, but did not induce dissociation of FKBP12 from SR vesicles. Rapamycin and FK506 produced a modulation of the $GABA_A$ receptor that was qualitatively similar to reported effects of ivermectin and lactones. The results suggest the existence of a macrolide/lactone binding site on the RyR.

Publications

During the course of this PhD study the following papers were published. Publications marked with an asterisk describe some of the work presented in this thesis.

Ahern, G.P., Junankar, P.R., and Dulhunty, A.F. (1994). Single channel activity of the ryanodine receptor calcium release channel is modulated by FK-506. FEBS Lett. *352*, 369-374.*

Dulhunty, A. F., Zhu, P-H., Patterson, M.F. and Ahern G. P. (1992) Actions of Perchlorate Anions on Rat Soleus Muscle Fibres. J. Physiol. Lond. *448*, 99-119.

Dulhunty, A.F., Junankar, P. R., Eager, K. R.; Ahern , G. P. and Laver, D. R. (1996). Ion channels in the sarcoplasmic reticulum of striated muscle. Eur. J. Physiol. (*In Press*).*

Kourie, J.I., Laver, D.R., Ahern, G.P., and Dulhunty, A.F. (1996). A calcium-activated chloride channel in sarcoplasmic reticulum vesicles from rabbit skeletal muscle. Am. J. Physiol. (*In Press*)

Laver, D.R., Roden, L.D., Ahern, G.P., Eager, K.R., Junankar, P.R., and Dulhunty, A.F. (1995). Cytoplasmic Ca^{2+} inhibits the ryanodine receptor from cardiac muscle. J. Membr. Biol *147*, 7-22.*

Premkumar, L.S. and Ahern, G.P. (1995). Blockade of a resting potassium channel and modulation of synaptic transmission by ecstasy in the hippocampus. J. Pharmacol. Exp. Ther. *274*, 718-722.

Commonly Used Abbreviations

AMP-PNP	5-adenylylimododiphosphate
ATP	Adenosine-5'triphosphate
BCl	"Big"-conductance chloride channel
CHAPS	3-[(3-cholamidopropyl)dimethylammonio]-2-hydroxy-1-propanesulfonate
CsA	Cyclosporin A
CyP	Cyclophilin
DMSO	Dimethylsulfoxide
FKBP	FK-binding protein
FKBP12	12 kDa FK506-binding protein
kDa	kilodalton
RyR	Ryanodine Receptor
SCl	"Small"-conductance chloride channel
SR	Sarcoplasmic Reticulum
TC	Terminal Cisternae

Parameters

F_o	frequency of opening , (s^{-1})
P_o	open probability
T_o	mean open time, (ms)
T_c	mean closed time, (ms)
I'	mean current, (pA)

Table of Contents

Chapter 1.

General Introduction

Ryanodine Receptor Calcium Release Channel

1.1 *RyR structure and localisation*

Ryanodine receptors (RyRs) are a class of intracellular Ca^{2+} release channels found in a variety of excitable and non-excitable tissue from invertebrates to vertebrates (reviewed by Coronado *et al.*, 1994). RyRs are so named because of their ability to bind with high affinity and specificity to the plant alkaloid, ryanodine (Pessah *et al.*, 1986; Imagawa *et al.*, 1987). In striated muscle, RyRs, located mainly at the terminal cisternae (TC) of sarcoplasmic reticulum (SR), are responsible for the rapid release of Ca^{2+} into the myoplasm which triggers contraction. In neurones and non-excitable cells, RyRs and inositol 1,4,5-trisphosphate receptor (IP_3R) calcium channels play an important role in Ca^{2+}-signalling (Berridge, 1993).

Purification of RyRs and gel electrophoresis studies showed that RyRs are aggregates of a single high molecular weight (> 300 kDa) peptide (Lai *et al.*, 1988; Smith *et al.*, 1988; Hymel *et al.*, 1988b; Anderson *et al.*, 1989). Subsequently, sequencing studies identified three major mammalian RyR isoforms: *RyR-1* (~ 565 kDa), *RyR-2* (~ 565 kDa) and *RyR-3* (~ 551 kDa) (Takeshima *et al.*, 1989; Zorzato *et al.*, 1990; Nakai *et al.*, 1990; Otsu *et al.*, 1990; Hakamata *et al.*, 1992). Each isoform is predominantly expressed in skeletal muscle, cardiac muscle, or brain and smooth muscle respectively. *RyR-3* is expressed in T-lymphocytes (Hakamata *et al.*, 1994) and ryanodine binding is detected in fibroblasts and liver (Larini *et al.*, 1995). *RyRs 1-3* are not detected in liver (Giannini *et al.*, 1995) suggesting the existence of a novel RyR isoform.

Hydropathy plots of RyR sequences suggest that the RyR protein consists of two major structural regions: a hydrophobic C-terminal pore region with between four (Takeshima *et al.*, 1989) and twelve (Zorzato *et al.*, 1990) possible membrane spanning segments and a large cytoplasmic region. Both the C- and N- terminal regions are probably cytoplasmic (Grunwald and Meissner, 1995). The morphological features of RyRs have been revealed by electron microscopy studies. The image displays fourfold symmetry with a four-leaf clover appearance (Lai *et al.*, 1988; Radermacher *et al.*, 1994;

Wagenknecht and Radermacher, 1995). This observation, the apparent sedimentation coefficient of 30 S (Lai *et al.*, 1988) and the ability of the proteins to cross-link (Lai *et al.*, 1989) indicate that the RyR exists as a homotetramer. The size of the tetramer, ~2.3 MDa, makes it the largest ion channel known. The cytoplasmic portion is 29 x 29 x 12 nm with a 12 x 12 x 7 nm base plate which inserts into the TC membrane. A low density structure runs down the centre of the transmembrane assembly and may constitute the ion channel pathway. This pore structure is apparently plugged near the cytoplasmic surface and branches into four radial canals which lead to the exterior of the transmembrane assembly (Radermacher *et al.*, 1994).

1.2 *Ion permeation and conductance*

The single channel properties of the RyR have been studied using the planar lipid bilayer technique, as the SR membrane is inaccessible to patch clamp recording. The RyR channel is cation selective and has a large conductance, ~ 100-150 pS (with 50 mM Ca^{2+} luminal or *trans*), ~ 580 pS (250 mM symmetric Na^{+}), ~ 525 pS (250 mM symmetric Cs^{+}) and ~ 750 pS (250 mM symmetric K^{+}) (Smith *et al.*, 1985; Smith *et al.*, 1986; Tinker *et al.*, 1992a). Thus, the conductance ratio monovalent/divalent cations is ~ 5-6. Under mixed ionic conditions the channel is weakly selective to Ca^{2+} over other cations with a permeability ratio (P_{Ca}/P_X) of between 5-14 for Na^{+} and K^{+} (Smith *et al.*, 1988; Liu *et al.*, 1989; Tinker *et al.*, 1992a). The lower Ca^{2+} conductance and the greater permeability of Ca^{2+} in mixed solutions has been explained by the presence of binding sites in the channel pore which have a higher affinity for Ca^{2+} compared with monovalent cations (Tinker *et al.*, 1992a). This explains the experimental results that the conductance of monovalent salts is decreased in the presence of Ca^{2+} (Smith *et al.*, 1988).

Multiple conductance levels in the RyR are frequently observed in studies using purified, detergent-solubilised RyRs. A consistent finding is the presence of discrete conducting levels at ~ 0.25, 0.5 and 0.75 of the maximum conductance (fractional conductance) (see *Table. 1-1*), although one study described multiple open levels composed of subunits with a fractional conductance of 0.05 (Hymel *et al.*, 1988a).

Subconductance states are less common in RyRs derived from native SR membrane preparations. The appearance of equally spaced conducting levels has been proposed to be due to the presence of a four-barrelled channel or a single barrelled channel with discrete conducting levels (Smith *et al.*, 1988, Liu *et al.*, 1989; Lai *et al.*, 1989).

Functional regulation of RyR

1.3 *Dihydropyridine receptor*

In skeletal and cardiac muscle, RyR Ca^{2+} release and contraction are tightly controlled by T-tubule membrane potential. The dihydropyridine receptor (DHPR) in the T-tubule is believed to be the voltage sensor (Rios and Brum, 1987): contraction in dysgenic muscle lacking the α_1 subunit of the DHPR is restored upon introduction of DHPR cDNA (Tanabe *et al.*, 1988). In cardiac muscle, contraction is dependent on Ca^{2+} inflow through DHPR channels (Cannell *et al.*, 1987; Nabauer *et al.*, 1989). In contrast, skeletal muscle contraction is independent of external Ca^{2+} (Armstrong *et al.*, 1972; Brum *et al.*, 1987) suggesting that the DHPR activates RyR Ca^{2+} release by another signalling pathway, possibly a mechanical coupling of the two receptors. Biochemical evidence supports an association between the DHPR and RyR in skeletal muscle. A small fraction of RyRs co-sediment with the α_1 subunit of the DHPR and both the RyR and DHPR can be co-immunoprecipitated by antibodies raised against the RyR or α_1, α_2, or β DHPR subunits (Marty *et al.*, 1994). A functional interaction has been demonstrated: a peptide corresponding to the 2-3 loop of the skeletal DHPR α_1 subunit activates the skeletal but not cardiac RyR (Lu *et al.*, 1994) and t-tubule depolarisation induces conformational changes in the skeletal RyR (Yano *et al.*, 1995a). Morphological studies support mechanical coupling but also indicate that only a subpopulation of RyRs are mechanically linked to DHPRs (Takekura *et al.*, 1994). The remaining unlinked RyRs may be activated by Ca^{2+} released initially through DHPR-linked RyRs. Ca^{2+} induced Ca^{2+} release (CICR) is observed in muscle fibres (Endo *et al.*, 1970; Ford and Podolsky, 1970) and micro-injection of fast-binding Ca^{2+} buffers modulate depolarisation induced SR Ca^{2+} release (Csernoch *et al.*, 1993; Yano *et al.*, 1995b).

Table 1-1. Subconductance states in RyR channels.

Reference	Preparation	Fractional Conductance
(Lai et al., 1988)	Purified, Rabbit SR	0.2, 0.4-0.5, 0.65
(Ma et al., 1988)	Purified, Rabbit SR	0.25, 0.5 *
(Smith et al., 1988)	Purified, Rabbit SR	0.25, 0.5, 0.75
(Hymel et al., 1988a)	Purified, Rabbit SR	0.05 multiples
(Liu et al., 1989)	Purified, Rabbit SR	0.25, 0.5, 0.75
(Ma, 1993)	Purified, Rabbit SR + ryanodine	0.25, 0.5 *
(Buck et al., 1992)	SR Vesicles, Rabbit + ryanodine	0.5
(Ma and Zhao, 1994)	SR Vesicles, Rabbit ± ryanodine	0.25, 0.5, 0.75
(Brillantes et al., 1994)	Cloned, FKBP12 deficient	0.25, 0.5, 0.75

* denotes subconductances observed in separate channels

1.4 *Regulation by endogenous ligands*

The ligand sensitivity of the RyR channel is identical to that of SR Ca^{2+} release. SR Ca^{2+} release and RyR channel activity are both regulated by cytoplasmic (*cis*) Ca^{2+}. The relationship between Ca^{2+} release and *cis* $[Ca^{2+}]$ is bell-shaped: RyRs are activated by micromolar and inhibited by millimolar Ca^{2+} concentrations (Kirino *et al.*, 1983; Meissner *et al.*, 1986; Fill *et al.*, 1990; Meissner, 1994). In skeletal RyRs the Ca^{2+} binding sites for activation and inhibition have affinities of ~ 1 and ~ 400 μM respectively and Hill coefficients of ~ 1 (Chu *et al.*, 1993; Laver *et al.*, 1995).

In vivo, Ca^{2+}-activation of RyRs may serve to amplify SR Ca^{2+} release initiated by T-tubule depolarisation, while Ca^{2+}-inhibition may then turn off CICR. CICR may also be terminated by a phenomenon known as "adaptation" or "increment detection" where channel activity is stimulated by changes in $[Ca^{2+}]$ and slowly decays in the presence of steady-state $[Ca^{2+}]$ (Gyorke and Fill, 1993; Valdivia *et al.*, 1995). However, there has been controversy regarding the caged-Ca^{2+} technique used in adaptation studies and in more recent experiments using rapid perfusion of Ca^{2+} solutions, adaptation was not observed (Sitsapesan *et al.*, 1995; Derek Laver unpublished observations).

Millimolar Mg^{2+} inhibits RyR channel activity. Mg^{2+} may act by competing with Ca^{2+} for the Ca^{2+}-activation site, binding to the Ca^{2+}-inhibition site and by binding in the pore as an open channel blocker (Kirino *et al.*, 1983; Meissner *et al.*, 1986; Smith *et al.*, 1986). Mg^{2+} may be an important physiological regulator of RyR channel function. Lowering myoplasmic Mg^{2+} from 1 mM to 50 μM produces spontaneous contractions in skinned muscle fibres (Lamb and Stephenson, 1991). Lamb and Stephenson (1991) have proposed that excitation-contraction coupling in skeletal muscle may operate through a change in Mg^{2+}-inhibition. A transient relief in Mg^{2+}-inhibition, possibly via a DHPR-RyR interaction, could allow for an ATP generated Ca^{2+} efflux through the RyR. A recent study has shown that Mg^{2+}-sensitivity is reduced 13-fold during depolarisation induced $^{45}Ca^{2+}$ release in isolated triads (Ritucci and Corbett, 1995).

SR Ca^{2+} efflux and channel activity are maximised in the presence of millimolar ATP. ATP acts directly on the RyR complex at an adenine nucleotide binding site since various, non-hydrolysable ATP analogues also stimulate channel activity (Ogawa and Ebashi, 1976; Meissner, 1984; Smith *et al.*, 1985; Smith *et al.*, 1986). ATP increases channel P_o without altering the Ca^{2+} activation and inactivation properties (Pessah *et al.*, 1987; Ma and Zhao, 1994). Thus, ATP may be a primary activator of the RyR in the absence of a Ca^{2+} stimulus.

1.5 *Phosphorylation*

The skeletal and cardiac RyRs are phosphorylated by various protein kinases although the functional significance of this remains unclear. In the cardiac receptor, phosphorylation of serine 2809 by Ca^{2+}/calmodulin dependent protein kinase (CaM kinase) increases channel activity (Witcher *et al.*, 1991). Binding of ^{3}H-ryanodine is either increased or decreased by phosphorylation with different kinases (Takasago *et al.*, 1991), suggesting that phosphorylation at different sites can increase or decrease P_o. Phosphorylation of the skeletal RyR presumably by CaM kinase can either increase (Herrmann-Frank and Varsanyi, 1993) or decrease (Wang and Best, 1992) channel activity. The difference may depend on which ligands are bound to the RyR. The Ca^{2+}/calmodulin dependent serine/threonine phosphatase, calcineurin, is associated with the skeletal RyR (Cameron *et al.*, 1995b, see below) and may interact with CaM kinase to alter channel function in a cyclical fashion.

1.6 *Miscellaneous endogenous regulators*

Many other endogenous factors are known to regulate the skeletal RyR channel, including physiological concentrations (3-30 mM) of inorganic phosphate (Fruen *et al.*, 1994), and fatty acids (μM) (el-Hayek *et al.*, 1993). The cardiac and skeletal RyR are activated by cyclic adenosine 5′-diphosphoribose (Lee, 1993; Meszaros *et al.*, 1993; Sitsapesan and Williams, 1995). Both channels are also affected by $[H^+]$. P_o is inhibited at low pH (< 7), but stimulated at high pH (> 7-7.5) (Ma *et al.*, 1988; Ma and Zhao, 1994).

Pharmacological agents commonly used to identify RyRs

1.7 *Ryanodine*

A fundamental characteristic of RyRs is the ability to bind the alkaloid drug ryanodine. Ryanodine has concentration-dependent effects on channel activity, with low concentrations (nanomolar to micromolar) locking the channel into a long-lived subconductance state (~ 0.5 maximum conductance with 250 mM symmetric K^+ or Cs^+) and high concentrations (>100 μM) completely blocking the channel (Lai *et al.*, 1989; Nagasaki and Fleischer, 1988; Rousseau *et al.*, 1987). These effects are consistent with whole muscle observations that ryanodine can cause a contracture and/or a decline in contractile force (see Ogawa, 1994). At least four binding sites have been identified with one high affinity (K_D ~ 1-5 nM) and three low affinity (K_D between 30 nM-5 μM) sites (see Coronado *et al.*, 1994). Ryanodine binding is slow, thus concentrations well in excess of the affinities are normally used in muscle or bilayer studies. Binding to the high affinity site is believed to induce the irreversible low conductance state while binding to the low-affinity sites is thought to close the channel (Nagasaki and Fleischer, 1988; Rousseau *et al.*, 1987), although one study has described at least four kinetically distinct states produced by ryanodine, suggesting a more complex interaction (Buck *et al.*, 1992). The mechanism by which ryanodine induces an open reduced conductance state is unknown. Smith *et al.* (1988) have proposed that the reduced conductance in the ryanodine modified channel may arise from selective opening of two of four putative ion conducting pathways in the tetrameric channel complex and that higher concentrations of ryanodine completely inhibit all of the pathways. Lindsay *et al.* (1994) have reported that ryanodine modification of the channel alters its permeation properties. Although ryanodine normally induces a unitary reduced conductance state, distinct subconductance states have been described in ryanodine modified CHAPS-solubilised RyRs and in ryanodine modified native channels (see *Table 1-1*).

1.8 *Caffeine*

Caffeine, in millimolar concentrations, has been used as an important pharmacological activator of RyR channels since it was first discovered to cause Ca^{2+} release from SR

vesicles (Weber, 1968; Weber and Herz, 1968) and to induce CICR in muscle fibres (Endo *et al.*, 1970). Caffeine directly stimulates single RyR channels (Nagasaki and Kasai, 1984; Liu *et al.*, 1989; Rousseau and Meissner, 1989). Although its binding site on the RyR has not been established it appears that caffeine exerts its effect by increasing the Ca^{2+} sensitivity of channel activation and by causing a modest increase in the maximum amount of Ca^{2+} released, or maximum P_o (Kurebayashi and Ogawa, 1986; Meissner *et al.*, 1986; Pessah *et al.*, 1987).

1.9 *Ruthenium red*

Ruthenium red is a polycationic dye first used to block mitochondrial Ca^{2+} transport (Moore, 1971). Later it was shown to inhibit SR Ca^{2+} release (Ohnishi, 1979; Meissner, 1984; Seiler *et al.*, 1984) and RyR channel activity (Smith *et al.*, 1985; Smith *et al.*, 1988; Hymel *et al.*, 1988a; Ma, 1993). Ruthenium red probably acts as an open channel blocker because, when added to the *cis* side of RyRs it causes a rapid voltage-dependent (positive potentials) flicker block (Ma, 1993). In contrast, when added to the *trans* side (at negative potentials) ruthenium red reduces channel conductance, indicating an asymmetric mode of action (Ma, 1993).

1.10 ***Proteins associated with the RyR***

In addition to the DHPR, a number of proteins are believed to interact with the RyR and modify its function. Calmodulin binds to the RyR at several sites (Seiler *et al.*, 1984; Tripathy *et al.*, 1995) and binding to one site is seen in cryo-electron microscopic analysis (Wagenknecht *et al.*, 1994). Calmodulin binding and its functional effects are Ca^{2+}-dependent. At least sixteen calmodulins bind in the presence of nanomolar Ca^{2+}, resulting in an increase in channel activity, whereas only four calmodulins bind with micromolar-millimolar Ca^{2+} resulting in a decrease in channel activity (Tripathy *et al.*, 1995; Smith *et al.*, 1989). These responses occur even in the absence of ATP, suggesting that calmodulin acts directly on the RyR and independently of a phosphorylation pathway.

Triadin, a 90 kDa protein in the SR membrane binds to the skeletal RyR (Kim *et al.*, 1990), specifically in the luminal domain (Guo and Campbell, 1995). A functional role of triadin in RyR function is suggested by the observation that anti-triadin antibodies inhibit the slow phase of depolarisation-induced Ca^{2+} release from SR vesicles (Brandt *et al.*, 1992) and that the association between triadin and the RyR is sensitive to ligands which activate or inhibit the calcium channel (Liu and Pessah, 1994).

Calsequestrin is a major SR Ca^{2+} binding protein which is anchored to the TC membrane by triadin (Guo and Campbell, 1995). A probable function of calsequestrin is to increase the Ca^{2+} storage capacity of the SR, but a direct action on the RyR is also suggested by conformational changes in calsequestrin that precede Ca^{2+} release (Ikemoto *et al.*, 1989).

Other proteins shown to interact with or affect the gating of RyR channels include the 12 kDa FK506 binding protein (discussed below), glyceraldehyde 3-phosphate dehydrogenase (Brandt *et al.*, 1990), aldolase (Brandt *et al.*, 1990), annexin VI (Diaz Munoz *et al.*, 1990), 170 kDa low-density-lipoprotein binding protein (Damiani and Margreth, 1991) and S-100 protein (Fano *et al.*, 1989; Marsili *et al.*, 1992).

FK506 Binding Protein (FKBP12)

1.11 *FKBP12 associates with the RyR*

The 12 kDa FK506-binding protein (FKBP12) is a cytosolic receptor for the immunosuppressive macrolide, FK506. FKBP12 is tightly associated with the skeletal RyR (Jayaraman *et al.*, 1992). The discovery of this association arose from proteolytic sequencing of highly purified rabbit skeletal muscle RyR, in which all but one of 31 peptides studied mapped to the published primary sequence of the RyR (Marks *et al.*, 1990; Marks *et al.*, 1989). The additional peptide was later identified as the N-terminal sequence of FKBP12 (Collins, 1991). An association between the RyR and FKBP12 was then demonstrated by the co-purification of the RyR and FKBP12 through chromatographic columns, the ability of anti-FKBP12 antibodies to immunoprecipitate

the RyR, and the co-localisation of both proteins to the terminal cisternae fraction of sarcoplasmic reticulum (Jayaraman *et al.*, 1992). A comparison of immunosuppressant (FK506 analogues) and high affinity ^{3}H-ryanodine binding indicated a stoichiometry of four FKBP12 monomers per channel complex ie. one FKBP12 monomer per RyR monomer (Timerman *et al.*, 1993). The tight association of FKBP12 with the RyR suggests that it may be involved in modulating RyR channel function.

1.12 *FKBP12, a proline isomerase and immunophilin*

FKBP12 is a member of a class of proteins with *cis-trans* peptidyl-proline isomerase (PPIase or rotamase) activity (Galat, 1993). Rotamases catalyse the interconversion of the *cis* and *trans* isomers of peptidyl-proline bonds in peptide and protein substrates. Rotamases were first isolated from porcine kidney (Fischer *et al.*, 1984) and mammalian thymocytes (Handschumacher *et al.*, 1984) but were later found in both the cytoplasm and internal membranes of many cell types from both prokaryotes (Hayano *et al.*, 1991) and eukaryotes (Harding *et al.*, 1986; Haendler *et al.*, 1987). Their presumed function is to accelerate the folding, assembly and trafficking of proteins (Galat, 1993; Galat and Metcalfe, 1995).

In addition, some rotamases selectively bind the potent and clinically useful immunosuppressants Cyclosporin A (CsA), FK506 and rapamycin and are consequently termed *immunophilins*. Based on their binding selectivity toward the immunosuppressive drugs, immunophilins may be divided into two superfamilies of proteins: cyclophilins (CyPs, CsA-binding proteins, Handschumacher *et al.*, 1984) and FK-binding proteins (FKBPs, FK506/rapamycin binding proteins, Harding *et al.*, 1989). The rotamase activity of cyclophilins and FKBPs is abolished following binding of their respective immunosuppressants (Harding *et al.*, 1989). For this reason it was originally proposed that the immunosuppression caused by these drugs was mediated by the inhibition of rotamase activity (Fischer *et al.*, 1989; Takahashi *et al.*, 1989). Later it was discovered that the immunosuppressive and other pharmacological effects of CsA and FK506 were mediated by inhibition of calcineurin, a Ca^{2+}/calmodulin dependent serine/threonine phosphatase (McCaffrey *et al.*, 1993). Calcineurin is inhibited

specifically by the CsA-cyclophilin and FK506-FKBP complexes, but does not interact with these drugs alone, or the Rapamycin-FKBP complex (Liu *et al.*, 1991). Rapamycin-FKBP binds to the 289 kDa RAFT1/FRAP proteins (Sabatini *et al.*, 1995) but the mechanism by which this inhibits T cell proliferation remains unclear.

1.13 *Structure of FK506, rapamycin and CsA*

The structures of FK506, rapamycin and CsA are shown in *Fig. 1-1*. FK506 and rapamycin are lipid soluble, macrocyclic lactones ie. they have a large ring structure with a characteristic ester moiety (shown here in position C1). Rapamycin (molecular mass 915) is larger than FK506 (molecular mass 822) and has 31 atoms in the ring whereas FK506 has 23 atoms. However, the C1-C14 region which binds to FKBP12 (Galat, 1993) is virtually identical in both drugs. High affinity binding involves the C2-N7 region or "pipecolinic ring" which is thought to mimic a proline residue. CsA is a large (molecular mass 1203) cyclic polypeptide structurally dissimilar to either FK506 or rapamycin.

1.14 *Regulation of RyR function by FKBP12*

The close association of FKBP12 and the RyR suggests that FKBP12 may modulate RyR channel function. Proline residues are found near the transmembrane region of the RyR (Takeshima *et al.*, 1989) and a *cis-trans* isomerisation of these residues may be involved in channel gating. In addition, binding by FKBP12, one per channel monomer, may be necessary to stabilise RyR structure which by itself may influence channel function.

When the first series of experiments in Chapter 4 were started there were no published reports addressing a functional role for the association of FKBP12 with the RyR. However, during the course of these experiments several studies investigating the role of FKBP12 on SR Ca^{2+} release, muscle tension and single channel properties of the RyR have been published, and are described below.

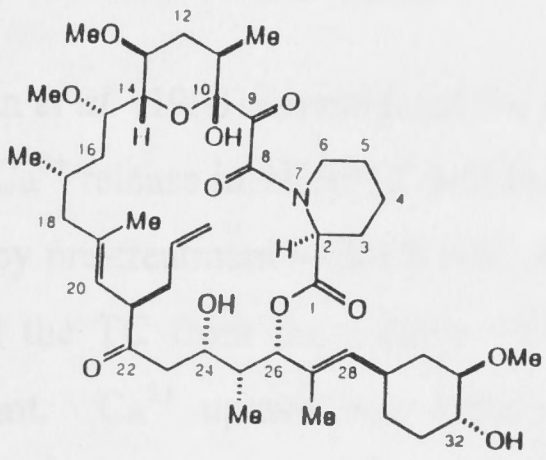

FK506

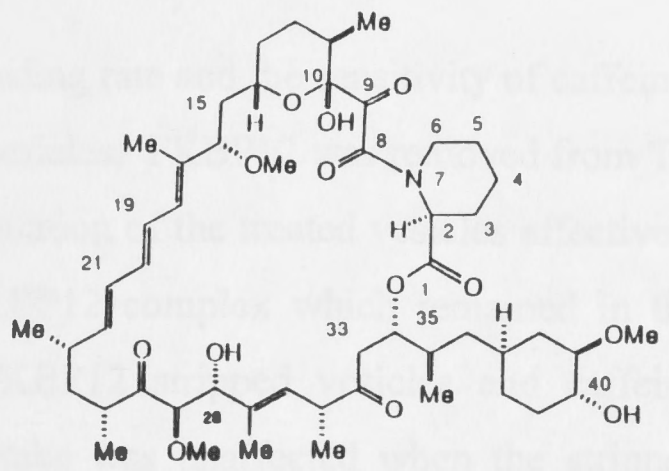

Rapamycin

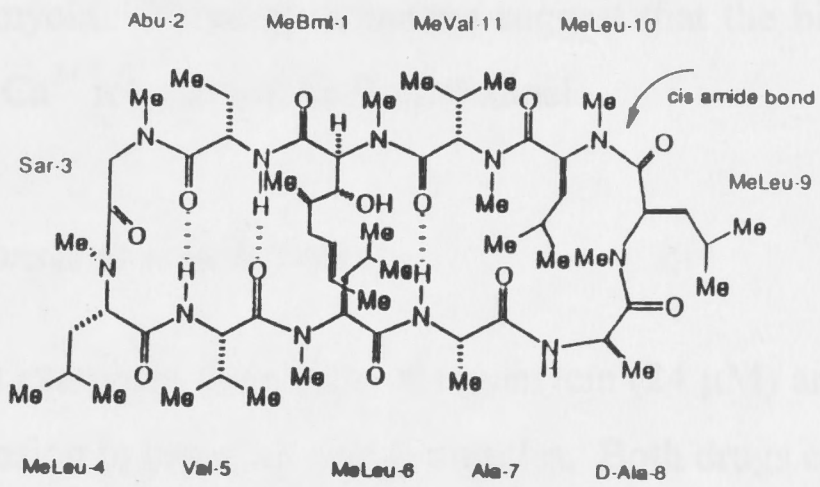

CsA

Fig. 1-1. Chemical structures of FK506 ($C_{44}H_{69}NO_{12}$, 803.547), rapamycin ($C_{56}H_{89}NO_{14}$, 999.7) and CsA ($C_{62}H_{111}N_{11}O_{12}$, 1201.948). CsA consists of 11 amino acids as labelled. Source: Galat and Metcalfe (1995)

1.15 *Ca^{2+} release from SR vesicles*

Timerman *et al.* (1993) investigated the Ca^{2+} loading rate and the sensitivity of caffeine-induced Ca^{2+} release in FKBP12 deficient TC vesicles. FKBP12 was removed from TC vesicles by pre-treatment with FK506. Sedimentation of the treated vesicles effectively separated the TC from the soluble FK506-FKBP12 complex which remained in the supernatant. Ca^{2+} uptake was reduced in FKBP12 stripped vesicles and caffeine induced Ca^{2+} release was enhanced. Ca^{2+} uptake was unaffected when the stripped vesicles were treated with the RyR inhibitor, ruthenium red, which demonstrated that the reduced uptake of the stripped vesicles was the result of enhanced release through the RyR. Brillantes *et al.* (1994) reported similar findings in SR vesicles treated directly with FK506 and rapamycin. These observations suggest that the binding of FKBP12 leads to a reduction in Ca^{2+} release via the RyR channel.

1.16 *Contractile responses in muscle fibres*

Brillantes *et al.* (1994) examined the effects of rapamycin (24 μM) and FK506 (12 μM) on caffeine induced tension in intact rat soleus muscles. Both drugs caused a significant increase in caffeine-induced tension that correlated with an increase in myoplasmic $[Ca^{2+}]$ and induced small amplitude muscle twitches prior to caffeine activation. These results are consistent with the hypothesis that removal of FKBP12 by rapamycin or FK506 activates the RyR but do not exclude the possibility of direct drug effects on the RyR. Lamb and Stephenson (1996) found that 1 μM FK506 and rapamycin caused a moderate (~ 20 - 30%), reversible potentiation of depolarisation induced contraction in skinned rat skeletal muscle fibres. In addition, 1 μM rapamycin enhanced the caffeine-induced tension response and this was also reversed upon washout. They explained their results as suggesting that the immunosuppressants had two separate effects: a direct activation of RyR Ca^{2+} release (hence the reversible nature of the activation) and an irreversible inhibition of excitation-contraction coupling possibly due to dissociation of FKBP12 from the RyR.

1.17 *Single channel recordings of RyRs lacking FKBP12*

Mayrleitner *et al.* (1994) recorded single channel RyR activity from TC vesicles which had been stripped of FKBP12 by pre-treatment with FK506. The RyR channel stripped of FKBP12 retained its characteristic sensitivity to Ca^{2+}, ryanodine, Mg^{2+} and ruthenium red and its unitary conductance was unchanged. However, caffeine sensitivity was increased compared to control channels and stripped channels had a greater P_o and longer mean open times over the Ca^{2+} range 70 nM to 1 μM. At 10 μM Ca^{2+} there was no difference in mean P_o. In two experiments 12 μM FK506 added directly onto the bilayer reactivated control channels that were closed by reducing cis Ca^{2+} to 55 nM. Furthermore, the addition of recombinant FKBP12 (3.3 nM) to a stripped channel, which was highly active in 70 nM Ca^{2+}, inhibited activity. These results support an inhibitory role for FKBP12 in RyR channel regulation. However, the possibility that pre-treatment with FK506 has additional effects on RyR channel activity could not be ruled out.

Brillantes *et al.* (1994) studied the single channel properties of the cloned, FKBP12 deficient RyR. The cloned RyR was expressed in insect cells, isolated membranes were solubilised and the RyR purified by sucrose density centrifugation, prior to incorporation into lipid bilayers. The FKBP12-deficient RyR exhibited a normal response to channel modulators: activated by Ca^{2+} (100 μM), caffeine (5 mM) and ATP (2 mM) and inhibited by Mg^{2+} (2 mM) and ruthenium red (20 μM). The channel had a maximum conductance of 515 pS and ryanodine (0.5 μM) characteristically locked the channel into a low conductance state. These observations indicated that the cloned FKBP12-deficient channel was functionally similar to the native RyR. However, the normal maximum conductance was only observed in 3/32 experiments. The channel mainly resided in substates that were ~ 0.25, 0.5 or 0.75 of the full open state ie. similar to results obtained with purified RyR channels (see *Table 1-1*). In contrast, in 40% of experiments where FKBP12 was co-expressed with the cloned RyR or added to the bilayer, the channel opened predominantly to the full conductance state. The presence of FKBP also modified channel open time and P_o. Open probability was markedly reduced in the presence of FKBP although the mean open time was longer. Similar

subconductance states were observed when native RyR channels were treated with FK506 or rapamycin, however, the immunosuppressive drugs had no effect, when applied to the FKBP deficient channel. The results suggested that FKBP has an inhibitory influence on RyR channel activity, and that it also stabilises the full conductance state of the channel. Furthermore, the results suggested that the increased frequency of subconductance states previously reported in purified RyR channels may have resulted from loss of FKBP12 in the purification process.

1.18 *FKBP12 action: binding or rotamase activity*

FKBP12 may regulate the RyR channel by binding *per se* to the channel and stabilising a conformational state, or via FKBP12-rotamase activity at proline residues. To discriminate between these two possibilities Timerman *et al.* (1995) measured the Ca^{2+} uptake characteristics of TC vesicles where wild type FKBP12 had been exchanged with recombinant FKBP12 which lacked rotamase activity on peptide substrates. To promote the exchange of FKBPs they utilised the observation that FKBPs dissociate and associate in a temperature dependent fashion. At 0°C exchange is very slow whereas at 37°C it proceeds rapidly. By incubating TC vesicles in a molar excess of recombinant mutants at 37°C they could fully replace wild type FKBP12 with mutants. In addition, they associated the mutants after first stripping wild type FKBP12 using FK506 analogues. Consistent with their earlier results they showed that removal of FKBP12 was inversely correlated with the rate of Ca^{2+} uptake, ie. removal of FKBP12 increased Ca^{2+} release. The drug action was shown to be mediated specifically by FKBP12 dissociation as uptake was not affected by the drug when the temperature was 4°C, and FKBP12 was not dissociated. Importantly, they demonstrated that exchange or re-association of stripped vesicles with mutant FKBPs restored Ca^{2+} uptake rates to that of control TC vesicles. These results suggest that binding of FKBP12 rather than FKBP12 rotamase activity mediates channel regulation. However, the authors only measured uptake in a narrow Ca^{2+} range, 10-50 μM and may have missed possible differences at other [Ca^{2+}]. For instance, Mayrleitner *et al.* (1994) reported that P_o of the FKBP12 stripped channel was greater than control channels with 70 nM to 1 μM cytoplasmic

Ca^{2+} but not different with 10 μM Ca^{2+}. It is also possible that RyR channel conductance or kinetics may have been affected without a net change in Ca^{2+} release.

1.19 *Modulation of Ca^{2+} release by bastadin: a macrocyclic compound which does not dissociate FKBP12*

Bastadins are a group of large macrocyclic compounds, isolated from the marine sponge *Ianthella basta*. Mack *et al.* (1994) showed that several of these compounds including bastadin 5, increased Ca^{2+} release from TC vesicles, ^{3}H-ryanodine binding and single channel open time and that these effects were antagonised in a dose-dependent fashion by FK506. In addition, bastadin 5 did not induce dissociation of FKBP12 but rather potentiated the dissociation due to FK506. The interpretation of these results is complex. The fact that FK506 antagonised bastadin action suggests that both compounds compete for a similar binding site, possibly on FKBP12. However, the observation that bastadin potentiates FK506-induced dissociation of FKBP12 argues against a competitive interaction. The opposite result would be expected, ie. a decrease in FKBP12 dissociation, if bastadin competed for the same site as FK506. Therefore it is not clear whether bastadin acts on FKBP12 or directly on the RyR.

1.20 *Rectification of the RyR by addition of FKBP12*

Chen *et al.* (1994) showed that when recombinant 7-14 nM FKBP12 was added to the purified skeletal RyR it induced asymmetric blockade of channel activity. FKBP12 added to the cytoplasmic side of the bilayer inhibited current flowing in the cytoplasmic to luminal direction but did not effect the luminal to cytoplasmic current. However, addition of FKBP12 to the *trans* chamber caused the opposite effect, a block of luminal to cytoplasmic current. This asymmetric current blockade could not be reversed by the addition of an FK506 analogue which would promote FKBP12 dissociation. Therefore it is unlikely that FKBP12 acted by binding to unoccupied FKBP12 binding sites on the cytoplasmic face of the RyR. It is possible that free FKBP12 , which has a small net positive charge, can cause a voltage-dependent block of the channel by binding to negatively charged residues lining the channel pore. Chen *et al.* also tested another 12 kDa positively charged protein but failed to observe any rectification. Ma *et al.* (1995)

observed that 300 nM FKBP12 induced a similar rectification in skeletal RyRs incorporated from native SR vesicles. These results suggest that unbound FKBP12 may regulate RyR function in a different way to bound FKBP12. There is a significant amount of free cytosolic FKBP12 in skeletal muscle (~ 3 μM, Timerman *et al.*, 1995) and the proportion bound to the RyR is in equilibrium with the cytosolic pool. Consequently, free FKBP12 would be able to block cytoplasmic to luminal ion flow through the RyR in a similar fashion to polyamines which block outward K^+ current in the inward rectifier K^+ channel (Ficker *et al.*, 1994; Lopatin *et al.*, 1994). Thus cytosolic FKBP12 may have a physiological role of preventing movement of Na^+ or K^+ into the lumen during RyR activation.

1.21 *Association of FKBPs and CyPs with other ion channels*

The specific association of FKBP12 with the skeletal RyR might indicate a specialised role for FKBP12 in the excitation-contraction coupling pathway at triadic junctions. However, FKBP association is not unique to the skeletal RyR. A 12.6 kDa FKBP has been found to be associated with the cardiac RyR (Timerman *et al.*, 1994), although the functional significance of this association is unknown. FKBP12 also associates with and regulates activity of the inositol trisphosphate receptor (IP_3R) (Cameron *et al.*, 1995a). There is evidence for functional association of CyPs with other ion channels. The mitochondrial transition pore is inhibited by CsA (Petronilli *et al.*, 1994) probably via the removal of an associated mitochondrial CyP (Nicolli *et al.*, 1996). CsA inhibits the association of homo-oligomers of the acetylcholine and serotonin receptors expressed in *Xenopus sp.* oocytes (Helekar *et al.*, 1994) and this inhibition can be reversed by over-expression of CyP. It is possible that FKBPs and CyPs associate with and regulate the functions of many other ion channels.

Chapter 2.

Materials and Methods

Materials and Methods

2.1 *Preparation of native SR vesicles*

SR vesicles were prepared using methods based on Saito *et al.* (1984). Unless otherwise indicated all reagents were purchased from Sigma. Back and leg muscles were dissected from New Zealand rabbits and stored at −70°C. Cubes of muscle were homogenised in a Waring blender in homogenising buffer (mM: imidazole, 20; sucrose, 300, adjusted to pH 7.1 with HCl). The homogenate was centrifuged (11,000 g, 15 min) and the pellet resuspended, rehomogenised (4 x 15 s) and centrifuged as above. The supernatant was filtered through cotton gauze and centrifuged at 110,000 g for 60 min. The crude SR vesicle pellet was resuspended in homogenising buffer and layered onto a discontinuous sucrose gradient containing 45%, 38%, 34%, 32% and 28% sucrose (in 20 mM imidazole, pH 7.1 adjusted with HCl), and centrifuged for 16 h at 20,000 rpm (Beckman SW28 rotor). Vesicles were collected from the following density interfaces: Band 1 (B1), 28%-32%; Band 2 (B2), 32%-34%; Band 3 (B3), 34%-38%; Band 4 (B4), 38%-45%. Vesicles were diluted 3-fold in 20 mM imidazole (pH, 7.1), pelleted at 125,000 g, resuspended in homogenising buffer (at 10 to 20 mg/ml protein), frozen and stored in liquid N_2. All procedures were performed at 4°C and all buffers contained the protease inhibitors: leupeptin, 1 μM; pepstatin A, 1 μM; benzamidine, 1 mM; phenylmethylsulphonyl fluoride, 0.7 mM. Protein was assayed (Lowry *et al.*, 1951) using bovine serum albumin (BSA) as a standard.

2.2 *Preparation of CHAPS-solubilised RyRs*

The method was based on previous reports (Lai *et al.*, 1988; Lindsay and Williams, 1991). Crude SR vesicles (2 mg protein per ml) were resuspended in 25 mM imidazole (pH 7.2) (BDH) containing L-a-phosphatidylcholine (2.5 mg/ml), 3-[(3-cholamidopropyl) dimethylammonio]-2-hydroxy-1-propanesulfonate (CHAPS) at either 0.5 or 1% (w/v), 1 M NaCl (Ajax), 0.1 mM EGTA, 0.15 mM $CaCl_2$ (BDH), 2 mM dithiothreitol. The mixture was homogenised using a glass Dounce homogeniser and incubated on ice for one hour. The insoluble material was removed by centrifugation at

100,000 g for 45 min before loading the supernatant onto a 5-25% linear sucrose gradient in the above buffer. This was allowed to sediment for 16 hr at 100,000 g in a SW28 rotor. Two millilitre fractions were collected from the bottom of the centrifuge tubes and aliquots of each fraction were subjected to sodium dodecyl sulfate (SDS)-polyacrylamide gradient gel electrophoresis (PAGE) and silver staining in order to identify the fraction containing the high molecular weight protein characteristic of the RyR. In some cases this was confirmed by Western blotting with anti-RyR antibodies.

Reconstitution of RyRs into proteoliposomes was achieved by dialysing fractions containing the RyR against a buffer containing (in mM): 100 NaCl, 0.1 [ethylene bis (oxyethylenenotrilo)] tetraacetic acid (EGTA), 0.15 $CaCl_2$, 25 imidazole, pH 7.2. Dialysis was carried out at 4°C overnight with at least three, changes of buffer. Sucrose was added to the proteoliposomes to a final concentration of 200 mM before snap freezing in liquid N_2.

2.3 *Preparation of FKBP12 stripped vesicles*

TC vesicles (2 mg protein per ml) were incubated with FK506 or rapamycin (0.05 to 40 μM) in 20 mM imidazole, 300 mM sucrose, pH 7.4, at either room temperature for one hour, or at 37°C for 15 mins. Buffers for control and immunosuppressant incubations contained 1% ethanol and the protease inhibitors 5 μg/ml leupeptin, 0.2 mM [4-(2 aminoethyl)-Benzenesulfonyl Fluoride Hydrochloride] (ICN Biomedicals). Membranes were pelleted at 436,000 g for 15 min in a Beckmann TL-100 centrifuge, washed once in the incubation buffer and resuspended at 2 mg/ml. Protein concentrations of treated vesicles were determined as for native vesicles (above).

2.4 *Preparation of anti-FKBP12 peptide antibodies*

A peptide, VQVETISPGDGRTFPKC, corresponding to the N-terminal sequence (2-17) of FKBP12 with an added cysteine residue was synthesised by the ANU Biomolecular Resource Facility. The peptide (5 mg) was coupled via the C-terminal cysteine to Keyhole Limpet Haemocyanin (KLH, 5 mg), activated with *m*-maleimidobenzoyl-N-hydroxysuccinimide ester using a method based on that of Green *et al.*, (1982). New

Zealand White rabbits were immunised subcutaneously with 0.8 mg of KLH-peptide conjugate in Freund's complete adjuvant. Booster injections in Freund's incomplete adjuvant followed; 0.8 mg and 0.5 mg at 3 week intervals. Pre-immune and immune (1 week following boosters) blood specimens were collected for testing.

Immunoglobulins were partially purified from the antisera by caprylic acid treatment and precipitation in 50% ammonium sulphate (GIBCO, BRL). After dialysis against 3 changes of phosphate-buffered saline, anti-FKBP12 peptide antibodies were purified by affinity chromatography. The peptide was conjugated to agarose beads via the C-terminal cysteine using the Pierce Immunpore Antigen/Antibody Immobilization kit#2. Antibodies that bound to the immobilised peptide were purified according to the manufacturer's instructions.

2.5 *Electrophoresis and Western Immunoblots*

TC proteins were solubilised in sample buffer at 100°C for 2 min, separated on a 15% SDS-polyacrylamide gradient gel using the buffer system of Laemmli (1970) and transferred to Immobilon-P membranes (Millipore) in 10 mM 3-[Cyclohexylamino]-1-propanesulfonic acid pH 11.0, 10% ethanol and 0.05% SDS at 75 V for 30 min. Membranes were blocked with 5% skim milk powder in 20 mM Tris, 500 mM NaCl, pH 7.5 (TBS) before incubating with either; anti-FKBP12 antibodies in rabbit serum (1:100), or affinity purified antipeptide immunoglobulin (20 µg/ml), or anti-FKBP12 monoclonal 3F4-70 (Fujisawa, 12 µg/ml); in 1% BSA, 20 mM Tris, 500 mM NaCl, pH 7.5 for 2 - 4 h at room temperature or overnight at 4°C. The secondary antibody (Silenus, 1:2000 dilution, incubated for 1 h at room temperature) was either an alkaline phosphatase conjugate, with colour developed as described by Blake *et al.* (1984), or a horseradish peroxidase conjugate, visualised using the enhanced chemiluminescence kit (Amersham) following the manufacturer's instructions.

2.6 *Densitometry*

Immunostaining, detected with the ECL kit, was scanned using a Novaline Gel Documentation System and digitally analysed using the Molecular Dynamics

ImageQuant Software Version 3.3. Relative amounts of FKBP12 in FKBP12-depleted vesicles were estimated from a standard curve, constructed from the signal obtained from known dilutions of TC vesicles which were electrophoresed and blotted on the same gel.

2.7 *Artificial lipid bilayers and SR vesicle fusion*

Lipid bilayers were formed from a mixture of palmitoyl-oleoyl-phosphatidylethanolamine, palmitoyl-oleoyl-phosphatidylserine and palmitoyl-oleoyl-phosphatidylcholine (5:3:2 by volume; Avanti Polar Lipids, Alabaster, Alabama). The lipid mixture was dried under N_2 and redissolved in *n*-decane at a final concentration of 50 mg/ml. Bilayers were formed over apertures (diameter 150 - 300 μm) in the wall of 1.5 ml delrin cups. Thinning of the thick lipid film to a bilayer was monitored visually with 20x magnification or electrically by measuring bilayer capacitance. Membrane capacitance was measured from the current response to a voltage ramp (1 V/s) and thinning produced an increase in capacitance to ~ 0.5 $\mu F/cm^2$. Incorporation of ion channels was achieved as described by Miller and Racker (1976). SR vesicles (B4) were added to a final concentration of 1 - 10 μg/ml and the solution stirred vigorously until the appearance of channel activity indicated vesicle fusion. The side of the bilayer to which vesicles were added was defined as *cis*, and the other side as *trans*. It was assumed that the cytoplasmic side of the SR membrane faced the *cis* chamber (Miller and Racker, 1976) and this was confirmed in tests of the sensitivity of RyR channels to ligands which are known to bind to the cytoplasmic domain of the protein (section 3.3(iii), *Figs. 3-3* and *3-4*, Ahern *et al.*, 1994).

2.8 *Solutions for bilayers*

Under standard conditions the *cis* chamber contained 250 mM CsCl (Aldrich), 10 mM *N*-tris-(hydroxymethyl)methyl-2-aminoethanesulphonic acid (TES) and 1 mM $CaCl_2$, pH 7.5 and the *trans* chamber contained 50 mM CsCl, 10 mM TES and 1 mM $CaCl_2$, pH 7.5 Free $[Ca^{2+}]$ was adjusted by perfusion with solutions containing 2 mM 1,2-bis(2-aminophenoxy)ethane-N, N, N′, N′-tetra-acetic acid (BAPTA) titrated to the desired free $[Ca^{2+}]$ with $CaCl_2$ using an ion meter (Radiometer ION83). Bilayer

chambers were perfused with 5 - 7 volumes of solution using a back-to-back syringe apparatus. Experiments were performed at 20 - 25°C.

2.9 *Chemicals and drugs*

Drugs/chemicals used on RyRs, and their manufacturers were: adensoine-5′triphosphate (ATP), 5-adenylylimidodiphosphate (AMP-PNP), ruthenium red, midecamycin (Sigma); CsA (Sandoz), deltamethrin (Alomone Laboratories); erythromycin (David Bull Laboratories), FK506 (gift from Fujisawa); ivermectin (gift from Merck); non-specific acid phosphatase (Calbiochem); rapamycin (gift from Wyeth-Ayerst); ryanodine (Calbiochem and Latoxan). Stock solutions of CsA, FK506, ivermectin and rapamycin were prepared at either 20 mM in ethanol or 60 mM in DMSO and stored at –70°C. Deltamethrin was prepared at 10 μM in ethanol and stored at –20°C. Non-specific acid phosphatase was dialysed against 250 mM CsCl solution overnight at 4°C. All other agents were dissolved in a 250 mM CsCl solution and stored at –4°C or –20°C. All drugs were added directly to the bilayer bath while stirring vigorously.

2.10 *Single channel recording*

Voltage was controlled and single channel activity recorded via an Axopatch 200 amplifier (Axon Instruments, Foster City, CA). The *cis* and *trans* chambers were connected to the amplifier head stage by Ag/AgCl electrodes in agar salt-bridges. Electrical potentials are given with respect to the *trans* chamber as ground and positive current is directed from the *cis* to *trans* chamber. Unless otherwise stated the bilayer potential was held at +40 mV (the Cl^- equilibrium potential) during recording of RyR currents. During the experiments the bilayer current and potential were monitored on an oscilloscope and recorded at a bandwidth of 5 kHz on videotape using pulse code modulation (Model 200; A.R. Vetter). The current signals were replayed, filtered (4-pole Bessel, –3 dB) at 1 or 2 kHz and digitised via a TL-1 DMA interface (Axon Instruments) at 2 or 5 kHz.

2.11 *Analysis of data*

Channel current levels and activity were analysed using an in-house programme, *Channel2*, developed by M. Smith and P.W. Gage. Detailed analysis of current levels was performed using the mean-variance method described by Patlak (Patlak, 1988). Briefly, a window of 10 data points was systematically moved along the record producing mean current versus variance pairs which were plotted as a histogram. Maintained current levels appear in these plots as low variance regions. Amplitude histograms were constructed from the bins of the mean-variance histogram that fall below a set variance level and which excludes high variance regions associated with transitions. Peaks in this amplitude histogram correspond to conductance levels and were fitted with multiple gaussian functions using the programme "*Peakfit*" (Jandel).

Single channel activity was evaluated using the following parameters: the mean open time (T_o); the frequency of opening (F_o); the mean closed time (T_c), the open probability (P_o, ie. the sum of all open times as a fraction of the total time) and the mean current (I', ie. the integral of the current divided by the total time). Open times were defined as intervals where the current exceeded a discriminator set above the baseline noise at ~ 10 - 20% of the maximum channel open level. The threshold for event detection was set between 10 and 20 % ~~there~~, rather than at 50% of the maximum open level, so as to include openings to subconductance levels. Unless otherwise stated P_o and I' were measured from >90 s of continuous data, except in Chapter 3 where P_o was also measured within "bursts" of openings. Bursts were defined as periods of activity terminated by closures of >1 s. This burst threshold was decided on the basis that nearly all the closed durations (as determined by closed time frequency distributions) were associated with exponential decay constants of <100 ms. Analysis of bilayers containing multiple channels was restricted to measurement of I'.

2.12 *Analysis of open durations for different conducting levels*

Analysis of open times of different open levels (section 5.11) was performed using the programme, EVPROC (written by Dr. Derek Laver, see Kourie *et al.*, 1996a). EVPROC fits the current signal with an idealised record of putative current transitions,

by evaluating the significance of each observed transition. A transition is considered significant if its amplitude exceeds two times the SE of the noise on adjacent current levels (calculated from the SD of the background noise), otherwise the adjacent levels are amalgamated. Dwell time analysis for subconductance and maximum conductances was performed by assigning a current range or "window" for each level (estimated from amplitude histograms) which was used as a threshold for event detection ie. a transition into the window was recorded as an opening and a transition out of the window was recorded as a closure. Open time distributions were plotted using the log-bin method of Sigworth and Sine (1987). Data were fitted with the sum of either two or three exponentials.

2.13 *Statistical Analysis*

Differences between mean values were evaluated for statistical significance using the Student's t-test. Significance was set at the 0.05 level. For comparison between two different groups of channels (horizontal comparison) a two sample, two-tailed t-test was used. For comparison before and after a given treatment for a single group of channels (longitudinal comparison) a paired t-test was used. A one-tailed t-distribution was used where paired tests involved small sample populations and were used to evaluate either a consistent increase or decrease in a given parameter. For some paired analyses in Chapter 4 (as indicated), data was first converted into the logarithmic form (on advice of ANU Statistical Consulting Unit) to allow for the wide variability in the magnitude of channel responses to agents. Heterogeneity in the ligand sensitivities of RyRs has been well documented (Ma, 1995; Laver *et al.*, 1995).

2.14 *Inhibitory synaptic currents in hippocampal neurons*

Synaptic currents were studied using conventional whole cell patch clamping in self-synapsing or "autaptic", hippocampal neurons (Bekkers and Stevens, 1991). Autaptic neurons were kindly provided by Dr. John Bekkers (Neurophysiology Group, JCSMR). Cells were dissociated from the CA1 region of newborn rats, and single neurons were grown separately on small spots of collagen and poly-D-lysine for 1 to 3 weeks before use. Under these conditions neurons formed profuse autaptic connections. For

electrophysiological studies, the bath solution contained 124 mM NaCl, 2.5 mM KCl, 2 mM $CaCl_2$, 26 mM $NaHCO_3$, 2.5 mM NaH_2PO_4 and was equilibrated with a gas mixture of 95% CO_2 and 5 % O_2 (pH 7.2-7.3). Patch electrodes were made from thick-walled borosilicate glass tubes (Clark Electromedical) and were filled with a solution that contained 140 mM K-gluconate, 2 mM $MgCl_2$, 10 mM HEPES, pH 7.3. Electrodes had resistances between 5 - 15 MΩ. Autaptic currents were elicited by a 2 ms depolarisation from either –80 mV to 0 mV, or –40 mV to +40 mV. Autaptic currents were either excitatory or inhibitory and these were distinquishable by their reversal potential, timecourse and pharmacological properties as outlined by Bekkers and Stevens, (1991). Briefly, excitatory autaptic currents reversed close to 0 mV; and displayed a rapid activating component which decayed completely within 25 ms and a slower activating component which was Mg^{2+} sensitive, and reduced at hyperpolarised potentials. These properties are consistent with the "non-NMDA" and *N*-methyl-D-aspartate (NMDA) class of glutamate receptors respectively (Bekkers and Stevens, 1991). In contrast, inhibitory currents reversed between –60 to –70 mV, consisted of a single fast-activating and slow-inactivating component (decay phase of the current ~ 100 ms) and were sensitive to the benzodiazepine, diazepam (see *Fig. 6-19B*). These properties are consistent with the $GABA_A$ class of receptors (Study and Barker, 1981; Bekkers and Stevens, 1991).

Cells under voltage clamp were perfused continuously with control solution from a 300 μM barrel positioned ~ 100 to 200 μM from the cells, and drugs were applied from another barrel moved into position with a hydraulic manipulator. Data was collected before, during and after application of FK506/rapamycin. In each case, the averages of 4 sweeps at 0.2 s^{-1} was collected. Data were filtered at 2 kHz and digitised at 5 kHz. The decay phase of inhibitory currents was fitted with a single exponential function. Currents were plotted minus the preceding capacitive transients.

Chapter 3.

Characterisation of the RyR

3.1 Introduction

Single channel RyR recordings were first published by Smith *et al.* (1985) who described a large conductance (~100 pS), Mg^{2+} sensitive, adenine nucleotide activated Ca^{2+} channel from skeletal muscle SR. Subsequent studies detailed the ion permeation properties and the Ca^{2+} and pharmacological sensitivity of RyR channels from both native and purified RyR preparations (Smith *et al.*, 1986; Imagawa *et al.*, 1987; Rousseau *et al.*, 1987; Smith *et al.*, 1988). The aim of the experiments described here was to identify RyR channels from native SR vesicles incorporated into lipid bilayers and to compare their properties with those described previously. Properties used to characterise the RyR channel included a high Cs^+ conductance, Ca^{2+} sensitivity, activation by adenine nucleotides, modification by ryanodine and inhibition by ruthenium red. Analyses of subconductance states and the ryanodine modified conductance are also presented.

Experiments were carried out using CsCl solutions with Cs^+ as the major permeant ion through RyR channels. A major advantage of using Cs^+ compared with Ca^{2+} is that Cs^+ is more conductive through the RyR channel (~ 525 pS with symmetric 250 mM Cs^+, Williams, 1992; compared with ~ 100 - 150 pS with 50 mM Ca^{2+} *trans*, Smith *et al.*, 1986) and so the current will have a better signal to noise ratio. Also RyR activity is sensitive to Ca^{2+}, so avoiding Ca^{2+} as the permeant ion allows a study of the Ca^{2+} dependence of channel activity. Another benefit of Cs^+, as opposed to other monovalent cations, is that it greatly diminishes the background current of SR K^+ channels (Coronado *et al.*, 1980). Cl^- channels are also present in SR membrane (see below, Tanifuji *et al.*, 1987; Rousseau, 1989). To minimise contamination from Cl^- currents when recording RyRs the bilayer potential was usually held close to the Cl^- equilibrium potential of +40 mV.

Results

3.2 *Fusion of SR vesicles with lipid bilayers*

The rate of fusion of B4 SR vesicles with lipid bilayers was dependent on vesicle concentration, bilayer surface area, osmotic gradient and *cis* [Ca^{2+}]. Fusion ordinarily occurred within 5 - 10 minutes of vesicle addition under standard conditions: 250/50 mM CsCl, 1/1 mM Ca^{2+} (*cis*/*trans*) with bilayer capacitances of 200 - 350 pF and 10 µg/ml of B4 vesicle protein. Several types of ion channels were observed: a large (~150 - 500 pS) Cs^+ conducting channel which was identified as the RyR (see below), a large conductance (269 pS) Cl^- channel similar to that described by (Tanifuji *et al.*, 1987) and a small conductance (100 pS) Cl^- channel (Kourie *et al.*, 1996a). Incorporation of RyRs (347 of 434 bilayers or 80%) occurred more frequently than Cl^- channels (55%). Incorporation of RyRs alone occurred in 45% of experiments. This value is considerably higher than the 14% reported using crude SR vesicles (Laver *et al.*, 1995), but is consistent with the greater RyR concentration in B4 compared with crude vesicle preparations. In addition, a large conductance (>500 pS) channel permeable to both Cs^+ and Cl^- was seen in 9 experiments (2%) using B4 vesicles. The properties of this channel were similar to the mitochondrial voltage-dependent anion channel (VDAC). VDAC-type channels were seen more frequently (22%) after solubilised SR preparations were incorporated into bilayers .

3.3 *Characterisation of the RyR*

(i) Current-voltage relationship and conductance

One type of Cs^+ channel was frequently observed after vesicle incorporation and identified as the RyR on the basis of its pharmacological and conductance properties as outlined below. *Fig. 3-1A* shows examples of Cs^+ channel activity recorded in 250/50 mM CsCl and 1/1 mM Ca^{2+} (*cis*/*trans*) at different bilayer potentials. Activity consisted of very short openings (<1 ms) and long openings (~100 ms). The majority of openings were to a single, maximal current level, however, transitions to smaller current levels (substates) were occasionally evident. For example, a clear open level at

~70% of the fully open level can be seen in the +80 mV trace. The current-voltage (I-V) relationship for the fully open level (250/50 mM CsCl and 1/1 mM Ca^{2+}) was non-linear (*Fig. 3-1B*). The line represents the best fit of a third-order polynomial function to the data. The channel passed more current at positive potentials (*cis* to *trans*) than at negative potentials (*trans* to *cis*) and the current reversed at −18.2 mV. Thus, under these conditions the channel passed more current in the outward (*cis* to *trans*) direction, or behaved as an "outward rectifier". This effect is shown clearly in a plot of slope conductance versus voltage (*Fig. 3-2D, solid line*). The conductance at +80 mV was 616 pS but fell in a hyperbolic fashion to 133 pS at negative potentials. The slope conductance at the reversal potential (−18.2 mV) was 166 pS.

(ii) Effects of trans Cs^+/Ca^{2+} concentrations on conductance

Previous investigations in solutions containing 5:1 *cis/trans* CsCl have obtained a linear I-V relationship, with a conductance of ~ 480 - 600 pS and a reversal potential close to +40 mV (see for eg. Williams, 1992). The differences between this study and earlier reports can be explained by the respective *trans* [Ca^{2+}] used (1 mM in this study versus <1 μM in previous reports). The RyR has a higher selectivity for divalent over monovalent cations (PCa^{2+}/PCs^+ ~ 6 - 8) but the conductivity of the monovalent cations far exceeds that of the divalent cations (Tinker *et al.*, 1992a; Smith *et al.*, 1988). Consequently, as [Ca^{2+}] rises, or [Cs^+] falls, then Ca^{2+} will competitively displace Cs^+ from binding sites within the pore, occupy the pore for longer periods and reduce the net current that passes through the channel. The presence of high Ca^{2+} concentrations will also shift the apparent reversal potential from E_{Cs} (−40 mV) toward E_{Ca} (0 mV). These effects are demonstrated in *Fig.3-2A* where the current at +40 mV increased 230% from 15.8 to 36 pA after *trans* Ca^{2+} was reduced from 1 mM to 1 μM. Reducing *trans* Ca^{2+} increased single channel current at all bilayer potentials, created a linear I-V relationship, shifted the reversal potential from −18 to −32.5 mV (*Fig. 3-2B*) and abolished the voltage-dependence of conductance (*Fig. 3-2D*). The slope conductance calculated at the reversal potential increased from 166 to 529 pS. A similar effect was observed by increasing *trans* [Cs^+] without changing [Ca^{2+}]. With symmetric 250 CsCl and 1 mM Ca^{2+} the slope conductance was 500 pS and the current reversed at 0 mV

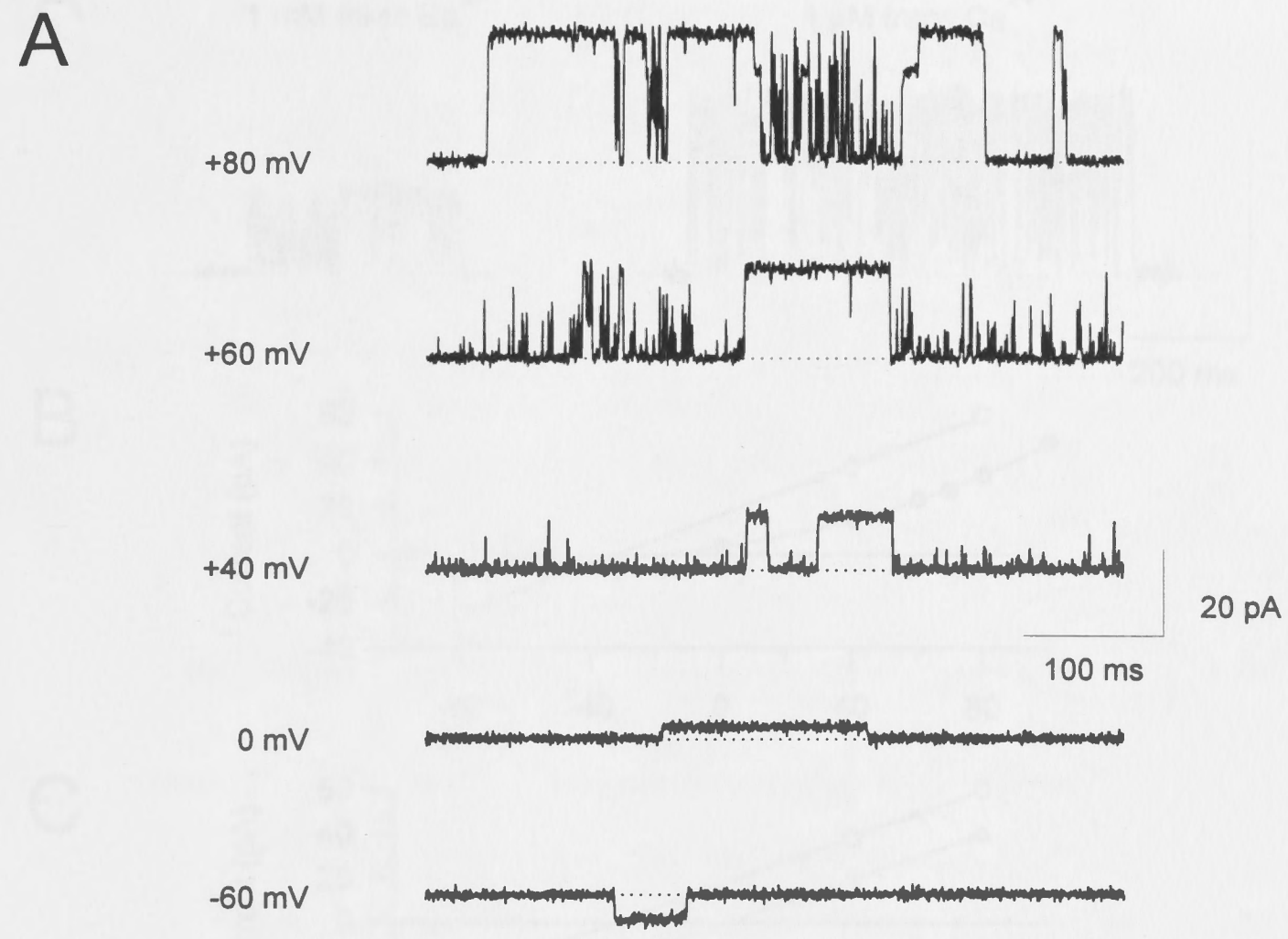

Fig. 3-1. Current-voltage relationship of RyR channels. (A) Representative current traces of a RyR channel at various bilayer potentials (*trans* = ground) with 250/50 mM CsCl, 1/1 mM Ca^{2+} (*cis*/*trans*). Channel openings are shown as upward deflections from the baseline (*broken line*). (B) Plot of maximum current (mean ±SD) versus voltage for five RyRs under the same conditions as (A). The line is a fit to a third-order polynomial function. The reversal potential was –18.2 mV.

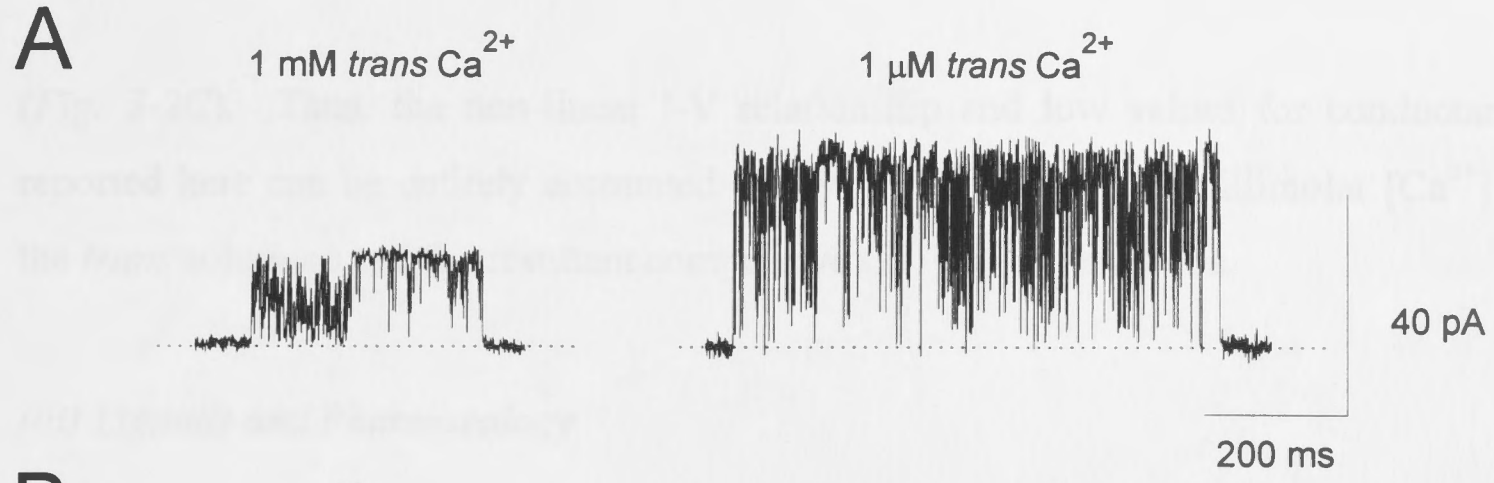

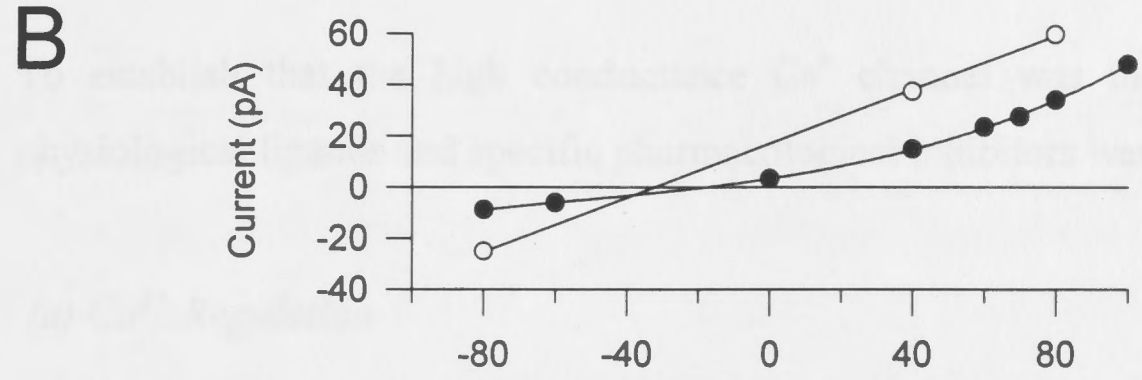

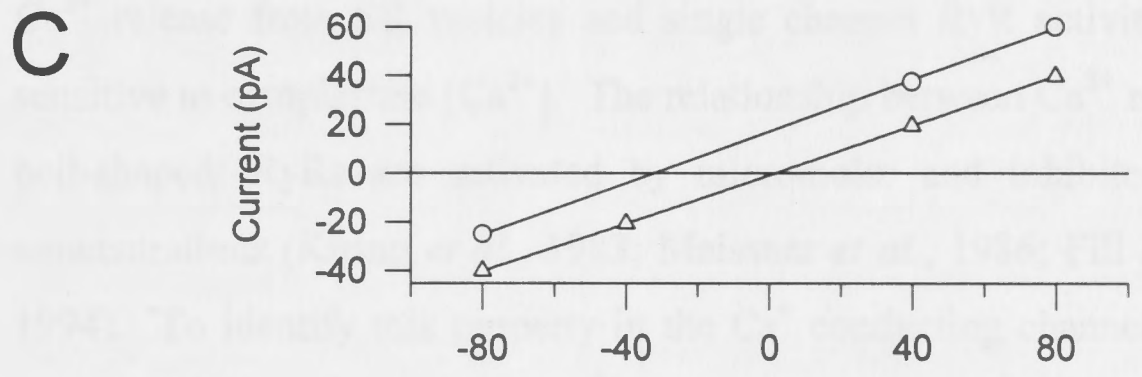

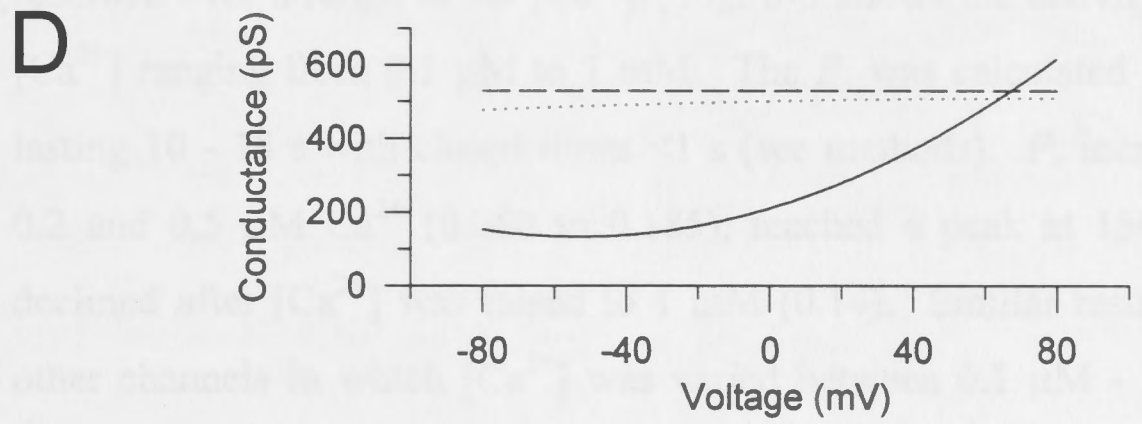

Fig. 3-2. Effect of *trans* Ca^{2+}/Cs^{+} concentration on RyR channel conductance. (A) Current traces at +40 mV with 250/50 mM CsCl (*cis*/*trans*) and 10 μM *cis* Ca^{2+}. Reducing *trans* $[Ca^{2+}]$ from 1 mM to 1 μM increased the current from 15.8 pA to 36 pA. (B) Plot of current versus voltage for RyR channels with 250/50 mM CsCl (*cis*/*trans*), 1 mM *cis* Ca^{2+} and either 1 mM (*closed circles*) or 1 μM (*open circles*) *trans* Ca^{2+}. Reducing *trans* Ca^{2+} increased current at all potentials, produced a linear I-V curve and shifted the reversal potential from −18.2 to −32.5 mV. (C) I-V curve for RyR with 1 μM *trans* Ca^{2+} (*open circles*) or symmetric 250 CsCl, 1 mM Ca^{2+} (~~*closed circles*~~ *open triangles*) shows that reducing *trans* $[Ca^{2+}]$ or raising *trans* $[Cs^{+}]$ had equivalent effects. (D) Plots of slope conductance versus voltage obtained by ~~deriving~~ *differentiating* the polynomial functions in (B) & (C), control (*solid line*), 1 μM *trans* Ca^{2+} (*dotted line*) and symmetric 250 mM CsCl (*dashed line*).

(*Fig. 3-2C*). Thus, the non-linear I-V relationship and low values for conductance reported here can be entirely accounted for by the low [Cs^+] and millimolar [Ca^{2+}] in the *trans* solutions and the resultant competitive Cs^+/Ca^{2+} interactions.

(iii) Ligands and Pharmacology

To establish that the high conductance Cs^+ channel was the RyR the effects of physiological ligands and specific pharmacological inhibitors were investigated.

(a) Ca^{2+} Regulation

Ca^{2+} release from SR vesicles and single channel RyR activity in lipid bilayers are sensitive to cytoplasmic [Ca^{2+}]. The relationship between Ca^{2+} release and *cis* [Ca^{2+}] is bell-shaped: RyRs are activated by micromolar and inhibited by millimolar Ca^{2+} concentrations (Kirino *et al.*, 1983; Meissner *et al.*, 1986; Fill *et al.*, 1990; Meissner, 1994). To identify this property in the Cs^+ conducting channel, channel activity was recorded over a range of *cis* [Ca^{2+}]. *Fig. 3-3* shows the activity of one channel at *cis* [Ca^{2+}] ranging from 0.1 μM to 1 mM. The P_o was calculated from bursts of activity lasting 10 - 15 s with closed times <1 s (see methods). P_o increased sharply between 0.2 and 0.5 μM Ca^{2+} (0.080 to 0.185), reached a peak at 150 μM Ca^{2+} (0.62) and declined after [Ca^{2+}] was raised to 1 mM (0.14). Similar results were obtained in 6 other channels in which [Ca^{2+}] was varied between 0.1 μM - 1 mM. Thus, the Cs^+ conducting channel reproduced the bell-shaped Ca^{2+} dependence of P_o that is characteristic of the RyR. A more detailed analysis of Ca^{2+} regulation is given below.

(b) Adenine Nucleotides

ATP is known to stimulate SR Ca^{2+} efflux and activate the RyR channel by binding directly to an adenine nucleotide binding site (Ogawa and Ebashi, 1976; Meissner, 1984; Smith *et al.*, 1985). ATP activation is independent of phosphorylation. *Fig. 3-4A* shows the effect of adenine nucleotides on Cs^+ channel activity. Control traces were recorded with 1 mM *cis* Ca^{2+} and activity was inhibited. After the addition of 1 mM ATP to the *cis* chamber (*left-hand trace*) the activity was dramatically increased and

characterised by long open times (n = 13). A similar effect was seen after the addition of a non-hydrolysable ATP analogue, AMP-PNP (*right-hand trace*) in this and 15 other channels, demonstrating that these compounds acted directly on the channel and that the effects were not due to donation of a phosphate group. Neither compound had an effect when added to the *trans* chamber (n = 3).

(c) Ryanodine and ruthenium red

Ryanodine (nanomolar to micromolar) characteristically locks RyR channels into a low conductance state (Lai *et al.*, 1989; Nagasaki and Fleischer, 1988; Rousseau *et al.*, 1987). The effect of 20 μM ryanodine on the Cs^+ conducting channel is shown in *Fig. 3-4B*. Ryanodine rapidly induced the characteristic long-lived sub-conductance state thus confirming that the Cs^+ conducting channel was the RyR. Similar results were seen in eight other channels. A more detailed analysis of ryanodine modification is given below. The polycationic dye, ruthenium red, is also known to block RyR channel activity (Smith *et al.*, 1985; Smith *et al.*, 1988; Hymel *et al.*, 1988a; Ma, 1993). Addition of ruthenium red to the *cis* chamber completely blocked activity of the ryanodine-modified channel within seconds (*Fig. 3-4B*, *bottom trace*). Ruthenium red blockade was observed in four other native RyR channels.

(d) Miscellaneous ligands

SR Ca^{2+} release and RyR channel P_o are sensitive to Mg^{2+} (see Meissner, 1994). Addition of 2 mM Mg^{2+} (when *cis* Ca^{2+} was 1 mM) inhibited channel activity in 2 of 2 bilayers. RyR channel activity has been shown to be strongly stimulated by inorganic phosphate (Fruen *et al.*, 1994), while acid phosphatase can increase channel activity presumably by de-phosphorylation of an unidentified phosphoprotein (Wang and Best, 1992). Addition of 10 mM HPO_4^{2-} (n = 2) or 10 - 15 units of non-specific acid phosphatase (n = 3) to the *cis* chamber, increased channel activity when RyRs were inhibited by 1 mM *cis* Ca^{2+} (data not shown).

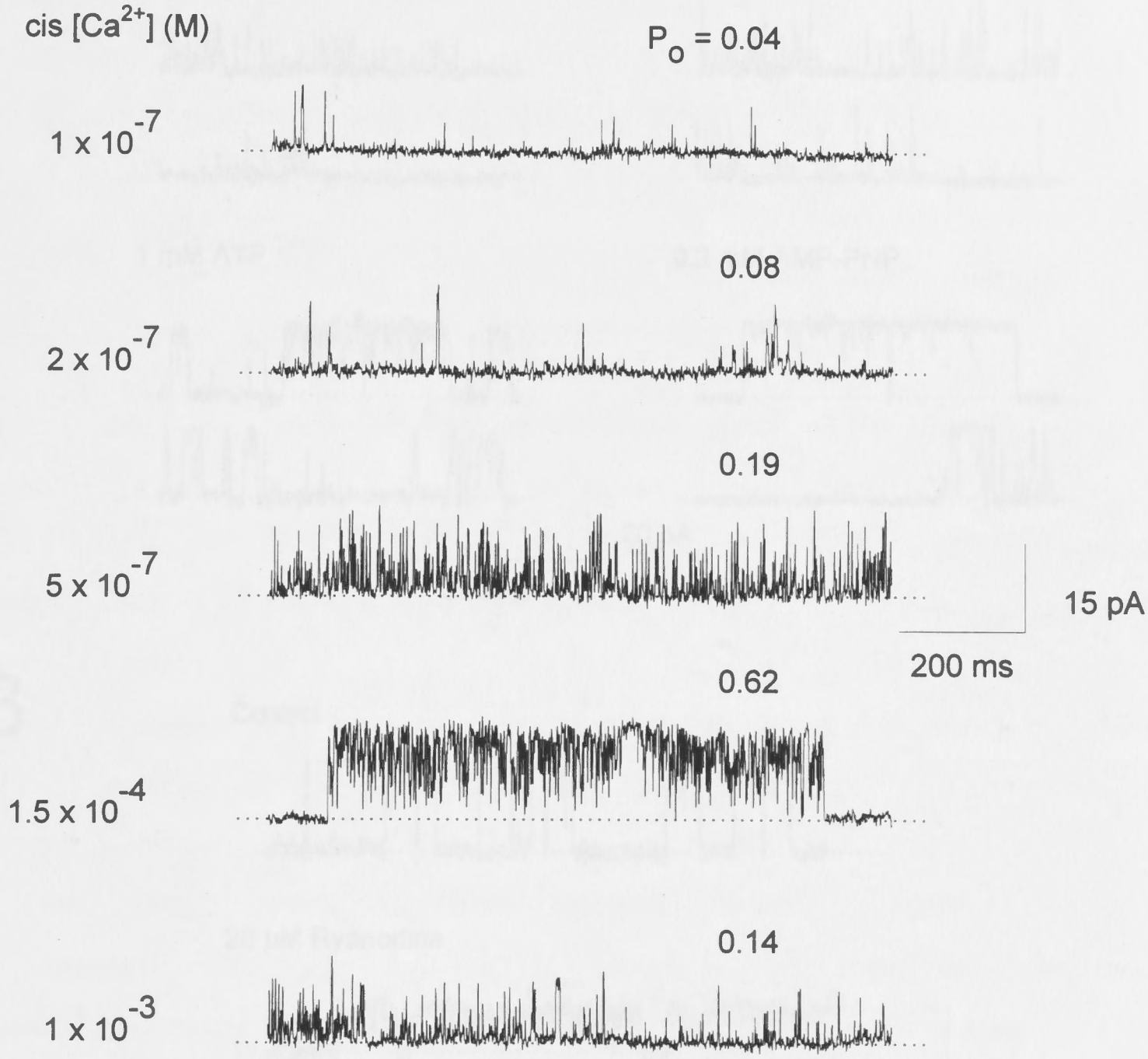

Fig. 3-3. Sensitivity of RyR channel activity to *cis* $[Ca^{2+}]$. Representative 1 s traces of channel activity at +40 mV (opening upwards) with *cis* $[Ca^{2+}]$ as indicated. The *cis* chamber was perfused with a buffered 0.1μM Ca^{2+} solution and $[Ca^{2+}]$ was further adjusted by addition of $CaCl_2$. P_o was calculated from within bursts (see text) and is indicated at top right of each trace.

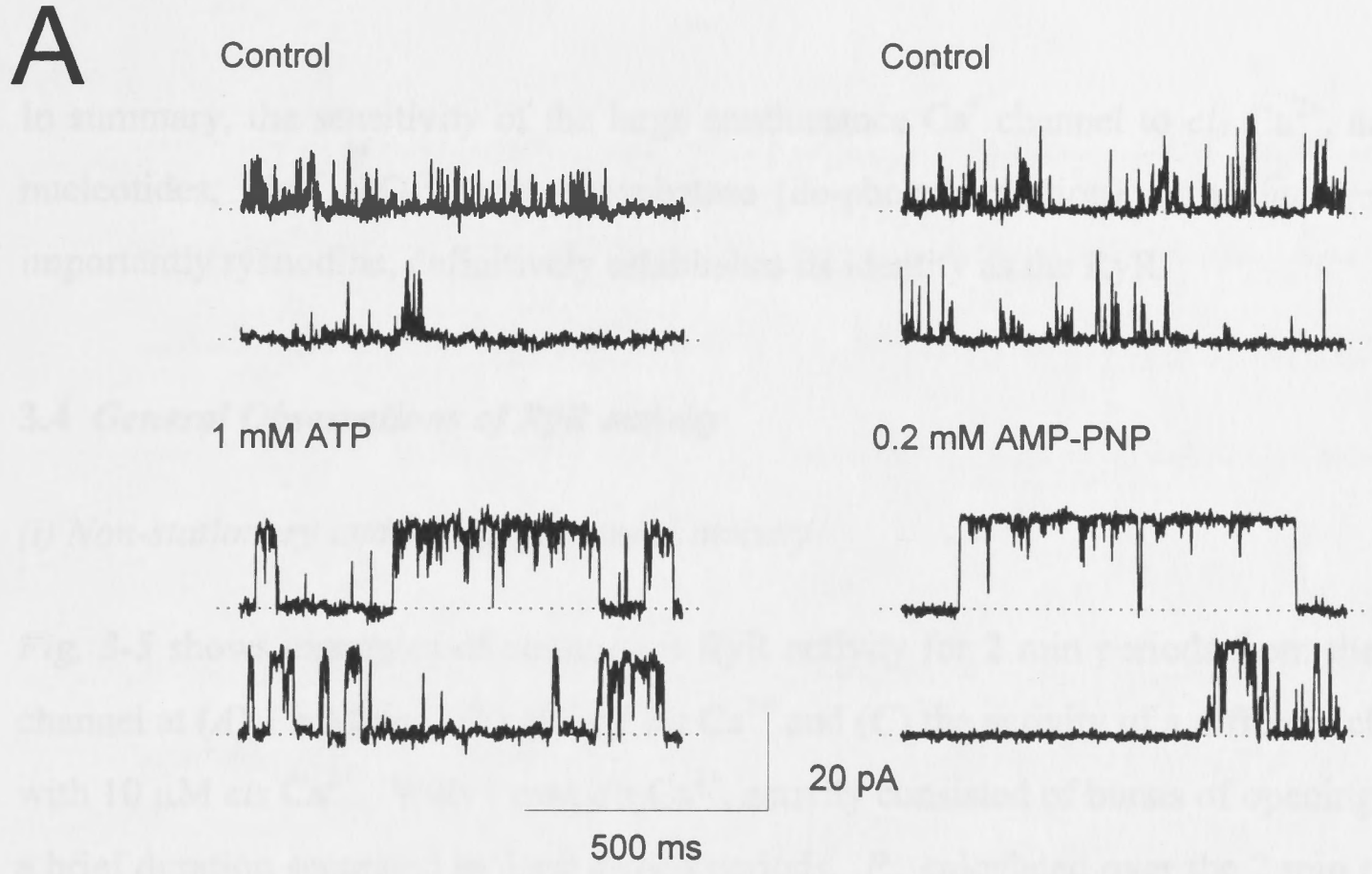

Fig. 3-4. Pharmacological characterisation of RyR channels. (A) Effect of addition of 1 mM ATP or 0.2 mM of the non-hydrolysable analogue AMP-PNP, on RyR channel activity with 1 mM *cis* Ca^{2+}. Both compounds activated the channels suggesting common action at a adenine-nucleotide binding site. (B) Effect of sequential addition of ryanodine and ruthenium red to the *cis* chamber of a RyR with 10 μM *cis* Ca^{2+}. Ryanodine characteristically locked the channel into a long-lived subconductance state. Ruthenium red completely blocked activity.

In summary, the sensitivity of the large conductance Cs^+ channel to *cis* Ca^{2+}, adenine nucleotides, Mg^{2+}, HPO_4^{2-}, acid phosphatase (de-phosphorylation), ruthenium red and importantly ryanodine, definitively establishes its identity as the RyR.

3.4 *General Observations of RyR activity*

(i) Non-stationary and bursting channel activity

Fig. 3-5 shows examples of continuous RyR activity for 2 min periods from the same channel at (*A*) 1 mM and (*B*) 10 μM *cis* Ca^{2+} and (*C*) the activity of a different channel with 10 μM *cis* Ca^{2+}. With 1 mM *cis* Ca^{2+}, activity consisted of bursts of openings with a brief duration separated by long closed periods. P_o, calculated over the 2 min period, was 0.012 and the mean open time (T_o) and the frequency of opening (F_o) were 0.92 ms and 13.7 s^{-1} respectively. When *cis* Ca^{2+} was reduced to 10 μM, P_o increased 10-fold to 0.11, T_o increased from 0.92 to 1.17 ms and F_o increased from 13.7 to 88.9 s^{-1}. In contrast in the second channel (*Fig. 3-5C*) with 10 μM *cis* Ca^{2+} activity consisted of very long bursts of up to 10 s in duration, separated by very long closures of up to 30 s in duration (P_o = 0.08, T_o = 4.71 ms, F_o = 16.6 s^{-1}). Thus, there was considerable variability between channels even with the same *cis* $[Ca^{2+}]$. The bursting nature of RyR activity and the non-stationarity is very apparent in a plot of P_o versus time. *Fig. 3-5D* shows a plot of P_o, averaged for each 10 s segment in the 2 min records. The striking feature is that P_o oscillated in a periodic fashion and that this pattern was apparently independent of $[Ca^{2+}]$ (compare *A* and *B*). The P_o pattern of channel *C* was far more variable than *B* despite the same $[Ca^{2+}]$, yet the average P_o for the 2 mins was similar for both channels. Oscillation in activity was seen in all channels in which continuous P_o analysis was performed (n = 8) and was apparent in the data records of most other channels (n >300). Oscillations were not obvious after channels had been modified by ryanodine. If the bilayer potential was switched during a long closed period (from +40 mV to –40 mV and back) channel activity was usually observed immediately after the voltage pulse, suggesting that channel activity was sensitive to bilayer potential. Recent studies have observed a voltage dependence in RyR channel activity particularly at large positive or negative potentials (>±80 mV) (Laver *et al.*, 1995; Ma, 1995; Ma *et al.*, 1995). However, in the present study channel activity at +40 mV was still observed

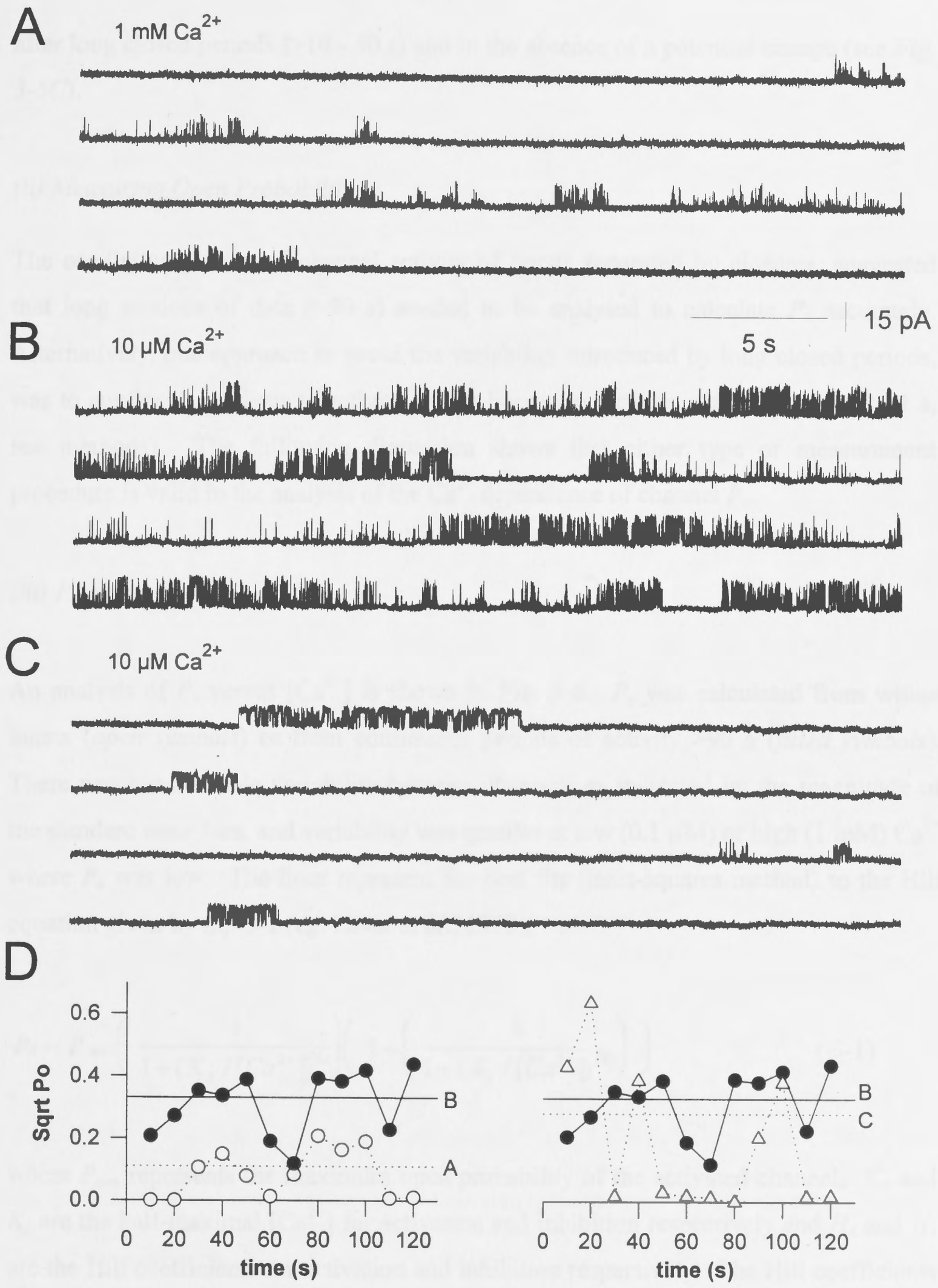

Fig. 3-5. Stationarity of RyR channel activity. Traces showing 2 minutes of continuous channel activity (opening upwards) of a RyR channel (A) with 1mM *cis* Ca^{2+} and (B) 10 µM *cis* Ca^{2+} and (C) activity from a separate channel with 10 µM *cis* Ca^{2+}. (D) Plots of P_o versus time (calculated for each 10 s segment) for the channel activity shown in A (open circles), B (filled circles) & C (triangles). Each horizontal line represents the mean P_o for that channel activity over the 2 min duration. Note the sqrt P_o scale used to clearly show low P_o values.

after long closed periods (>10 - 30 s) and in the absence of a potential change (see *Fig. 3-5C*).

(ii) Measuring Open Probability

The oscillating pattern of channel activity of bursts separated by closures, suggested that long sections of data (>90 s) needed to be analysed to calculate P_o accurately. Alternatively, one approach to avoid the variability introduced by long closed periods, was to confine P_o analysis to activity within bursts (ie. activity with closed times <1 s, see methods). The following discussion shows that either type of measurement procedure is valid in the analysis of the Ca^{2+} dependence of channel P_o.

(iii) P_o versus Ca^{2+}

An analysis of P_o versus [Ca^{2+}] is shown in *Fig. 3-6*. P_o was calculated from within bursts (*open symbols*) or from continuous periods of activity >90 s (*filled symbols*). There was considerable variability between channels as indicated by the magnitude of the standard error bars, and variability was smaller at low (0.1 μM) or high (1 mM) Ca^{2+} where P_o was low. The lines represent the best fits (least-squares method) to the Hill equation given by *Eq. 3-1* (eg. Laver *et al.*, 1995),

$$P_o = P_{max}\left(\frac{1}{1+(K_A/[Ca^{2+}])^{H_A}}\right)\left(1-\left(\frac{1}{1+(K_I/[Ca^{2+}])^{H_I}}\right)\right) \qquad (3\text{-}1)$$

where P_{max} represents the maximum open probability of the activated channel, K_A and K_I are the half-maximal [Ca^{2+}] for activation and inhibition respectively and H_A and H_I are the Hill coefficients for activation and inhibition respectively. The Hill coefficients represent the number of Ca^{2+} ions which bind co-operatively to produce either channel activation or inhibition. The P_o versus [Ca^{2+}] curve was bell-shaped, rising between 0.1 μM and 1 μM, reaching a peak at 10 μM - 100 μM and declining at 1 mM [Ca^{2+}], which agrees with previous reports (Smith *et al.*, 1986; Fill *et al.*, 1990; Chu *et al.*, 1993). As expected, P_o calculated from within bursts was greater than P_o measured

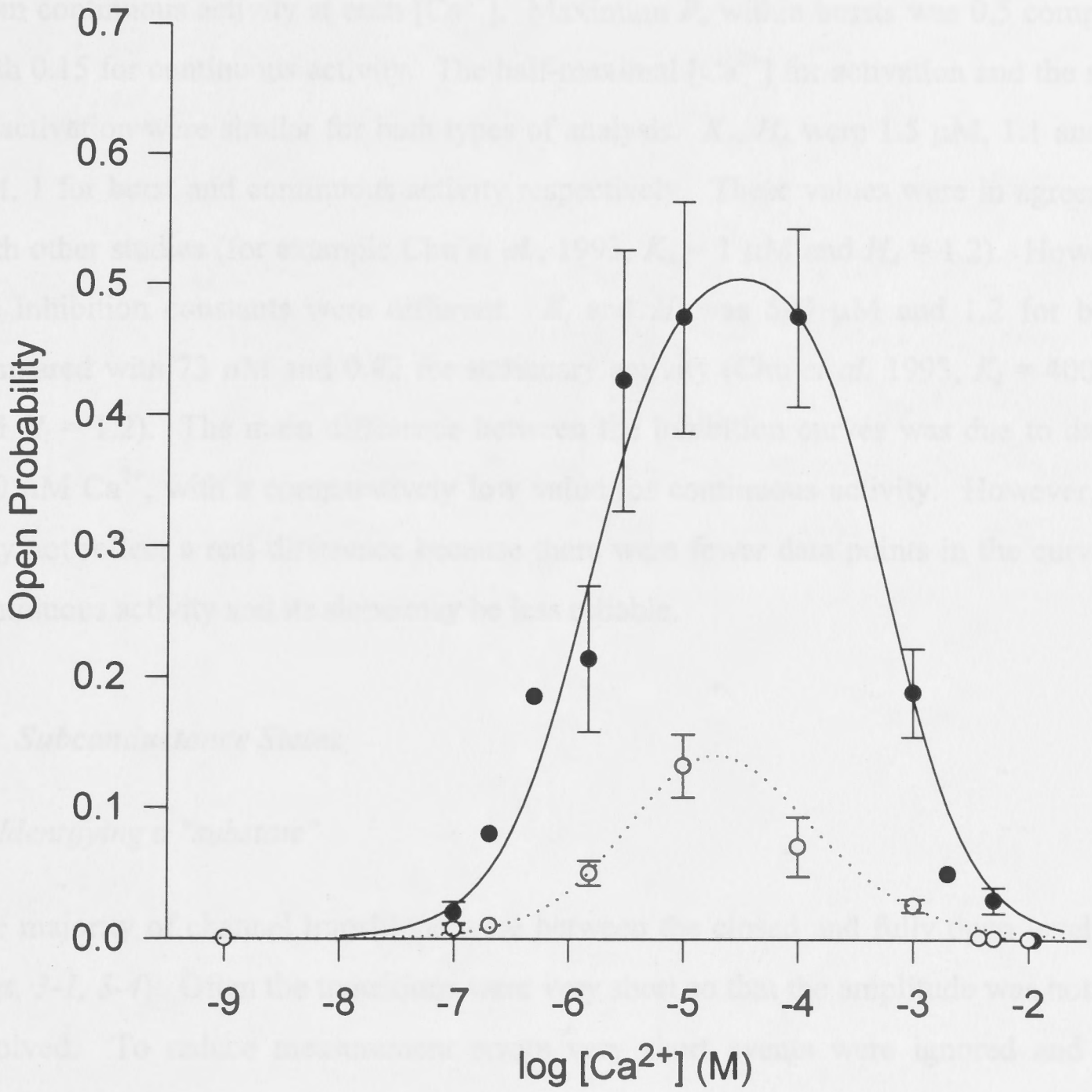

Fig. 3-6. Ca^{2+} dependence of RyR channel activity. Solutions contained 250/50 mM CsCl (*cis*/*trans*), 1 mM Ca^{2+} *trans*. *Cis* [Ca^{2+}] was adjusted by perfusion with Ca^{2+} buffered solutions. P_o measured within bursts (*filled circles*, mean ± sem of 72 RyRs) or from continuous activity >90 s (*open circles*, mean ± sem of 58 RyRs). Data without error bars are single observations. The lines represent the solutions to *Eq. 3-1* for the following parameter values: (*solid line*) $P_{max} = 0.54$, $K_A = 1.5$ μM, $H_A = 1.1$, $K_I = 590$ μM and $H_I = 1.2$; (*dotted line*) $P_{max} = 0.24$, $K_A = 5.1$ μM, $H_A = 1$, $K_I = 73$ μM and $H_I = 0.82$.

from continuous activity at each [Ca^{2+}]. Maximum P_o within bursts was 0.5 compared with 0.15 for continuous activity. The half-maximal [Ca^{2+}] for activation and the slope of activation were similar for both types of analysis. K_A, H_A were 1.5 μM, 1.1 and 5.1 μM, 1 for burst and continuous activity respectively. These values were in agreement with other studies (for example Chu *et al.*, 1993, K_A = 1 μM and H_A = 1.2). However, the inhibition constants were different. K_I and H_I was 590 μM and 1.2 for bursts compared with 73 μM and 0.82 for stationary activity (Chu *et al.* 1993, K_I = 400 μM and H_I = 1.2). The main difference between the inhibition curves was due to data at 100 μM Ca^{2+}, with a comparatively low value for continuous activity. However, this may not reflect a real difference because there were fewer data points in the curve for continuous activity and its slope may be less reliable.

3.5 *Subconductance States*

(i) Identifying a "substate"

The majority of channel transitions were between the closed and fully open level (see *Figs. 3-1, 3-4*). Often the transitions were very short so that the amplitude was not well resolved. To reduce measurement errors very short events were ignored and only amplitudes of levels made up of at least three data points were considered. For quantitation, amplitude histograms were constructed using mean-variance analysis (Patlak, 1988) incorporated into "Channel2". Multiple gaussian functions were then used to fit the peaks in the histograms. The peak amplitudes were normalised and expressed as a fraction of the maximum conductance (fractional conductance). Using these methods, a number of current levels smaller than the main open level (subconductance states or substates) were observed in ~ 20% of channels. For example a substate at ~ 0.7 of the maximum open level was seen in the channel shown in *Fig. 3-1A* and this level is evident in the +80 mV trace. *Fig. 3-7A* shows examples of substate activity from this channel at different bilayer potentials while *Fig. 3-7B* shows a plot of current versus voltage for the maximum open level and the substate. Each curve is the best fit to a third order polynomial function. Both the maximum open level and the substate level reversed at ~ −15 mV and the slope conductances at this potential were 173 and 124 pS respectively. It is arguable that the 124 pS level represents the activity

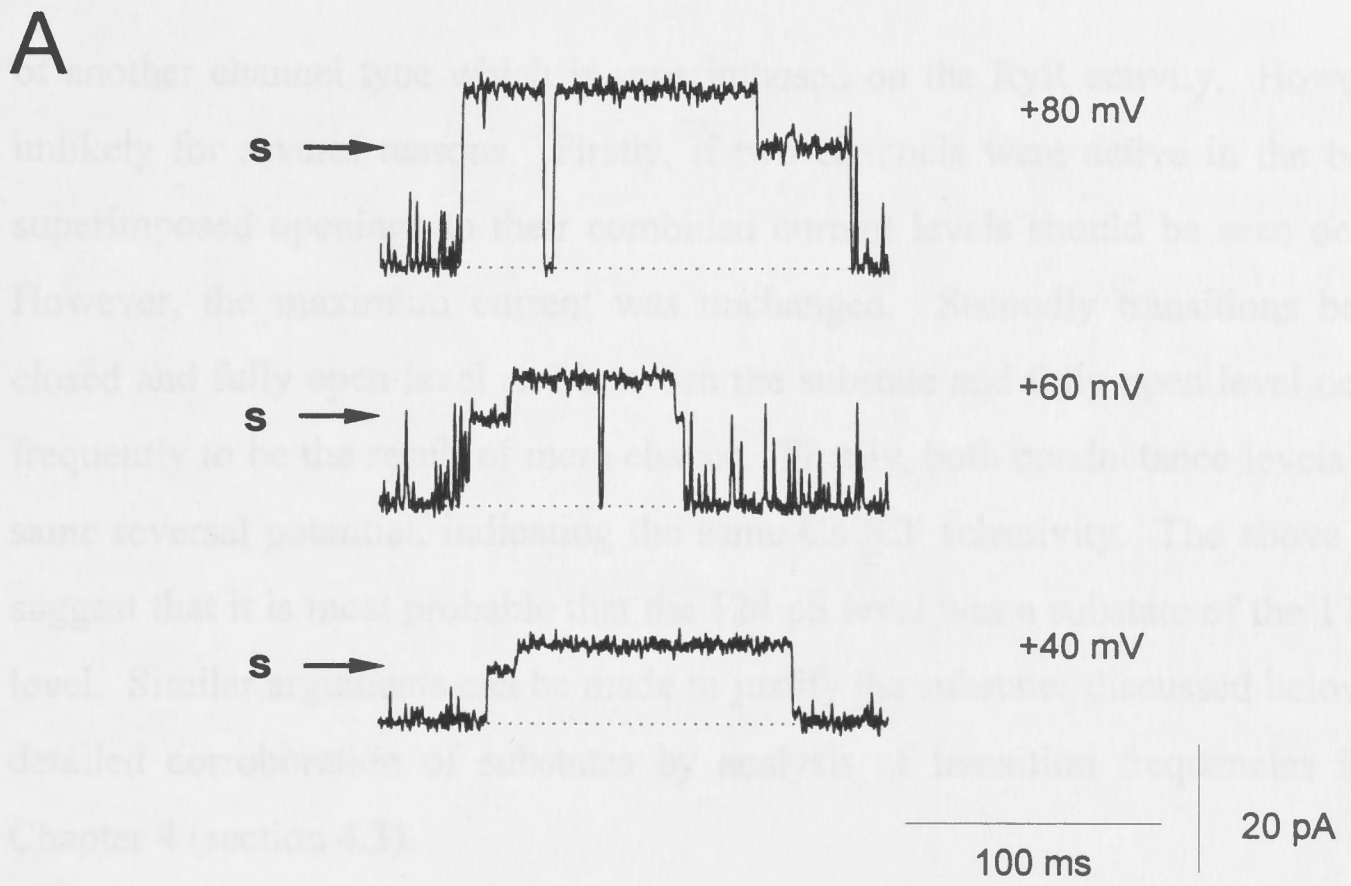

Fig. 3-7. Characterisation of RyR channel substate activity. (A) RyR current traces from the same channel shown in *Fig. 3-1* showing the substate level,"s", at different bilayer potentials. (B) I-V plot for the maximal open level and the substate level. The reversal potential for both levels was ~ –15 mV and the slope conductances at that potential were 173 and 124 pS respectively.

of another channel type which is superimposed on the RyR activity. However this is unlikely for several reasons. Firstly, if two channels were active in the bilayer then superimposed openings to their combined current levels should be seen occasionally. However, the maximum current was unchanged. Secondly transitions between the closed and fully open level and between the substate and fully open level occurred too frequently to be the result of mere chance. Finally, both conductance levels shared the same reversal potential, indicating the same Cs^+/Cl^- selectivity. The above arguments suggest that it is most probable that the 124 pS level was a substate of the 173 pS open level. Similar arguments can be made to justify the substates discussed below. A more detailed corroboration of substates by analysis of transition frequencies is given in Chapter 4 (section 4.3).

(ii) Subconductance levels

Clear substates were observed in ~ 20% of native RyR channels (23 of 107 channels studied). Substates occurred at numerous levels mostly between 0.15 and 0.85 of the maximum current. Typically, only one or two substate levels were seen in each of these channels. The most frequent were characteristically long-lived, with amplitudes which varied between 11 - 33% of the maximum current. Examples of these substates labelled "S1" are shown in *Figs. 3-8A, 8B, 9A* and *9B*. Their fractional conductances derived from gaussian fits to the histograms were 0.31, 0.29, 0.20 and 0.11 respectively. These small substates often occurred after a burst of activity and in a transition from the fully open state. However, bursting activity exclusively to substate levels was also seen. In the channel shown in *Fig. 3-8B* channel flickering to the main open level gave way to a burst of longer-lived openings to the S1 level before the resumption of flickering activity again.

Some channels exhibited multiple substates and at least 3 to 4 levels in addition to the closed and fully open levels were evident in the channels shown in *Fig. 3-9*. In *Fig. 3-9A* the levels S1 - S3 had fractional conductances of 0.20, 0.59 and 0.90 while in *Fig. 3-9B* the levels S1a, S1b, S2 & S3 had values of 0.11, 0.28, 0.41 and 0.71 respectively. In another channel (*Fig. 3-10*) three substates, S1 - S3, were identified at +40 mV and also

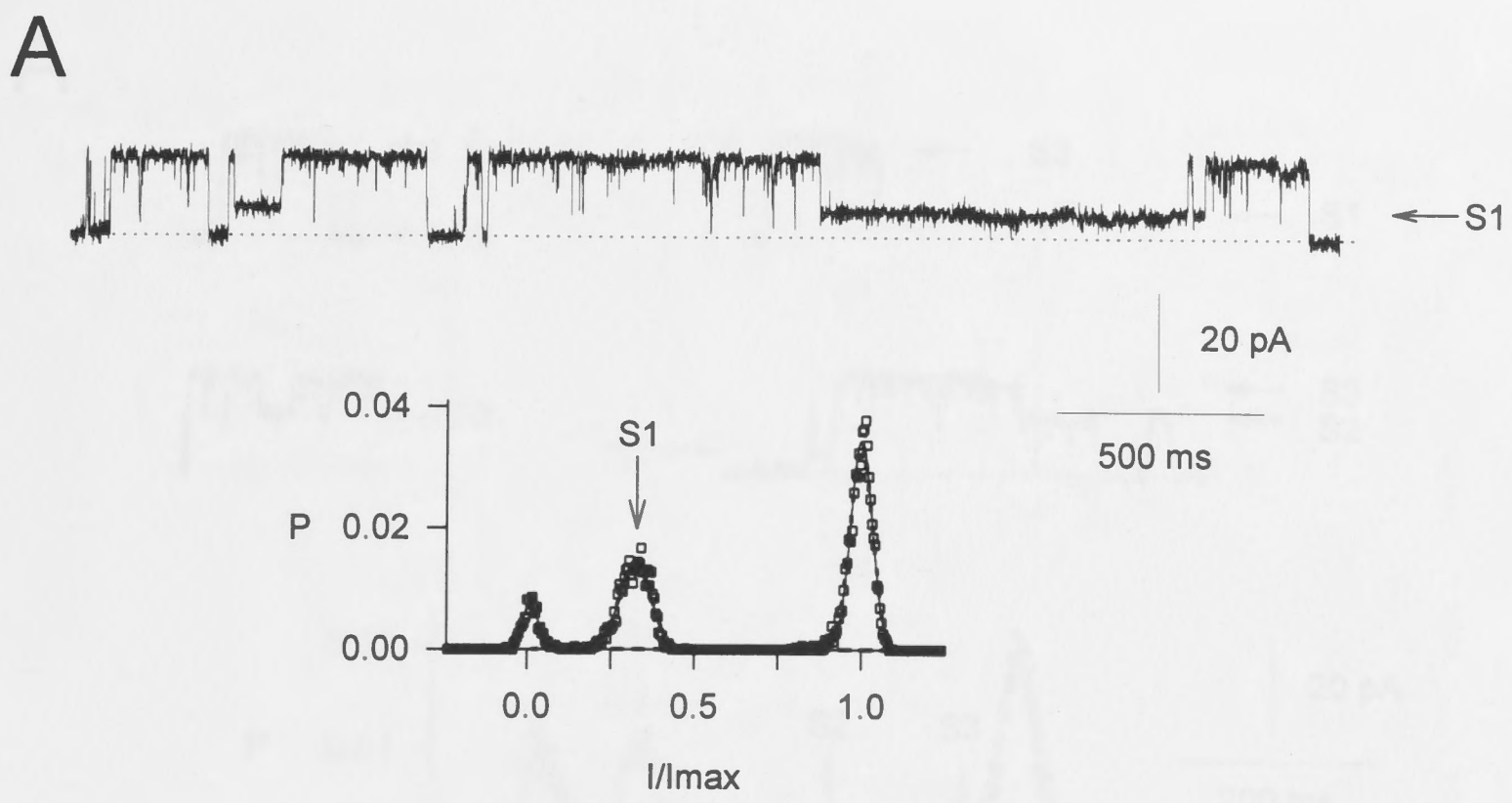

Fig. 3-8. Representative substate activity in two RyRs. Examples of channel activity showing common low conductance levels marked "S1" (*upper panels*) and amplitude histograms constructed by mean-variance analysis of 3 - 5 s of selected data (*lower panels*). For histograms, current was normalised to the maximum value and the peaks were fitted by multiple gaussian functions. (A) Channel activity at 10μM *cis* Ca^{2+} with long-lived openings to level S1 (fractional conductance = 0.31). (B) Another RyR channel recorded with 0.1μM Ca^{2+} and 2 mM ATP *cis*, showing openings to the maximum level punctuated by a burst of activity to level S1 (fractional conductance =0.29).

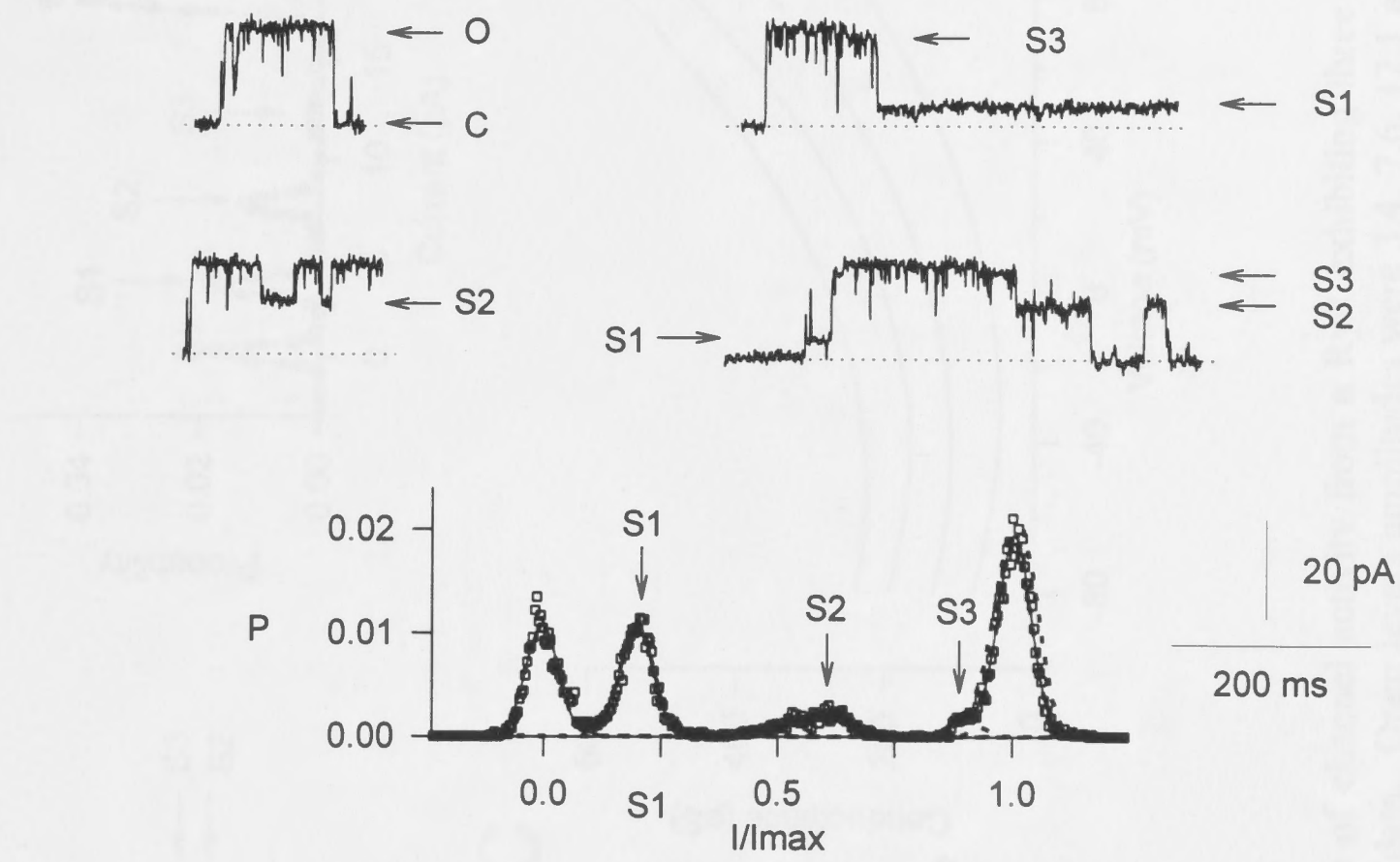

Fig. 3-9. Multiple substate activity in RyR channels. (A) Examples of substate activity from a channel showing the closed level "C", the fully open level "O" and three substate levels "S1 - S3". The normalised amplitudes of S1 - S3 were 0.2, 0.59 and 0.90 respectively. (B) Activity from another RyR channel showing four substate levels S1a, S1b, S2 and S3 with respective values of 0.11, 0.28, 0.41 and 0.71. Values for the substate levels were derived from gaussian fits to the amplitude histograms constructed from mean-variance analysis of 1.2 - 3 s of selected data. Note that substate activity was concentrated at the S1 level.

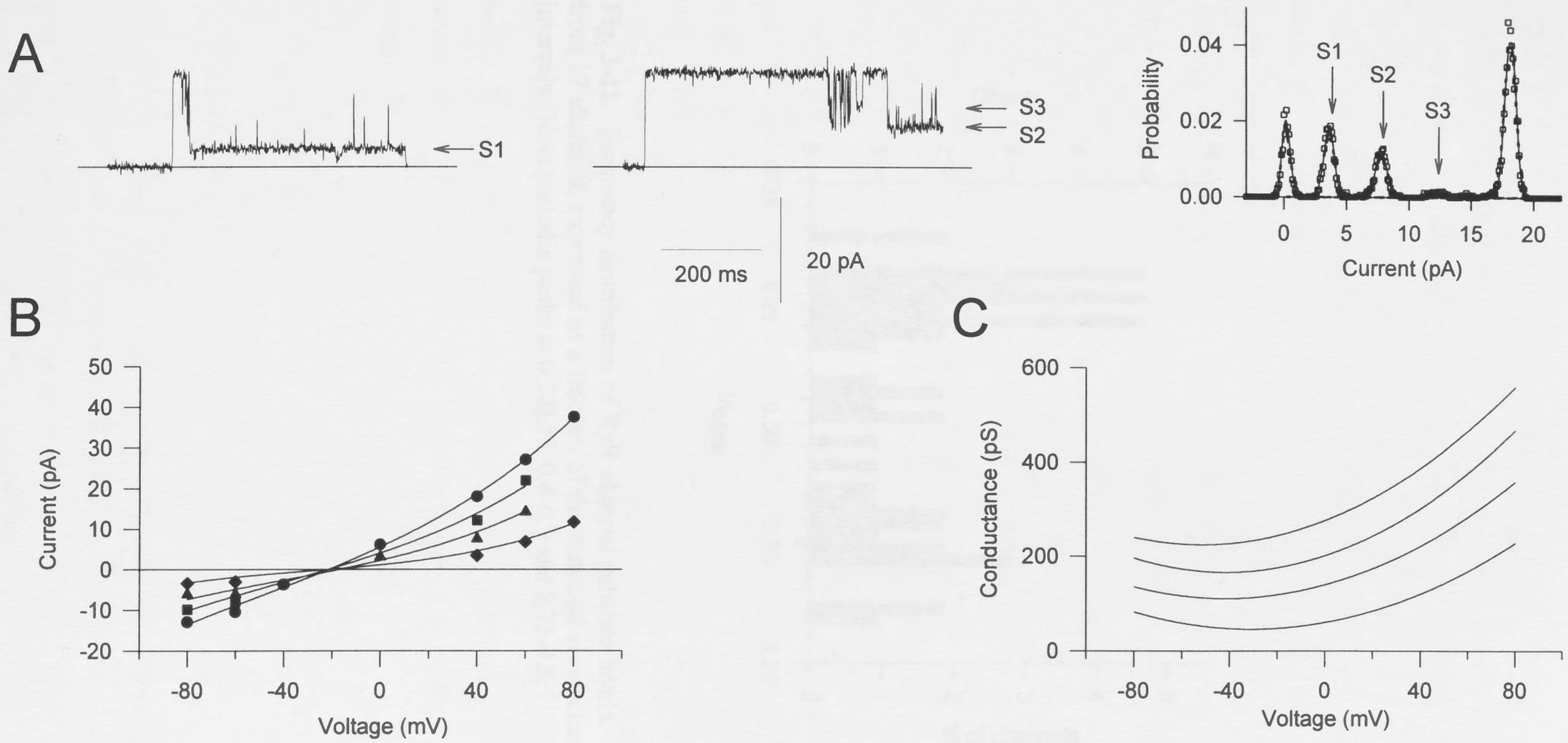

Fig. 3-10. Voltage dependence of substate conductance in a RyR channel. (A) Example of channel activity from a RyR exhibiting three distinct substates S1-S3 and a histogram constructed from mean-variance analysis of 3 s of selected data. Open levels amplitudes were 3.4, 7.6, 12.1 and 17.9 pA. Bilayer potential was +40 mV with 10 μM *cis* Ca^{2+}. (B) Current-voltage plot of the maximum open level and the three substates. The currents all reversed at ~ –20 mV. (C) Plot of slope conductance versus voltage shows that the conductance of each open level had a similar voltage dependence (see text).

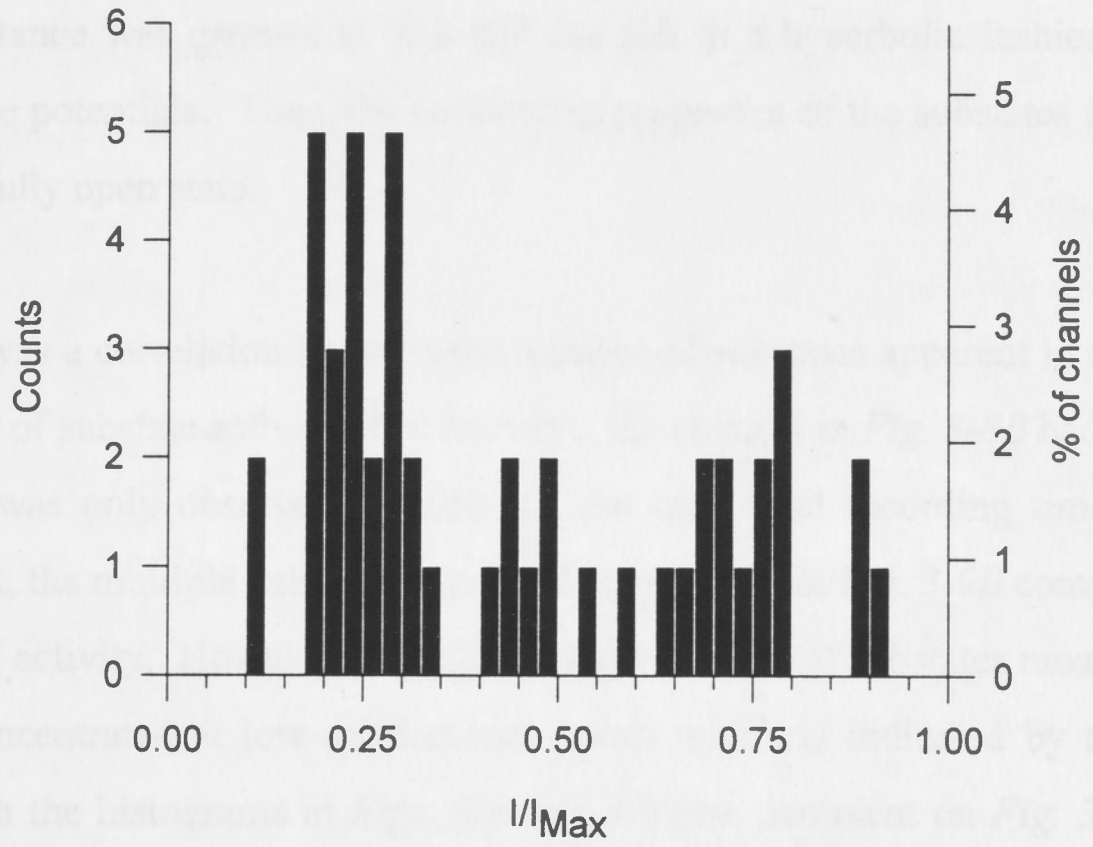

Fig. 3-11. Frequency distribution of RyR channel substate levels. Values were obtained from 17 channels, expressed as a fraction of the maximal conductance and binned in 0.05 intervals. Note periodic peaks at 0.2-0.25, 0.4-0.5 and 0.75-0.8.

at other bilayer potentials. The I-V relationship for this channel (*Fig. 3-10B*) shows that the three substates and the maximal open level shared the same reversal potential of ~ –20 mV (as did the open levels in the channel shown in *Fig. 3-7*). The slope conductances at that potential were 47, 118, 175 and 243 pS respectively. *Fig. 3-10C* shows that the conductance of all the open levels showed the characteristic voltage sensitivity caused by the presence of millimolar *trans* Ca^{2+} shown in *Fig. 3-2D*. The conductance was greatest at +80 mV but fell in a hyperbolic fashion with increasing negative potentials. Thus, the conductive properties of the substates are similar to that of the fully open state.

There was a correlation between the number of substates apparent in a channel and the amount of substate activity. For example, the channel in *Fig. 3-8B* had a single S1 level which was only observed for 650 ms out of a total recording time of 4 mins. In contrast, the multiple substate activity of the channel in *Fig. 3-9B* comprised 56% of the channel activity. However, regardless of the number of substates most substate activity was concentrated at low conductance levels which is indicated by the prominent S1 peaks in the histograms in *Figs. 3-8* and *3-9* (see comment on *Fig. 3-9*). While there was variability between individual channels in both the number and magnitude of substates the levels appeared to be clustered at discrete amplitudes. A frequency distribution of substates in fifteen channels (*Fig. 3-11*) revealed that most had fractional conductances between 0.20 - 0.30, 0.40 - 0.55 or 0.70 - 0.85. The most frequent levels were ~ 25%. Thus small conductance levels comprised most of the substate activity within individual channels and were the most frequently seen levels between different channels.

3.6 Ryanodine Substate

(i) General Observations

The plant alkaloid ryanodine radically alters the gating and conductance properties of the RyR (*Fig. 3-4C*). After ryanodine treatment the average time before onset of ryanodine gating was 68 ± 22 s (range 10 to 210 s, n = 8) at 10 μM - 1 mM *cis* Ca^{2+}. As found previously (Nagasaki and Fleischer, 1988), the induction of the ryanodine

substate was dependent on channel P_o. In two channels where *cis* Ca^{2+} was 0.1μM and P_o was ~ 0, no channel activity was seen in the bilayer lifetime (6 - 10 mins).

RyR current amplitudes were measured before and after treatment with ryanodine (1-20 μM). In 8/9 channels ryanodine induced a unitary current level with an amplitude 51 ± 1% of the control current at +40 mV. The I-V relationship for a ryanodine modified channel is compared with untreated channels in *Fig. 3-12A*. Ryanodine treatment reduced the current at all bilayer potentials without significantly changing the reversal potential (–18.2 mV for control, –21 mV for ryanodine treated). The current was attenuated more at positive potentials compared with negative potentials. The plot of slope conductance versus voltage (*Fig.3-12B*) shows that ryanodine caused a modest reduction and "flattening" of the control curve. Because of this effect the size of the ryanodine substate relative to the maximum open level was dependent on the voltage at which measurements were made. The ratio of the ryanodine-modified to control conductance was 0.47, 0.42 and 0.4 at –40 mV, +40 mV and +80 mV respectively.

(ii) Comparison of ryanodine substate with pre-existing substates

One interesting question regarding the ryanodine substate is whether it is related to the substates occasionally seen in channels the absence of ryanodine as described above. Ryanodine treatment induced a unitary current level at 51% of the control current at +40 mV. Therefore it is possible that the ryanodine induced substate might be related to the 40 - 50% level seen in untreated channels. However the results of one experiment argues against this hypothesis (*Fig. 3-13*). In this experiment, ryanodine was added to a native channel which already exhibited three prominent substate levels (S1 - S3). Ryanodine did not induce a unitary substate nor eliminate the pre-existing substate activity, but instead reduced the amplitude of each open level. Values for the substate and maximum open levels at +40 mV were 3.4, 7.6, 12.1 and 17.9 pA for control activity and 2.2, 4.4, 6.9 and 8.8 pA after ryanodine treatment. Furthermore, the I-V relationship for each open level in this channel was obtained before and after ryanodine treatment (*Fig. 3-14A & B*). The striking feature is that ryanodine treatment uniformly reduced the magnitude of each substate and made the I-V curves linear. The

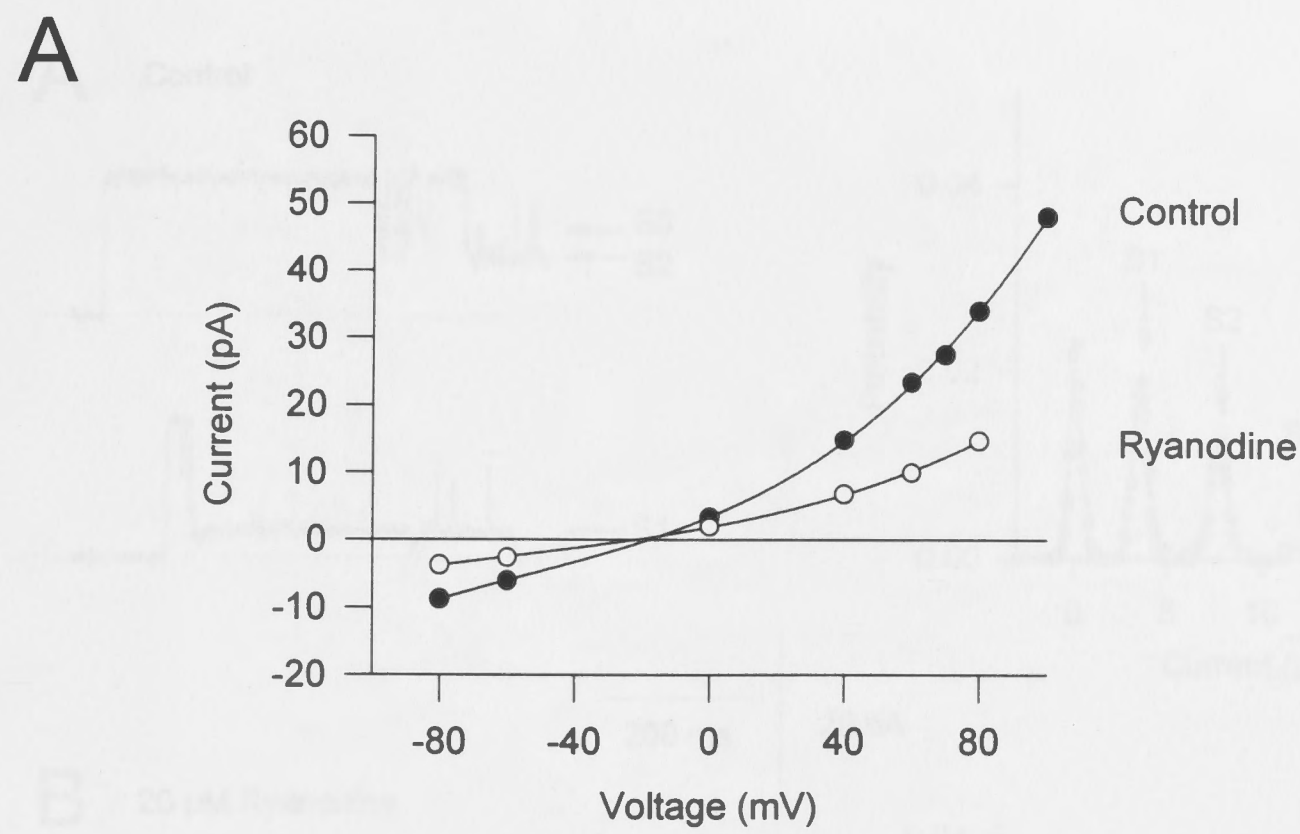

Fig. 3-12. Effects of ryanodine on RyR channel conductance. (A) I-V plot for 5 control channels (*filled symbols*) and a separate channel after treatment with 10 μM ryanodine (*open symbols*). Solutions contained 250/50 mM CsCl 1/1 mM Ca^{2+} (*cis/trans*). Lines represent the fits to third-order polynomial equations. Ryanodine treatment reduced the current at all potentials, without affecting the reversal potential (–18.2 mV for control, –21.2 mV for ryanodine treated). (B) Voltage dependence of conductance obtained by plotting the derivative functions of the polynomial fits in (A). Ryanodine treatment caused a slightly greater reduction in conductance at positive compared with negative potentials. The ryanodine treated/control conductance was 0.47, 0.42 and 0.40 at –40 mV, +40 mV and +80 mV respectively.

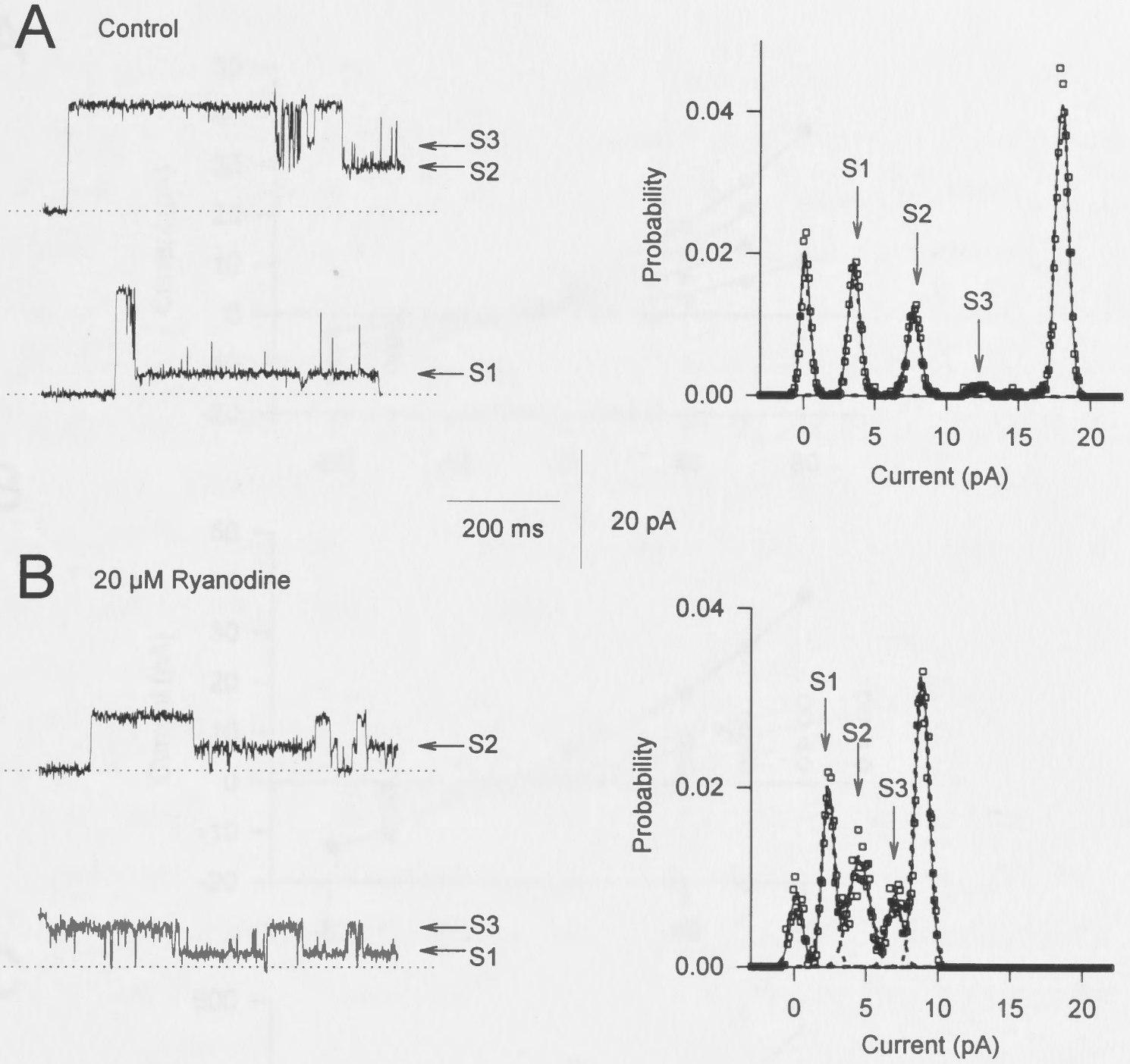

Fig. 3-13. Effect of ryanodine on pre-existing RyR channel substates. (A) Control channel activity at 10μM Ca^{2+} exhibiting three distinct substates S1-S3. (B) Activity from the same channel after treatment with 20 μM ryanodine. Ryanodine did not induce a unitary substate level but instead reduced the conductance of each open level. Amplitude histograms were constructed from mean-variance analysis of 2-3 s of selected data. Peaks in the histograms were fitted with multiple gaussian functions and correspond to the levels marked in the current traces. Values of S1 - O were 3.4, 7.6, 12.1, 17.9 pA and 2.2, 4.4, 6.9, 8.8 pA before and after ryanodine treatment respectively.

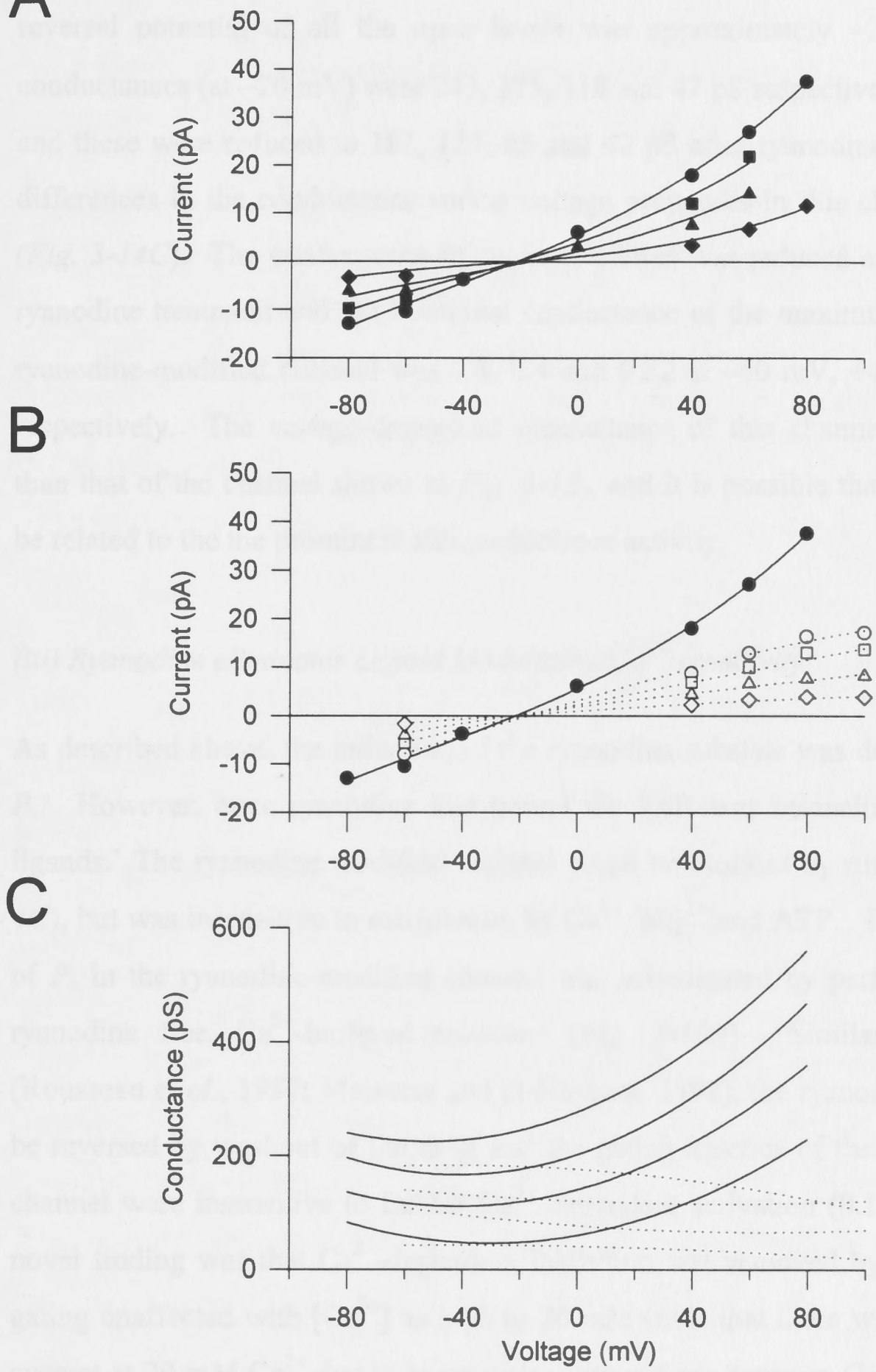

Fig. 3-14. Effect of ryanodine on RyR channel substate conductance. (A) I-V plot of maximum open level and three substates from channel in *Fig. 3-12*. Lines represent the fits to third-order polynomial equations. The reversal potential for all levels was approximately –20 mV. (B) Current-voltage relationship of each open level after ryanodine treatment (*open symbols*) compared with maximum control activity (*filled circles*). Ryanodine reduced the amplitude of each open level and linearised the curves. (C) Plot of slope conductance versus voltage showing that ryanodine caused a proportional reduction in the conductance of each open state and eliminated the rectification.

reversal potential of all the open levels was approximately –20 mV. The slope conductances (at –20 mV) were 243, 175, 118 and 47 pS respectively before ryanodine, and these were reduced to 181, 125, 85 and 42 pS after ryanodine modification. The differences in the conductance versus voltage properties in this channel were marked (*Fig. 3-14C*). The conductance of each open level was reduced and made linear after ryanodine treatment and the fractional conductance of the maximum open level in the ryanodine-modified channel was 0.8, 0.4 and 0.22 at –40 mV, +40 mV and +80 mV respectively. The voltage-dependent conductance of this channel was much greater than that of the channel shown in *Fig. 3-12* , and it is possible that the difference may be related to the the prominent subconductance activity.

(iii) Ryanodine eliminates Ligand Modulation/Ca^{2+} sensitivity

As described above, the induction of the ryanodine substate was dependent on channel P_o. However, once ryanodine had bound the RyR was insensitive to most channel ligands. The ryanodine modified channel could be blocked by ruthenium red (*Fig. 3-4C*), but was insensitive to modulation by Ca^{2+}, Mg^{2+} and ATP. The Ca^{2+} dependence of P_o in the ryanodine-modified channel was investigated by perfusing the bath with ryanodine free, Ca^{2+}-buffered solutions (*Fig. 3-15A*). Similar to earlier reports (Rousseau *et al.*, 1987; Meissner and el-Hashem, 1992), the ryanodine effect could not be reversed by washout of the drug and the gating kinetics of the ryanodine modified channel were insensitive to further Ca^{2+}-dependent activation (0.1 - 10 μM Ca^{2+}). A novel finding was that Ca^{2+}-dependent inhibition was removed by ryanodine with the gating unaffected with [Ca^{2+}] as high as 20 mM (note that there was a reduction in the current at 20 mM Ca^{2+} due to competitive interactions between Ca^{2+} and Cs^{+}). The P_o of ryanodine modified channels was close to unity and independent of [Ca^{2+}] over the range 1 nM to 20 mM (*Fig. 3-15B*). The results are consistent with the effects of ryanodine on CICR from SR vesicles (Meissner, 1986).

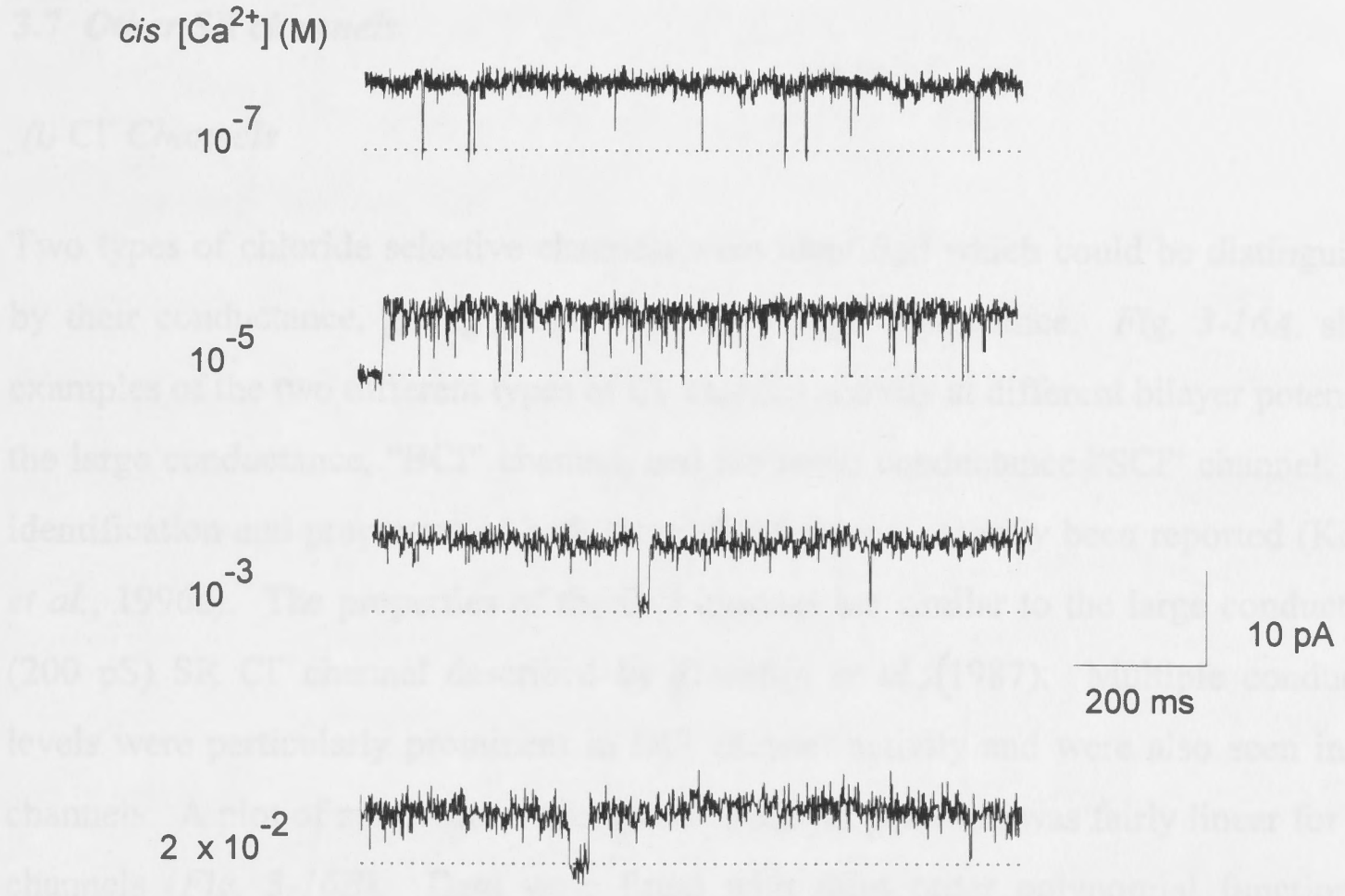

Fig. 3-15. Ryanodine abolishes Ca^{2+} sensitivity of RyR channels. (A) Typical current traces of ryanodine modified channels with *cis* [Ca^{2+}] ranging from 0.1 μM to 20 mM. (B) Ca^{2+} dependence of P_o (calculated within bursts) of untreated channels (*filled symbols*) or ryanodine-modified channels (*open symbols*). Ryanodine locked channels in an open state and eliminated Ca^{2+}-dependent activation and inactivation.

3.7 *Other SR channels*

(i) Cl^- *Channels*

Two types of chloride selective channels were identified which could be distinguished by their conductance, gating properties and voltage dependence. *Fig. 3-16A.* shows examples of the two different types of Cl^- channel activity at different bilayer potentials, the large conductance, "BCl" channel, and the small conductance "SCl" channel. The identification and properties of both these channel have recently been reported (Kourie *et al.*, 1996a). The properties of the BCl channel are similar to the large conductance (200 pS) SR Cl^- channel described by (Tanifuji *et al.*, (1987). Multiple conducting levels were particularly prominent in BCl channel activity and were also seen in SCl channels. A plot of maximum current versus bilayer potential was fairly linear for both channels (*Fig. 3-16B*). Data were fitted with third order polynomial functions to calculate reversal potentials and the conductance for each channel was calculated at the reversal potential. The BCl channel had a maximal conductance of 269 pS , while the SCl channel had a maximal conductance of 100 pS with 250/50 mM CsCl, 1/1 mM Ca^{2+} (*cis/trans*). Currents from both channels reversed at ~ +30 mV (BCl channel +32.1 mV, SCl channel +28.1 mV). In symmetric CsCl conditions the SCl channel reversed at ~ 0 mV and there was no change in maximal conductance (105 pS). The BCl channel had a high P_o at all bilayer potentials, especially at positive potentials where there were few closures, while the SCl channel opened in bursts separated by long (~1 s) closures. The SCl but not BCl channel exhibited a voltage dependence. P_o was fairly stationary at 0 mV but decreased within a few seconds after a voltage step to large positive or negative potentials. Channel activity recovered after returning the bilayer potential to 0 mV, or more rapidly, by a brief voltage step with the opposite sign of the initial step. A rigorous analysis of SCl channel voltage dependence is given by Kourie *et al.*, (1996a).

(ii) VDAC-type non selective channel

Large conductance channels permeable to Cs^+ and Cl^- were seen in only 9 of 434 bilayers using B4 vesicles but were seen more frequently (10 of 44 bilayers) following

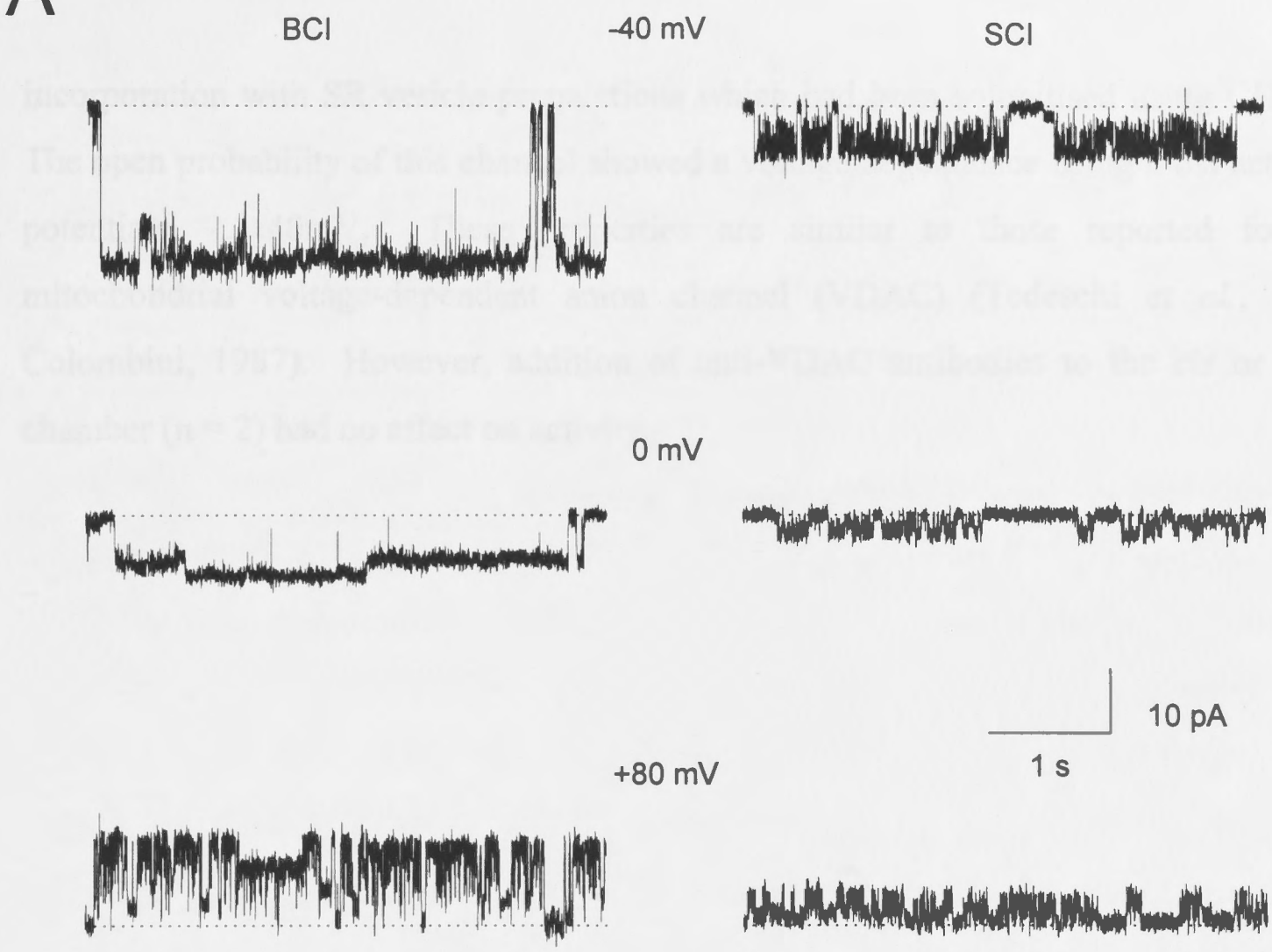

Fig. 3-16. Types of SR Cl^- channel activity. (A) Example of channel activity of the large (BCl) channel and the small conductance (SCl) channel at various bilayer potentials with 250/50 mM CsCl, 1/1 mM Ca^{2+} (*cis*/*trans*). (B) I-V relationship of the maximum current level under same conditions as in A, BCl (*filled circles*, mean of 4 channels), SCl (*open circles*, mean of 3 channels) and a SCl channel in symmetric 250 mM CsCl, 1 mM Ca^{2+} (*triangles*). Each curve is a fit to a third order polynomial function. The reversal potential and slope conductance were +32.1 mV and 269 pS respetively for the BCl channel, and +28.1 mV and 100 pS respectively for the SCl channel using asymmetric solutions. With symmetric solutions the SCl channel reversed at ~ 0 mV and its slope conductance was 105 pS.

incorporation with SR vesicle preparations which had been solubilised using CHAPS. The open probability of this channel showed a voltage dependence being most active at potentials ~ ±40mV. These properties are similar to those reported for the mitochondrial voltage-dependent anion channel (VDAC) (Tedeschi *et al.*, 1987; Colombini, 1987). However, addition of anti-VDAC antibodies to the *cis* or *trans* chamber (n = 2) had no affect on activity.

Discussion

3.8 *Characterisation of the RyR*

The incorporation of B4 SR vesicles into lipid bilayers with a CsCl buffer produced RyR channel activity and several types of Cl^- channel activity. RyR channels were easily identifiable by their characteristic permeation properties and their sensitivity to well known RyR channel modulators. In symmetric 250 mM Cs^+ the channel had a linear I-V relationship and a conductance of ~ 500 pS which is similar to published values of between 480 - 600 pS. The RyR channel displayed typical sensitivity to *cis* $[Ca^{2+}]$, adenine nucleotides, Mg^{2+}, ryanodine and ruthenium red. These observations suggest that the RyR channel studied here was functionally the same as that described in a number of earlier studies. In addition the results confirm the reports of Fruen *et al.* (1994) and Wang and Best (1992) that RyR channel activity is stimulated by HPO_4^{2-} and non-specific acid phosphatase respectively.

3.9 *Trans $[Ca^{2+}]$ modifies Cs^+ conductance*

When bilayer solutions contained asymmetric 250/50 mM *cis/trans* the Cs^+ conductance was sensitive to *trans* $[Ca^{2+}]$. Millimolar *trans* Ca^{2+} produced a non-linear I-V relationship and reduced gCs^+ in a voltage-dependent manner. Conductance was little affected at large positive potentials but fell in a hyperbolic fashion with more negative potentials. In contrast, the I-V relationship was made linear and the conductance was restored to ~ 500 pS when *trans* Ca^{2+} was reduced to micromolar concentrations. These effects can explained by a competitive interaction between Ca^{2+} and Cs^+ for permeation through the ion channel pore. The channel is selective for Ca^{2+} over Cs^+ and consequently Ca^{2+} will tend to displace Cs^+ as the permeant ion and reduce gCs^+ (Tinker *et al.*, 1992a; Smith *et al.*, 1988) The reduction in gCs^+ was voltage dependent because Ca^{2+} competes with Cs^+ more effectively at negative potentials ie. when current is flowing from the lower $[Cs^+]$ *trans* (50 mM Cs^+) to *cis* (250 mM Cs^+).

3.10 *Non-stationary and variable activity of RyRs*

RyR channel activity showed significant temporal variation. Typically a burst of channel openings would be separated by closed periods of variable duration. This variability showed up as oscillations in P_o plotted against time . The cause of this variability is unknown but non-stationary kinetics and mode-shifting behaviour have been previously documented in RyRs (Smith *et al.*, 1986; Ashley and Williams, 1990; Zahradnikova and Palade, 1993). Large variations in activity were apparent between different channels as evidenced by the standard errors in the P_o versus Ca^{2+} curves. The sensitivities of RyRs to both Ca^{2+} activation and inhibition are reported to vary widely (Laver *et al.*, 1995). Variations between channels may arise because (i) RyRs have different oxidation or phosphorylation states (Witcher *et al.*, 1991; Herrmann-Frank and Varsanyi, 1993; Abramson *et al.*, 1988); (ii) associated proteins eg. calmodulin, triadin, calsequestrin, FK506 etc. (Kim *et al.*, 1990; Seiler *et al.*, 1984; Guo and Campbell, 1995; Jayaraman *et al.*, 1992) may be removed from some RyRs; (iii) RyRs are partially degraded by endogenous calpain II (Rardon *et al.*, 1990); (iv) RyRs have different voltage sensitivities. For example channel activity has been reported to decline rapidly in a fraction of skeletal RyRs at large potentials (Ma, 1995; Ma *et al.*, 1995) and more slowly in cardiac RyRs at +40 mV (Laver *et al.* 1995). Such variability in the voltage sensitivity may be due to other mentioned variables above.

3.11 *Analysis of channel open probability*

The non-stationary channel activity of RyRs suggested that long sections of data would be necessary (at least 90 s) to accurately measure P_o. However, the Ca^{2+} dependence of P_o was similar when P_o was calculated from within bursts or from continuous sections of activity. Both analyses produced bell-shaped curves with a maximal P_o of ~ 0.5 and ~ 0.15 from analysis of burst and continuous activity respectively. Values for K_A were ~ 1 μM from both types of analysis but K_I from continuous analysis was somewhat lower (75 μM) than that measured from analysis within bursts (400 μM). The difference probably reflected the smaller sample population in continuous activity group and greater variability introduced by long closed times. An advantage of measuring P_o from within bursts is that it is far easier to sample a large population of

channels, because you are not limited to selected bilayers with long lifetimes. However, a disadvantage of limiting P_o analysis to within bursts is that it ignores factors such as long closed times and burst frequency, which are clearly important in terms of total channel activity. Moreover drugs which modulate RyR activty may primarily alter closed times. Consequently P_o analysis in subsequent chapters was measured from continuous segments of data.

3.12 *Subconductance states*

A notable feature of RyR channel activity was the appearance of subconductance states which were prominent in 20% of channels. It is possible that subconductance states represented the activity of another smaller conductance channel in the bilayer. This was unlikely because a summation of open levels was never observed and the frequencies of transitions between the substate and maximum open level occurred too frequently to support the involvement of independent channels. Moreover, substates had the same permeation properties as the maximum open level ie. the same reversal potential and voltage-dependent conductance. While there was some variability in substate amplitude the most frequently occurring levels had fractional conductances of ~ 0.25, 0.45 and 0.75. A similar substate pattern has been observed in a number of studies particularly with detergent solubilised RyRs but also in native RyR channels (see *Table 1-1*). The existence of four main open levels (three substates and a maximum open level) and the known tetrameric structure of the RyR have led to the hypothesis that the channel may be composed of four coupled, ion conducting pathways (Smith *et al.*, 1988, Liu *et al.*, 1989; Lai *et al.*, 1989). Coupling of the pathways would be necessary to explain how the channel normally opens to the maximum level. The results here are consistent with the hypothesis of coupled pathways but do not prove the hypothesis. The smallest substates (fractional conductances of ~ 0.15 - 0.25) were more frequent than other levels and events at those levels of longer duration. This might be expected if the open levels were due to the activity of four independent subunits each with a $P_o <$ ~ 0.2. However, the open level amplitudes do not follow the binomial distribution because in most channels the frequency of openings to the maximum level is too great.

3.13 *Ryanodine modification: evidence for altered Ca^{2+}/Cs^{+} selectivity*

Ryanodine treatment locked channels into a typical long-lived substate with a fractional conductance of ~ 0.5 (250/50 mM Cs^{+} 1/1 mM Ca^{2+} *cis/trans*, +40 mV). The ryanodine- modified channel was insensitive to Ca^{2+}-dependent activation or inhibition. Loss of Ca^{2+}-activation has been documented in ryanodine-treated channels (Rousseau *et al.*, 1987; Meissner and el-Hashem, 1992). Whereas removal of Ca^{2+}-inhibition by ryanodine has been observed in SR vesicles (Meissner, 1986) ~~but~~ it has not been previously described in single channels (this is reported in Laver *et al.*, 1995). An interesting finding was that ryanodine treatment modified the I-V relationship and voltage-dependent conductance apparent in mixed Cs^{+}/ Ca^{2+} solutions. A consequence of this was that the fractional conductance of the ryanodine-induced substate was dependent on the bilayer potential (although the magnitude of this voltage dependence was different in the two channels studied). One explanation for these effects is that ryanodine modifies Ca^{2+}/Cs^{+} permeability. As described above, the non-linear I-V relationship and the voltage dependence of conductance in 250/50 mM CsCl was due to the presence of millimolar *trans* Ca^{2+} which competes with and reduces Cs^{+} permeation through the channel. Therefore, it is possible that the linearisation of the I-V curve and a reduction in the voltage-dependence of conductance after ryanodine treatment, without removing Ca^{2+}, may have resulted from a change in Ca^{2+}/Cs^{+} selectivity. Ion selectivity changes following ryanodine modification have recently been reported (Tu *et al.*, 1994; Lindsay *et al.*, 1994). Tu *et al.* found that divalent/monovalent cation selectivity was reduced fourfold after ryanodine treatment and that this was due to an increase in monovalent and a decrease in divalent cation permeability. Lindsay *et al.* also reported decreased divalent/monovalent cation selectivity and increased ion binding affinities after ryanodine modification. It would be necessary to compare the effects of ryanodine in solutions with and without Ca^{2+}, to establish that a shift in the P_{Ca}/P_{Cs} is responsible for the conductance changes observed in ryanodine modified channels.

3.14 *The ryanodine modified conductance is distinct from naturally occurring substates*

The mechanism by which ryanodine increases channel P_o and reduces conductance is unknown. As described above one model of RyR structure is that it is composed of four ion conducting pores. Consequently, (Smith *et al.*, 1988) have proposed that ryanodine may induce a near 50% reduction in conductance by selectively blocking a number of these ion conduction pathways. However, the observation from one channel in the present study that an equal number of subconductance states were seen before and after ryanodine modification, albeit with a reduced conductance, strongly argues against this hypothesis. Instead, these results suggest that the substates observed in untreated RyRs are distinct from the ryanodine induced substate. Furthermore, if the RyR is composed of four conducting pores then ryanodine must uniformly reduce the conductance through each pore. Lindsay *et al.* (1994) have reported that ryanodine reduces the rate of ion translocation through the RyR by increasing the affinity of ion binding in the channel pore. In their study they found that ryanodine modification caused a greater increase in ion binding affinity for divalent compared with monovalent cations. Consequently the ryanodine substate had a fractional conductance of 0.6 - 0.65 with monovalent permeant cations but only 0.25 with divalent cations.

The dramatic changes in channel gating and conductance produced by ryanodine in RyRs is not a unique phenomenon. Similar effects are produced by a number of naturally occurring toxins in other types of ion channels. The alkaloids, batrachotoxin and veratridine, interact with voltage-sensitive Na^+ channels and produce an increased P_o and a reduced single channel conductance (Moczydlowski *et al.*, 1984; Garber and Miller, 1987). Peptides in dendrotoxin (a snake venom) induced subconductance events in maxi Ca^{2+}-activated K^+ channels (Lucchesi and Moczydlowski, 1991). The alterations in conductance induced by these toxins are likely to result from conformational changes in the channel proteins which alter ion translocation (Garber and Miller, 1987; Lucchesi and Moczydlowski, 1991). The similarity of the actions of these toxins and ryanodine suggests a common mode of action. Possible mechanisms by which ryanodine reduces RyR conductance ~~is~~ are discussed in more detail in Chapter 5 (sections 5.20 & 5.21).

Chapter 4.

Modulation of RyR channel activity by FK506 and rapamycin

4.1 Introduction

A regulatory action of FKBP12 on RyRs was first described by Timerman *et al.* (1993) who showed that Ca^{2+} uptake was decreased and caffeine-induced Ca^{2+} release enhanced in SR vesicles stripped of FKBP12. Mayrleitner *et al.* (1994) subsequently showed that the P_o of RyRs stripped of FKBP12 was greater than that of native RyRs over the Ca^{2+} range 70 nM to 1 μM and that addition of FK506 to a bilayer activated a RyR when *cis* Ca^{2+} was 55 nM. Preliminary findings of the present study showed that FK506 activated RyRs with *cis* Ca^{2+} between 0.1 μM and 1 mM (Ahern *et al.*, 1994). The effects of FK506 treatment on RyR channel activity are presented here in further detail. FK506 may regulate RyR channel activity in a number of ways. FK506 inhibits FKBP12 rotamase activity (Harding *et al.*, 1989) and dissociates FKBP12 from the RyR (Timerman *et al.*, 1993). Either of these mechanism could influence RyR activity. The FK506/FKBP12 complex inhibits the serine/threonine phosphatase, calcineurin (Liu *et al.*, 1991), which is anchored to the RyR by FKBP12 (Cameron *et al.*, 1995b) and may be an endogenous regulator of RyR activity. Phosphorylation of the skeletal muscle RyR at serine-2843 activates the calcium channel (Herrmann-Frank and Varsanyi, 1993). Therefore an inhibition of calcineurin by FK506 may enhance channel phosphorylation and activity. To investigate this possibility the single channel effects of the immunosuppressant rapamycin was tested. Rapamycin is an analogue of FK506 with similar interactions with FKBP12, except that the rapamycin-FKBP12 complex does not inhibit calcineurin (Liu *et al.*, 1991).

Results

4.2 *FK506 activates RyRs and induces submaximal conductances*

FK506 (0.75 to 40 μM) activated and modulated RyR gating. An example of these two distinct changes in RyR activity is shown in *Fig. 4-1*. (*A*) shows representative bursts of channel activity while (*B*) shows a plot of P_o averaged for each 30 s period of the experiment. Note that P_o is expressed as sqrt (P_o) for a better display of the data. Under control conditions, with 0.1 μM *cis* Ca^{2+}, channel activity was low (mean P_o = 0.0005) but increased 3 min after addition of 10 μM FK506 to the *cis* chamber (mean P_o = 0.023). Channel activity in the presence of FK506 consisted of bursts of openings to the maximum open state (*dashed line*) and to submaximal levels (*arrows*). When ryanodine was added to the *cis* chamber activity was reduced for 30 min at which stage the channel abruptly entered into a long-lived reduced conductance state ("Ry") that is characteristic of the ryanodine poisoned channel. The 30 min delay before the onset of ryanodine modified gating was atypical (see below). Submaximal currents were still observed in the ryanodine modified channel.

FK506 increased RyR channel activity in 30 of 33 bilayers (P_o changes for single channels are summarised in section 4.10). The maximal channel conductance was not affected by FK506 (249 ± 9 pS for control, 250 ± 9 pS after FK506, n = 13) but subconductance activity became prominent in all treated channels. Substate activity typically consisted of long sojourns at levels between 20 - 50% the maximal conductance, accompanied by shorter openings to higher current levels. A particularly good example is shown in *Fig. 4-2*. In this experiment control channel activity with 1 mM *cis* Ca^{2+} consisted of frequent transitions between open (O) and closed (C). Within 30 s of addition of 20 μM FK506 to the *cis* chamber, gating was radically altered and P_o increased from 0.04 to 0.37 with long-lived openings pre-dominantly to a level at 0.27 of the maximal conductance ("FK"). Subconductance levels were also seen at 0.15 and 0.54 as shown by the all points histogram. Addition of ryanodine (10 μM) inhibited activity for 150 s before onset of a characteristic ryanodine gating mode (amplitude= 7.7 pA, P_o = 0.99, T_o = 308 ms) However, a substate with a fractional conductance of 0.28, corresponding to level "FK", was still apparent in the ryanodine modified channel.

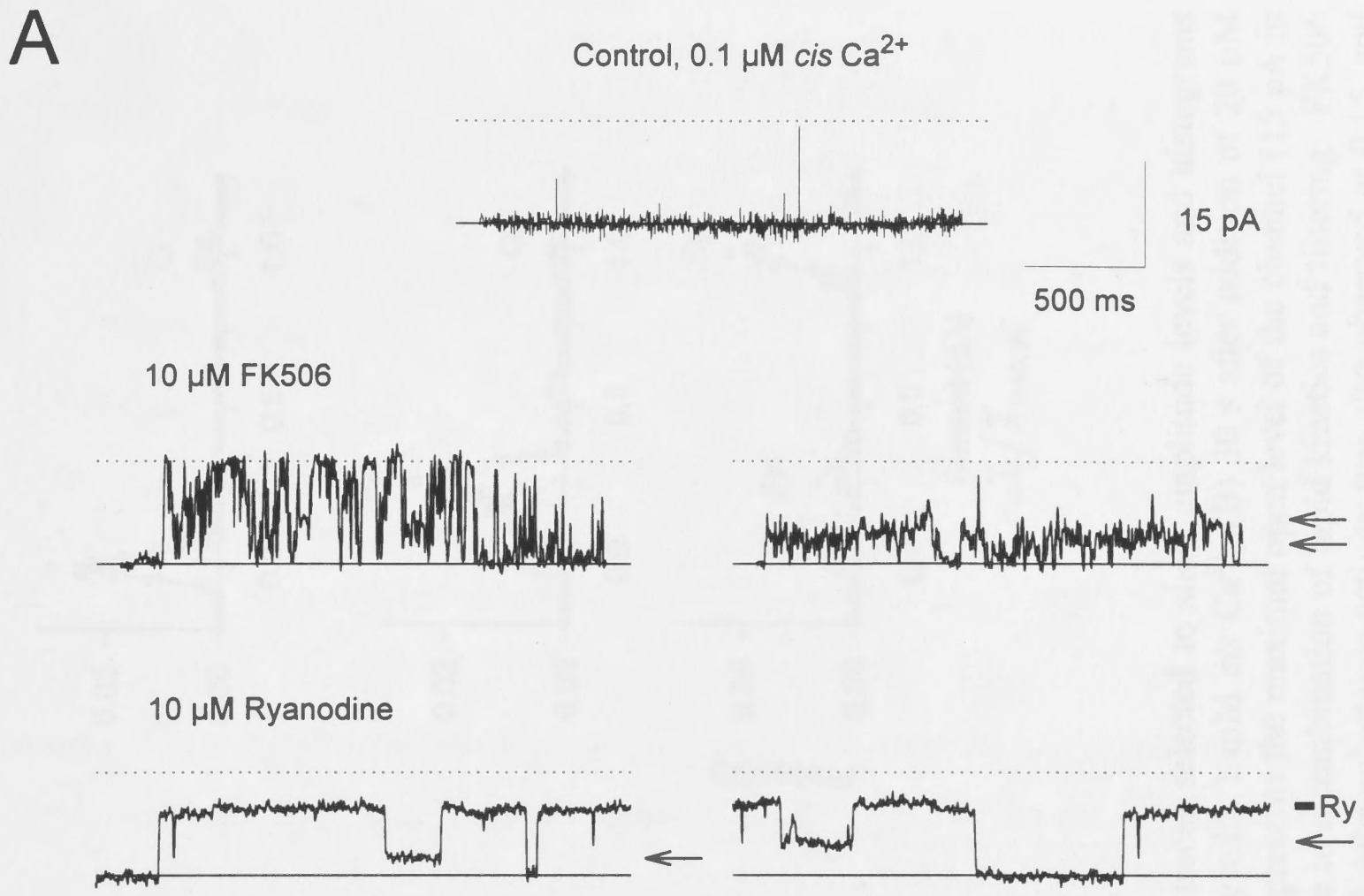

Fig. 4-1. FK506 activates and alters conducting states of the RyR channel. (A) Representative bursts of channel activity with 0.1 μM cis Ca^{2+} (*top*), 6 min after addition of 10 μM FK506 to the cis chamber (*middle*) and 30 min after addition of 10 μM ryanodine to the cis chamber (*bottom*). Arrows indicate substate levels. (B) Continuous plot of P_o averaged for each 30 s period for the experiment in (A). Solid bars are the mean P_o values for the separate conditions. Note the sqrt P_o scale used for better illustration of data.

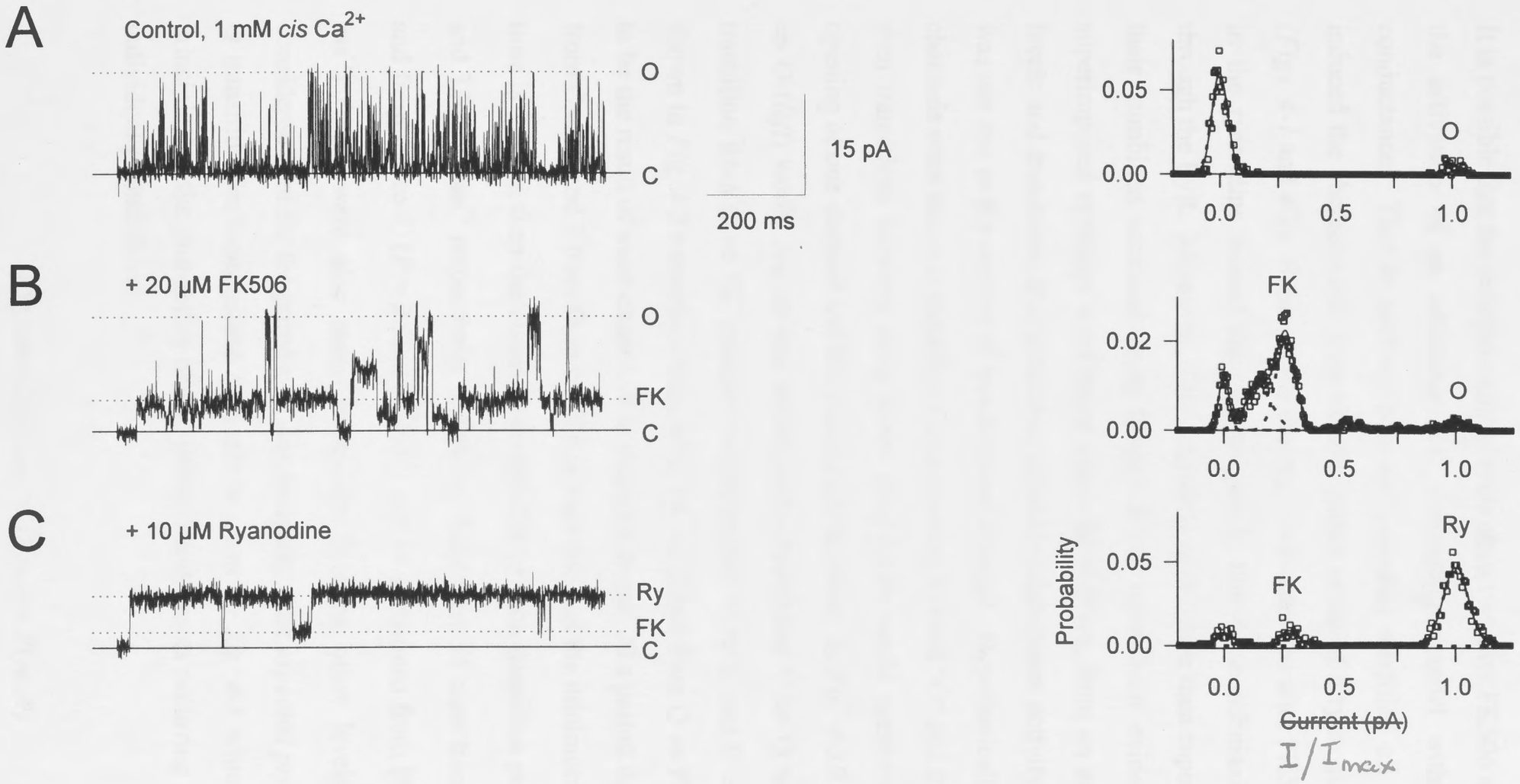

Fig. 4-2. Example of subconductance states in a FK506 treated RyR channel. Current traces selected to show amplitude levels and histograms constructed from mean-variance analysis of 1-2 s of data for (A) control channel activity with 1 mM *cis* Ca^{2+}, (B) 30 s after addition of 20 μM FK506 to the cis chamber and (C) 150 s after addition of 10 μM ryanodine. Level "O" represents the maximal open level of the channel (15 pA in (A), 17.2 pA in (B)). Note that the maximum open level in (A) was not fully resolved due to a combination of rapid kinetics and filtering. FK506 produced a prominent substate at 0.27 of the maximum conductance ("FK"), but marked subconductance activity was also observed at 0.15, and 0.54. After ryanodine treatment the maximal open level was reduced to 7.7 pA (45% of pre-ryanodine maximum) but the substate level ("FK") was still observed at 0.28 (see text).

4.3 *Submaximal conductance levels produced by FK506 are substates of the RyR*

It is possible that the reduced current levels observed after FK506 addition resulted from the activation of an additional Cs^+ conducting channel with a different unitary conductance. This is unlikely because ryanodine modified all channel activity and induced the characteristic slow kinetic, gating mode of a ryanodine poisoned channel. (*Figs. 4-1* and *4-2*). Submaximal current levels observed after FK506 addition remained in the ryanodine treated channel suggesting that these submaximal currents flowed through the RyR. Moreover, if two channels were active then superimposed openings to their combined maximal open levels should have been evident. However, such superimposed openings were never seen. In addition, from an analysis of the current levels and transitions it is clear that reduced conductance activity produced by FK506 was not due to the activity of an additional channel. Hypothetically, if two independent channels were active in the bilayer, one opening to level "O" and the other to level "FK" then transitions between these levels (*Fig.4-3B*) would necessitate the simultaneous opening of one channel and the closing of the other. In *Fig. 4-3B*, a transition from FK $\Rightarrow$ O (*left*) would require the simultaneous transitions C $\Rightarrow$ O and FK $\Rightarrow$ C, while a transition from O $\Rightarrow$ FK (*middle*) would require O $\Rightarrow$ C and C $\Rightarrow$ FK. In the bilayer shown in *Fig. 4-2* transitions from level FK $\Rightarrow$ O and from O $\Rightarrow$ FK were too numerous to be the result of mere chance. For example, in one 20 s period there were 8 transitions from C $\Rightarrow$ O and 7 from O $\Rightarrow$ C. If it is assumed that the minimum resolvable transition time is ~ 1 ms, then the observed probability of each transition per ms (P), was 4×10^{-4} and 3.5×10^{-4} ~~ms~~$^{-1}$ respectively. Likewise, there were 51 clear transitions from C $\Rightarrow$ FK and from FK $\Rightarrow$ C ($P = 2.55\times10^{-3}$ ~~ms~~$^{-1}$) and 34 transitions from FK $\Rightarrow$ O ($P = 1.7\times10^{-3}$ ~~ms~~$^{-1}$) (there were also many transitions between other levels, but these are not considered here for the purpose of this analysis). The *expected probability* of the FK $\Rightarrow$ O transition for independent channels is given by *Eq. 4-1* which simply restates the principle that the probability of two independent events occurring is the product of their individual probabilities:

$$\text{Expected } P_{(\text{FK} \Rightarrow \text{O})} = P(_{C \Rightarrow O}) \times P(_{FK \Rightarrow C}) \qquad (4\text{-}1)$$

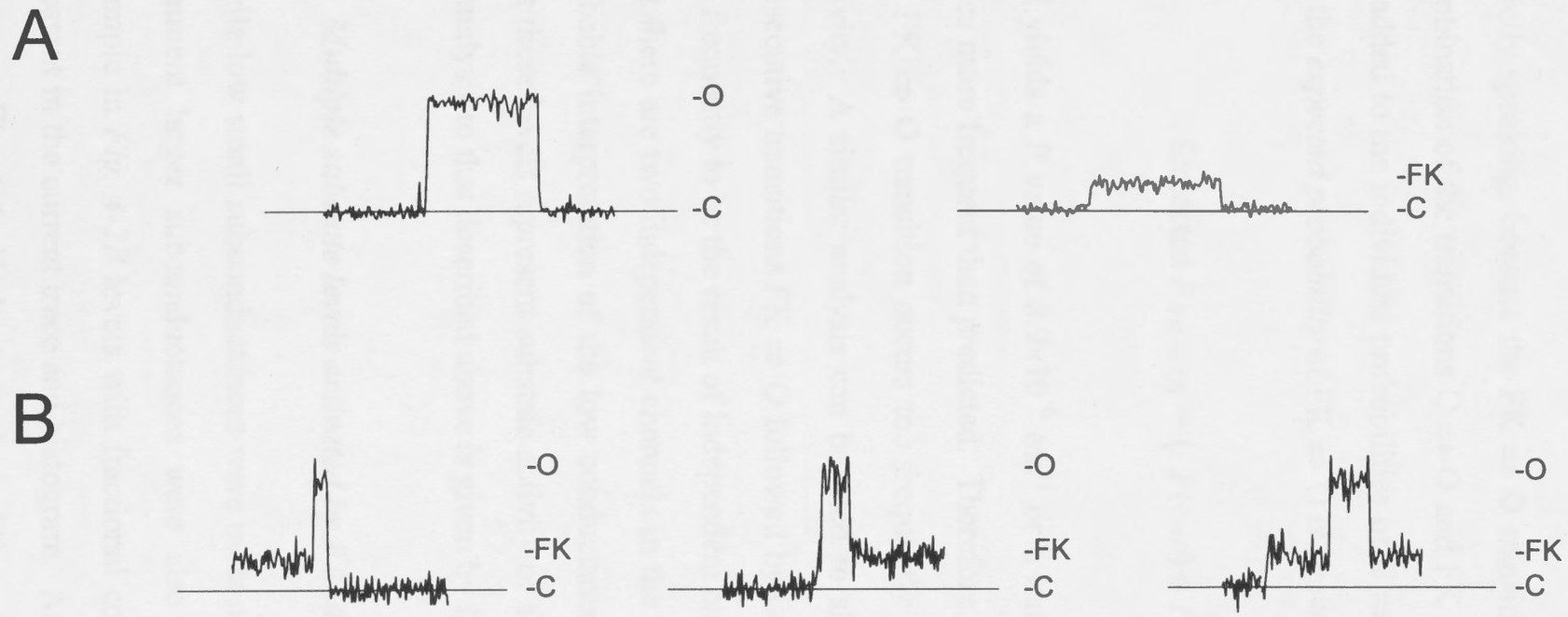

Fig. 4-3. Examples of current transitions between the fully open level (~16pA) the closed level and a FK506 activated substate. (A) An independent channel hypothesis with one channel opening to level "O" (*left*) and the other activated by FK506 opening to level "FK" (*right*). (B) Activity from the channel shown in *Fig. 4-2* showing transitions between level FK and O (*left*), O and FK (*middle*) and a sequential transition FK to O to FK (*right*). The frequency of the transitions is too ~~numerous~~ high to be caused by the simultaneous transitions of independent channels (see text).

ie. the probability of the first channel opening multiplied by the probability of the second channel closing. Solving this equation from the observed data above produces an *expected probability* for FK ⇒ O, of 1×10^{-6} ~~ms~~$^{-1}$, or one transition every 1000 s, whereas the transition actually occurred every 0.59 s; ~ 1700 times more frequently than predicted.

Strictly speaking, because the FK ⇒ O transition is assumed in this analysis to be the combination of the transitions C ⇒ O and FK ⇒ C, then the observed $P_{(FK \Rightarrow O)}$ should be added to the individual probabilities of C ⇒ O and FK ⇒ C. This revised equation for the *expected probability* of FK ⇒ O is shown in *Eq. 4-2*,

$$\text{Expected } P_{(FK \Rightarrow O)} = \left(P(C \Rightarrow O) + P(FK \Rightarrow O) \right) \times \left(P(FK \Rightarrow C) + P(FK \Rightarrow O) \right) \quad (4\text{-}2)$$

and yields a *P* value of 8.9×10^{-6} ~~ms~~$^{-1}$ or a transition every 112 s, which is still ~ 190 times more frequent than predicted. Therefore, by either form of analysis it is clear that the FK ⇒ O transition occurs too frequently to be the result of independent channel activity. A similar analysis can be used to show that transitions from O ⇒ FK and consecutive transitions FK ⇒ O followed by O ⇒ FK (*Fig. 4-3B*, *right trace*) occur far too frequently to be the result of independent channel activity. Therefore, the hypothesis that there are two independent channels in the bilayer is extremely unlikely. The more probable interpretation of the low conductance levels seen after FK506 application is that these levels represent substate activity of a single channel. Note that a similar type of analysis to that described above is given by Jahr and Stevens (1987).

4.4 *Multiple substate levels activated by FK506*

While low small subconductances were most prominent in channel records after FK506 treatment larger subconductances were also observed, albeit less frequently. For example in *Fig. 4-2B* levels with fractional conductances of 0.54 and ~ 0.75 - 0.8 are apparent in the current trace and histogram. An example of multiple substate activity is shown in *Fig. 4-4*. Under control conditions (*A*) the channel opened predominantly to

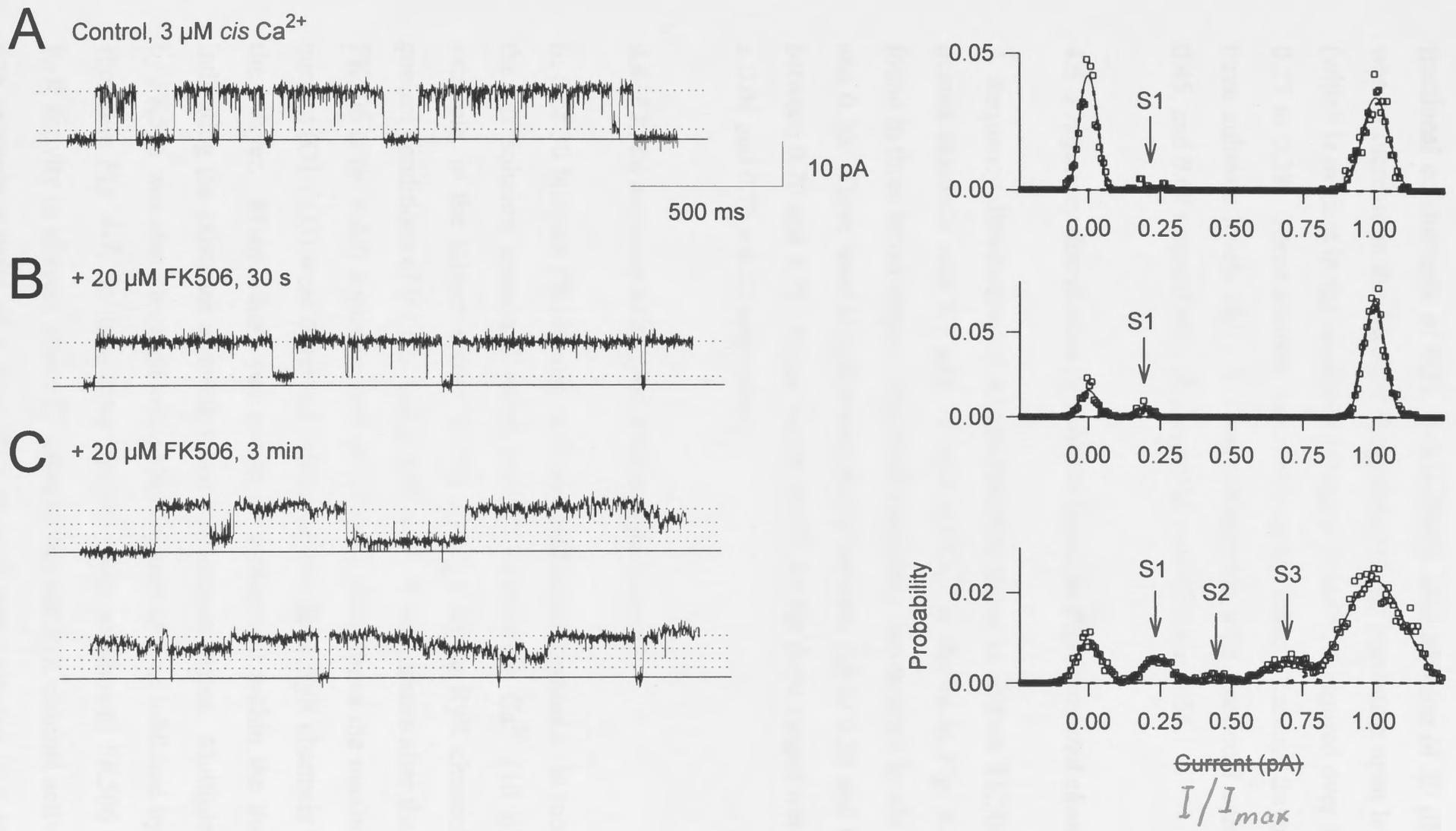

Fig. 4-4. Multiple subconductance states in a FK506 treated RyR channel. Representative channel activity recorded at +30 mV and histograms constructed from mean-variance analysis of 4 - 5 s of data. (A) Control channel activity (opening upwards) with 3 μM cis Ca^{2+} shows transitions from the closed to the fully open level and an occasional subconductance state (S1) with a fractional conductance of 0.21. (B) Actvity from the same channel 30 s after the addition of 20 μM FK506 to the cis chamber. FK506 stabilised openings at the fully open level and the S1 level (fractional conductance = 0.19). (C) After 3 min, several substate levels (S1-S3) were apparent with fractional conductances of 0.23, 0.45, and 0.68 respectively. Note that dotted lines represent open levels obtained by gaussian fits to the peaks in the histogram.

the maximal open level but occasional substates were observed at level S1 which had a fractional conductance of 0.21. Immediately after addition of 20 μM FK506 (*B*) there was an increase in the duration of openings to the maximum open level and to level S1 (which is evident in the amplitude histogram) and P_o measured over 30 s increased from 0.27 to 0.38. Three minutes later the channel current became fragmented and at least three substate levels (S1 - S3) were detectable with fractional conductances of 0.23, 0.45, and 0.68 respectively. P_o measured over 45 s was 0.56.

4.5 *Frequency distribution of substate levels in FK506 treated channels*

A frequency distribution of subconductance states in sixteen FK506 (0.75 to 40 μM) treated channels with 0.1 μM - 1 mM cis Ca^{2+} is shown in *Fig. 4-5*. Substates were found in three broad ranges. The most frequently encountered levels were between 0.18 and 0.30. There were also frequent levels between 0.4 to 0.55 and less frequent levels between 0.70 and 0.75. Mean values (±SD) for the three ranges were 0.25 ± 0.06, 0.49 ± 0.06 and 0.73 ± 0.03 respectively.

4.6 *FK506 activates additional channels in bilayer*

In 6 of 30 bilayers FK506 also activated additional channels. In most of these bilayers the *cis* solution contained either maximal activating Ca^{2+} (10 μM) or ATP. For example, in the bilayer shown in Fig. *4-6A*, a single RyR channel was active under control conditions of 0.1 μM and 2 mM ATP. Two minutes after the addition of 20 μM FK506 (*Fig. 4-6B*) superimposed openings to three times the maximum single channel current (O1 - O3) were observed indicating that three RyR channels were now active in the bilayer. Many other open levels were observed within the three maximal levels indicating the existence of multiple subconductance states. Multiple channel activation by FK506 was also observed when channel activity was inhibited by low pH (n = 2) as shown in *Fig. 4-7*. In three other bilayers (data not shown) FK506 was able to initiate RyR activity in bilayers where Cl^- channel but not RyR channel activity was evident. In one example activity of a large BCl channel was recorded in a bilayer for 30 mins. Addition of FK506 to the *cis* chamber of the bilayer activated a RyR channel within 30 seconds, even though several perfusions of the *cis* chamber had removed all remaining

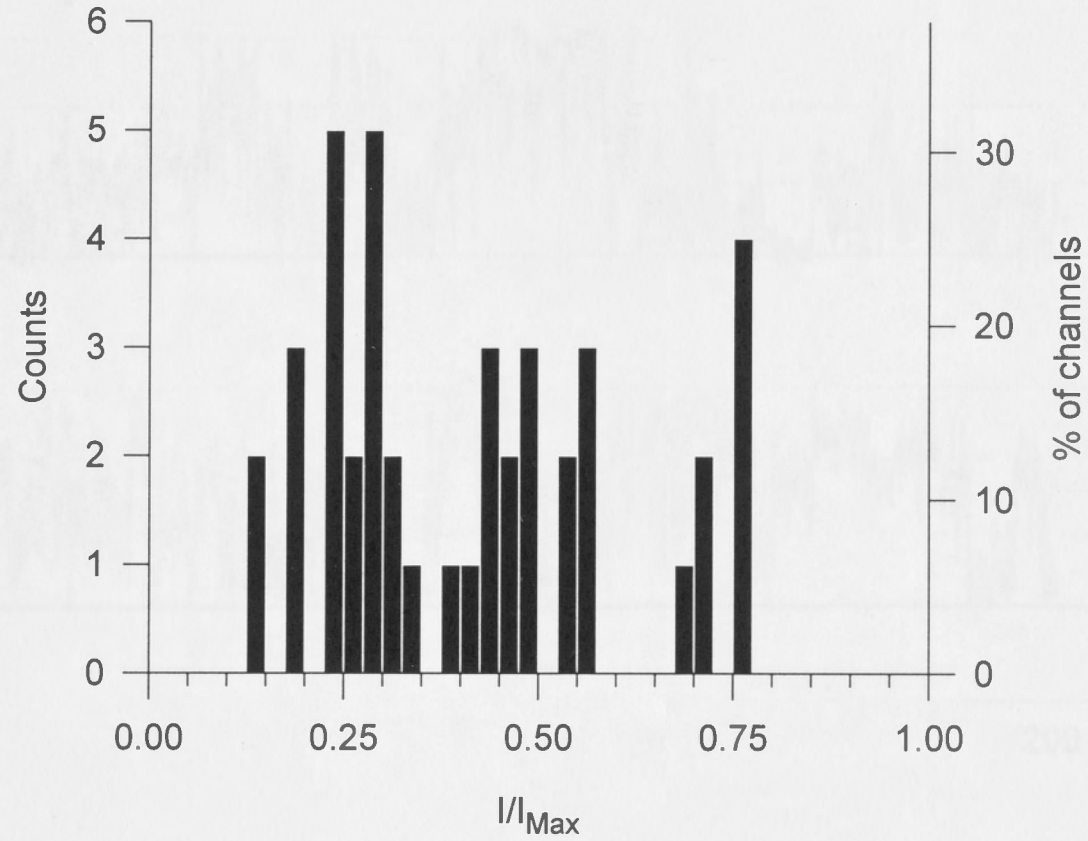

Fig. 4-5. Frequency distribution of subconductance levels in FK506 treated RyR channels. Values were obtained from 16 channels (with a bilayer potential of +40 mV), expressed as a fraction of the maximum conductance and binned in 0.025 intervals. Three broad peaks were obtained with mean values (± SD) of 0.25 ± 0.06, 0.49 ± 0.06 and 0.73 ± 0.03.

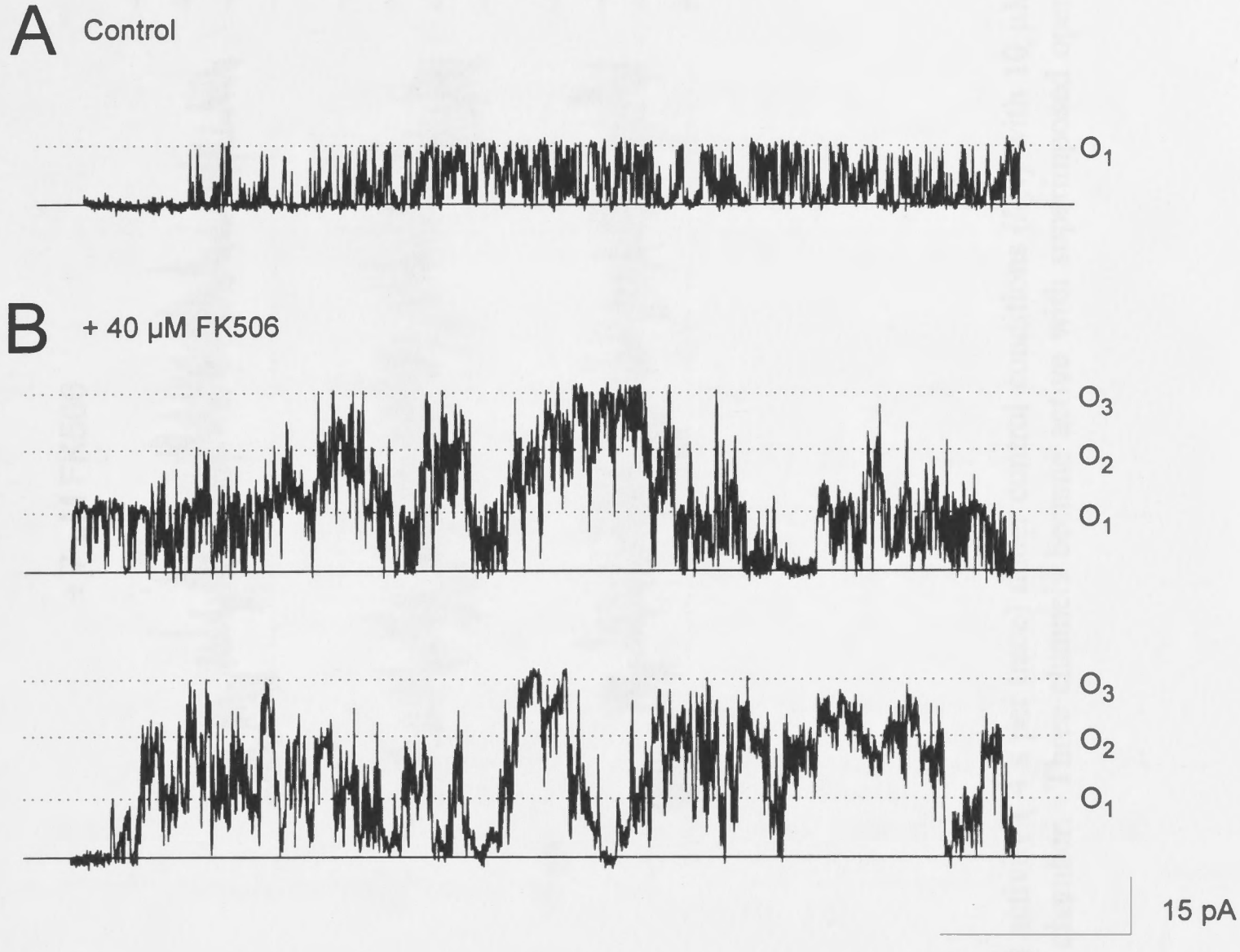

Fig. 4-6. FK506 activates multiple RyR channels. (A) Activity of a single RyR channel opening to level O_1 with 0.1 μM Ca^{2+}/2 mM ATP. (B) Activity from the same bilayer after addition of 40 μM FK506 to the *cis* chamber. Superimposed openings of three RyR channels (O_1-O_3 at ~ 15.5, 32 and 47 pA) are evident as well as multiple subconductance states. I' (measured over periods of 20 s) increased from 3.6 pA to 8.3 pA.

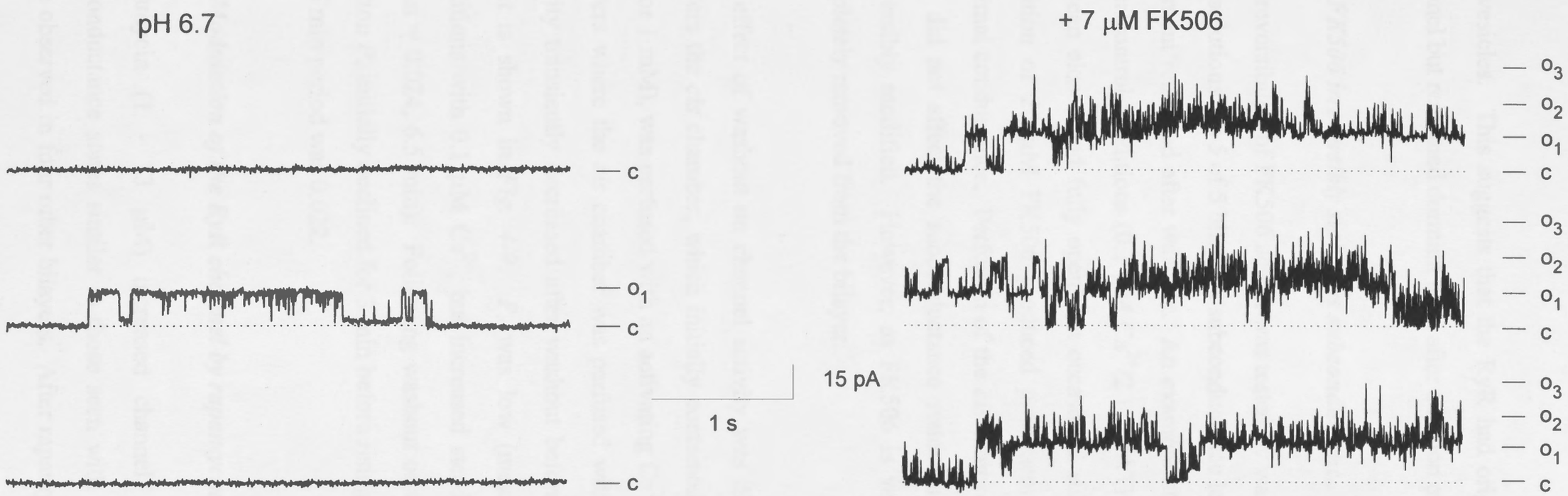

Fig. 4-7. FK506 activates RyR channels at low pH. Representative channel activity (4 s per trace) under control conditions (*left*) with 10 μM *cis* Ca^{2+} and pH 6.7 and (*right*) 30 s after addition of 7 μM FK506 to the *cis* chamber. Three channels became active with superimposed openings between levels O_1 - O_3.

SR vesicles. This suggests that the RyR had originally co-incorporated with the Cl^- channel but remained dormant until after addition of FK506.

4.7 *FK506 irreversibly stabilises subconductance states*

The reversibility of FK506 action was tested by washing out the *cis* chamber with drug-free solutions. In 5 of 5 bilayers, subconductance levels that were stabilised with FK506 treatment remained after washout. An example of this is shown in *Fig. 4-8*. Activity under control conditions (0.1 μM Ca^{2+}/2 mM ATP *cis*) consisted mainly of transitions between closed and fully open, but occasional substates were also observed (*arrow*). Addition of 20 μM FK506 produced prominent substates at ~ 0.25 and 0.45 the maximal conductance. Perfusion of the *cis* chamber with a solution containing 10 μM Ca^{2+} did not affect the subconductance states suggesting that the channel had been irreversibly modified. However, as FK506 is very lipophilic it may not have been completely removed from the bilayer.

The effect of washout on channel activity was difficult to interpret because in three bilayers the *cis* chamber, which initially contained a non-activating Ca^{2+} solution (0.1 μM or 1 mM), was perfused with an activating Ca^{2+} solution (10 μM Ca^{2+}). In the two bilayers where the *cis* chamber was perfused with the same control solution channel activity transiently decreased after washout before rising again. An example of this effect is shown in *Fig. 4-9*. P_o was low (mean = 0.001, 2.5 min) under control conditions with 0.1 μM Ca^{2+}, but increased steadily after addition of 10 μM FK506 (mean = 0.024, 6.5 min). Following washout of the *cis* chamber with a 0.1 μM Ca^{2+} solution P_o initially declined for 3 min before rising again. The mean P_o calculated over the 5 min period was 0.022.

4.8 *Modulation of the RyR channel by rapamycin*

Rapamycin (1 - 13 μM) increased channel P_o and I' and produced marked subconductance states similar to those seen with FK506 (*Fig. 4-10*). Similar results were observed in four other bilayers. After rapamycin treatment I' increased from 1.93

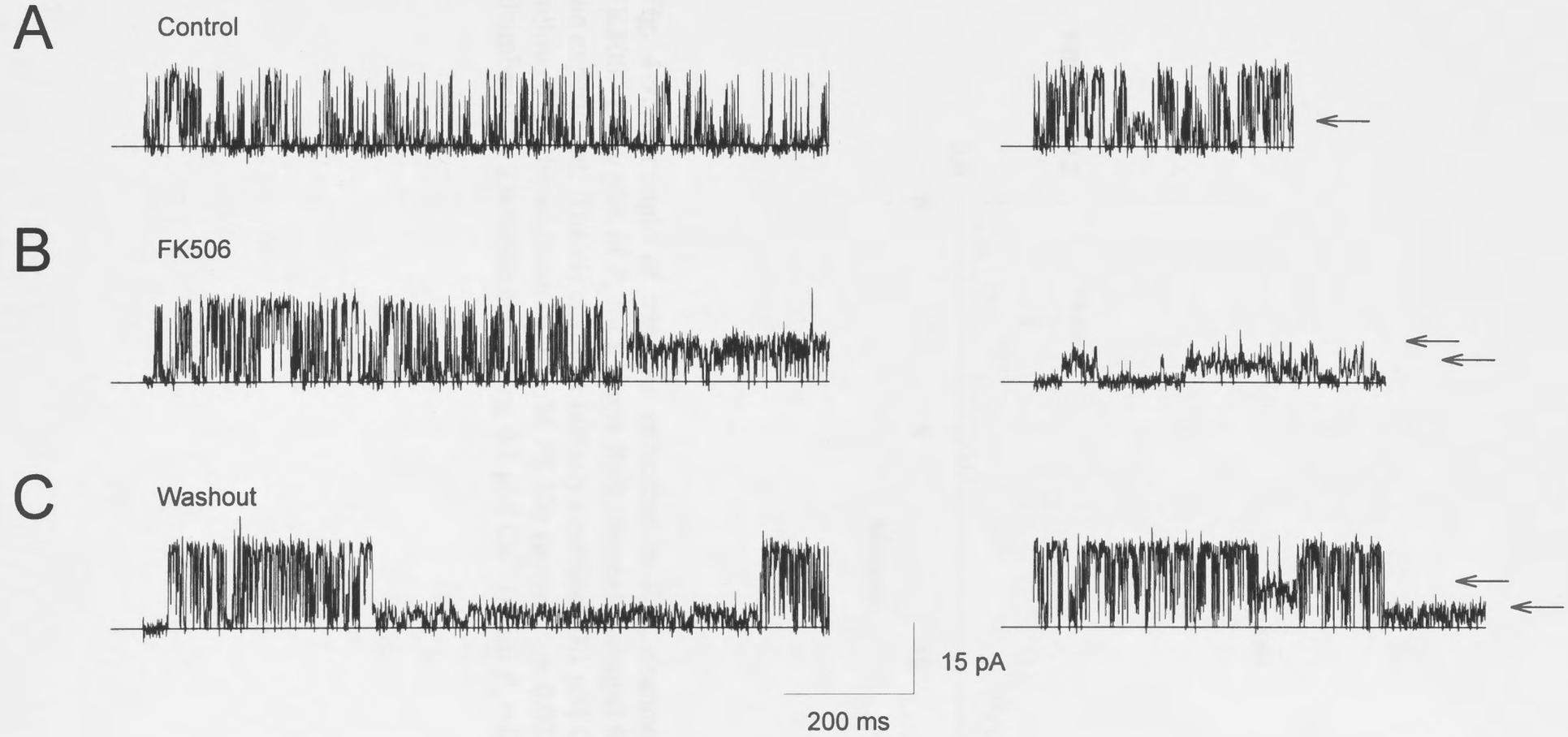

Fig. 4-8. FK506 irreversibly stabilises subconductance states in a RyR channel. (A) Example of channel activity from a single RyR with 0.1 μM Ca^{2+} and 2 mM ATP *cis*, showing transitions mainly between the closed (*solid line*) and fully open level, and occasional subconductance state (*arrow*) at ~ 0.4 - 0.45 of the maximum conductance. (B) Activity from the same channel after addition of 20 μM FK506 to the *cis* chamber showing prominent subconductance states at ~ 0.25 and 0.45 of the maximal conductance (*arrows*). (C) Washing out the *cis* chamber with a drug-free solution containing 10 μM Ca^{2+} did not eliminate the subconductance states.

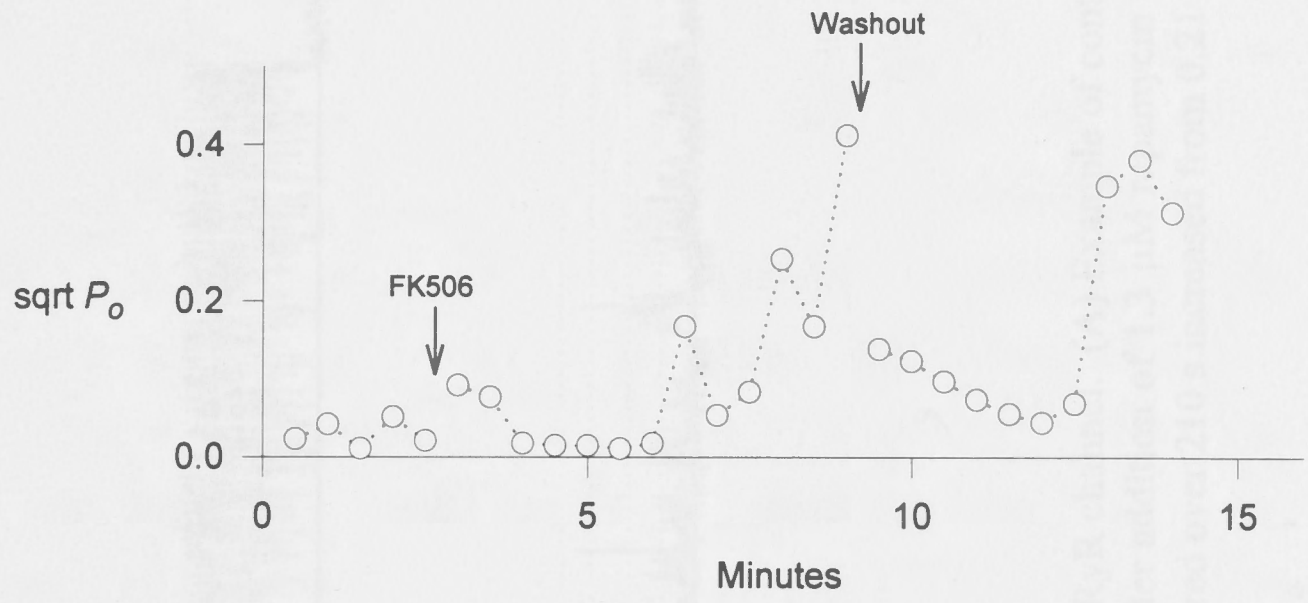

Fig. 4-9. Example of transient reduction in RyR channel P_o after washout of FK506. Diary plot of P_o for a single RyR channel averaged for each 30 s section of the experiment. The *cis* chamber initially contained 0.1 μM Ca^{2+} (mean P_o= 0.001), followed by the addition of 10 μM FK506 (mean P_o = 0.024) and washout of the chamber with a solution containing 0.1 μM Ca^{2+} (mean P_o = 0.022) (see text).

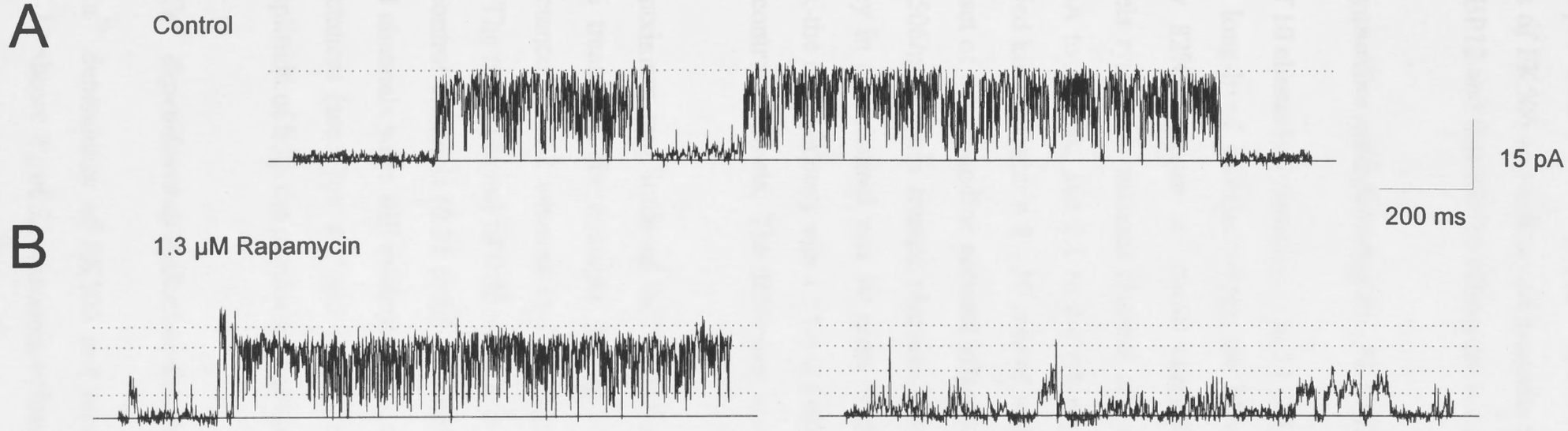

Fig. 4-10. Rapamycin activates and produces subconductance states in a native RyR channel. (A) Example of control channel activity with 10 μM *cis* Ca^{2+} (bilayer potential + 40 mV) and (B) activity from the same channel after addition of 1.3 μM rapamycin to the *cis* chamber. The dotted lines represent open levels drawn by eye at 4.9, 9.6, 14.9 and 19.2 pA. P_o measured over 210 s increased from 0.21 to 0.28.

± 0.52 pA to 5.34 ± 1.47 pA (n = 5, P<0.05, paired t-test). The similarity between the effects of FK506 and rapamycin suggests that both drugs act by disrupting the function of FKBP12 and that FK506 effects are not mediated through calcineurin.

4.9 *Ryanodine modulation of the FK506/rapamycin treated RyR channel*

In 8 of 10 channels, ryanodine (7 to 33 μM) locked the FK506 or rapamycin treated RyR into a long-lived substate within the bilayer lifetime (4 - 33 min), compared with a similar 82% response in control channels (*Fig. 4-11A*). In the other two treated channels ryanodine reduced channel activity (I' measured over 240 s, decreased from 3.01 pA to 1.2 pA, and 2.1 to 0.6 pA respectively) but did not induce the ryanodine-modified kinetics within 8 - 10 min of addition, when the bilayers broke. The delay in the onset of the ryanodine substate after ryanodine addition (latency) was more variable in FK506/rapamycin treated channels compared with control channels (*Fig. 4-11B*). Latency in one channel was 30 mins as shown in *Fig. 4-1*. Excluding that value (>> 2xSD), the mean latency was 1.51 ± 0.4 mins (n = 6) compared with 1.1 ± 0.4 mins (n = 8) for control channels. The difference was not significant (P = 0.53, two-sample t-test).

The maximum amplitude of the ryanodine substate tended to be more variable after FK506 treatment, for example in *Fig. 4-1* the ryanodine substate had a fractional conductance of 0.62 whereas in *Fig. 4-2* the substate had a fractional conductance of 0.45. The mean (±sem) of 0.55 ± 0.03 (n = 6) was not statistically different (P<0.198) from control channels (0.51 ± 0.01, n = 9). Interestingly, substates apparent in FK506 treated channels were still evident after ryanodine treatment and with similar fractional conductances (see *Figs. 4-1* and *4-2*) ie. ryanodine caused a proportional reduction in the amplitude of both the maximum open level and the substate levels.

4.10 *Ca^{2+} dependence of RyR channel activation by FK506 and rapamycin*

The Ca^{2+} dependence of FK506 and rapamycin channel activation was investigated. *Fig. 4-12* shows P_o of 23 channels before and after treatment with FK506 (0.75 - 20 μM) or rapamycin at [Ca^{2+}] ranging from 1 nM to 1 mM (without ATP). FK506 and rapamycin increased P_o at all Ca^{2+} concentrations. The differences were significant

A

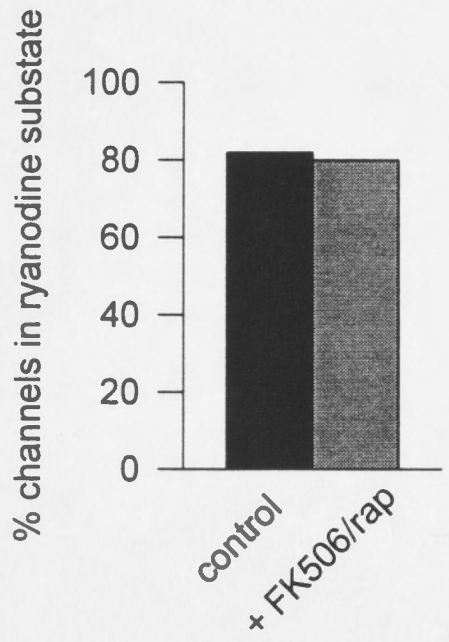

B

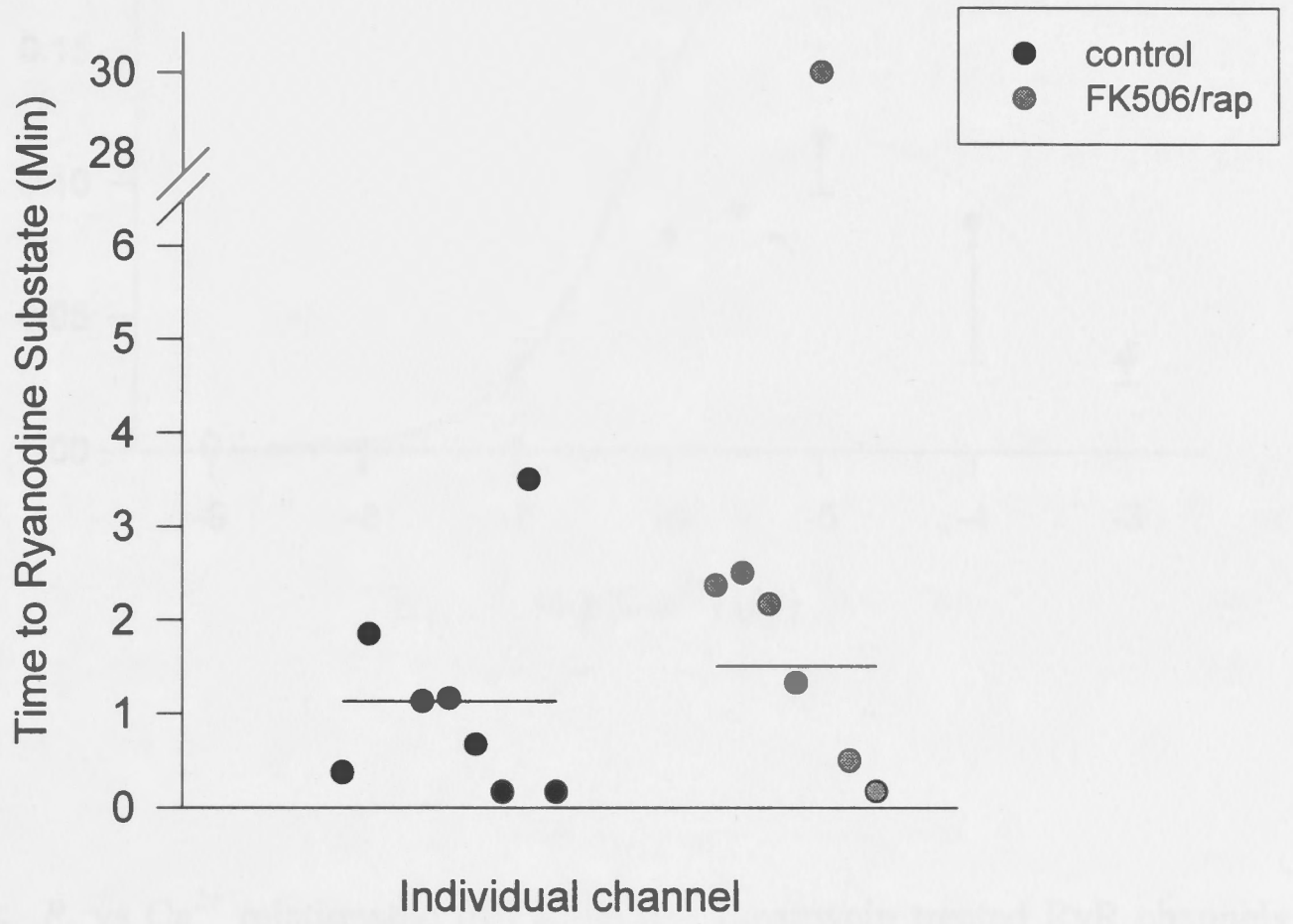

Fig. 4-11. Effects of ryanodine on channels treated with FK506 and rapamycin. (A) Percentage of control (*solid bar*) and FK506/rapamycin treated (*grey bar*) channels modified by ryanodine (1-20 μM) within the bilayer lifetime (4 - 33 min). (B) Latency of ryanodine substate in control (*filled circles*) and FK506/rapmycin treated (*grey circles*) channels. *Cis* Ca^{2+} was 1 μM - 1 mM.

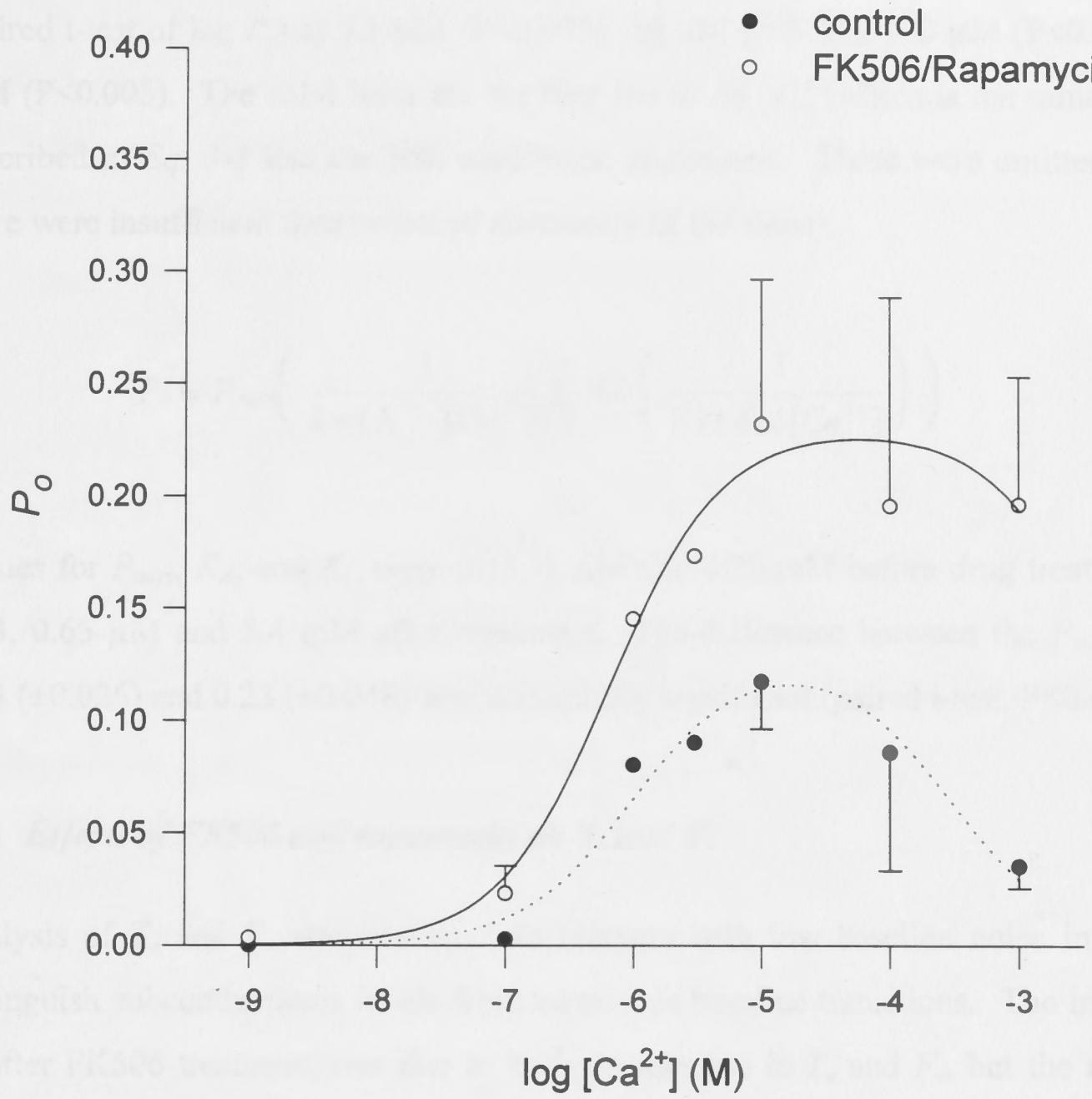

Fig. 4-12. P_o vs Ca^{2+} relationship of FK506 and rapamycin treated RyR channels. P_o (mean ± sem) of 24 channels before (*filled circles*) and after treatment with FK506 or rapamycin (*open circles*). Points without error bars are single observations. The drugs produced a significant increase (paired student's t-test of log P_o) at 0.1 μM ($P<0.005$), 10 μM ($P<0.05$), 100 μM ($P<0.05$) and 1 mM ($P<0.005$). Lines are the best fit to *Eq. 4-3*. Parameter values for P_{max}, K_A *and* K_I were 0.13, 1 μM and 0.29 mM respectively for control channels and 0.23, 0.65 μM and 5.4 mM respectively for drug treated channels (see text).

(paired t-test of log P_o) at 0.1 μM (P<0.005), 10 μM (P<0.05), 100 μM (P<0.05) and 1 mM (P<0.005). The solid lines are the best fits to *Eq. 4-3* (which is the same function described in *Eq. 3-1* less the Hill coefficient parameters. These were omitted because there were insufficient data points to accurately fit the slope).

$$P_o = P_{max}\left(\frac{1}{1+(K_A/[Ca^{2+}])}\right)\left(1-\left(\frac{1}{1+(K_I/[Ca^{2+}])}\right)\right) \qquad (4\text{-}3)$$

Values for P_{max}, K_A, and K_I were 0.13, 1 μM and 0.29 mM before drug treatment and 0.23, 0.65 μM and 5.4 mM after treatment. The difference between the P_{max} values, 0.13 (±0.026) and 0.23 (±0.048) was statistically significant (paired t-test, P<0.05).

4.11 *Effects of FK506 and rapamycin on T_o and F_o*

Analysis of T_o and F_o was restricted to bilayers with low baseline noise in order to distinguish subconductance levels from erroneous baseline transitions. The increase in P_o after FK506 treatment was due to both an increase in T_o and F_o, but the responses were Ca^{2+} dependent. In 3 of 3 channels with 1 mM *cis* Ca^{2+}, T_o increased from 1.50 ± 0.49 ms to 3.48 ± 0.70 (P<0.05, paired t-test of log values) and F_o increased from 23 ± 11 s^{-1} to 87 ± 23 s^{-1} (P<0.01). A similar response was seen in 4 of 4 channels with 0.1 μM Ca^{2+}. T_o increased from 0.83 ± 0.17 ms to 1.65 ± 0.31 ms (P<0.05) and F_o increased from 0.8 ± 0.2 s^{-1} to 10.8 ± 2.4 s^{-1} (P<0.01). With 10 μM *cis* Ca^{2+} there were variable responses. T_o increased in four channels from 5.83 ± 4.33 ms to 15.67 ± 12.4 ms (P<0.01) but decreased in two other channels from 38.66 ± 28.04 ms to 2.89 ± 0.49 ms (not significant) while F_o increased in four channels from 11.7 ± 6.5 s^{-1} to 61.7 ± 18.7 s^{-1} (P<0.05), but decreased in two others from 90.6 ± 48.4 s^{-1} to 43.4 ± 16.7 s^{-1} (not significant). The variability in the response was probably related to the highly variable channel kinetics prior to FK506 addition (see *Fig. 3-5* for an example of kinetic variability at 10 μM Ca^{2+}).

Similar Ca^{2+}-dependent changes in T_o and F_o were observed after rapamycin treatment in three channels. In one channel at 1 mM *cis* Ca^{2+} T_o and F_o increased from 1.02 to 2.10

ms, and 7.2 to 52 s^{-1} respectively. With 100 μM *cis* Ca^{2+} T_o decreased from 5.50 to 5.07 ms and F_o increased from 6.9 to 30 s^{-1}. While at 10 μM *cis* Ca^{2+} T_o increased from 1.54 to 3.74 ms but F_o decreased from 139 to 60 s^{-1}.

4.12 *Specificity of FK506/rapamycin action*

Several lines of evidence suggest that FK506 and rapamycin interacted directly and specifically with the RyR complex. Firstly, as described above, addition of ryanodine in the majority of cases eliminated all channel activity and locked the channel into the ryanodine substate mode. Secondly, FK506 and rapamycin did not induce channel activity when added to the bilayer alone (n = 5) , nor did they alter the activity of the large (BCl, n = 3) or small (SCl, n = 4) chloride channels. Lastly, addition of equivalent concentrations of the solvents used to dissolve the drugs, ethanol (0.33%, n = 2) or DMSO (0.066%, n = 4), had no effect on RyR channel activity.

Discussion

4.13 *FK506 modulates RyR activity and conductance levels*

The experiments in this chapter examined the effects of FK506 and rapamycin on the single channel properties of RyRs. FK506 produced a number of distinct effects. FK506 increased channel activity (P_o and I'), activated additional channels and induced prominent submaximal current levels. The increase in P_o was due to a rise in T_o and F_o. Mayrleitner *et al.* (1994) have previously reported that the open times of RyRs stripped of FKBP12 are enhanced by up to 6-fold. The submaximal current levels were most likely subconductance states of the RyR and not the activity of an independent channel because the frequency of transitions between substate and maximum open levels were higher than expected for independent channels. Moreover, substates persisted in ryanodine poisoned channels and their amplitudes were reduced by ryanodine in the same proportion as the maximal current.

A frequency distribution of subconductance states in FK506 treated channels showed that there were three main levels at 0.25, 0.49 and 0.73 of the maximal conductance. Similar subconductance levels have been observed in the RyR channel expressed without FKBP12 (Brillantes *et al.*, 1994). In contrast to that study, the subconductance states observed here did not occur with equal frequency. In most channels the S1 levels at ~0.15 - 0.25 were seen more frequently and these levels dominated substate activity within channels (see *Figs. 4-1, 4-2*, *4-4* and *4-8*). Recently, (Ma *et al.*, 1995) have also observed that small substate levels are very prominent when native RyR channels are treated with FK506. In the present study substate levels with fractional conductances of ~ 0.25, 0.45 were occasionally evident prior to FK506 treatment and were enhanced following addition of the drug (*Figs. 4-4*, *4-8*). The frequency distribution of substate levels in untreated channels (see *Fig. 3-11*) was similar to the distribution observed in FK506 treated channels. These observations support the idea that FK506 stabilised rather than induced subconductance activity.

4.14 *Mechanism of action of FK506*

The modulation of RyR channel activity by FK506 may have been mediated through FK506/FKBP12 inhibition of calcineurin, a serine/threonine phosphatase which is anchored to the RyR via FKBP12 (Cameron *et al.*, 1995b). To investigate whether calcineurin signalling was involved in activation by FK506, I investigated the actions of rapamycin, an FK506 analogue, which binds to FKBP12 but does not inhibit calcineurin. Like FK506, rapamycin increased single channel activity of RyRs, activated additional channels and stabilised multiple subconductance states. These results are consistent with the study by Brillantes *et al.* (1994) which showed that rapamycin produces subconductance states in RyRs and increases caffeine-induced tension responses in skeletal muscle.

The observation that rapamycin had the same effect as FK506 suggests that FK506 acted independently of calcineurin. However, while the rapamycin-FKBP12 complex does not directly inhibit calcineurin, rapamycin does induce dissociation of FKBP12 from the RyR, and thus would remove calcineurin from the RyR (Cameron *et al.*, 1995b). It is possible that there is a direct association between calcineurin and the RyR which is critical for a functional interaction between the two proteins. Consequently, it may not be correct to assume that rapamycin acts completely independently of calcineurin. On the other hand, in the bilayer, an involvement by calcineurin as a phosphatase is not supported by the fact that these experiments were undertaken in the absence of ATP and Mg^{2+} which are necessary to support phosphorylation processes. Two other pieces of evidence suggest FK506 and rapamycin acted specifically by dissociating FKBP12 or disrupting its rotamase activity. Firstly, the subconductance states induced by FK506 treatment were irreversible and could not be eliminated by washing the drug out of the bilayer. Such an irreversible action would be expected if FK506 and rapamycin acted via removal of FKBP12. Secondly, channel activity tended to increase with time in the presence of FK506. A progressive channel activation would be predicted if FK506 acted by binding to FKBP12 because the kinetics of this reaction are known to be temperature dependent and would proceed more slowly under bilayer conditions, (~ 25°C) than at 37°C (Timerman *et al.*, 1995). However, channel activity

was transiently reduced by washing out FK506 suggesting that a component of channel activation may be reversible and therefore independent of FKBP12.

4.15 *Ryanodine modification of FK506/rapamycin treated channels*

Ryanodine binding is known to be correlated with channel P_o so any agent which increases P_o should also stimulate ryanodine binding. Using this line of reasoning one would predict that FK506 and rapamycin should also stimulate ryanodine binding. However, as shown in *Fig. 4-11*, the latency of the ryanodine substate after ryanodine addition, a simple measure of ryanodine affinity in single channels, was not reduced after treatment with FK506 and rapamycin despite a substantial increase in P_o. In addition the fractional conductance of the ryanodine substate tended to be larger and more variable, in the presence of FK506 compared with untreated channels, although the differences were not significant. These results raise the possibility that FK506 or rapamycin treatment may modify the ryanodine affinity of the channel. Alternatively, the results may reflect intrinsic variability of the channel rather than effects of the drugs. Ma (1995) has shown recently that latency of the ryanodine substate is quite variable in single RyR channels ranging from 1 - 2 min up to 30 min. However, a complex interaction between FK506/rapamycin treatment and ryanodine binding is suggested by ^{3}H-ryanodine binding studies. FK506 increases maximum ryanodine binding, but decreases the average affinity in skeletal muscle (Mack *et al.*, 1994) while FK506 and rapamycin inhibit maximum binding in cardiac muscle (Kaftan *et al.*, 1995) and in liver respectively (Kraus-Friedmann and Feng, 1994). In summary, the single channel data presented here do not give a conclusive answer as to the effects of FK506/rapamycin treatment on ryanodine affinity.

4.16 *Ca^{2+} dependence of activation by FK506 and rapamycin*

FK506 and rapamycin increased RyR channel P_o over a 1 nM - 1 mM Ca^{2+} range . The P_o versus Ca^{2+} relationship was broader after FK506 treatment particularly at inhibiting $[Ca^{2+}]$ ($\geq$ 0.5 mM). The relaxation of Ca^{2+}-inhibition is consistent with previous studies which showed that the Mg^{2+} sensitivity of Ca^{2+} release is reduced in SR vesicles stripped of FKBP12 (Timerman *et al.*, 1993; Timerman *et al.*, 1995). Those results

suggested that FKBP12 also affected low affinity Ca^{2+} sensitivity because Ca^{2+} and Mg^{2+} are thought to share the same low affinity inhibition site on the RyR (see Meissner, 1994; Derek Laver, unpublished observations). Channel agonists, like ATP, which act independently of Ca^{2+} binding, increase P_o without altering the Ca^{2+} sensitivity of activation or inhibition (for example, Ma and Zhao, 1994). Therefore the observation here that FK506 increased maximal P_o and broadened the bell-shaped Ca^{2+} versus P_o relationship, suggests that FK506 action may have Ca^{2+}-dependent and independent components. A Ca^{2+}-independent action is also supported by the observation that FK506 activates channels inhibited by low pH, since low pH inhibits RyR P_o independently of Ca^{2+} (Ma and Zhao, 1994).

Previously it has been shown that the P_o of FKBP12-stripped RyR channels is elevated over the sub-activating Ca^{2+} range 70 nM to 1 μM but not at maximal activating, 10 μM Ca^{2+} (Mayrleitner *et al.*, 1994), suggesting that removal of FKBP12 selectively modifies the Ca^{2+} sensitivity of channel activation. There are two likely explanations which may account for ~~explain~~ the differences between the Mayrleitner study and the results reported here. Firstly, in contrast to the present study, Mayrleitner *et al.* used 2 mM ATP as a co-agonist. The maximum P_o in the presence of optimal 10 μM Ca^{2+} and millimolar ATP was ~ 0.8, so a further stimulation of RyR activity by removal of FKBP12 may have been prevented. Secondly, FK506 and rapamycin may have a direct stimulatory action on the RyR independent of FKBP12 (see Chapter 6). This would explain a difference between channels that have been pre-treated with FK506 as opposed to channels which are directly treated with the drug in the bilayer. A direct action of the drugs on the RyR is suggested by Lamb and Stephenson (1996), who observed that 1 μM FK506 and rapamycin caused a moderate (~ 20 - 30%), reversible increase in the contractile responses of skinned muscle fibres.

4.17 *Summary*

FK506 and rapamycin increased RyR channel P_o at 10^{-9} M - 10^{-3} M *cis* Ca^{2+}. FK506 increased T_o and F_o. Both drugs induced the appearance of prominent subconductance states, especially at ~ 0.25 the full conductance, and subconductances remained with

similar fractional conductances in channels subsequently modified by ryanodine. That FK506 and rapamycin had similar effects suggests that it is unlikely that inhibition of calcineurin is involved in the action of FK506. Rather the irreversible nature of the subconductance states suggests that both drugs acted by removing FKBP12, although a direct action of the drugs on the RyR protein cannot be ruled out.

Chapter 5.

RyR channels stripped of FKBP12

5.1 Introduction

FK506/rapamycin treatment of RyRs in the bilayer increased channel activity and stabilised subconductance levels (Chapter 4). The actions of FK506/rapamycin may be due to dissociation of FKBP12 from the RyR and hence a loss of a channel regulatory function of FKBP12. However, dissociation of FKBP12 occurs slowly at room temperature (see below) and is likely to be incomplete within the limited lifespan of bilayers (80% bilayers <10 min). Therefore it is not clear whether the effects observed in the bilayer are due to FKBP12 dissociation and/or a direct effect of FK506/rapamycin on the RyR protein. To address this question a different approach was used. TC vesicles were pre-treated with FK506/rapamycin to remove FKBP12 prior to vesicle incorporation into bilayers and the amount of FKBP12 remaining was estimated by densitometric analysis of Western blots. The advantage of this approach was that it avoided possible direct effects of the drugs on the RyR, since FK506/rapamycin was washed out after the incubation period prior to vesicle incorporation. In addition the pre-treatment procedure allowed for the correlation of channel activity with the level of FKBP12 dissociation.

FKBP12 has been implicated in stabilising RyR channel activity at the maximum conductance level because cloned RyRs, expressed without FKBP12, display prominent subconductance levels (Brillantes *et al.*, 1994). In contrast, Mayrleitner *et al.* (1994) reported that native skeletal RyRs stripped of FKBP12 by FK506 pre-treatment had normal conductance properties and ligand sensitivity, except that their P_o was greater over the Ca^{2+} range 70 nM to 1 μM. The cloned RyR channel may differ from its native counterpart in the extent of post-translational protein modifications and in the presence of associated proteins other than FKBP12. Therefore, it was also of interest to confirm whether the native FKBP12-stripped channel has different properties to the cloned channel.

Results

5.2 *Dissociation of FKBP12 from SR vesicles*

TC vesicles were stripped of FKBP12 by treatment with FK506/rapamycin (see methods). SR FKBP12 was identified by Western blot analysis using either, a rabbit anti-peptide sera that recognised a 16 amino acid sequence in the N-terminus of FKBP12 (Dr. P. Junankar), or a monoclonal mouse anti-human FKBP12 antibody, 3F4-70 (Fujisawa). Immunostaining with the anti-peptide sera detected prominent proteins at ~ 12 and 30 kDa and a less prominent protein at ~50 kDa (*Fig.5-1A*). The 12 kDa protein is likely to be FKBP12 due to its molecular weight and the observation that it was selectively removed from SR preparations by FK506/rapamycin treatment (*lanes 2* and *3*) but not affected by solvent treatment alone (1% ethanol, *lane 1*). Rapamycin was slightly more effective than FK506 in removing FKBP12, which is consistent with the greater affinity of rapamycin for FKBP12 (Schreiber, 1991). Dissociation of FKBP12 was temperature dependent and occurred more slowly at room temperature (22 - 25°C) compared with 37°C. Incubation with 20 μM FK506 or rapamycin for one hour at room temperature did not completely dissociate FKBP12 (*Fig. 5-1A*). Whereas, near complete dissociation of FKBP12 occurred within 15 min at 37°C with ~10 μM rapamycin (*Fig. 5-1B*). Immunostaining of untreated B4 vesicles (data not shown) was similar to the solvent control indicating that temperature alone did not induce FKBP12 dissociation.

The immunoblot shown in *Fig. 5-1B* was stripped and reprobed with the monoclonal anti-FKBP12 antibody, 3F4-70 (*Fig. 5-2A*) which resulted in a single band at ~ 12 kDa, confirming the identity of this protein as FKBP12. In addition, this indicated that the higher molecular weight proteins identified in *Fig 5-1* probably resulted from non-specific antibody binding and/or cross-reactivity. Varying the rapamycin concentrations from 0 μM to 10 μM (15 min at 37°C) produced a dose-dependent dissociation of FKBP12 (*Fig. 5-1B* and *5-2A*). FKBP12 content was estimated by densitometry and expressed as a percentage of the untreated control value. *Fig. 5-2B* shows a plot of percentage of FKBP12 remaining versus rapamycin concentration obtained from four

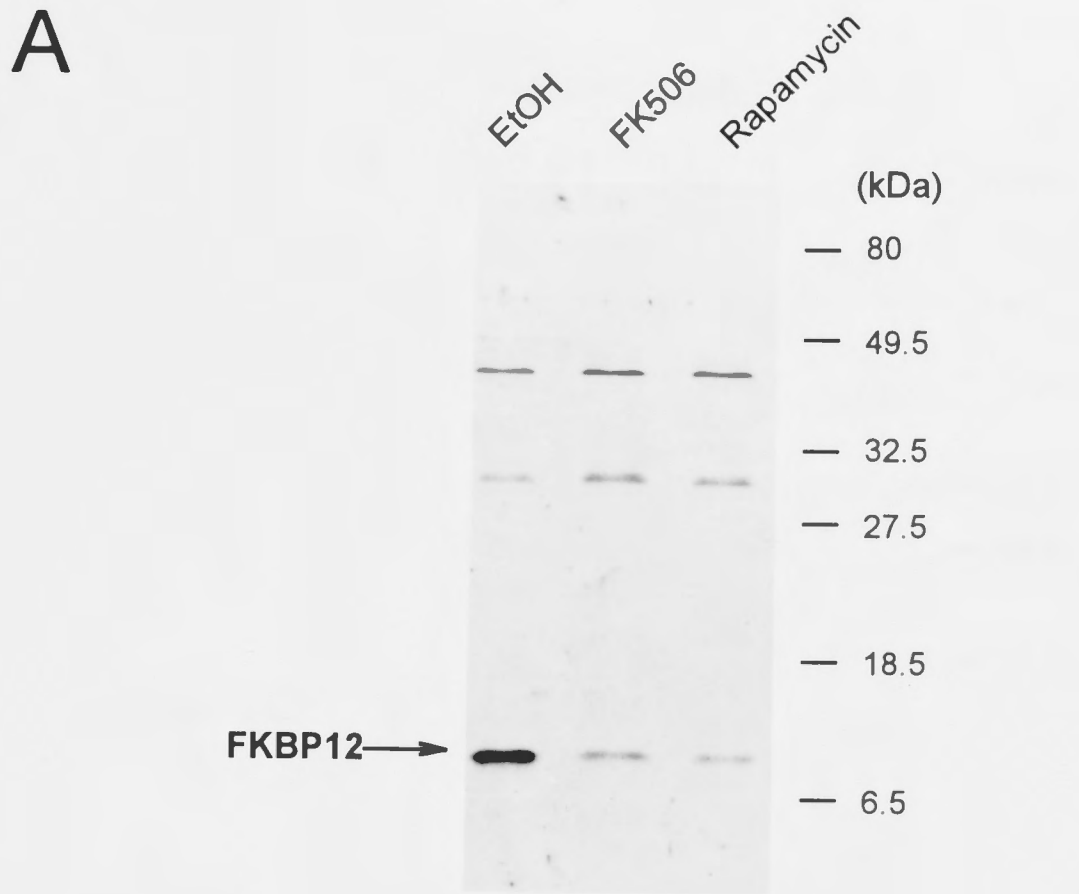

Fig. 5-1. FK506/Rapamycin induced dissociation of FKBP12 from SR vesicles. Western immunoblot analysis of FKBP12 in 10 μg of B4 SR vesicles probed with rabbit anti-peptide sera (see methods). (A) Effect of SR vesicle incubation with 1% ethanol, solvent control, (*lane 1*), 20 μM FK506 (*lane 2*) and 20 μM rapamycin (*lane 3*) for 1 hour at room temperature. The blot was developed using an alkaline phosphatase-conjugated secondary antibody. (B) Dose-dependent dissociation of FKBP12 with rapamycin (0-10 μM) incubation for 15 min at 37 °C. The blot was developed using an HRP-conjugated secondary antibody and the enhanced chemiluminescence detection system. The higher molecular weight bands are non-specific (see Fig. 5-2).

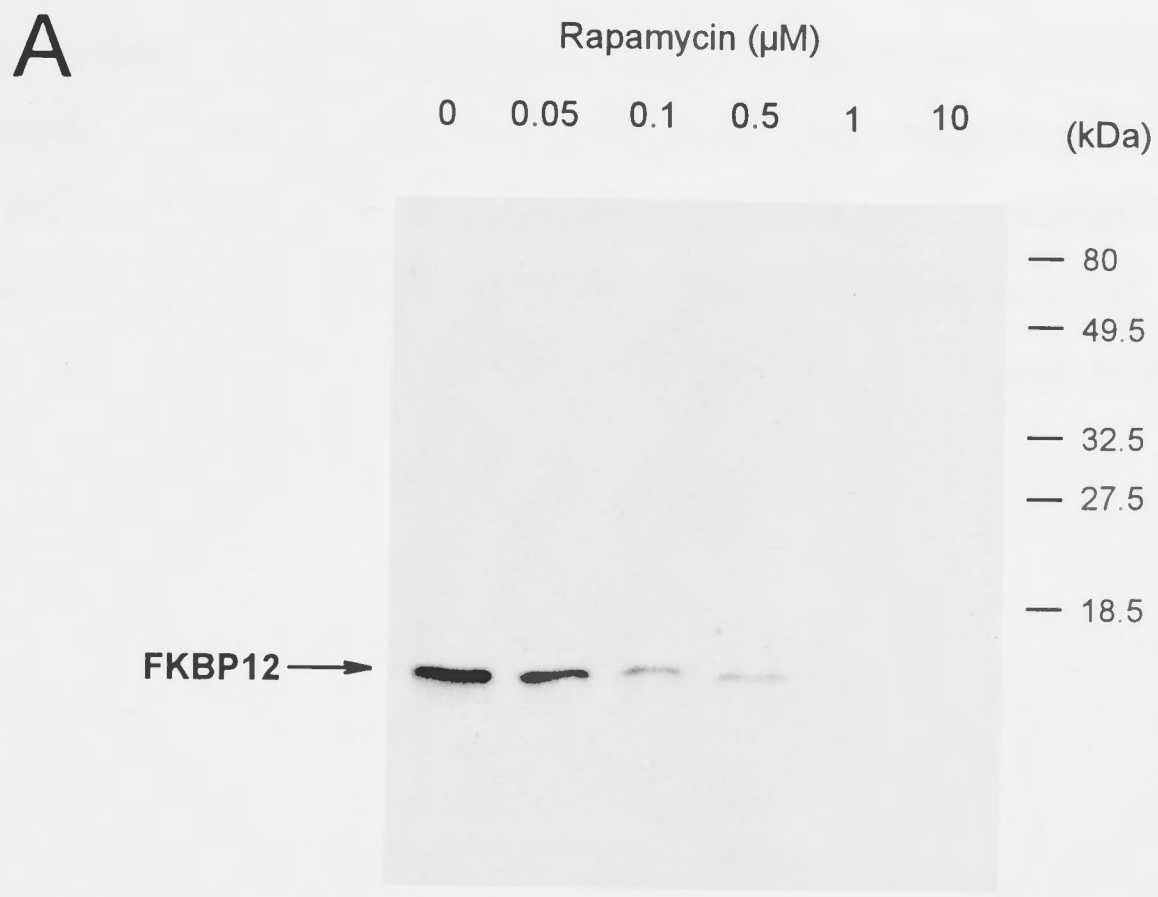

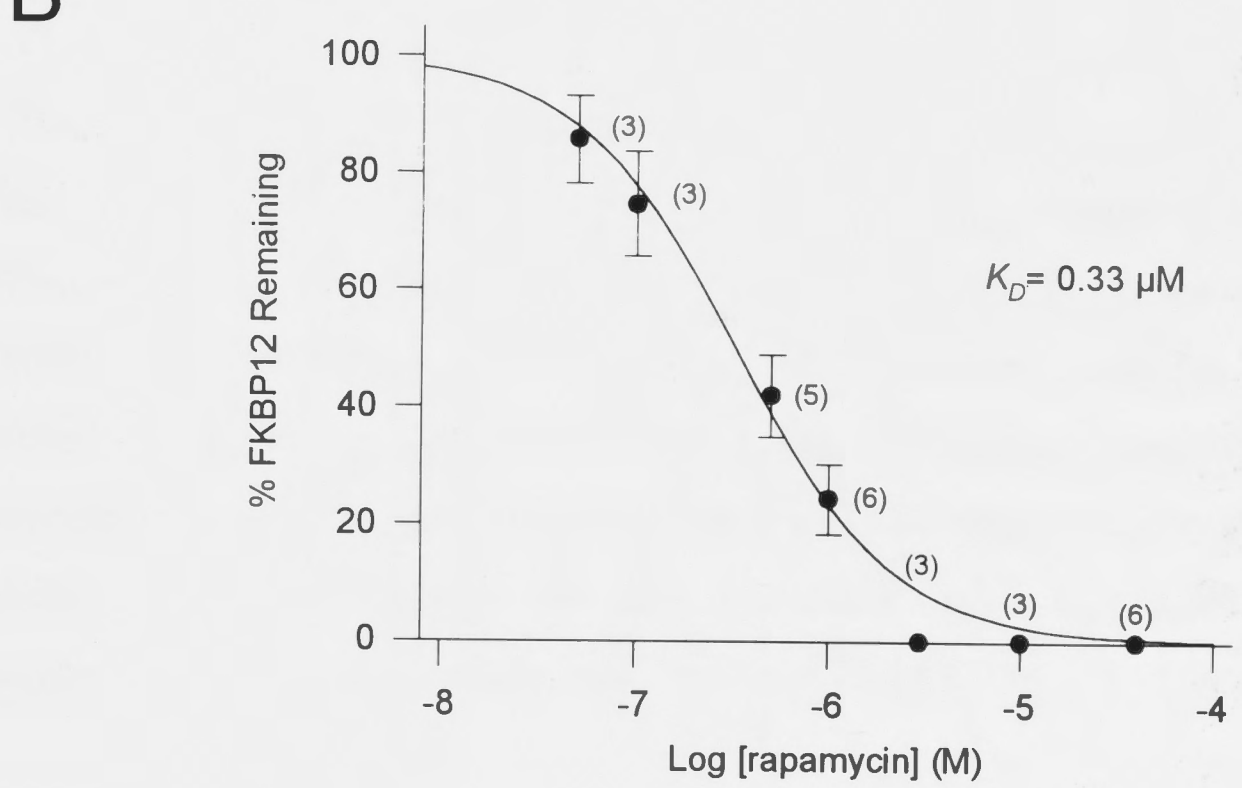

Fig. 5-2. Dose-dependent dissociation of FKBP12 by rapamycin (A) the same immunoblot as in Fig. 5-1B, stripped and reprobed with monoclonal anti-FKBP12 antibodies produced a single band at ~12 kDa, confirming that this protein was FKBP12. (B) Plot of relative amount (%) of FKBP12 remaining in SR vesicles versus log [rapamycin] (M). Immunoblot chemiluminescence was quantified by densitometric analysis (see methods). Data are the mean ± sem and the number of experiments is indicated alongside each point. The solid line is the best fit to Equation 5-1. K_D = 0.33 μM and H = 1.

experiments. Importantly, while the data values at 10 μM rapamycin indicated ~ 100% removal of FKBP12 this probably did not represent complete dissociation but the limit of the detection method. To estimate the detection limit, standard dilutions of untreated vesicles were analysed and FKBP12 was found to be undetectable at ~90 - 95% dilution. The solid line in *Fig. 5-1B* is the best fit (least squares method) to a Hill equation (*Eq. 5-1*)

$$F = 100\% \times \left(1 - \left(\frac{1}{1 + (K_D / [rap])^H} \right) \right) \qquad (5\text{-}1)$$

where F is the percentage of FKBP12 remaining, K_D is the half-maximal concentration of rapamycin for FKBP12 dissociation and H is the Hill co-efficient for dissociation, since nine RyR in ten had no associated FKBP12 monomer. Values for K_D and H were 0.33 μM and 1 respectively. The curve fit predicted that at 10 μM rapamycin, ~ 2.6% of FKBP12 remained ie. one RyR in ten had an associated FKBP12 monomer. The K_D value represents the rapamycin concentration at which 2/4 FKBP12 monomers are removed from each RyR and is similar to an earlier study (Timerman *et al.*, 1993) (K_D of ~ 0.4 - 1 μM) in which SR vesicles were stripped of FKBP12 by FK506 treatment. However, in the Timerman study the incubation was carried out for one hour at room temperature. The greater sensitivity of FKBP12 dissociation reported here is consistent with the reported higher affinity of rapamycin for FKBP12 (Schreiber, 1991). The Hill co-efficient of 1 is consistent with a 1:1 stoichiometry of binding between rapamycin and FKBP12.

5.3 *General observations of RyRs stripped of FKBP12*

Vesicles that had been pre-treated with rapamycin or its solvent alone (1% ethanol) were incorporated into lipid bilayers. In total, sixty channels were studied which were derived from seven separate rapamycin treatments of five vesicle preparations. The majority of channels were incorporated from vesicles that had been pre-treated with ≥ 10 μM rapamycin, at 37°C for ≥ 15 min (ie. 100% FKBP12 stripped). Others were incorporated from vesicles pre-treated with 0.1 μM (~ 25% stripped), 0.5 μM (~ 50% stripped) and 1 μM rapamycin (~ 75% stripped) each at 37°C for 15 min ; or 10 μM

FK506, for 1 hour at room temperature (~ 75% stripped). For simplicity, channels are referred to as being stripped of the same percentage of FKBP12 as the vesicles from which they were incorporated. This may not be strictly accurate; it is likely that there was some variation in FKBP12 association between RyRs from the same population of treated vesicles because stripping of FKBP12 may not have been homogenous. Variability between channels would be greatest in vesicles partially stripped of FKBP12 but should have decreased as FKBP12 dissociation of the vesicles approached 100%. Therefore, in this study 100% stripped vesicles were mostly used in bilayer studies.

The vesicle incorporation frequency was unaffected by the incubation procedure, with 90% of incorporations from stripped and unstripped vesicles occurring in less than 10 min. Pre-treatment with rapamycin and/or 37°C incubation had no apparent effect on SR Cl^- channels.

5.4 *Ligand sensitivity of FKBP12 stripped RyRs*

Dissociation of FKBP12 had profound effects on RyR channel activity and conductance properties, yet channels retained their characteristic ligand sensitivity. The effects of FKBP12 dissociation are particularly well summarised in the channel shown in *Fig. 5-3*. A burst of activity at 1 mM *cis* Ca^{2+} (*top trace*) consisted of long openings (50 - 100 ms) to a small substate level (S1) and transitions to shorter lived, higher current levels. After the addition of 1 mM ATP (*second trace*) to the *cis* chamber, openings to the higher current levels were longer and at least four open levels were evident. The channel remained sensitive to ryanodine (100 μM, *third trace*) with a characteristic ~ 50% reduction in the maximum open level. However pre-existing substate activity remained prominent in the ryanodine modified channel. Finally, 80 μM ruthenium red (*bottom trace*) completely blocked all activity within seconds of addition to the *cis* chamber. In summary, ATP activation was seen in 10/10 stripped RyRs, ryanodine modification in 17/21 channels and ruthenium red block in 8/9 channels. The ryanodine modification is discussed in more detail below. In conclusion, the FKBP12-stripped RyR could still be identified as a RyR by its characteristic ligand sensitivity.

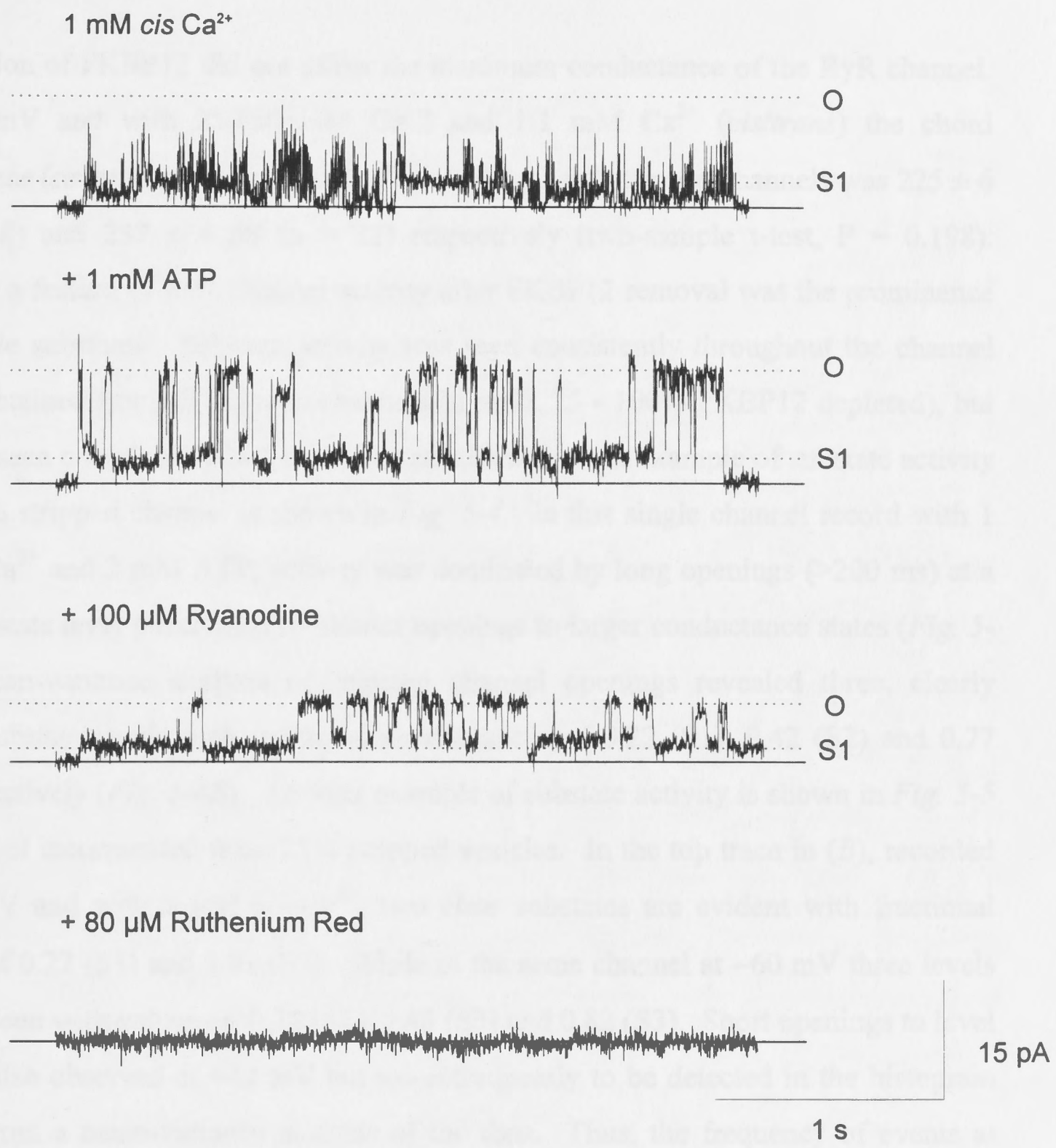

Fig. 5-3. Ligand sensitivity of the FKBP12-stripped RyR channel. Representative channel activity from a single RyR incorporated from 100% FKBP12-stripped vesicles. The channel mainly opened to the maximum open level (O) and a subconductance level (S1). The bilayer potential was +40 mV and activity was recorded with 250/50 mM CsCl and 1/1 mM Ca^{2+} (*cis/trans*) (*top trace*), followed by sequential addition of 1 mM ATP (*second trace*), 100 µM ryanodine (*third trace*) and 80 µM ruthenium red (*bottom trace*) to the *cis* chamber.

5.5 *Conductance levels of the FKBP12 stripped RyR channel*

Dissociation of FKBP12 did not affect the maximum conductance of the RyR channel. At +40 mV and with 250/50 mM CsCl and 1/1 mM Ca^{2+} (*cis*/*trans*) the chord conductance (reversal potential = –20 mV) of control and stripped channels was 225 ± 6 pS (n = 8) and 237 ± 4 pS (n = 32) respectively (two-sample t-test, P = 0.198). However, a feature of RyR channel activity after FKBP12 removal was the prominence of multiple substates. Substate activity was seen consistently throughout the channel records obtained from all stripped channels (n = 60, 25 - 100% FKBP12 depleted), but was only seen occasionally in 4 of 14 control channels. An example of substate activity in a 100% stripped channel is shown in *Fig. 5-4*. In this single channel record with 1 mM *cis* Ca^{2+} and 2 mM ATP, activity was dominated by long openings (>200 ms) at a small substate level punctuated by shorter openings to larger conductance states (*Fig. 5-4A*). Mean-variance analysis of selected channel openings revealed three, clearly defined substate levels with fractional conductances of 0.22 (S1), 0.42 (S2) and 0.77 (S3) respectively (*Fig. 5-4B*). Another example of substate activity is shown in *Fig. 5-5* in a channel incorporated from 25% stripped vesicles. In the top trace in (*B*), recorded at +40 mV and with 1 μM *cis* Ca^{2+}, two clear substates are evident with fractional currents of 0.22 (S1) and 0.81 (S3). While in the same channel at –60 mV three levels could be seen with values of 0.28 (S1), 0.45 (S2) and 0.82 (S3). Short openings to level S2 were also observed at +40 mV but too infrequently to be detected in the histogram derived from a mean-variance analysis of the data. Thus, the frequency of events at each substate level may have a small voltage dependence, although this was not examined in detail. A plot of current versus voltage for each open level (*Fig. 5-6*) shows that the different open levels all reversed around –18 to –20 mV. The slope conductance at –18 mV was 211, 160 and 60 pS for the maximal open level (*filled circles*), S3 (*open circles*) and S1 (*open triangles*) respectively. Note that there were insufficient data to fit a curve to S2 (*open squares*).

A frequency distribution of current levels in thirty-nine stripped channels at +40 mV (1 μM to 1 mM *cis* Ca^{2+}, with or without 1 mM ATP) confirmed that there were three main substate levels with fractional conductances (mean ± SD) of 0.25 ± 0.05, 0.49 ± 0.03

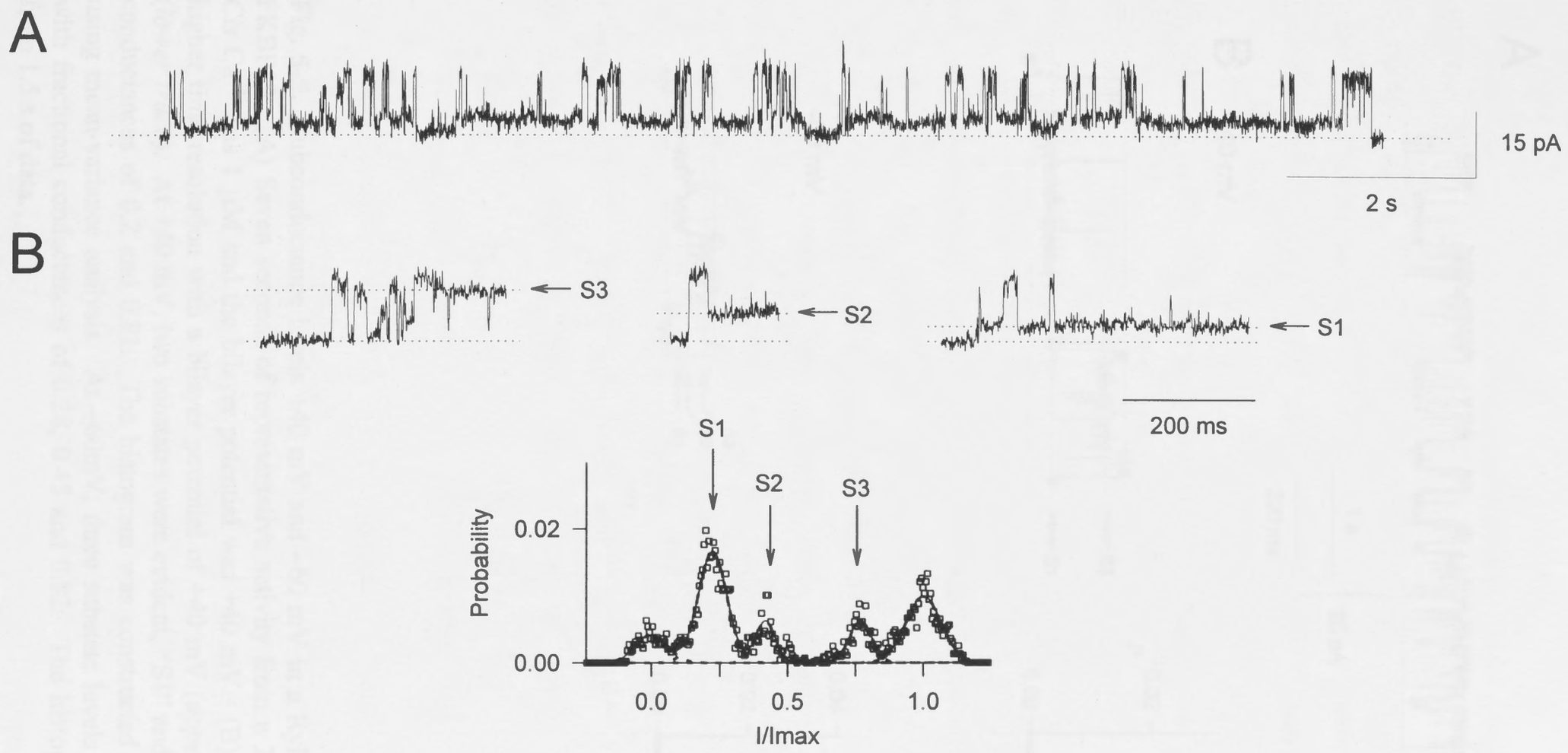

Fig. 5-4. Subconductance levels in the FKBP12-stripped RyR channel. (A) A 12 s segment of channel activity from the same 100% stripped channel in *Fig. 5-3*, with 1 mM $Ca^{2+}$and 1 mM ATP in the *cis* chamber. Openings to a low substate level are prominent, punctuated by transitions mainly to the fully open level. (B) Selected openings at higher time resolution showing openings to levels "S1", "S2" and "S3" and a amplitude histogram constructed from mean-variance analysis of 2 s of selected data. The fractional conductance of levels S1 - S3 derived from the peaks in the histogram was 0.22, 0.42 and 0.77 respectively.

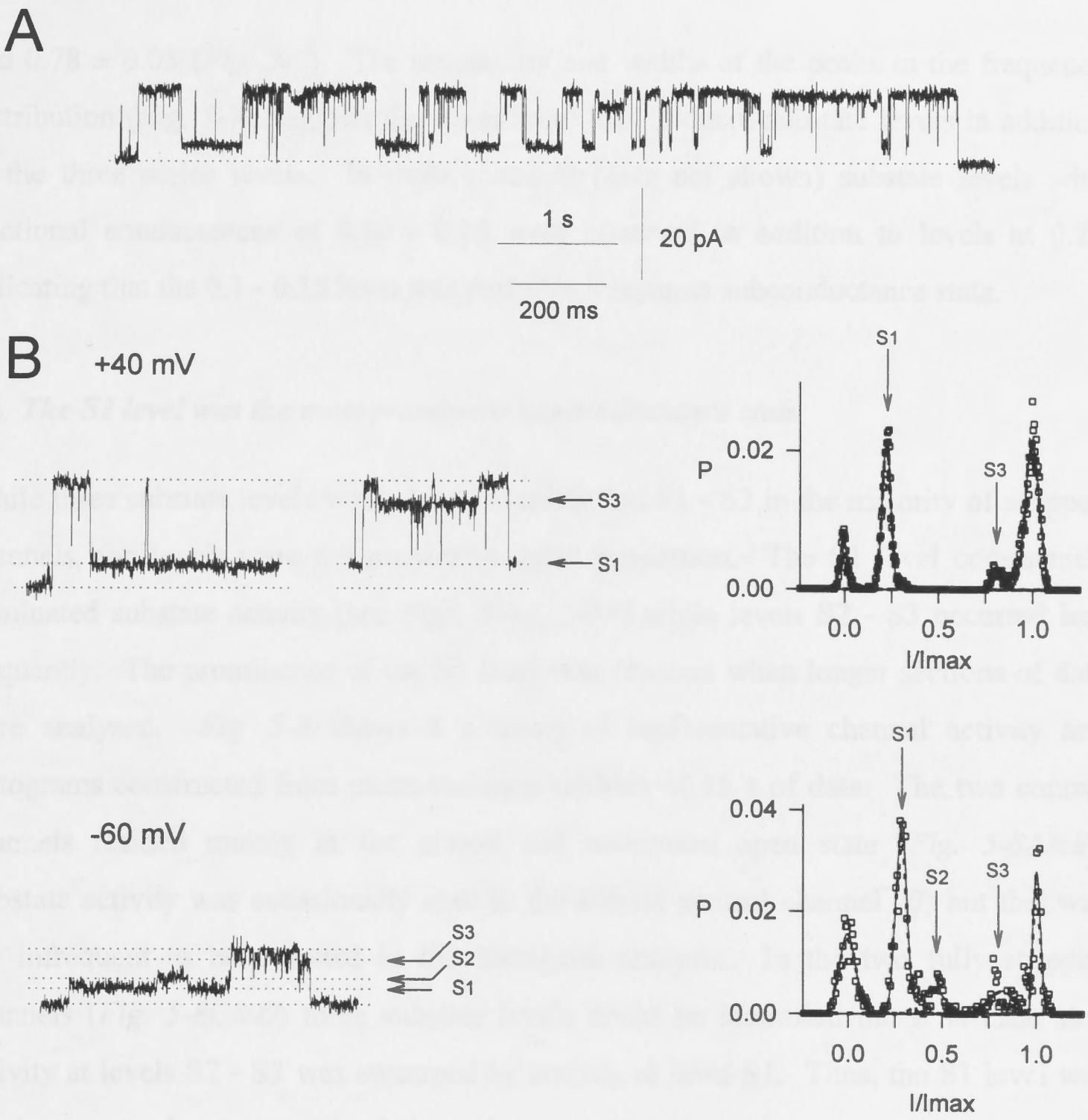

Fig. 5-5. Subconductance levels +40 mV and –60 mV in a RyR partially stripped of FKBP12. (A) Seven seconds of representative activity from a 25% stripped channel. *Cis* Ca^{2+} was 1 μM and the bilayer potential was +40 mV. (B) Selected openings at higher time resolution with a bilayer potential of +40 mV (*upper trace*) and –60 mV (*lower trace*). At +40 mV, two substates were evident, "S1" and "S3", with fractional conductances of 0.2 and 0.81. The histogram was constructed from the data in (A) using mean-variance analysis. At –60mV, three substate levels were evident, S1-S3, with fractional conductances of 0.28, 0.45 and 0.82. The histogram was constructed from 1.5 s of data.

and 0.78 ± 0.05 (*Fig. 5-7*). The asymmetry and widths of the peaks in the frequency distribution (*Fig. 5-7*) suggests that there were less frequent substate levels in addition to the three major levels. In three channels (data not shown) substate levels with fractional conductances of 0.10 - 0.15 were observed in addition to levels at 0.25 indicating that the 0.1 - 0.15 level was probably a separate subconductance state.

5.6 *The S1 level was the most prominent subconductance state*

While three substate levels were clearly identified at S1 - S3 in the majority of stripped channels, the levels were not present in equal proportion. The S1 level consistently dominated substate activity (see *Figs. 5-4A*, *5-5A*) while levels S2 - S3 occurred less frequently. The prominence of the S1 level was obvious when longer sections of data were analysed. *Fig. 5-8* shows 8 s traces of representative channel activity and histograms constructed from mean-variance analysis of 15 s of data. The two control channels resided mainly in the closed and maximum open state (*Fig. 5-8A&B*). Substate activity was occasionally seen in the second control channel (*B*) but this was too infrequent to be detected in the histogram analysis. In the two fully stripped channels (*Fig. 5-8C&D*) three substate levels could be identified but it is clear that activity at levels S2 - S3 was swamped by activity at level S1. Thus, the S1 level was the dominant substate in stripped channels.

5.7 *Variation in relative activity of subconductance states and maximum open state*

There was considerable variability in the proportion of substate to maximum open state activity. For example, the channel in *Fig. 5-8C* opened mostly to the maximal conductance while the channel in *Fig. 5-8D* opened mostly to S1 even though both channels were obtained from vesicle preparations that were nominally 100% stripped. This variation was seen in 43 fully stripped channels studied. Of these, 20 channels opened mainly to the maximal open level while 23 channels opened mainly to level S1. One explanation for the variability is the possibility that there were heterogenous populations of stripped channels in each vesicle preparation with some only partially stripped or with at least one FKBP12 monomer remaining. This is unlikely for several reasons. Firstly, the probability of incorporating a channel with one associated FKBP12

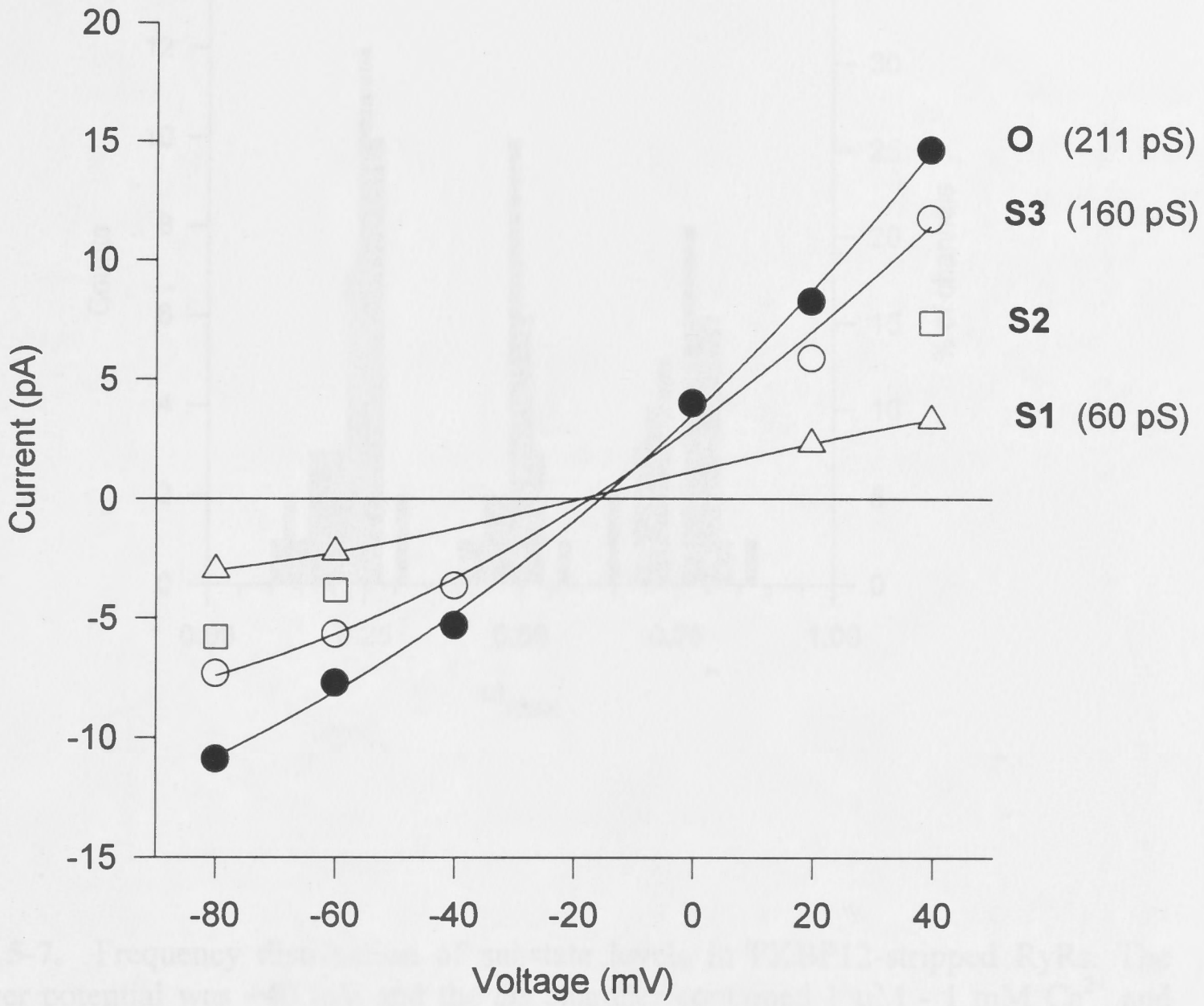

Fig. 5-6. Current-voltage relationship for open levels in a stripped RyR channel. Data were obtained from the four open levels, O and S1 - S3, in the channel shown in *Fig. 5-4*. The solid lines are the best fits to a third-order polynomial function. The currents all reversed close to −18 mV and the slope conductances, as indicated on right, were calculated at this potential. Note that there was insufficient data to fit level S2.

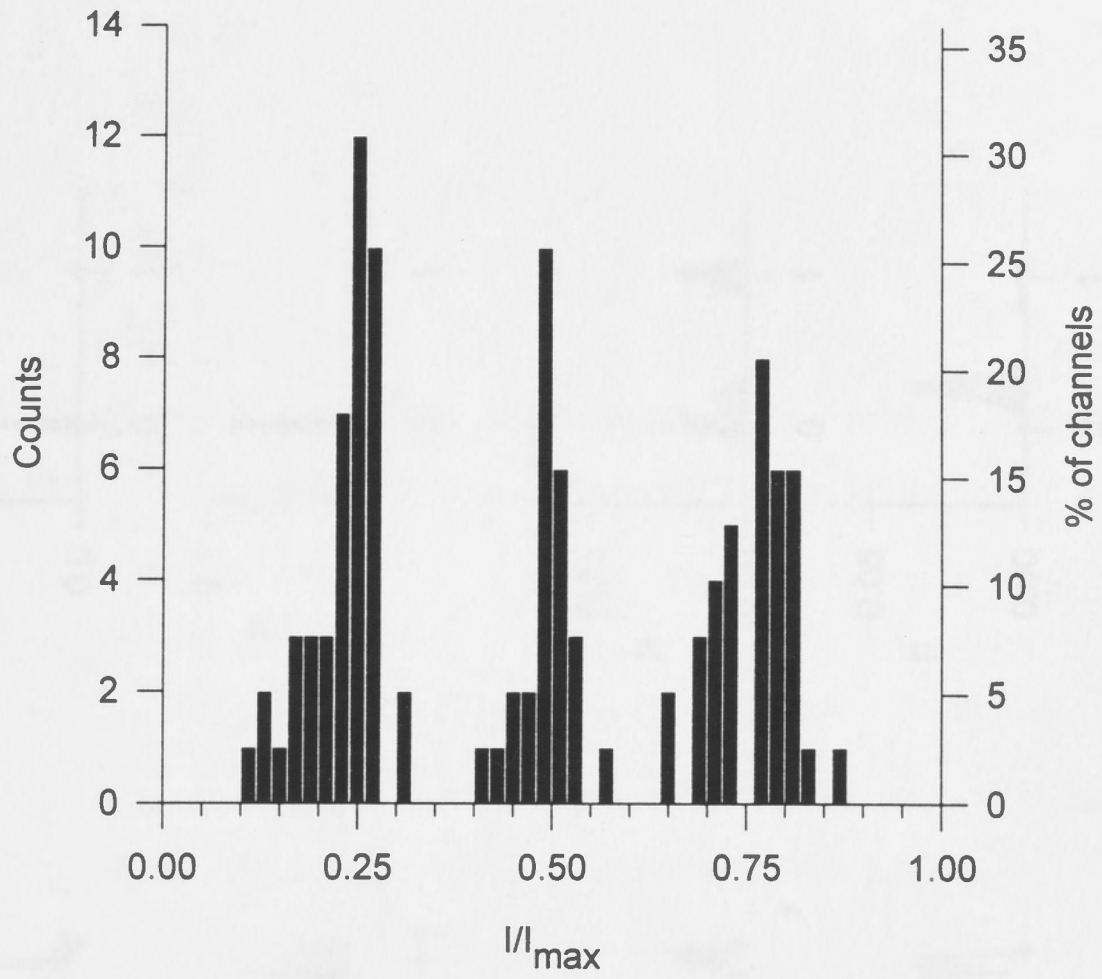

Fig. 5-7. Frequency distribution of substate levels in FKBP12-stripped RyRs. The bilayer potential was +40 mV and the *cis* chamber contained 1 μM - 1 mM Ca^{2+} and 0 - 1 mM ATP. Values were obtained from 39 channels (25 - 100% stripped), expressed as a fraction of the maximum conductance and binned in 0.02 intervals. Three major peaks are evident with respective means (± SD) of 0.25 ± 0.05, 0.49 ± 0.03 and 0.78 ± 0.05.

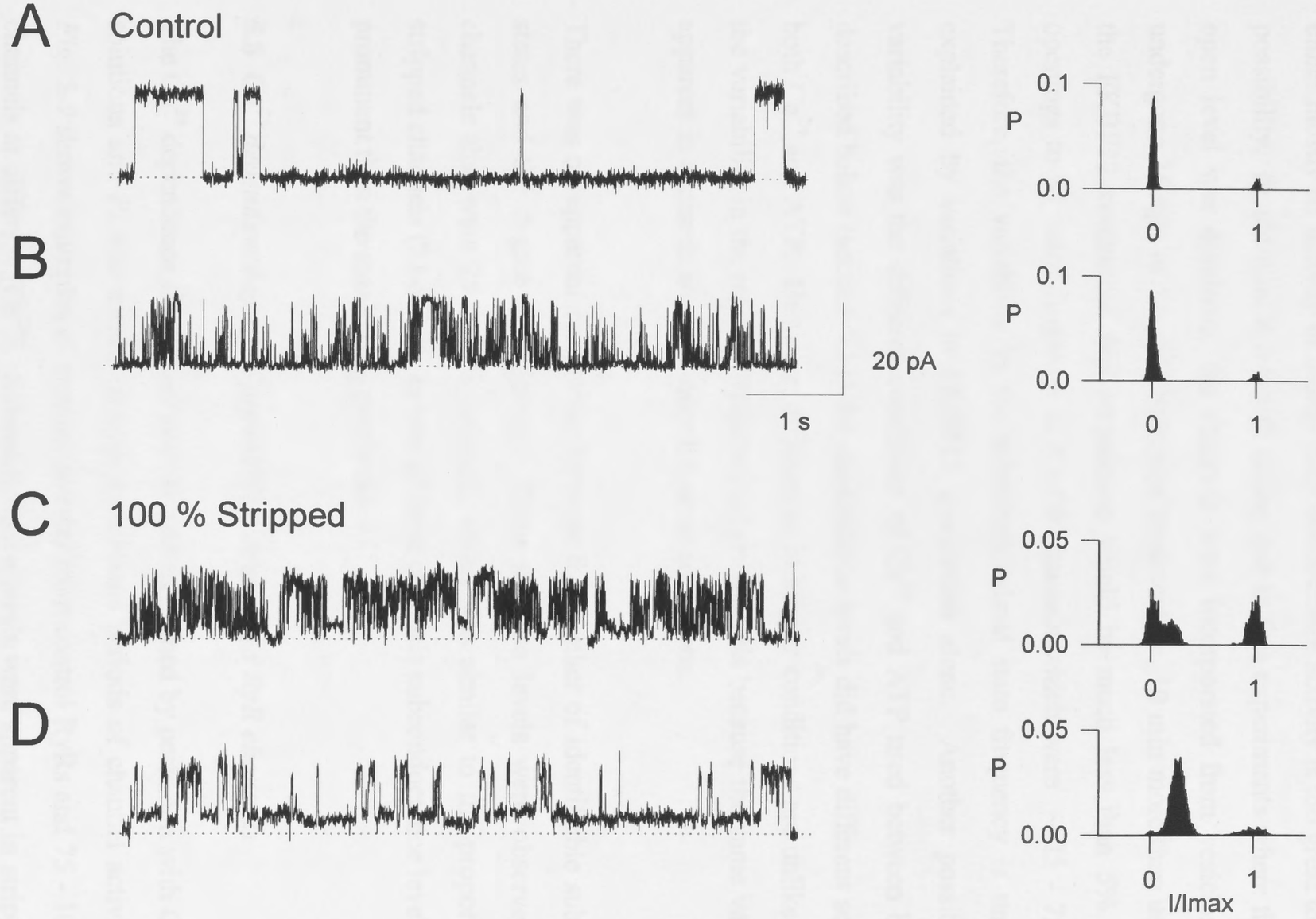

Fig. 5-8. Relative frequency of substate activity. Representative 8 s traces of channel activity and amplitude histograms constructed from 15 s of continuous channel activity. (A&B) Activity of two unstripped RyRs recorded with 10 μM *cis* Ca^{2+}. (C&D) Activity of two 100 % stripped channels recorded with 1 mM *cis* Ca^{2+} and 1 mM Ca^{2+} + 1 mM ATP respectively. After stripping, subconductance activity is concentrated at low levels. Note the differences between the stripped channels.

monomer from vesicles with ~ 5% FKBP12 remaining would be about 1 in five, assuming homogenous stripping of channels. The frequency of channels exhibiting either mostly S1 activity or mostly fully conductance activity is too great to support this possibility. In addition, it is worth noting that in five experiments where the maximum open level was dominant, the channels were incorporated from vesicles which had undergone 25 min of 10 μM rapamycin treatment, ie. 10 min more than usual. Hence, the FKBP12 content of this preparation would be much less than 5%. Moreover, openings to S1 were dominant in 4 of 9 channels which were ~ 25 - 75% stripped. Therefore, the variability in the substate/maximal state frequency is unlikely to be explained by variations in FKBP12 association alone. Another possible cause of variability was the different conditions of Ca^{2+} and ATP used between bilayers. As described below (section 5.11) the conductance levels did have different sensitivities to both Ca^{2+} and ATP. However, differences in bilayer conditions are unlikely to explain the variability in the relative frequency of open levels because the same variability was apparent in channels studied under the same conditions.

There was no apparent correlation between the number of identifiable subconductance states and the degree of stripping. Three substate levels were observed in 3 of 5 channels that were 25 - 50% stripped, which was similar to the proportion in fully stripped channels (23 of 30). In two of those channels subconductance levels were more prominent than the maximum open level.

5.8 *Ca^{2+} dependence of open probability for stripped RyR channels*

The Ca^{2+} dependence of channel activity was examined by perfusion with Ca^{2+}-buffered solutions and P_o was measured over continuous periods of channel activity for >90s. *Fig. 5-9* shows examples of channel activity from control RyRs and 75 - 100% stripped channels at different [Ca^{2+}]. Subconductance levels were apparent in stripped channels at all [Ca^{2+}] but not in control channels. Stripped channels were more active at 0.1 μM and 1 - 5 mM Ca^{2+} but not very different at 10 μM Ca^{2+}. The Ca^{2+} dependence of P_o for channels incorporated from control vesicles incubated with solvent (1% ethanol) was indistinguishable from those incorporated from non-incubated channels (*Fig. 5-10).*

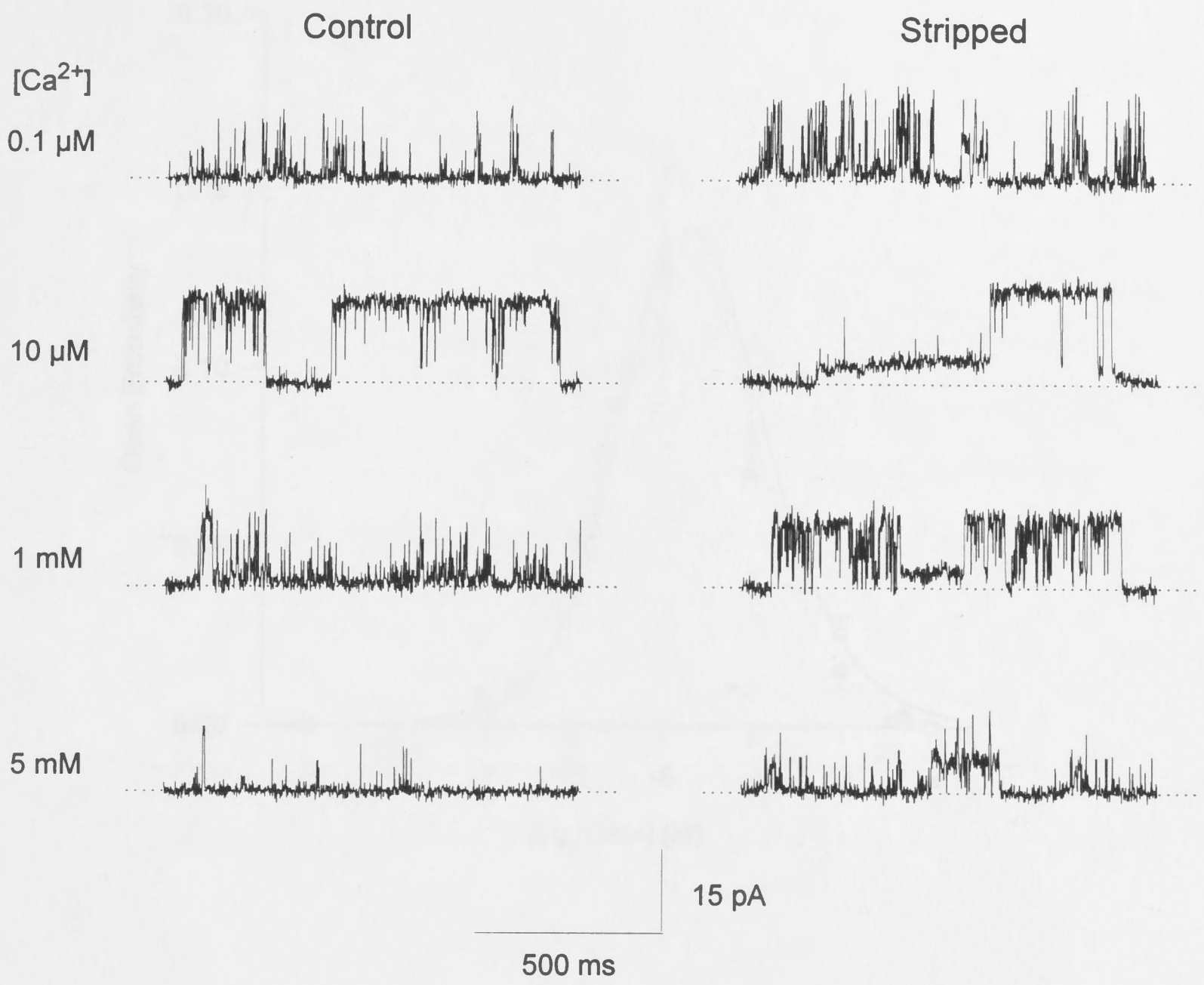

Fig. 5-9. Ca^{2+} dependence of FKBP12-stripped RyR channel activity. Representative bursts of activity in 1.1 s recordings from control and 75 - 100 % stripped channels. Solutions contained 250/50 mM CsCl (*cis*/*trans*), 1 mM Ca^{2+} *trans* and *cis* [Ca^{2+}] as indicated. The bilayer potential was +40 mV.

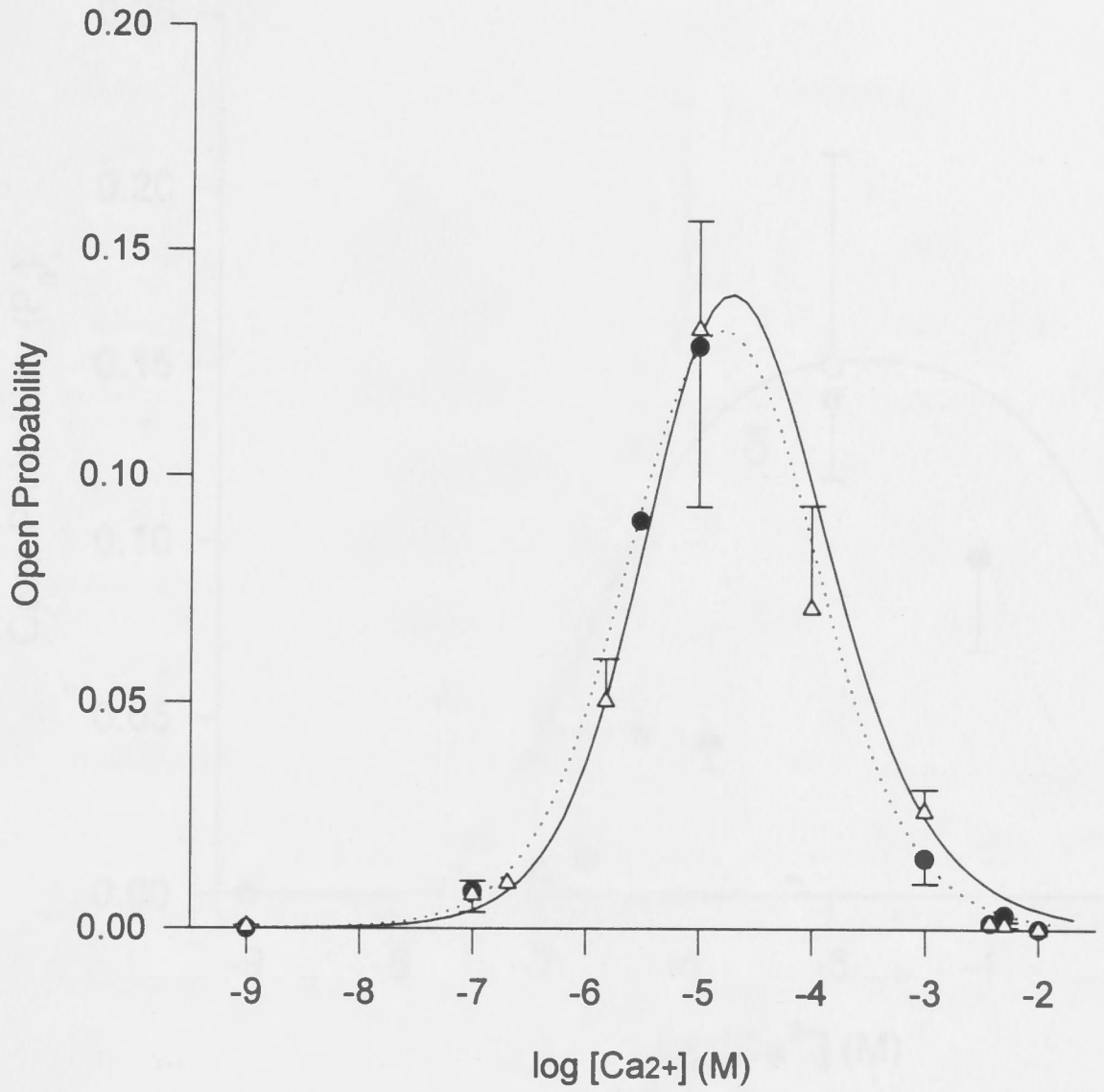

Fig. 5-10. P_o versus Ca^{2+} relationship for control and solvent-incubated (1% ethanol, 37°C, 15 min) RyR channels. Solutions contained 250/50 mM CsCl (*cis/trans*), 1 mM Ca^{2+} *trans* and *cis* [Ca^{2+}] was adjusted by perfusion with Ca^{2+}-buffered solutions. Control channel data (*triangles*, mean ± sem, n = 55) are from *Fig. 3-6* and were fitted with *Eq. 3-1* (*solid line*). Solvent-incubated data (*circles*, mean ± sem, n = 26) were fitted with *Eq. 4-3* (*broken line*, see text). Parameter values for P_{max}, K_A *and* K_I were 0.24, 5.1 μM and 73 μM respectively for the control group and 0.18, 2.8 μM and 93 μM respectively for the solvent-incubated group.

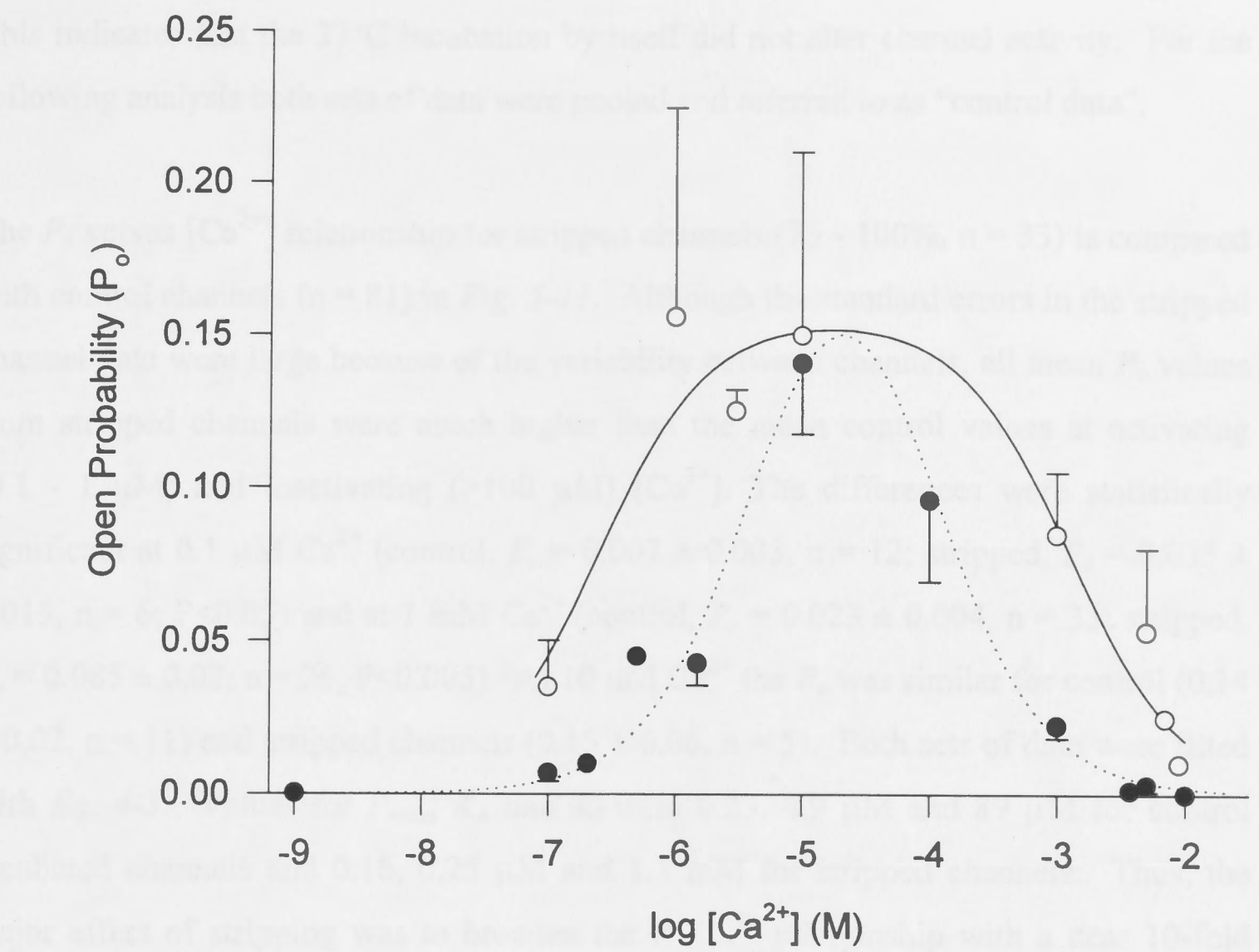

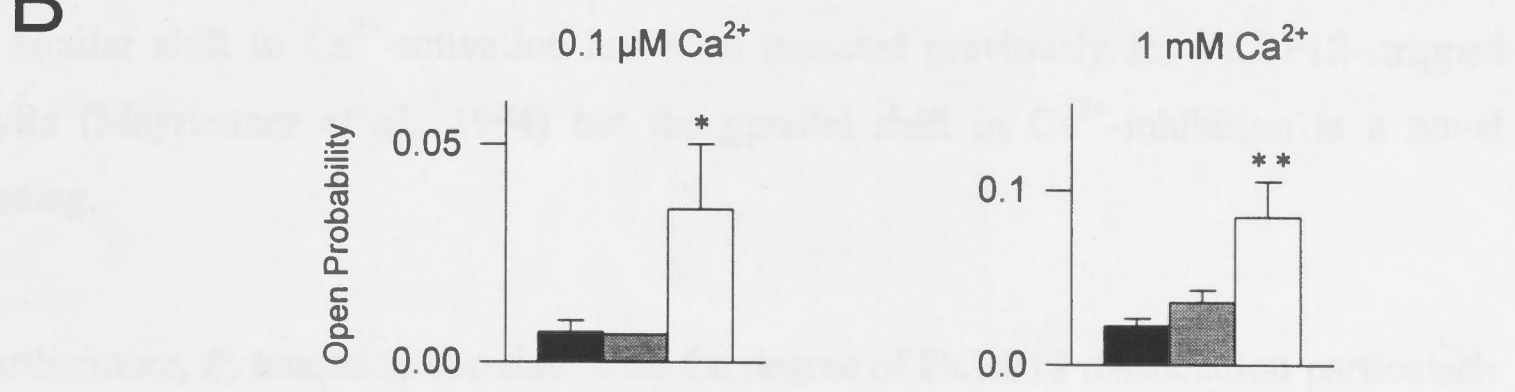

Fig. 5-11. P_o versus Ca^{2+} relationship for FKBP12-stripped RyR channels. (A) Open probability of control channels (*filled circles*, mean ± sem, n = 81) and 75 - 100% stripped channels (*open circles*, mean ± sem, n = 50). Points without error bars are single observations. Lines are the best fits to *Eq. 4-3*. Parameter values for P_{max}, K_A *and* K_I were 0.23, 4.9 μM and 89 μM respectively for control incubated channels and 0.16, 0.25 μM and 1.3 mM respectively for stripped channels. (B) Correlation between FKBP12 dissociation and channel activity. P_o with 1 mM and 0.1 μM *cis* Ca^{2+} for control (*solid bars*, n = 33 and 12), 25 - 50% stripped (*grey bars*, n = 2 and 1) and 75 - 100% stripped (*white bars*, n = 26 and 6) channels. Statistical differences between control and 75 - 100% stripped channels were measured using a two-tailed student's t-test (** P<0.005, * P<0.05).

This indicates that the 37°C incubation by itself did not alter channel activity. For the following analysis both sets of data were pooled and referred to as "control data".

The P_o versus [Ca^{2+}] relationship for stripped channels (75 - 100%, n = 33) is compared with control channels (n = 81) in *Fig. 5-11*. Although the standard errors in the stripped channel data were large because of the variability between channels, all mean P_o values from stripped channels were much higher than the mean control values at activating (0.1 - 1 μM) and inactivating (>100 μM) [Ca^{2+}]. The differences were statistically significant at 0.1 μM Ca^{2+} (control, P_o = 0.007 ± 0.003, n = 12; stripped, P_o = 0.035 ± 0.015, n = 6; P<0.05) and at 1 mM Ca^{2+} (control, P_o = 0.023 ± 0.004, n = 33; stripped, P_o = 0.085 ± 0.02, n = 26; P<0.005). At 10 μM Ca^{2+} the P_o was similar for control (0.14 ± 0.02, n = 11) and stripped channels (0.15 ± 0.06, n = 5). Both sets of data were fitted with *Eq. 4-3*. Values for P_{max}, K_A *and* K_I were 0.23, 4.9 μM and 89 μM for control incubated channels and 0.16, 0.25 μM and 1.3 mM for stripped channels. Thus, the major effect of stripping was to broaden the P_o-Ca^{2+} relationship with a near 10-fold increase in the sensitivity of/and a 10-fold decrease in the sensitivity of Ca^{2+}-inhibition. A similar shift in Ca^{2+}-activation has been reported previously for FKBP12-stripped RyRs (Mayrleitner *et al.*, 1994) but the parallel shift in Ca^{2+}-inhibition is a novel finding.

Furthermore, P_o tended to correlate with the degree of FKBP12 dissociation particularly at the extreme ends of the range of [Ca^{2+}] used. However there was an insufficient number of partially stripped channels (25 - 50% stripped) to draw any conclusions from these results. Previously, Timerman *et al.* (1995) have shown that the degree of FKBP12 removal correlates with reduced Ca^{2+} uptake from SR vesicles.

5.9 *Ca^{2+} dependence of I′ for FKBP12-stripped channels*

The increase in substate activity following stripping, particularly the prominence of small open levels at 10 - 25% of the maximum open level, presented technical difficulties in measuring P_o. To include small substate activity the open channel discriminator was set above baseline noise. However, despite this it was impossible to

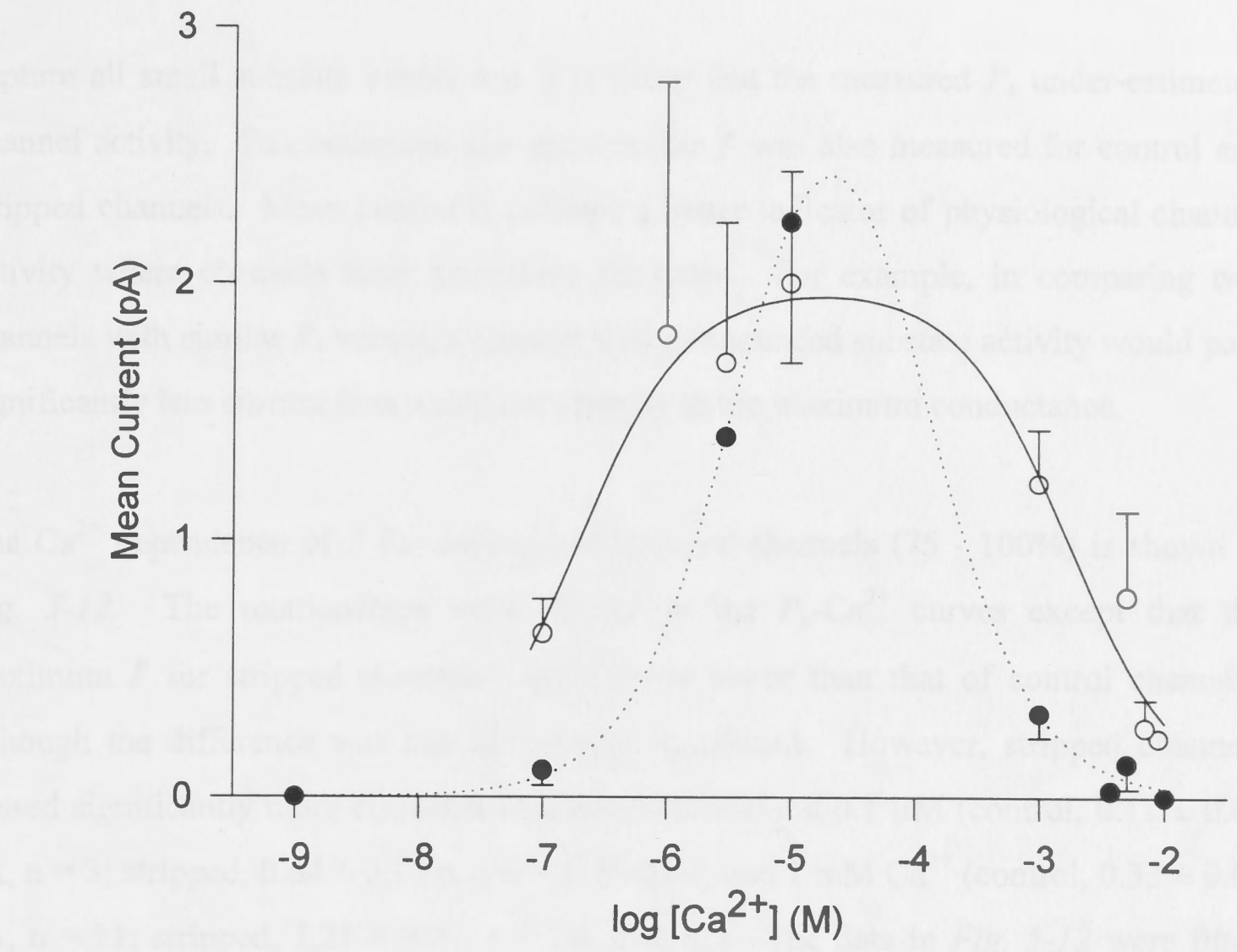

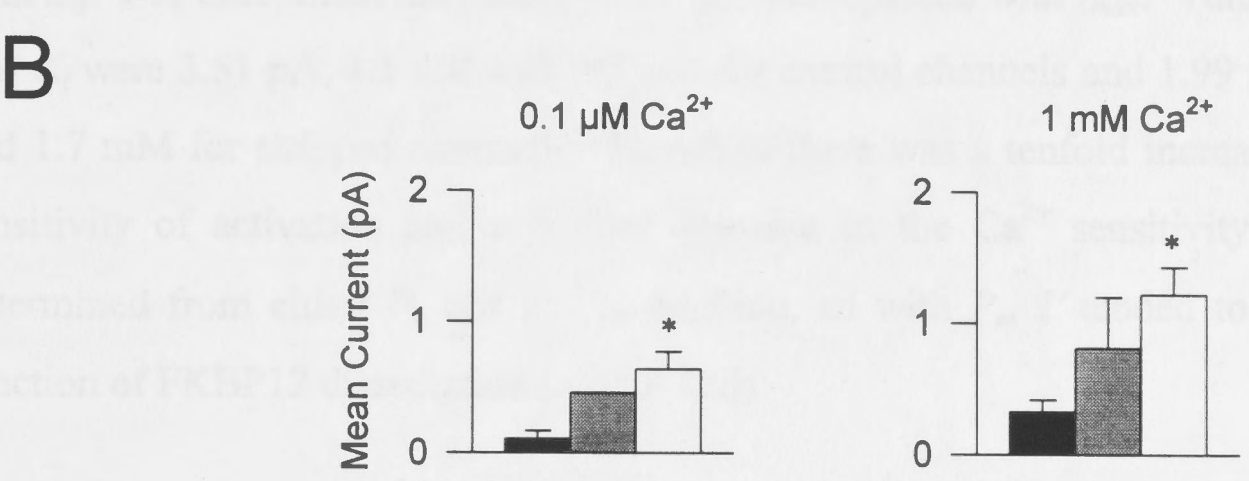

Fig. 5-12. *I′* versus Ca^{2+} relationship for FKBP12-stripped RyR channels. (A) *I′* of 75 - 100% stripped channels (*open circles*, mean ± sem, n = 50) and control channels (*filled circles*, mean ± sem, n = 26). Lines are the best fits to *Eq. 4-3*. Parameter values for I_{max}, K_A *and* K_I were 3.51 pA, 4.3 μM and 103 μM respectively for control channels and 1.99 pA, 0.197 μM and 1.7 mM respectively for stripped channels. (B) *I′* with 1 mM and 0.1 μM *cis* Ca^{2+} for control (*solid bars*, n = 3 and 11), 25 - 50% stripped (*grey bars*, n = 1 and 2) and 75 - 100% stripped (*white bars*, n = 6 and 26) channels. Statistical differences between control and 75 - 100% stripped channels were measured using a two-tailed student's t-test (* $P<0.05$).

capture all small substate events and it is likely that the measured P_o under-estimated channel activity. To circumvent this problem the I' was also measured for control and stripped channels. Mean current is perhaps a better indicator of physiological channel activity where channels have prominent substates. For example, in comparing two channels with similar P_o values, a channel with pronounced substate activity would pass significantly less current than a channel opening to the maximum conductance.

The Ca^{2+} dependence of I' for control and stripped channels (75 - 100%) is shown in *Fig. 5-12*. The relationships were similar to the P_o-Ca^{2+} curves except that the maximum I' for stripped channels tended to be lower than that of control channels, although the difference was not statistically significant. However, stripped channels passed significantly more current than control channels at 0.1 μM (control, 0.11 ± 0.06 pA, n = 3; stripped, 0.64 ± 0.13 pA, n = 6; $P<0.05$) and 1 mM Ca^{2+} (control, 0.33 ± 0.09 pA, n = 11; stripped, 1.21 ± 0.21, n = 26; $P<0.05$). The data in *Fig. 5-12* were fitted with *Eq. 4-3*, except that the parameter, P_{max}, was replaced with I_{max}. Values for I_{max}, K_A *and* K_I were 3.51 pA, 4.3 μM and 103 μM for control channels and 1.99 pA, 0.197 μM and 1.7 mM for stripped channels. Therefore there was a tenfold increase in the Ca^{2+} sensitivity of activation and a similar decrease in the Ca^{2+} sensitivity of inhibition determined from either P_o and I'. In addition, as with P_o, I' tended to increase as a function of FKBP12 dissociation (*Fig. 5-12B*).

5.10 *Mean open time, mean closed time and opening frequency of FKBP12-stripped RyRs*

A systematic analysis of open and closed time durations was not performed because of difficulty in measurement of transitions to small subconductance levels which would distort open and closed times. However, in several channels with low noise and clean transitions, these parameters could be measured unambiguously. *Table 5-1* compares the average T_o, T_c and event frequency (F_o) of these stripped channels with control channels at 0.1 μM, 10 μM and 1 mM *cis* Ca^{2+}. At 0.1 μM Ca^{2+}, F_o was ~ 8 fold greater in stripped channels compared with control channels, but T_o was not significantly different. At 10 μM Ca^{2+} there was no significant difference in any of the parameters,

Table 5-1. Single channel kinetics of control and FKBP12-stripped RyRs

	Control				Stripped		
$[Ca^{2+}]$	n	F_o (s^{-1})	T_o (ms)	T_c (ms)	n	F_o (s^{-1})	T_o (ms)	T_c (ms)
0.1 μM	8	3.8 ± 2.1	0.83 ± 0.09	983 ± 286	5	30 ± 13.3*	1.15 ± 0.19	128 ± 70*
10 μM	8	37.7 ± 16.0	14.05 ± 6.13	83 ± 27	5	48.1 ± 11.3	4.25 ± 1.26	53 ± 39
1 mM	22	15.5 ± 3.1	0.78 ± 0.05	160 ± 34	13	61.6 ± 11.9***	1.97 ± 0.48**	36 ± 14**

Mean ± sem for n channels; F_o, number of events per second; T_o, mean open time and T_c, mean closed time.
Values significantly different from control: * $P < 0.05$, ** $P < 0.01$, *** $P<0.0001$ (student's two-tailed t-test).

although T_o tended to be smaller in stripped channels. At 1 mM Ca^{2+}, F_o and T_o were ~ 4 and ~ 2.5 fold greater, respectively, in stripped channels.

5.11 *The maximum conductance state and S1 subconductance states have different Ca^{2+}-inhibition sensitivities*

It was very apparent from an inspection of channel records that the small S1 subconductance level had longer open durations than the maximum open level especially at inhibiting [Ca^{2+}]. A good example of this differential Ca^{2+} sensitivity is shown in *Fig. 5-13A* which shows channel activity from a single stripped RyR with 10 μM *cis* Ca^{2+}. Current transitions occurred mainly between the closed, S1 and maximum open level. *Fig. 5-13B* shows activity from the same channel after *cis* Ca^{2+} was increased to 1 mM. It is obvious from the trace that openings to the maximum level were more inhibited by high Ca^{2+} than openings to the S1 level. To quantify this, the duration of events at each level was compiled using the programme EVPROC (see methods). Briefly a current range ("window") was assigned for each level from amplitude histogram analysis (~ 1 - 4 pA for the substate analysis and ~ 9 - 15 pA for the maximum open state analysis). EVPROC detected as events, any current transitions that crossed the window ie. a transition into the window was recorded as an opening and a transition out of the window was recorded as a closing. Open duration histograms were plotted using the log-bin scaling method devised by Sigworth and Sine (1987). With 10 μM *cis* Ca^{2+} (*Fig. 5-13A, right*), the durations of the maximal (*filled symbols*) and substate (*open symbols*) levels were very similar and both distributions could be fitted by the sum of three exponentials (τ_1 = 0.7 ms, τ_2 = 5.9 ms and τ_3 = 28.9 ms for the maximum level; τ_1 <0.5 ms, τ_2 = 4.4 ms and τ_3 = 40.4 ms for the substate level). With 1 mM *cis* Ca^{2+} open durations for the maximum open level were reduced and the distribution could be adequately fitted by a double exponential (τ_1 <0.5 ms, τ_2 = 2.2 ms). In contrast, the substate open time distribution was less affected by the increase in [Ca^{2+}] (τ_1 <0.5 ms, τ_2 = 4.7 ms and τ_3 = 31 ms). However, the event probability of τ_2 and τ_3 were decreased. Overall, when Ca^{2+} was raised from 10 μM to 1 mM, T_o for the maximum state decreased from 9.3 to 1.2 ms (~ 8-fold change), whereas T_o for the substate level decreased from 15.6 to 4.1 ms (~ 4-fold change). Therefore, the Ca^{2+}

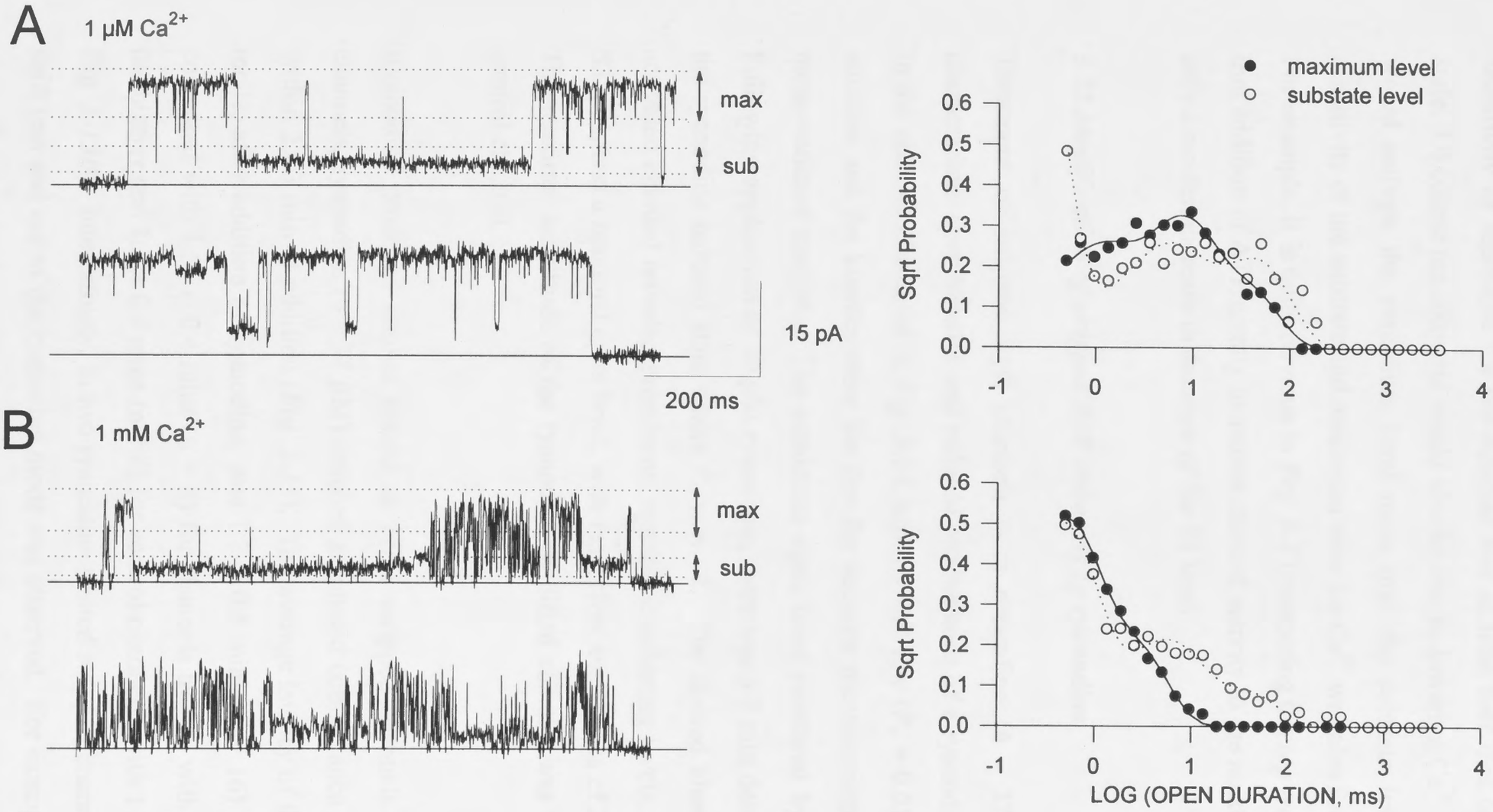

Fig. 5-13. Different Ca^{2+} sensitivity of the maximum open state and a subconductance state in a stripped RyR channel. Representative channel activity (*left*) and open time distributions (*right*) from a single RyR with (A) 1 μM *cis* Ca^{2+} and (B) 1 mM *cis* Ca^{2+}. The current level fluctuated mainly between the closed, fully open and S1 subconductance state. The duration of events at the maximum and subconductance levels were compiled by detecting transitions into and out of the current windows (indicated on the traces) using the programme EVPROC (see text). Open duration histograms for the maximum level (*solid symbols*) and substate level (*open symbols*) were plotted using the log-bin method of Sigworth and Sine (1987). In (A), the lines show the sum of three exponentials fitted to the data. For the maximum level (*solid line*) $\tau_1 = 0.7$ ms, $\tau_2 = 5.9$ ms and $\tau_3 = 28.9$ ms and for the substate level (*dotted line*) $\tau_1 < 0.5$ ms, $\tau_2 = 4.4$ ms and $\tau_3 = 40.4$ ms. In (B), the maximum level data was fitted with a double exponential (*solid line*), $\tau_1 < 0.5$ ms, $\tau_2 = 2.2$ ms and the substate level data was fitted with the sum of three exponentials (*dotted line*), $\tau_1 < 0.5$ ms, $\tau_2 = 4.7$ ms and $\tau_3 = 31$ ms.

sensitivity of inhibition for the substate was at least half that of the maximum open state. Of course the converse would also be true ie. lowering Ca^{2+} from 1 mM to 10 μM would activate the maximum level more than the substate level. The differential sensitivity of the substate and maximum state for Ca^{2+} was also found to apply for ATP. For example, it is quite obvious in *Fig. 5-3* (comparing the *top trace* and *second trace*) that addition of ATP greatly increased channel activity to the maximum open level with only a modest increase in duration of the S1 level.

5.12 *Modification of stripped RyR channels by ryanodine*

Treatment of stripped RyR channels with ryanodine (4 - 37 μM) produced the characteristic slow kinetics and reduced conductance of a ryanodine poisoned channel. In the channel illustrated in *Fig. 5-14*, activity was low (P_o = 0.019) prior to ryanodine addition and the kinetics were too fast for accurate measurement of amplitudes using mean-variance analysis. The maximum open level measured by eye was ~16.2 pA. Following application of 30 μM ryanodine, there was a 3 min delay before the onset of the ryanodine induced state where P_o was ~1. The slowed kinetics of the ryanodine activated channel revealed prominent, multiple conducting levels; three substate levels, S3 - S1, and a maximal open level, with respective amplitudes of 2, 3.5, 6.6 and 8.4 pA The maximal amplitude of the ryanodine-modified channel was therefore 52% of the control channel.

Ryanodine produced similar results in 17/21 stripped channels. In the majority of channels, ryanodine (4 - 37 μM) induced a reduced conductance open mode, typically within 2 - 3 min of addition (*Fig. 5-15*). The average latency of the ryanodine substate mode, after addition of ryanodine, was 1.2 ± 0.3 mins (n = 16) for stripped channels compared with 1.51 ± 0.4 mins (n = 6) for channels treated with FK506/rapamycin in the bilayer and 1.1 ± 0.4 mins (n = 8) for control channels (with 1 μM - 1 mM *cis* Ca^{2+}, *Fig. 5-15B*). Interestingly, in two ryanodine treated stripped channels a transient gating shift into and out of the ryanodine mode was observed. For example, in *Fig. 5-16A* the channel entered a ryanodine modified mode (as indicated by the arrow) with a reduced maximal conductance, 30 s after the addition of 7μM ryanodine. However, 1 min later

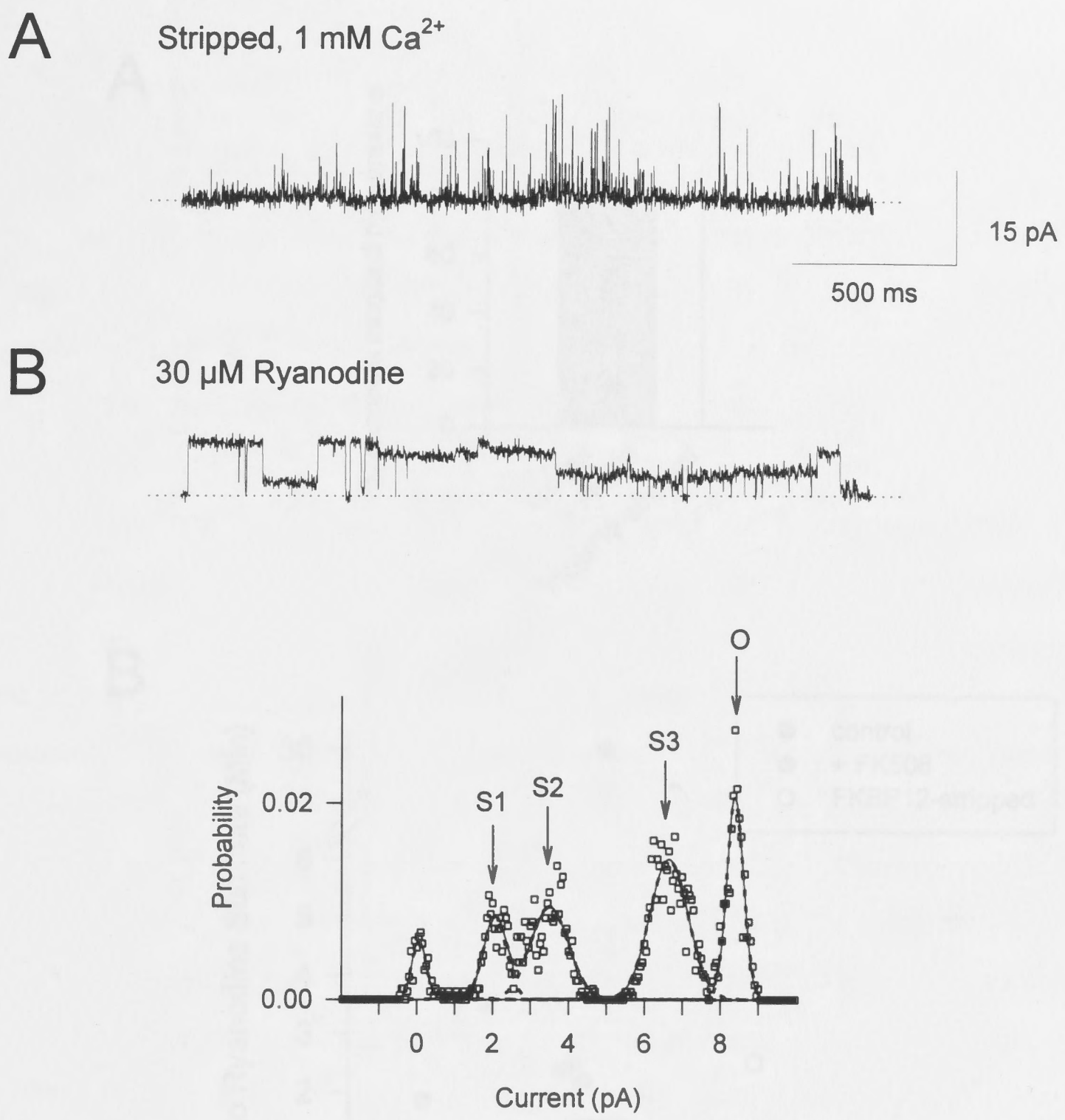

Fig. 5-14. Effect of ryanodine treatment on activity of the FKBP12-stripped RyR channel. (A) Current trace showing channel activity of a 100% stripped RyR with a bilayer potential of +40 mV and 1 mM *cis* Ca^{2+}. Activity was low ($P_o = 0.019$) and the kinetics were too rapid to measure amplitudes by histogram analysis. The peak amplitude measured by eye was 16.2 pA. (B) Activity from the same channel 3 min after the addition of 30 μM ryanodine to the *cis* chamber. P_o was increased to ~ 1 and the kinetics were dramatically slowed. Four distinct open levels were evident (S1-S3 and O) with respective amplitudes of 2, 3.5, 6.6 and 8.4 pA derived from the histogram. Thus, the maximum amplitude of the ryanodine-activated channel was 52% of the control value.

A

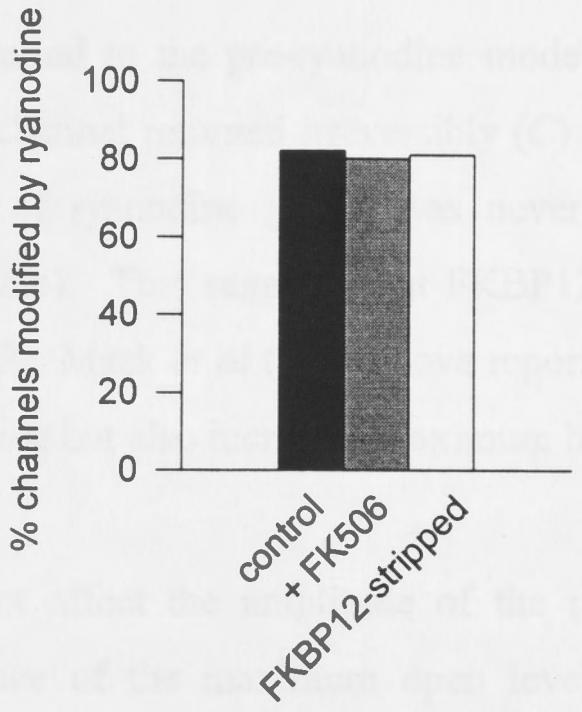

B

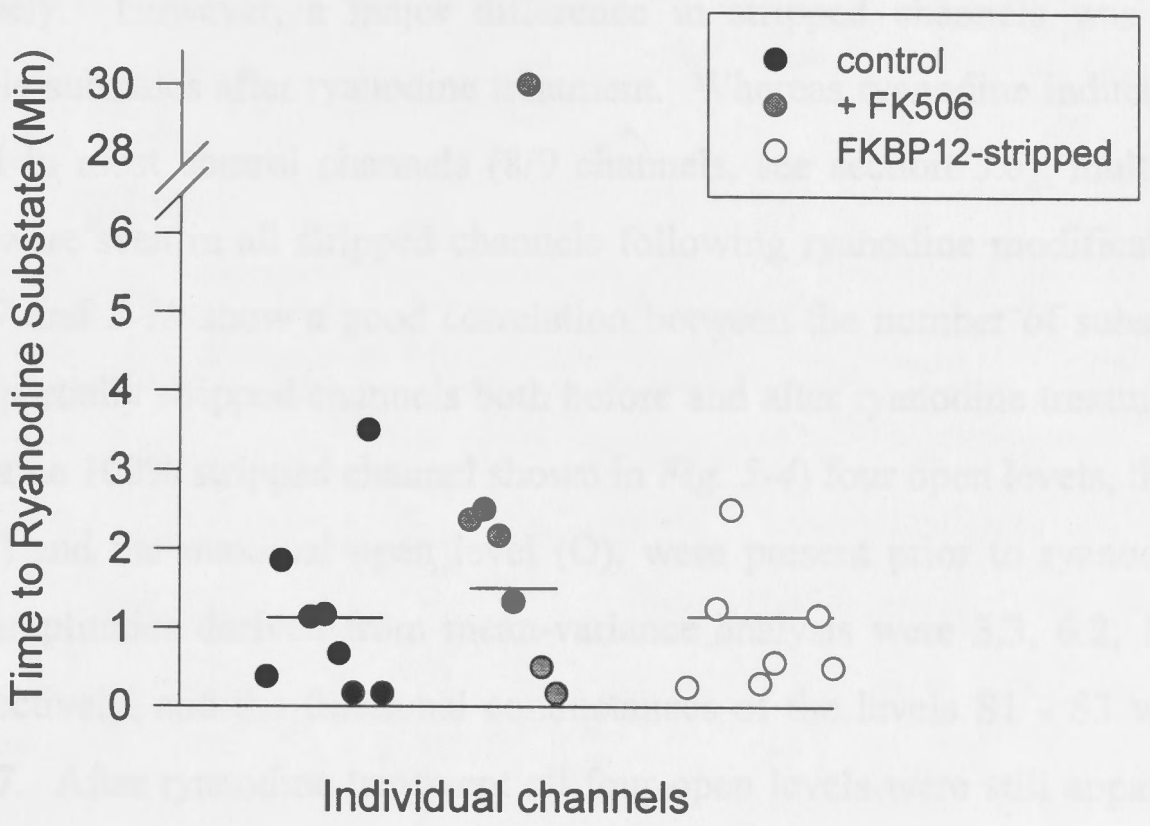

Fig. 5-15. Summary of ryanodine action in control, FK506/rapamycin treated and FKBP12-stripped RyR channels. (A) Percentage of channels modified by ryanodine within bilayer lifetime; control channels (*solid bar*), FK506/rapamycin treated channels (*grey bar*) and FKBP12 stripped channels (*open bar*). (B) Latency of ryanodine induced gating after addition of ryanodine, for control (*filled circles*), FK506/rapamycin treated (*grey circles*) and FKBP12-stripped (25-100%, *open circles*) channels. *Cis* Ca^{2+} was 1 μM - 1 mM and [ryanodine] was 4 - 37 μM. Note break in time scale at 10 min.

(*B*) the channel abruptly reverted to the pre-ryanodine mode with a return to control conductance. 15 s later the channel returned irreversibly (*C*) to the ryanodine induced state. A transient reversal of ryanodine gating was never observed in unstripped channels (1 - 20 μM ryanodine). This suggests that FKBP12 dissociation may affect ryanodine affinity for the RyR. Mack *et al* (1994) have reported that FK506 decreases the affinity of ryanodine binding but also increases maximum binding.

Removal of FKBP12 did not affect the amplitude of the ryanodine substate. The average fractional conductance of the maximum open level in ryanodine modified channels was 0.506 ± 0.01 (n = 15) and 0.51 ± 0.01 (n = 9) for stripped and control channels respectively. However, a major difference in stripped channels was the presence of multiple substates after ryanodine treatment. Whereas ryanodine induced a solitary open level in most control channels (8/9 channels, see section 3.6), multiple conducting levels were seen in all stripped channels following ryanodine modification (17/17). *Figs 5-17* and *5-18* show a good correlation between the number of substate levels in fully and partially stripped channels both before and after ryanodine treatment. In *Fig. 5-17*, (the same 100% stripped channel shown in *Fig. 5-4*) four open levels, three substates (S1 - S3) and the maximal open level (O), were present prior to ryanodine treatment. Their amplitudes derived from mean-variance analysis were 3.3, 6.2, 11.4 and 14.9 pA, respectively, and the fractional conductances of the levels S1 - S3 were 0.22, 0.42 and 0.77. After ryanodine treatment all four open levels were still apparent but with reduced current amplitudes. Values for S1 - S3 and O were 2, 3.9, 5.6 and 8.3 pA, respectively. The fractional conductances for S1 - S3 were 0.24, 0.47 and 0.68. Therefore, fractional conductances for S3 - S1 were similar before and after ryanodine treatment, although the S3 level was a little smaller in the ryanodine-activated state. The relative frequency of S2 and S3 activity increased following ryanodine treatment (normalised area under the curve increased from 10 to 23% for S2 and from 11 to 29% for S3) which suggests that ryanodine can modify the gating mechanism of each substate. A similar result is shown in *Fig. 5-18* with the same 25% stripped channel depicted in *Fig. 5-5*. Three open levels were evident, a prominent S1 substate, a less prominent S3 substate and the maximal open level (O). Their amplitudes were 3.5, 12.9 and 15.5 pA respectively. The fractional conductances for S1 and S3 were 0.23 and

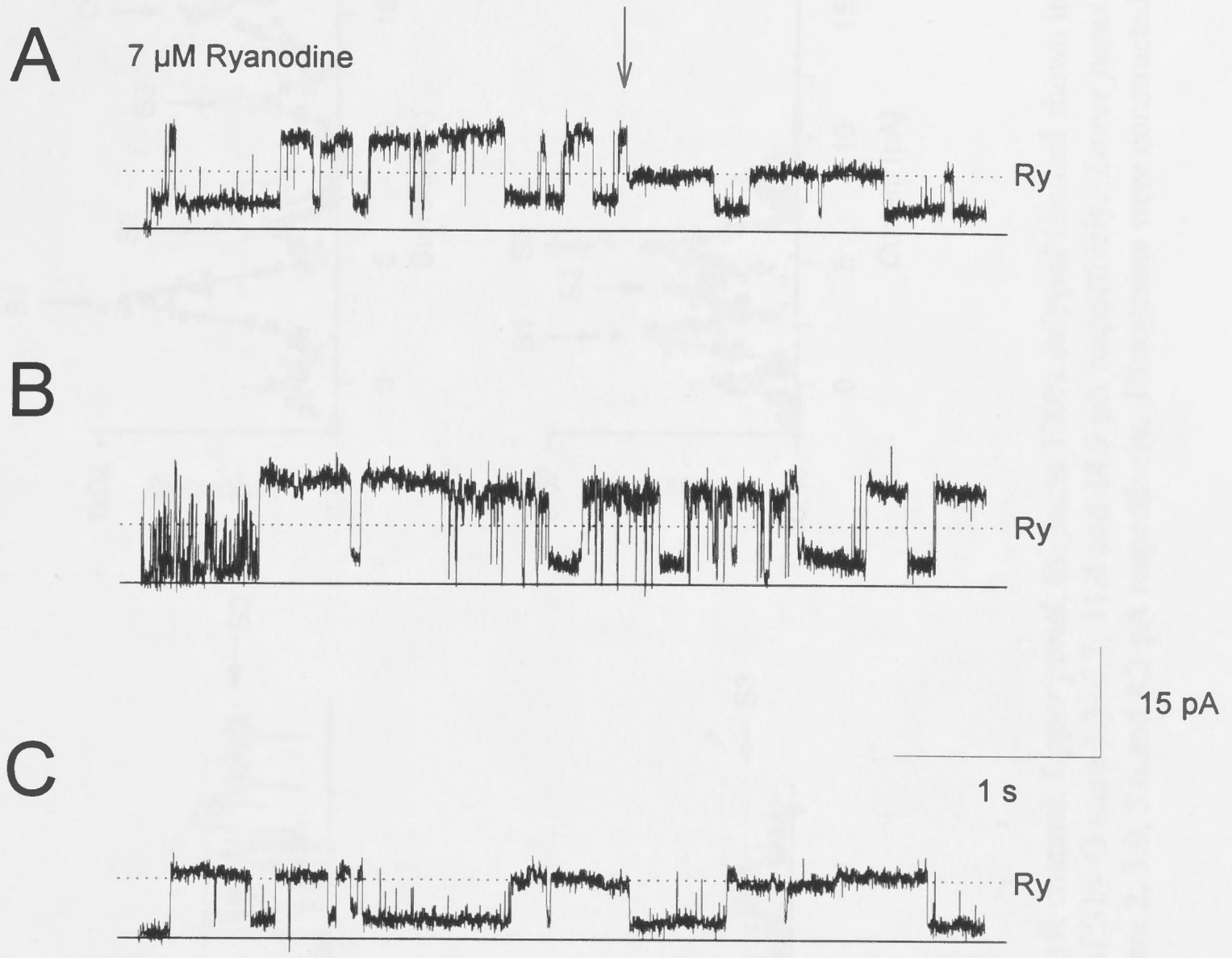

Fig. 5-16. Transient ryanodine modification in a FKBP12-stripped RyR channel. Current traces from a single RyR at +40 mV, with 1 μM *cis* Ca^{2+}, (A) shows induction of reduced conductance ryanodine state (*arrow*) 30 s after addition of 7 μM ryanodine, (B) a transient reversion to pre-ryanodine gating mode 1 min later and (C) irreversible return to ryanodine state 15 s later.

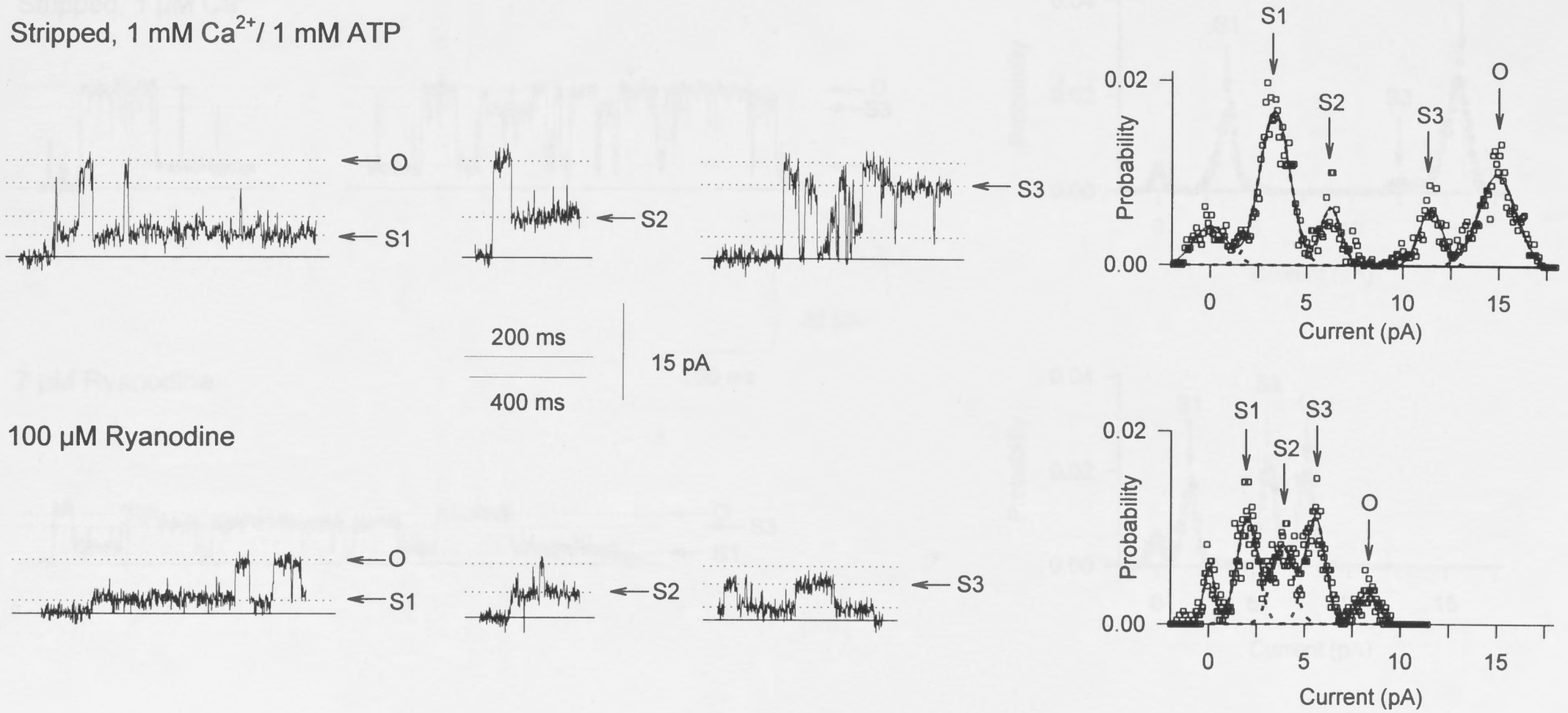

Fig. 5-17. Effect of ryanodine on multiple substates in FKBP12-stripped RyR channel. *Upper panel*, the same 100% stripped channel shown in *Fig. 5-4* with three substates, S1 - S3, and the maximal open level, O. Amplitudes of S1 - O were 3.3, 6.2, 11.4 and 14.9 pA respectively. *Lower panel*, 100 µM ryanodine reduced the current of each open level. Amplitudes for S1 - O were 2, 3.9, 5.6 and 8.3 pA respectively. Histograms were constructed from 3 - 4 s of selected data.

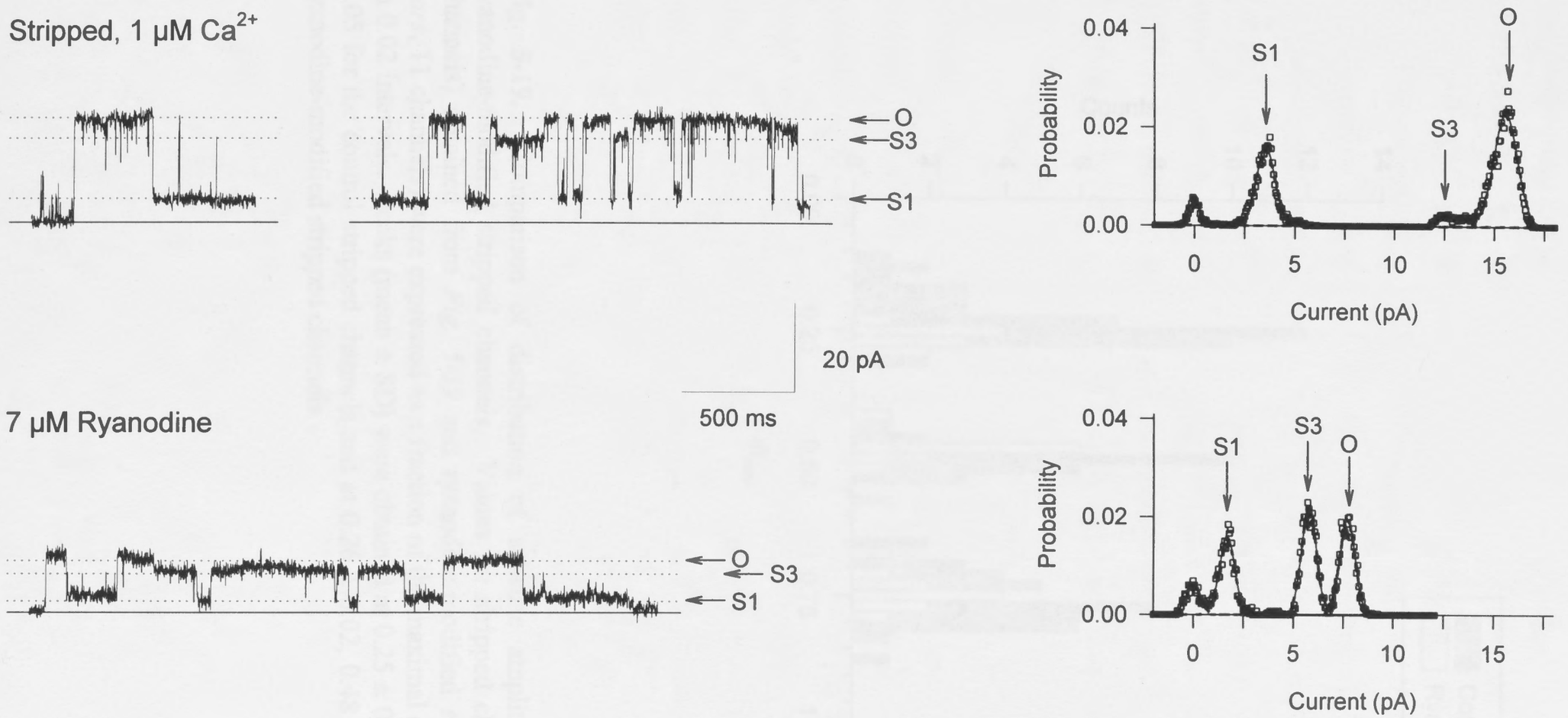

Fig. 5-18. Effect of ryanodine on partially stripped RyR channel. *Upper panel*, the same 25% stripped channel shown in *Fig. 5-5* with two substates, S1 and S3 and a maximum open level, O. Their amplitudes were 3.5, 12.9 and 15.5 pA respectively. *Lower panel,* after treatment with 7 μM ryanodine, three open levels were still observed with amplitudes of 1.7 (S1), 5.8 (S3) and 7.7 pA (O). Histograms were constructed from 7 and 3 s of data respectively.

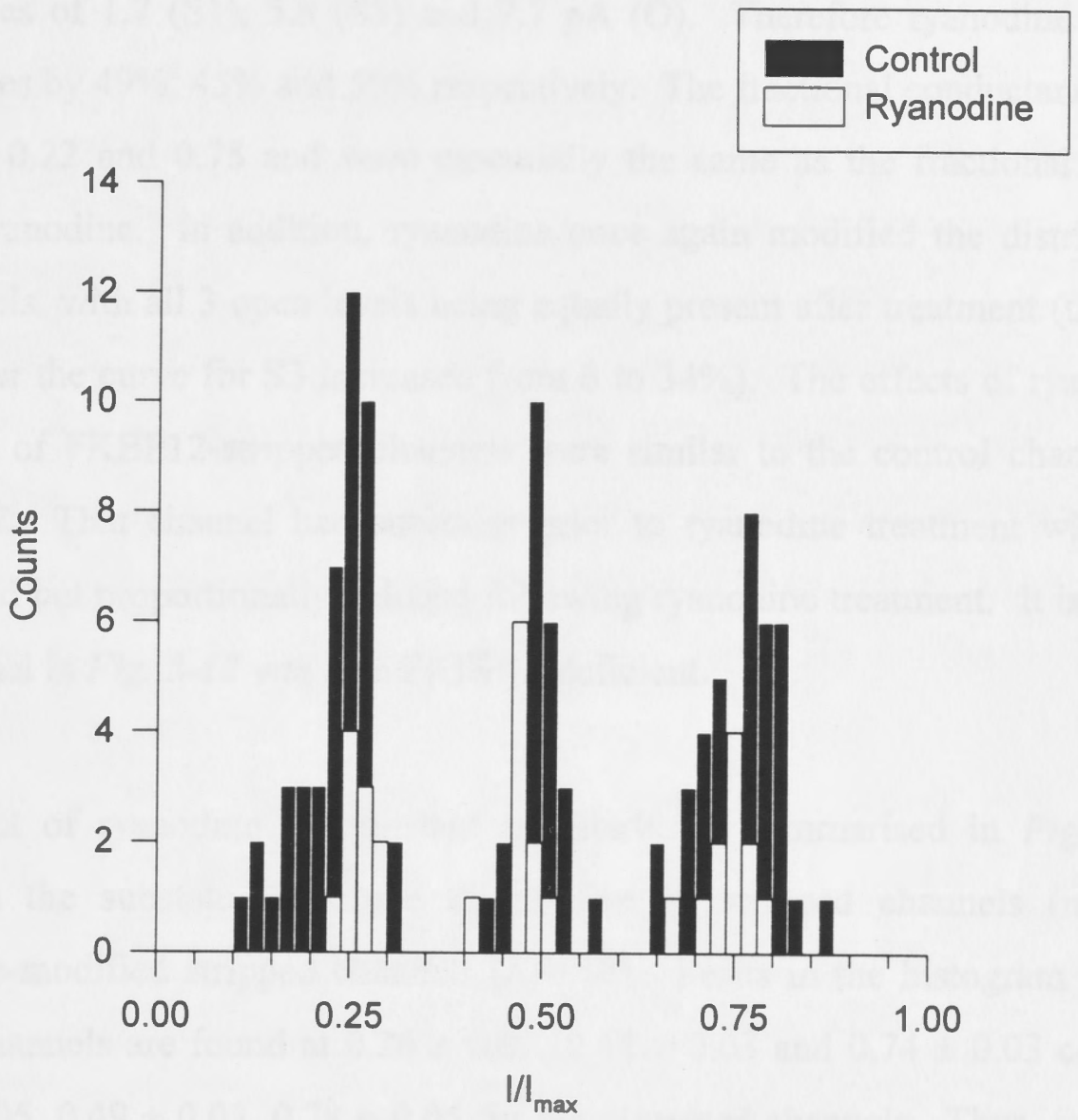

Fig. 5-19. Comparison of distribution of substate amplitudes for stripped and ryanodine-modified stripped channels. Values for stripped channels (*solid bars*, 39 channels) obtained from *Fig. 5-39* and ryanodine-modified stripped channels (*open bars*, 11 channels) were expressed as a fraction of the maximal conductance and binned in 0.02 intervals. Peaks (mean ± SD) were obtained at 0.25 ± 0.05, 0.49 ± 0.03, 0.78 ± 0.05 for the control stripped channels and at 0.26 ± 0.02, 0.48 ± 0.03, 0.74 ± 0.03 for ryanodine-modified stripped channels.

0.83. After treatment with 7 μM ryanodine, three open levels were still observed with amplitudes of 1.7 (S1), 5.8 (S3) and 7.7 pA (O). Therefore ryanodine reduced their amplitudes by 49%, 45% and 50% respectively. The fractional conductances for S1 and S3 were 0.22 and 0.75 and were essentially the same as the fractional conductances before ryanodine. In addition, ryanodine once again modified the distribution of the open levels, with all 3 open levels being equally present after treatment (the normalised area under the curve for S3 increased from 6 to 34%). The effects of ryanodine on the substates of FKBP12-stripped channels were similar to the control channel shown in *Fig. 3-12*. That channel had substates prior to ryanodine treatment which were not eliminated but proportionally reduced following ryanodine treatment. It is arguable that the channel in *Fig. 3-12* was also FKBP12 deficient.

The effect of ryanodine on substate amplitudes is summarised in *Fig. 5-19* which compares the substate amplitude distribution of stripped channels (n = 39) with ryanodine-modified stripped channels (n = 11). Peaks in the histogram for ryanodine treated channels are found at 0.26 ± 0.02, 0.48 ± 0.03 and 0.74 ± 0.03 compared with 0.25 ± 0.05, 0.49 ± 0.03, 0.78 ± 0.05 for the untreated channels. Thus, four main open levels were observed in both cases and the fractional amplitudes of substates were not affected by ryanodine treatment.

Discussion

5.13 *FKBP12 dissociation and identification of stripped channels*

In this set of experiments the role of FKBP12 in RyR function was examined by pre-stripping FKBP12 from SR vesicles prior to incorporation into lipid bilayers. Incubation with 10 μM rapamycin for 15 min at 37°C removed >90 - 95% of FKBP12 from SR vesicles.* RyR channels stripped of FKBP12 could still be identified by their characteristic ligand sensitivity. The channels were activated by ATP and blocked by ruthenium red in the same manner as unstripped RyR channels. In addition, stripped channels were sensitive to ryanodine, entering a long-lived reduced conductance mode after ryanodine treatment, and were activated and inhibited by micromolar and millimolar *cis* [Ca^{2+}] respectively, two fundamental properties of the native RyR (discussed further below).

5.14 *Subconductance states in FKBP12-stripped channels*

An important finding of this study was that FKBP12-stripped RyRs exhibited prominent subconductance states. Three major substates were observed with average fractional conductances of 0.25, 0.49 and 0.78. These results indicate that the subconductance states observed in RyRs treated with FK506/rapamycin in the bilayer (Chapter 4) were due to FKBP12 dissociation. Similar fractional conductances have been reported for the cloned, FKBP12-deficient RyR, expressed in insect cells (Brillantes *et al.*, 1994). In contrast, Mayrleitner *et al.*, (1994) did not report observing prominent substates in native FKBP12-stripped RyRs. There is no obvious explanation to account for the differences between the present study and that of Mayrleitner *et al*, but it is possible that substates were less apparent in the latter because of the presence of multiple channels in the bilayers. Multiple conductance levels in the RyR have previously been reported especially in studies using purified, detergent-solubilised channels (see *Table 1-1*). Most of those studies reported discrete conducting levels with fractional conductances of ~ 0.25, 0.5 and 0.75, although not necessarily all within a single channel. The similarity between the open levels observed in the cloned channel, the purified RyR channels and the FKBP12-stripped channels in this study, suggest that all of these

* While the degree of FKBP12 association could not be determined for a single channel, the quantitative immunoblotting analysis allowed for the prediction of the probability of such an association. Thus with 10μM rapamycin it was assumed that ~nine out of ten RyRs did not have an associated FKBP12 monomer.

channels may be FKBP12-deficient. However it is important to note: (a) that while the average substate levels reported here were fairly equally spaced, this was not always the case for individual channels, and (b) that less frequent substate levels occurred in addition to the three major levels. These points are addressed further below.

A notable feature of the substate activity was that the levels occurred with different frequencies. The S1 level was most prominent especially in amplitude analysis of longer (>15 s) sections of data (this might be expected if the open levels were due to the activity of four independent subunits with equivalent $P_o < \sim 0.2$. However, the binomial distribution is not followed because in most channels the frequency of openings to the maximum level is too great). In contrast, Brillantes *et al.*, (1994) showed that activity of the FKBP12 deficient channel was fairly equally distributed between all subconductance levels. However, they do not say whether their data is representative of activity as a whole. In this study there was considerable variability between channels in the proportion of substate to maximum open state activity observed ie. approximately half the channels opened mainly to the maximum level whereas the other half opened mainly to subconductance levels (particularly level S1). The same variability was equally evident in fully stripped and partially stripped channels which suggests that it was not due to differences in the level of FKBP12 association between channels. This result raises the possibility that factors other than FKBP12 may be required to stabilise maximum channel conductance, for example the phosphorylation state of the channel or the presence of other associated regulatory proteins such as calmodulin, triadin and calsequestrin. That factors other than FKBP12 may be required to stabilise channel conductance is also implicated by the results of Brillantes *et al.* (1994) who observed that co-expression of RyRs with FKBP12 only stabilised normal maximum conductance properties in 40% of channels. In addition, Brillantes *et al.* observed that only 3 of 32 FKBP12-deficient RyR channels exhibited openings to the normal maximum conductance level, whereas the majority of stripped channels in the present study opened, at least occasionally, to this level. An obvious explanation for the difference is that the FKBP12-stripped channels in the present study were still likely to be associated with other regulatory proteins or modified by muscle-specific post-translational processes, whereas, this may not be the case for the cloned channels expressed in an

insect cell line. Another possibility is that the differences were due to bilayer conditions, for example in the Brillantes study bilayer potential was 0 mV and caffeine was used to activate channels whereas in the present study channel activity was mostly recorded at +40 mV in the absence of caffeine. That membrane potential may influence the distribution of conductance levels in stripped channels is suggested by the different number of substates observed at +40 mV and –60 mV (*Fig.5-5*).

5.15 *FKBP12 stripped channels are more sensitive to Ca^{2+}-activation and less sensitive to Ca^{2+}-inhibition*

P_o and I' were greater in stripped compared with control channels at sub-activating and inhibiting [Ca^{2+}] but not at maximum activating [Ca^{2+}]. K_A *and* K_I were both shifted ~10-fold. An increase in the affinity of Ca^{2+}-activation (from ~ 1 μM to 0.2 μM) has previously been reported for FKBP12-stripped channels (Mayrleitner *et al.*, 1994), but a novel finding of the present study is the decrease in the Ca^{2+} affinity of inhibition. Such a decrease is consistent with the reduced Mg^{2+} sensitivity of Ca^{2+} release from stripped SR vesicles (Timerman *et al.*, 1993; Timerman *et al.*, 1995), since it is likely that both Ca^{2+} and Mg^{2+} act on the same inhibitory binding site (see Meissner, 1994; Derek Laver, unpublished observations). The parallel shift in K_A *and* K_I indicates that FKBP12 modulates the Ca^{2+} binding sites of both activation and inhibition. It is unlikely that FKBP12 directly interacts with these binding sites because they are believed to be located on separate regions of the RyR complex. Evidence for a spatial separation of Ca^{2+} binding sites is provided by the observation that caffeine selectively increases sensitivity of activation to Ca^{2+} without affecting Ca^{2+}-inhibition (Pessah *et al.*, 1987). It is more likely that removal of FKBP12 induces conformational changes in the RyR which affects binding of Ca^{2+}, and other ligands, at multiple sites. Consistent with this idea is the observation that activity of FKBP12 stripped channels are more sensitive to caffeine compared with control channels (Timerman *et al.*, 1993; Mayrleitner *et al.*, 1994).

An interesting observation is that the P_o and I' of FKBP12-stripped channels at any given [Ca^{2+}] retained the variability of control channels. This suggests that a difference

in the level of FKBP12 association between native RyRs, by itself, cannot explain the inherent variability commonly observed in native channels. As described above to account for the variability in conductances, it is likely that other factors such as phosphorylation, or oxidation state of the channel, or the presence of other associated proteins also have important roles in regulating channel activity.

The average T_o of FKBP12 stripped channels was greater than control channels at 1 mM *cis* Ca^{2+} but not significantly different at 0.1 μM Ca^{2+}. Instead the increase in P_o at 0.1 μM Ca^{2+} was mainly due to an increase in average F_o. This is in contrast to the results of Mayrleitner *et al.* (1994) who reported that, the open times of stripped channels with 0.4 μM *cis* Ca^{2+}/2 mM ATP were up to ~ 6-fold greater than control channels. The different results may be explained by the use of ATP in the Mayrleitner study, because the effects of FKBP12 removal and ATP may be synergistic. Alternatively, the open times in the present study may have been underestimated because of the presence of small unmeasurable subconductances which were not apparent or ignored in the Mayrleitner study.

An interesting observation was that the S1 subconductance level was less sensitive to inhibiting [Ca^{2+}] than the maximum open level. The open levels also displayed differential sensitivity to ATP. Similarly, different sensitivities to Ca^{2+}-activation have been reported for the low and high conductance states of the SR SCl channel (Kourie *et al.*, 1996b). Substates and main states in other channels, are also known to differ in their sensitivity to voltage (Tyerman *et al.*, 1992) and to channel blockers (Takeda and Trautmann, 1984). Differential ligand sensitivity of RyR conductance states has not been previously described, although low pH is known to favour the opening of small conductance levels in the native channel (Ma and Zhao, 1994). Ma and Zhao suggest that low pH may cause a partial dissociation of the RyR tetrameric complex and thus favour opening of individual subunits. However, in terms of a physical model of the RyR, the results reported here argue against a complex of four identical ion-conducting pores, because one might expect identical pores to have similar ligand sensitivities (see section 5.17).

5.16 *Ryanodine modification of stripped channels*

FKBP12-stripped RyRs displayed normal sensitivity to ryanodine, ie. ryanodine readily locked the channels open and reduced the maximum channel conductance by ~ 50%. However, a notable difference in stripped channels compared with control channels was that ryanodine did not induce a unitary conductance. Instead pre-existing substates which were prominent in stripped channels were retained after ryanodine modification and ryanodine reduced the conductance of each open level by ~ 50%. Earlier studies have reported subconductances in ryanodine activated channels (Buck *et al.*, 1992; Ma, 1993; Ma and Zhao, 1994). In particular, Ma and Zhao (1994) observed four equally spaced substates in native ryanodine treated channels with fractional conductances of ~ 0.25, 0.5 and 0.75. However, it was unclear in those studies how the substates in ryanodine treated channels related to substates in untreated channels. A novel finding in this study was that the three main substates induced by FKBP12 dissociation were observed before and after ryanodine treatment and that the fractional conductances of these substates remained fairly constant.

Previously, it has been suggested that the reduced conductance of the ryanodine activated channel might be due to the selective closing of ion-conducting pores in a multi-pore channel. However, the observation that the four major open levels evident in stripped channels were retained after ryanodine treatment with the same fractional conductances argues against this hypothesis. Furthermore, not only did ryanodine reduce the conductance of each open level it also increased the lifetime of each level, an effect which is very obvious in *Fig. 5-14*. In addition, ryanodine altered the relative frequency of each open state, with longer openings at levels S2 and S3 (see *Figs. 5-17* and *5-18*) suggesting that the conductance levels are regulated in a co-operative manner.

An interesting observation in two ryanodine treated stripped channels was the occurrence of a transient shift in channel activity from the ryanodine gating mode to the pre-ryanodine state (*Fig. 5-16*). This phenomenon was never observed in unstripped channels and may therefore represent a modification in the stability of the ryanodine state arising from FKBP12 deficiency. Shifts in RyR channel activity out of the

ryanodine-modified state have been observed previously with low ryanodine concentrations (~ 10 nM) in native RyRs (Buck *et al.*, 1992) and with greater ryanodine concentrations (4 μM) in a cloned, CHAPS-solubilised RyR (Chen *et al.*, 1993). Given that CHAPS-solubilised RyRs are possibly FKBP12-deficient this suggests a link between FKBP12 association and ryanodine binding. Indeed, Mack *et al* (1994) reported that FK506 treatment of SR vesicles decreased ryanodine binding affinity but also increased maximum binding.

5.17 *Implications of substates for channel structure: single, variable-diameter pore, or multi-barrelled pore?*

The existence of four equally spaced conductance levels in FKBP12 stripped channels has interesting implications for RyR structure. It has been suggested, based on this observation and the tetrameric channel structure, that the RyR consists of four separate ion permeation pathways or barrels (Smith *et al.*, 1988, Liu *et al.*, 1989; Lai *et al.*, 1989). Support for this hypothesis is given by electron microscopic studies which show an apparent low density region, which may constitute a channel pore, on the luminal side of the RyR, branching to form four radial canals exiting on the cytoplasmic side (Radermacher *et al.*, 1994). Multi-barrelled or oligomeric channels have previously been postulated to account for multiple "integer" amplitudes observed in chloride channels from *Torpedo electropax* (Miller and White, 1984), alveolar epithelium (Krouse *et al.*, 1986) and a renal tubule K^+ channel (Hunter and Giebisch, 1987). *Fig. 5-20A* shows a cartoon of a possible multi-barrel structure for the RyR with four equivalent conductive pathways in parallel. Each barrel has a separate gate. In the presence of FKBP12 (*blue*) the gates are coupled tightly and therefore open in unison, whereas in the absence of FKBP12 coupling is weaker and the gates act more independently. Consequently, this would account for four conductance levels. However, it is clear that FKBP12 cannot be the sole determinant of coupling between individual barrels because if this was the case then the frequency of conductance levels in stripped RyRs would follow a binomial distribution, (assuming equal P_o of each barrel) which they obviously did not. An alternative to the multi-barrel model, is a scheme consisting of a single barrel which has a gate and a variable calibre pore (*Fig. 5-20B*). To account for the four major open levels in stripped RyRs the pore diameter

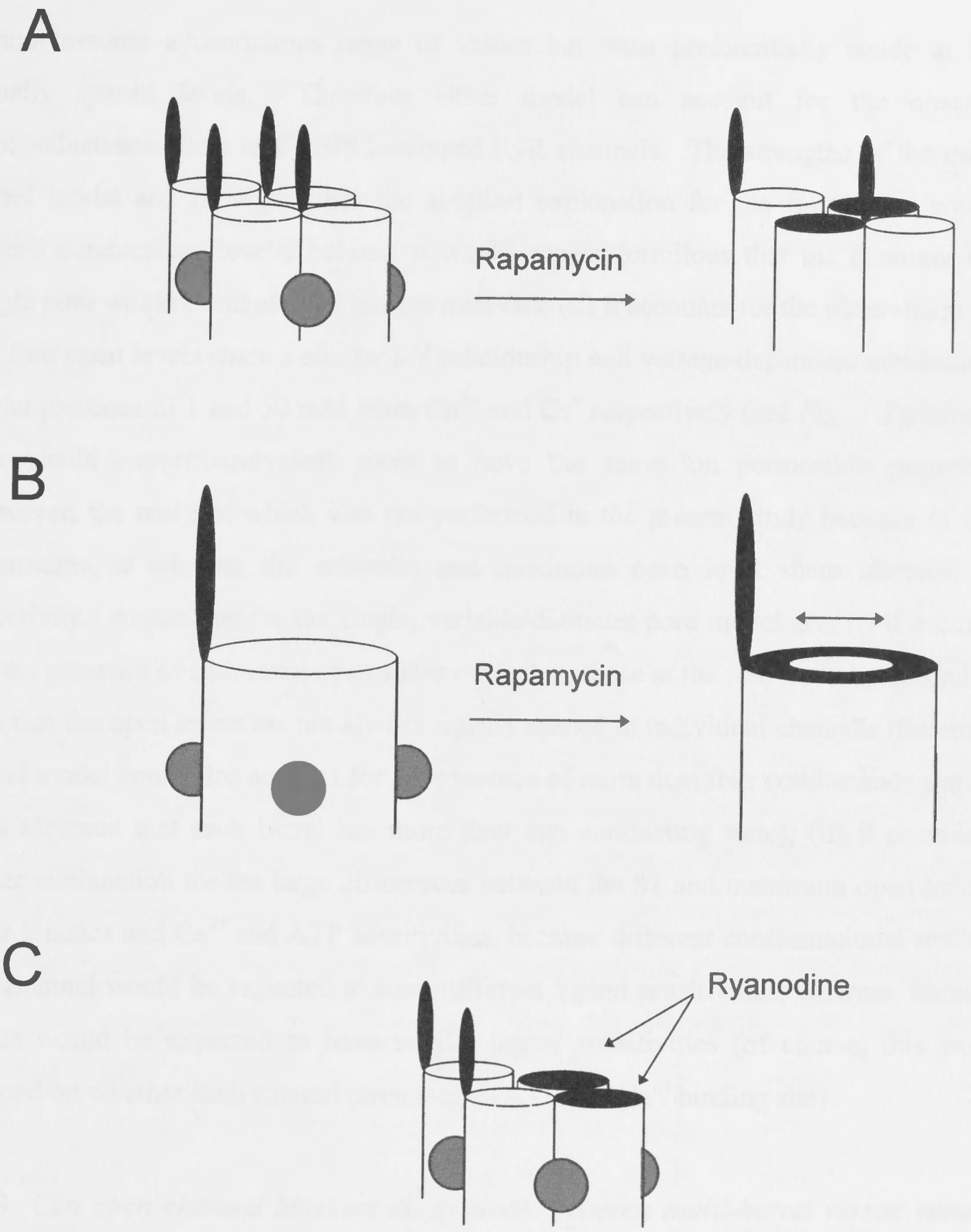

Fig. 5-20. Models of RyR channel structure. (A) Multi-barrel model, with four cylindrical pores and lids to represent possible independent gating. Associated FKBP12 monomers (*blue*) may regulate co-operativity so that the barrels open in unison, while dissociation of FKBP12 by rapamycin leads to independent gating of the individual pores. (B) Single, variable-diameter pore model. In control situation the pore diameter is fixed by FKBP12 so that openings of the gate produces unitary maximum conductances. Removal of FKBP12 allows pore diameter to fluctuate between four discrete diameter values. (C) A previously postulated action of ryanodine, closing two of four barrels in a multi-barrel channel.

cannot assume a continuous range of values but must preferentially reside at four equally spaced levels. Therefore either model can account for the observed subconductance states in FKBP12-stripped RyR channels. The strengths of the multi-barrel model are: (i) it provides the simplest explanation for the four major equally spaced conductance levels, because it would appear fortuitous that the diameter of a single pore would occur at four discrete intervals; (ii) it accounts for the observation that the four open levels share a similar I-V relationship and voltage-dependent conductance in the presence of 1 and 50 mM *trans* Ca^{2+} and Cs^{+} respectively (see *Fig. 3-2*), because you would expect equivalent pores to have the same ion permeation properties. However, the real test which was not performed in the present study because of time constraints, is whether the substates and maximum open level share identical ion selectivity. Arguments for the single, variable-diameter pore model are: (i) it accounts for the presence of additional open states other than those at the four main levels and the fact that the open levels are not always equally spaced in individual channels (the multi-barrel model could also account for the presence of more than four conductance states if it is assumed that each barrel has more than one conducting state); (ii) it provides a better explanation for the large differences between the S1 and maximum open level in their kinetics and Ca^{2+} and ATP sensitivities, because different conformational states of the channel would be expected to have different ligand sensitivities, whereas, identical pores would be expected to have similar ligand sensitivities (of course, this would depend on whether each subunit possesses an ATP and Ca^{2+} binding site).

5.18 *Can open channel blockers discriminate between multi-barrel versus variable pores in RyR?*

One way of establishing whether the RyR is multi-barrelled would be to test the effect of open channel blockers on the conductance. For example, the Mg^{2+} block of cardiac inwardly rectifying K^{+} channels produces subconductances at 0.33 and 0.66 the maximum amplitude (Matsuda, 1991). Matsuda interpreted this as suggesting that the channel was composed of three identical conducting units and that each unit was independently blocked by Mg^{2+}. Similarly, if the RyR is composed of four conducting units then an open channel blocker which independently blocked each unit would produce a amplitude distribution with four open levels. Recently, Tinker *et al.* (1992b)

and Tinker and Williams (1993), investigated the effects of large organic cations (tetrabutyl and tetrapentyl ammonium) and a charged local anaesthetic (QX314) on channel conductance in cardiac RyRs. Each drug produced a single distinct substate at ~ 21%, 14% and 34% of the maximum conductance respectively, when applied to the cytoplasmic side of RyRs only, and the occurrence of the substate was voltage dependent. The authors attributed this "substate block" to these agents binding and partially occluding the channel pore. *Prima facie* therefore, the absence of multiple substate levels in RyRs treated with open channel blockers argues against the multi-barrel hypothesis.

5.19 *A single barrel branching to form four radial pores?*

Neither model of channel structure, as outlined above, appears sufficient to adequately explain the properties of the conductance levels observed in FKBP12-stripped RyRs. While the multi-barrel model provides the simplest explanation of the observed conductance levels, a single-barrel model more adequately explains their differential ligand sensitivities and the observation that block of unstripped RyRs by large organic anions and local anaesthetics, produces unitary subconductances. Perhaps a more accurate model would be a composite of the two (*Fig. 5-21*), with a single-pore branching into four separate pathways on the cytoplasmic surface, as suggested by electron microscopic studies (Radermacher *et al.*, 1994). An advantage of this composite model is that it retains the multiple barrels which account for the discrete conductances and that it comprises a single barrel portion, presumably in the trans-membrane region where open channel blockers can interact, thereby accounting for a unitary blocked state. However, a composite model still fails to account for differential ligand sensitivity of the open levels.

5.20 *How does ryanodine reduce conductance of RyRs?*

It has been suggested that ryanodine produces a reduction in channel conductance by selectively blocking one or two pores in a multi-pore channel (see *Fig. 5-20C*). Hypothetically, if ryanodine blocked 2 of 4 pores then this would account for a near 50% reduction in current amplitude. Furthermore, it is postulated that additional

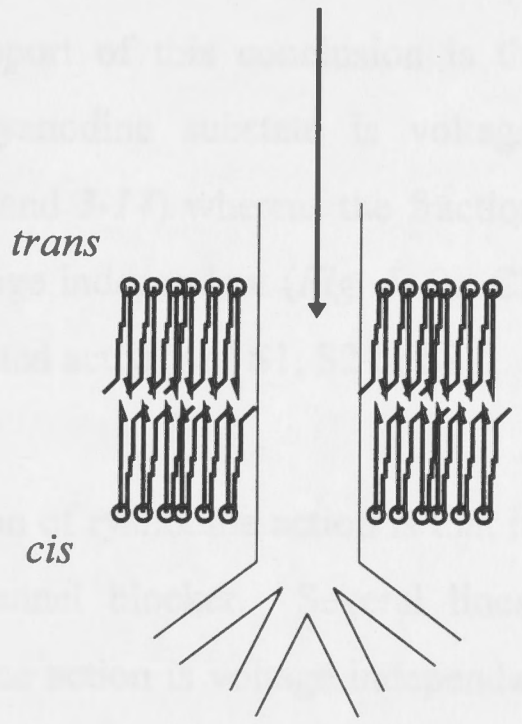

Fig. 5-21. Cartoon of a composite single-barrel/multi-barrel RyR structure. A tranverse view showing a single transmembrane pore branching to form four radial canals on the cytoplasmic surface of the protein, as suggested by electron microscopic studies (Radermacher *et al.*, 1994). As with the previous models in *Fig. 5-20*, FKBP12 may regulate co-operativity of the canals so that they open in unison. This structure may account for the unitary subconductances observed in native RyRs after treatment with agents that partially occlude the channel pore, because an open channel blocker may pass up the radial canals and bind in the transmembrane region. Occlusion of current flow in this region would produce a unitary substate in an unstripped channel, but a disproportionate reduction in the open levels of a stripped channel (see text).

ryanodine (>500 μM) may block the remaining barrels and therefore totally block the channel. Assuming that RyR conductance levels can be explained by a multi-pore channel structure, then the observation that ryanodine produces an equal reduction in conductance of each level indicates that ryanodine does not selectively inhibit individual pores, rather this indicates a current reduction independent of the gating of the pores. Other evidence in support of this conclusion is the observation that the fractional conductance of the ryanodine substate is voltage dependent under mixed ionic conditions (*Figs. 3-12* and *3-14*) whereas the fractional conductances of the substates, S1 - S3, are fairly voltage independent (*Fig. 5-6*). Clearly, the ryanodine induced state is not the result of selected activity of S1, S2 or S3.

The simplest explanation of ryanodine action is that it partially occludes the pore of the RyR like an open channel blocker. Several lines of evidence argue against this mechanism, (i) ryanodine action is voltage independent and essentially irreversible; (ii) the ryanodine substate is an "all or none" response, and does not display the dose-dependent continuum expected for an open channel blocker; (iii) ryanodine simultaneously modifies both the conductance and kinetics suggesting actions at multiple sites (Lai *et al.*, 1989; Nagasaki and Fleischer, 1988; Rousseau *et al.*, 1987). This last point suggests that ryanodine binding produces conformational changes in channel structure. Lindsay *et al.* (1994) have proposed that a stearic effect of ryanodine binding may alter ion affinity of the channel. Conductance saturates at lower ion concentrations and divalent/monovalent cation selectivity is reduced in the ryanodine modified channel (Lindsay *et al.*, 1994). Hence, changes in ion binding affinity within the channel pore(s) are likely to explain ryanodine induced changes in conductance.

5.21 *How does ryanodine produce a proportional reduction in the conductance of each open level?*

How does ryanodine produce a proportional reduction in the amplitude of the four major open levels? A simple explanation is that ryanodine alters the ion binding affinity and thus conductance, at a site upstream or downstream of the channel region responsible for multiple conductances ie. the four parallel pathways or variable-diameter region of

the channel pore. However, if ryanodine acted by merely adding a set, series resistance to ion flow then one would not expect to see an equal reduction in substate amplitude. A simple way of assessing this is with an equivalent circuit diagram (*Fig. 5-22A*). The essential features of the equivalent circuit are a battery representing electrochemical potential connecting four parallel resistors $R_{1\text{-}4}$ which each have a switch. Each resistive path represents a putative barrel in a multi-barrel channel or a set pore diameter in a single barrel channel. Thus, the circuit is valid for either the multi-barrel model, or the single, variable-diameter barrel model, at least in terms of describing conductance levels. Note that the circuit ignores the resistance of ion flow in solution which is assumed to be constant. If all switches are closed then the total resistance and conductance through the circuit are given by:

$$\frac{1}{R_{Total}} = \frac{1}{R_1} + \frac{1}{R_2} + \frac{1}{R_3} + \frac{1}{R_4}$$

$$G_{Total} = G_1 + G_2 + G_3 + G_4$$

and the G_{Total} will have a nominal value of 1. If the resistances $R_{1\text{-}4}$ are equal then the possible combination of open/closed switches will give a current distribution of 0.25, 0.5, 0.75, and 1. This arrangement accounts for four open levels of equal magnitude. To account for a reduction in conductance by ryanodine another resistance must be introduced into the circuit, R_{Ry}, the resistance due to ryanodine binding. R_{Ry} could be inserted in series with the parallel resistances at location (a) or (b) (*Fig. 5-22B*). In either case then,

$$R_{Total} = R_{1\text{-}4} + R_{Ry}$$

$$\frac{1}{G_{Total}} = \frac{1}{G_{1\text{-}4}} + \frac{1}{G_{Ry}}$$

When all switches are closed (unstripped channel) and if for simplicity $R_{Ry} = R_{1\text{-}4}$ then R_{Total} will merely double and the conductance will be halved. Thus, this would account for a 50% reduction in conductance following ryanodine treatment. However, if some of the switches are open (stripped channel) then the conductances will not be equally

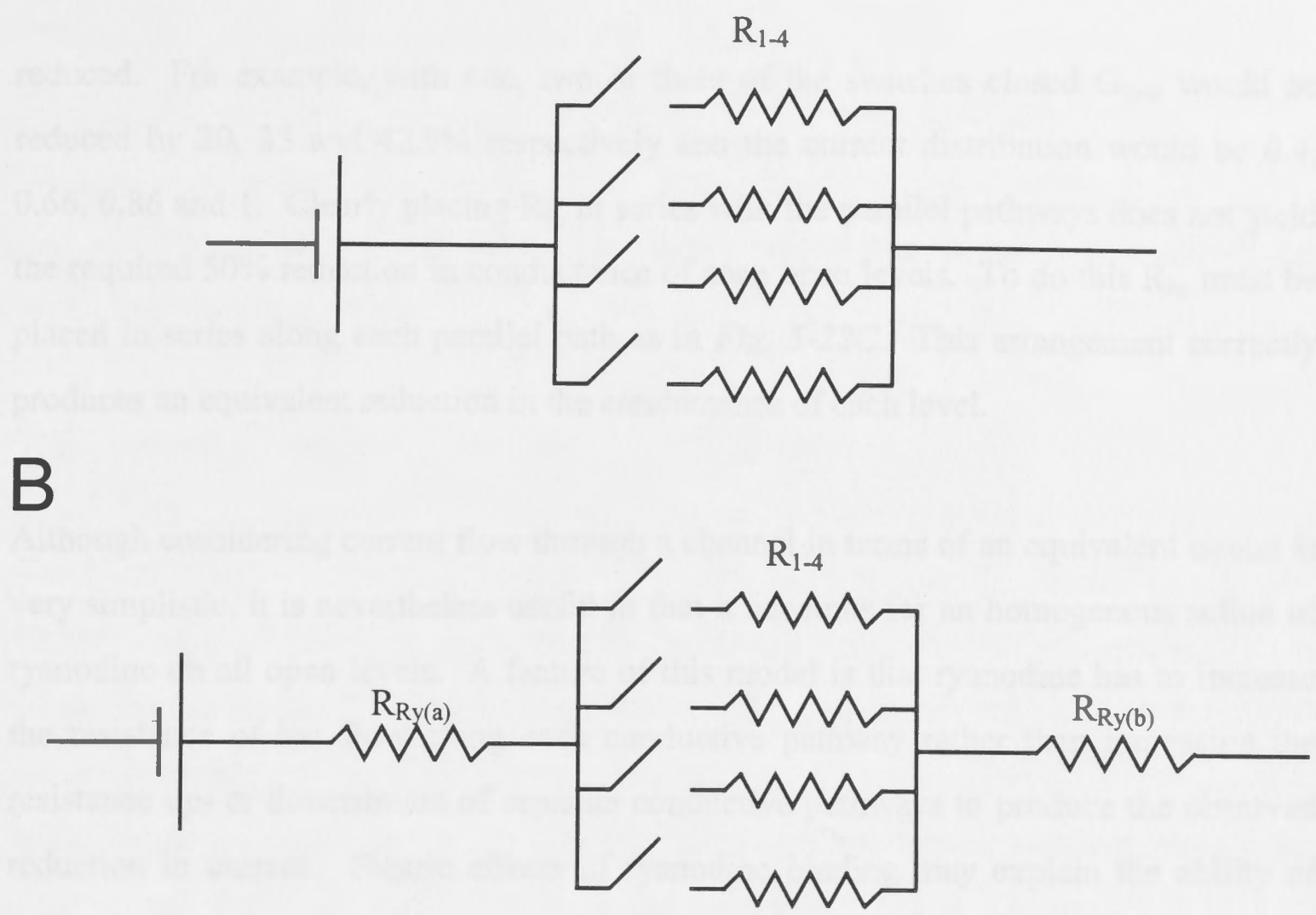

Fig. 5-22. Equivalent circuit representations of current flow in a stripped RyR channel and possible effects of ryanodine modification. (A) Control situation for a FKBP12 stripped channel, with a battery connected to four parallel, resistive pathways each with a separate switch. This circiut allows for four distinct open states with fractional conductances of 0.25, 0.5, 0.75 and 1 (assuming $R_{1\text{-}4}$ are equal). Note that the circuit ignores the resistance of ion flow in solution, which is assumed to be constant. (B) Possible introduction of an additive resistance by ryanodine either upstream or downstream of the four parallel pathways ($R_{Ry(a)}$ or $R_{Ry(b)}$). (C) An alternative possibility that ryanodine introduces a set resistance along each parallel pathway, $R_{Ry(1\text{-}4)}$. The model in (C) is more favourable because unlike (B) it predicts that ryanodine modification will produce a proportional reduction in the conductance of each pathway (see text).

reduced. For example, with one, two or three of the switches closed G_{Total} would be reduced by 20, 33 and 42.9% respectively and the current distribution would be 0.4, 0.66, 0.86 and 1. Clearly placing R_{Ry} in series with the parallel pathways does not yield the required 50% reduction in conductance of each open levels. To do this R_{Ry} must be placed in series along each parallel path as in *Fig. 5-22C*. This arrangement correctly produces an equivalent reduction in the conductance of each level.

Although considering current flow through a channel in terms of an equivalent circuit is very simplistic, it is nevertheless useful in that it accounts for an homogenous action of ryanodine on all open levels. A feature of this model is that ryanodine has to increase the resistance of ion flow along each conductive pathway rather than increasing the resistance up- or downstream of separate conductive pathways to produce the observed reduction in current. Steric effects of ryanodine binding may explain the ability of ryanodine to act at multiple sites and would be consistent with the observation that ryanodine also modified the relative frequency (ie. gating) of each open level (*Figs. 5-17* and *5-18)*. Finally, it would be interesting to investigate the effects of agents which partially occlude the channel pore, on the conductance of each open level in stripped RyRs. For example, if the RyR has a structure as depicted in *Fig. 5-21* then block in the single pore region upstream of the barrels would produce a disproportionate reduction in the conductance of each open level. Perhaps this would be a useful test to predict the ~~strutter~~ structure of the conduction pathway?

5.22 *Summary*

The major results of this study were:

(i) the FKBP12-stripped RyR exhibited three main subconductance levels (S1 - S3) that were equally spaced at ~ 0.25, 0.5 and 0.75 fractions of the maximal conductance. Other subconductances were also observed but much less frequently. Substate activity was concentrated at the S1 (0.25) level.

(ii) activity of stripped channels (P_o and I) was increased compared with unstripped channels at both sub-activating and inhibiting [Ca^{2+}] but not at maximal activating

$[Ca^{2+}]$. Increased P_o was due to both an increase in T_o and F_o. Conductance levels displayed differential sensitivity to Ca^{2+} and to ATP.

(iii) subconductances were seen with similar fractional conductances before and after ryanodine modification.

The presence of multiple conductance levels in stripped channels compared with a mostly unitary conductance in unstripped channels suggests that FKBP12 plays a role in stabilising activity to the maximum conductance. An alteration in channel structure by FKBP12 removal may explain the dual effects on the sensitivity of Ca^{2+}-activation and -inhibition. In terms of models of channel structure, the results could be used to support either a multi-barrel model, a single-variable diameter pore model or a composite of both. While the results are not entirely consistent with any model, the complexity of the conductance properties favours the composite model.

Chapter 6.

FKBP12-independent activation of the RyR by macrolides

6.1 Introduction

The results in Chapter 4 & 5 showed that the maximum P_o of RyR channels was not affected by FKBP12 removal (*Fig. 5-11*) whereas maximum P_o increased when FK506 and rapamycin were added to normal channels in bilayers (*Fig. 4-12*). How can one explain the difference between channels treated with FK506/rapamycin in the bilayer and channels stripped of FKBP12? The simplest explanation is that FK506 and rapamycin have additional actions on the RyR independent of FKBP12. Alternatively, the drugs may act solely on FKBP12 but cause a transient modification of channel properties in bilayers when they bind and dissociate FKBP12 monomers, ie. time-dependent effects of FKBP12 dissociation.

This chapter describes experiments designed to test for direct actions of FK506 and rapamycin on RyR activity. The first and simplest approach was to investigate the effect of rapamycin on RyRs fully stripped of FKBP12. In previous studies, Brillantes *et al.* (1994) reported that FK506 and rapamycin had no effect on the activity of RyRs expressed without FKBP12 and Timerman *et al.* (1995) showed that FK506 did not alter the Ca^{2+} uptake rate of TC vesicles when they were incubated at a temperature (4°C) which inhibited FKBP12 dissociation, suggesting no independent action of the drugs. In contrast, Lamb and Stephenson (1996) found that 1 μM FK506 and rapamycin caused a moderate (~ 20 - 30%), reversible potentiation of depolarisation-induced contraction in skinned, rat skeletal muscle fibres. In addition, 1 μM rapamycin enhanced caffeine-induced tension responses and this was also reversed upon washout. The reversibility of these actions suggests that they are mediated independently of FKBP12 dissociation.

The second approach was to investigate the effects of rapamycin on the CHAPS-solubilised RyR channel. Single channel studies using detergent solubilised RyRs have reported multiple conductance levels (*see Table 1-1*) similar to the FKBP12-deficient channel (Brillantes *et al.*, 1994) and the FKBP12-stripped RyR (Chapter 5), suggesting the possibility that detergent treatment causes the dissociation of FKBP12 monomers. Therefore, detergent solubilisation of RyRs may be a useful method of producing FKBP12-deficient channels and for studying direct effects of FK506 and rapamycin. In

particular, this method avoids the complications of pre-treating TC vesicles with FK506/rapamycin and ensuring complete removal of the drugs prior to bilayer studies.

The third approach was to investigate the single channel responses to addition of macrocyclic lactones, which do not dissociate FKBP12. Mack *et al.* (1994) have shown that "bastadins", a group of macrocyclic compounds with structural similarities to macrolides, modulate RyR activity without dissociating FKBP12. Bastadin 5 increased Ca^{2+} release from TC vesicles , ^{3}H-ryanodine binding and single RyR channel open time, and these effects were antagonised in a dose-dependent fashion by FK506. In addition, bastadin 5 was able to enhance FK506-dependent dissociation of FKBP12. The authors interpreted these results as suggesting that the bastadins interacted with FKBP12 at a different binding site to FK506 and rapamycin. However, another possibility is that bastadins act directly on the RyR.

I investigated the single channel effects of two commercially available macrolides, ivermectin and midecamycin.

Ivermectin (the 22,23-dihydro derivative of avermectin B_1) is a potent anti-parasitic drug widely used in veterinary medicine and for treatment of river blindness in humans (Campbell *et al.*, 1983). A feature of the chemical structure of ivermectin (*Fig. 6-1*) is the 18 member macrolactone ring. The therapeutic actions of ivermectin arise from it binding to and modifying vertebrate and invertebrate, type A γ-amino butyric acid ($GABA_A$) receptors (Sigel and Baur, 1987; Fritz *et al.*, 1979; Kass *et al.*, 1980; Mellin *et al.*, 1983; Duce and Scott, 1985) and invertebrate, glutamate-gated chloride channels (Duce and Scott, 1985; Cully *et al.*, 1994). Central nervous system effects in vertebrates are limited because ivermectin does not easily cross the blood-brain barrier (Campbell *et al.*, 1983). Binding studies suggest that ivermectin interacts with the channel at a site that is separate, but allosterically linked to the binding sites for benzodiazepines, barbiturates and picrotoxin (Pong *et al.*, 1982). A study of the effects of ivermectin on $GABA_A$ channels expressed in *Xenopus* oocytes reported showed actions (Sigel and Baur, 1987). The major effect of ivermectin was a potentiation of the whole cell GABA evoked current (K_A for ivermectin ~ 0.1 μM) with an increase in GABA affinity and a

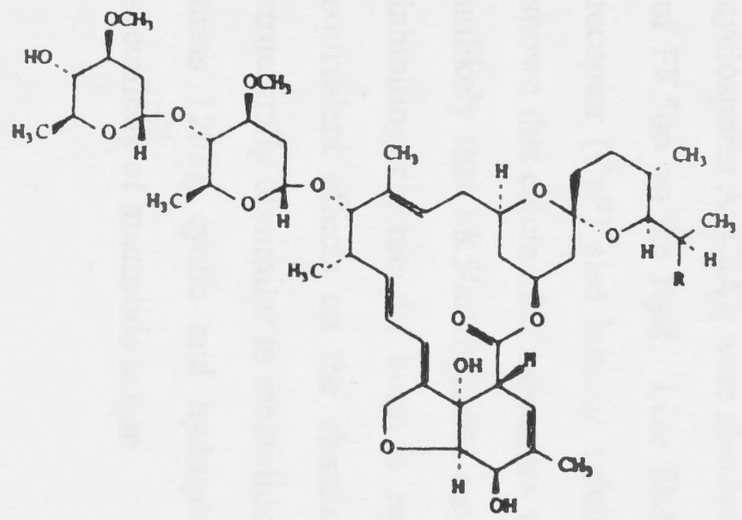

Ivermectin

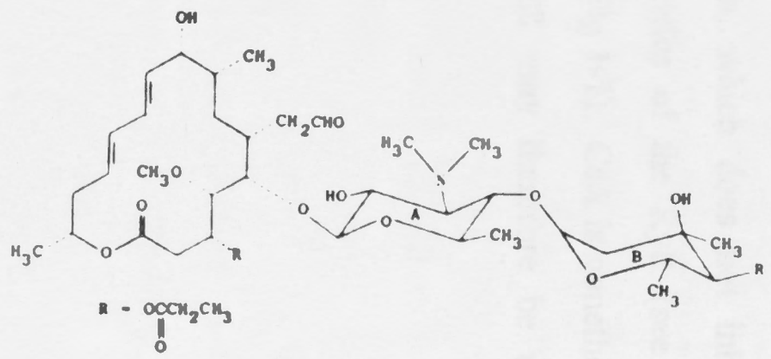

Midecamycin A_1

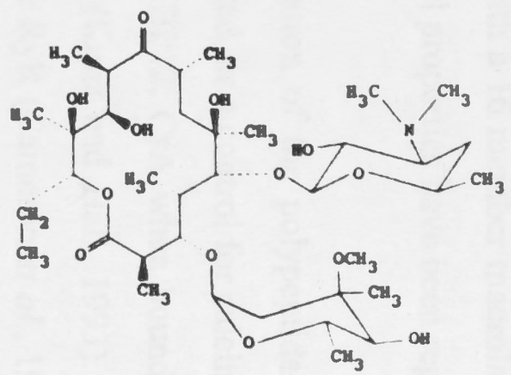

Erythromycin A

Fig. 6-1. Chemical structure of the macrolides, ivermectin, midecamycin and erythromycin. Source: The Merck index, 11th ed., Rahwey, N.J., 1989.

reduction in current desensitisation, however, a time-dependent reduction in current amplitude was also observed. Similarly, isomers of butyro-lactones have been shown to have concentration and structure dependent agonistic and antagonistic effects on $GABA_A$ receptor activity (Holland *et al.*, 1991; Peterson *et al.*, 1994).

Midecamycin is a macrolide antibiotic with a 16 member macrolactone ring (*Fig. 6-1*). No effects of midecamycin on ion channel properties have been reported.

The single channel responses to application of the polypeptide immunosuppressant, cyclosporin A (CsA), were also investigated, as a control for calcineurin specific actions of FK506 on the RyR. Like FK506-FKBP12, CsA when bound to its immunophilin receptor (CyP) also inhibits calcineurin (Kunz and Hall, 1993). A recent study has shown that calcineurin associates with the RyR (Cameron *et al.*, 1995b). However, it is unlikely that FK506 mediates any of its actions on the RyR (at least in bilayers) by inhibiting calcineurin because rapamycin, which does not inhibit calcineurin, has equivalent effects on the channel properties of the RyR (see Chapter 4). While structurally dissimilar to macrolides (see Fig 1-1), CsA is nonetheless large (molecular mass 1203), cyclic and hydrophobic and may therefore be useful in testing the specificity of macrolide action.

Results

6.2 *Rapamycin effect on FKBP12 stripped channels*

An example of the effect of rapamycin on the FKBP12-stripped RyR channel is shown in *Fig. 6-2*. This channel was derived from vesicles which had been treated with 10 μM rapamycin for 25 min at 37 °C, ie. 10 min longer than the time required to remove 97% FKBP12. Therefore, it would be reasonable to assume that these vesicles were fully stripped of FKBP12. Three subconductance states (S1 - S3) were observed in this channel with fractional conductances of ~ 0.23, 0.5 and 0.76. *Fig. 6-2A* shows a selected burst of activity with openings to S1, S3 and O (maximal open level). The presence of substates is consistent with the channel being stripped of FKBP12. In addition the P_o for this channel was 0.12 (with 1 mM *cis* Ca^{2+}), which is considerably higher than the average P_o for control channels of 0.023 ± 0.004 (n = 33), but closer to the mean for fully stripped channels (0.085 ± 0.02, n = 26). Therefore, the relatively high P_o of this channel is also consistent with it being stripped of FKBP12. *Fig. 6-2B* shows activity from the same channel after *cis* Ca^{2+} was reduced to 0.1 μM (*top trace*). The P_o was reduced to 0.012. The short open times made it difficult to measure distinct current levels but openings to level(s) just above the baseline and flickering activity to higher current levels are evident. After addition of 2.7 μM rapamycin to the *cis* chamber, P_o increased 2-fold to 0.025 (*second trace*) and after a total of 5.4 μM rapamycin was added, P_o increased a further 6-fold to 0.164 (*third trace*). Finally, washout of rapamycin from the *cis* chamber by perfusion with a solution containing 0.1 μM Ca^{2+}, reduced P_o to 0.047 (*bottom trace*). An analysis of the effects of rapamycin on the activity and kinetics of this channel is shown in *Fig. 6-3*. (*A&B*) show that both P_o and I' increased with rapamycin treatment in a dose-dependent manner and both were reduced by washout of rapamycin. (*C&D*) show that the increase in activity was the result of both an increase in T_o and F_o. The responses of T_o and F_o were dose-dependent. At 2.7 μM rapamycin, T_o was unchanged and the increase in channel activity was entirely due to a ~ 50% increase in F_o from 17.6 to 36.9 s^{-1}. At 5.4 μM rapamycin, F_o increased further to 161 s^{-1} and T_o increased from 0.68 to 1 ms. Upon washout, T_o

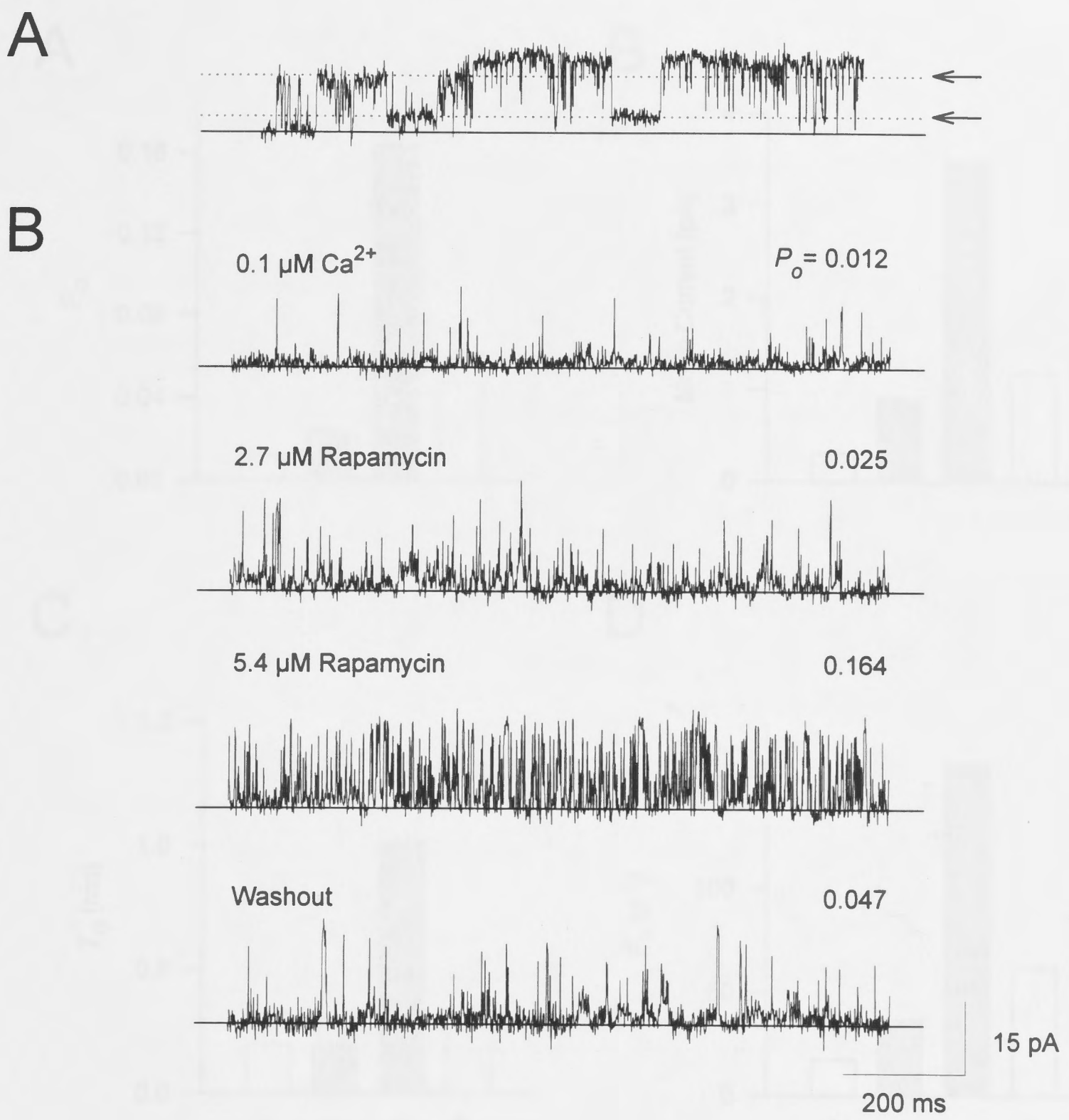

Fig. 6-2. A FKBP12 stripped RyR channel is reversibly activated by rapamycin. (A) Selected burst of channel activity from a single RyR incorporated from vesicles which had been stripped of FKBP12 by pre-treatment with 10 μM rapamycin, for 25 min at 37°C. Note the presence of subconductance states (*arrows*) which are characteristic of the FKBP12-stripped RyR channel. *Cis* Ca^{2+} was 1 mM and the bilayer potential was +40 mV. (B) Activity from the same channel after *cis* Ca^{2+} had been reduced to 0.1 μM Ca^{2+} (*upper trace*) followed by the successive addition of 2.7 μM rapamycin (*second trace*), 5.4 μM rapamycin (*third trace*) and washout of the *cis* chamber with a 0.1 μM Ca^{2+} solution (*bottom trace*). P_o is indicated at upper right of each trace and was calculated from >90 s of continuous channel activity for the top three traces and 50 s for the bottom trace.

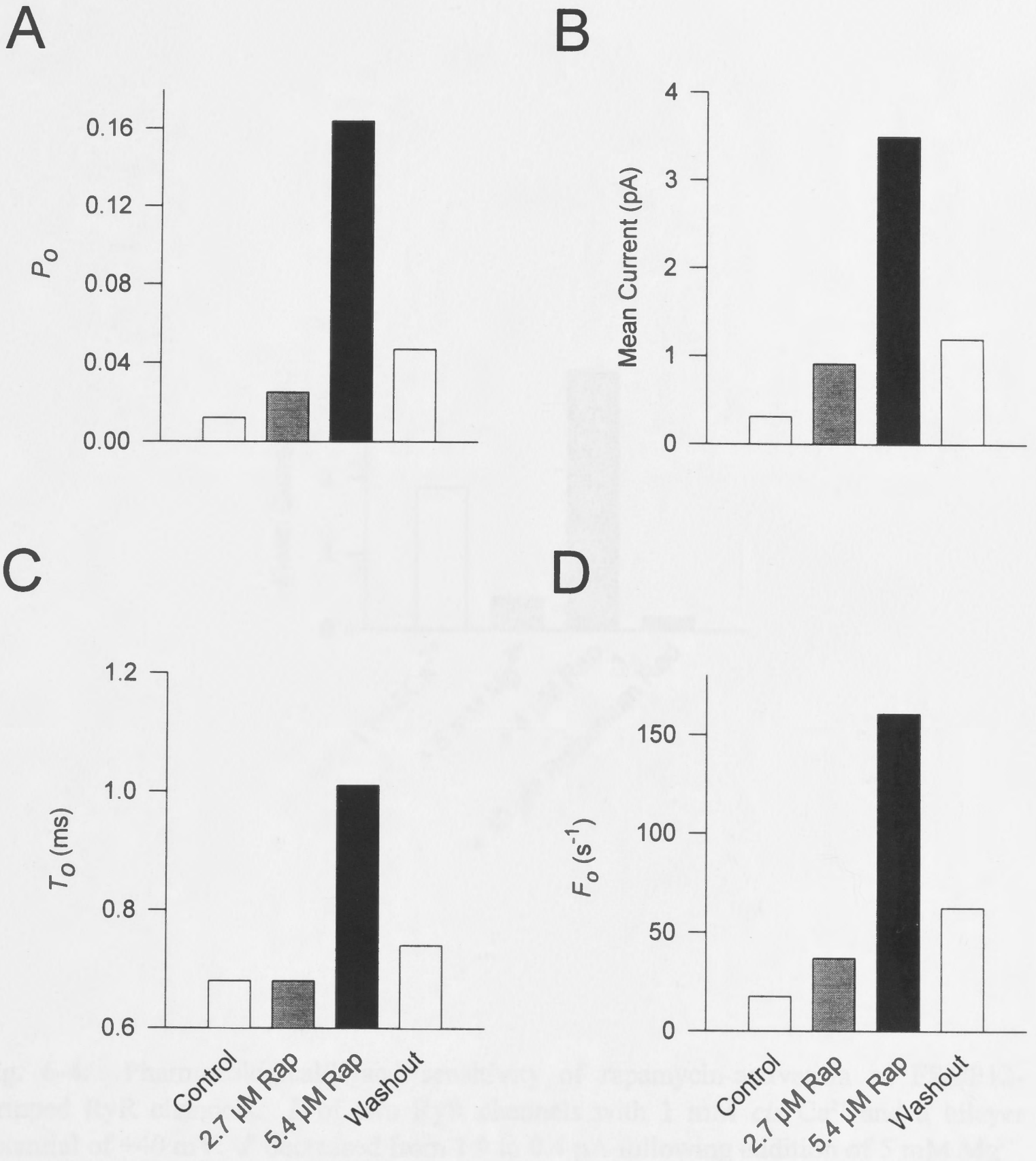

Fig. 6-3. Changes in channel activity and kinetics induced by rapamycin in a FKBP12-stripped RyR. Analysis of experiment shown in *Fig. 6-2* shows (A) P_o (B) mean current (I) (C) T_o and (D) F_o, for control, 2.7 μM rapamycin, 5.4 μM rapamycin and washout conditions as indicated.

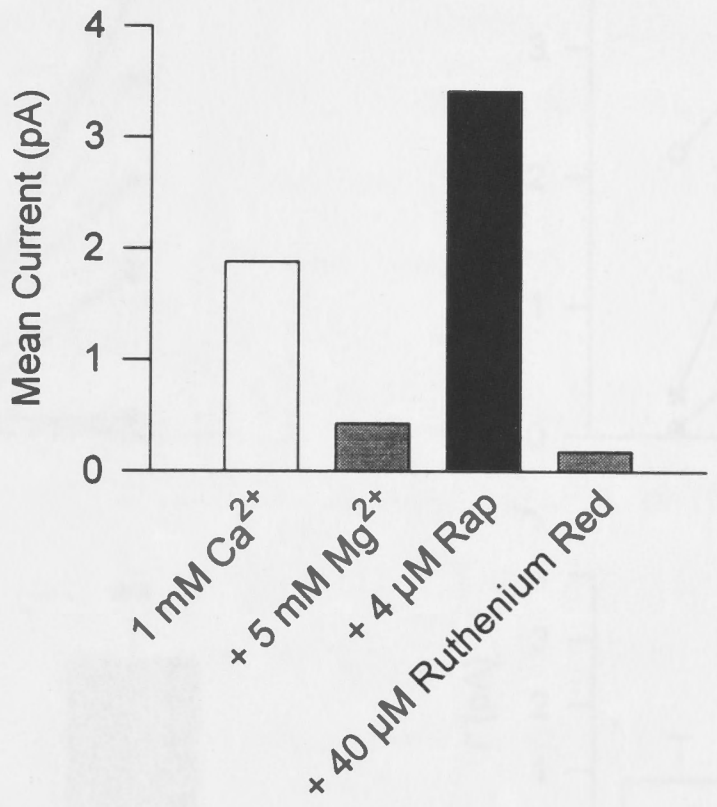

Fig. 6-4. Pharmacological/ligand sensitivity of rapamycin-activation of FKBP12-stripped RyR channels. *I'* of two RyR channels with 1 mM *cis* Ca^{2+} and a bilayer potential of +40 mV. *I'* decreased from 1.9 to 0.4 pA following addition of 5 mM Mg^{2+}. Subsequent addition of 4 μM rapamycin increased *I'* to 3.41 pA. Finally, addition of 40 μM ruthenium red blocked most of the current showing that the channels were RyRs. *I'* was measured from at least 90 s of continuous activity for each treatment.

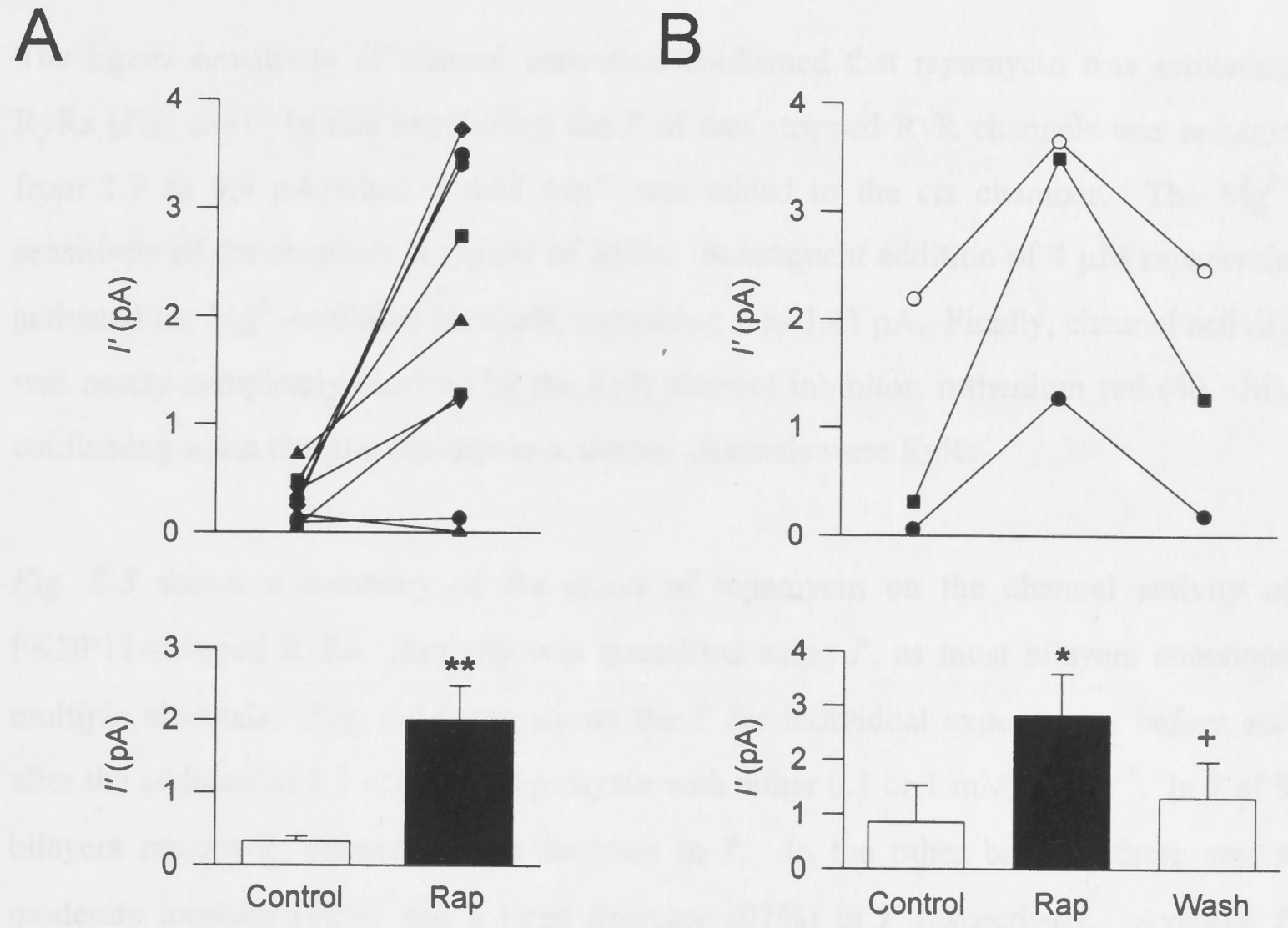

Fig. 6-5. Summary of reversible effect of rapamycin on channel activity of FKBP12 stripped RyRs. (A) *I′* before and after addition of rapamycin for nine separate experiments (*top*) and average response (mean ± sem) of same data (*bottom*). (B) *I′* for control, rapamycin and washout conditions in three separate experiments (*top*) and average values (*bottom*). Data in open symbols are values for the second addition of rapamycin for that channel. *Cis* Ca^{2+} in all experiments was either 0.1 μM or 1 mM. Statistical significance was evaluated with a paired t-test, * $P<0.05$, ** $P<0.005$ between control and rapamycin groups; $^{+}$ $P < 0.05$ between rapamycin and washout groups.

rapidly returned to the control value (0.7 ms) and F_o was substantially reduced to 62.5 s^{-1}.

The ligand sensitivity of channel activation confirmed that rapamycin was activating RyRs (*Fig. 6-4*). In this experiment the I' of two stripped RyR channels was reduced from 1.9 to 0.4 pA when 5 mM Mg^{2+} was added to the *cis* chamber. The Mg^{2+} sensitivity of the channels is typical of RyRs. Subsequent addition of 4 μM rapamycin activated the Mg^{2+}-inhibited channels, increasing I' to 3.41 pA. Finally, channel activity was nearly completely blocked by the RyR channel inhibitor, ruthenium red (40 μM), confirming again that the rapamycin-activated channels were RyRs.

Fig. 6-5 shows a summary of the effect of rapamycin on the channel activity of FKBP12-stripped RyRs. Activity was quantified using I', as most bilayers contained multiple channels. *Fig. 6-5A*, *top* shows the I' for individual experiments before and after the addition of 1.3 - 5.4 μM rapamycin with either 0.1 or 1 mM *cis* Ca^{2+}. In 7 of 9 bilayers rapamycin caused a large increase in I'. In the other bilayers there was a moderate increase (42%) and a large decrease (97%) in I' respectively. Average I' (*bottom*) increased significantly from 0.32 ± 0.07 pA to 2.00 ± 0.48 pA (± sem, n = 9, $P<0.005$, paired t-test). Furthermore, in three bilayers held while the *cis* chamber was perfused with drug-free solution, the channel activation caused by rapamycin was reduced by 70, 80 and 89% respectively after washout (*Fig. 6-5B, top*). Average I' in those three experiments (*bottom*) increased significantly after application of rapamycin from 0.85 ± 0.67 pA to 2.81 ± 0.77 pA ($P<0.05$) and fell significantly after washout, to 1.3 ± 0.66 pA ($P<0.05$).

6.3 *Reduction in maximal conductance by rapamycin*

In 8/9 experiments the maximum current level of the FKBP12 stripped channels was unaffected by rapamycin and the channels continued to display characteristic substate activity. However, in one channel the addition of rapamycin caused a dramatic increase in channel activity and reduced the amplitude of all the open levels, an effect very similar to that of ryanodine. *Fig. 6-6A* shows the gross changes in this channel in

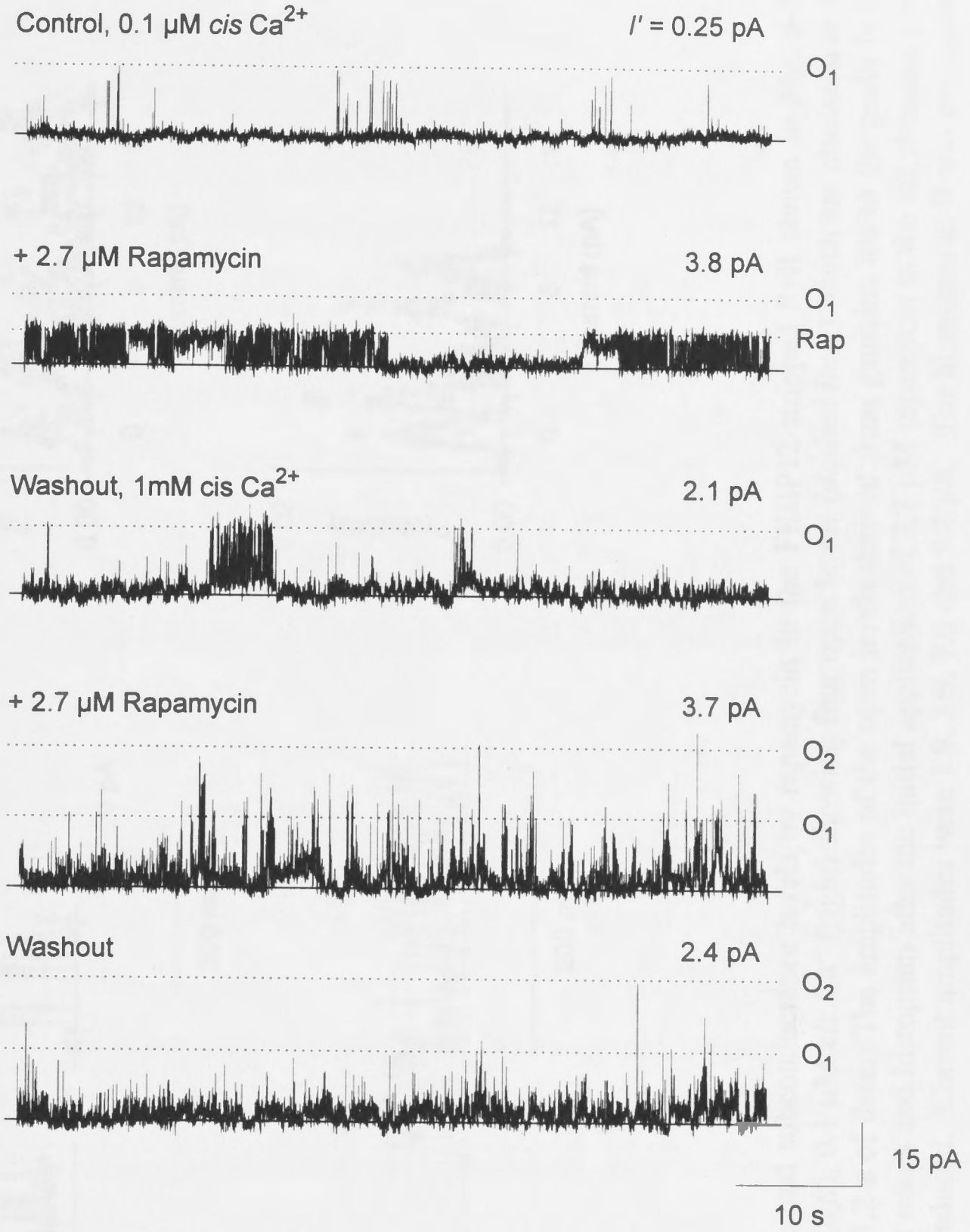

Fig. 6-6A. Reversible activation and reduction in maximal channel conductance by rapamycin in one FKBP12-stripped RyR. Traces show 60 s of continuous channel activity from a stripped RyR channel (bilayer potential +40 mV) with 0.1 µM *cis* Ca^{2+} (*top trace*) and after addition of 2.7 µM rapamycin (*second trace*), washout with solution containing 1 mM Ca^{2+} (*third trace*), re-addition of 2.7 µM rapamycin (*fourth trace*) and washout again (*bottom trace*). The initial application of rapamycin reduced the maximal open level from "O1" to "rap" and after the second application two channels became active in the bilayer (see text). Note that every 10th point has been plotted.

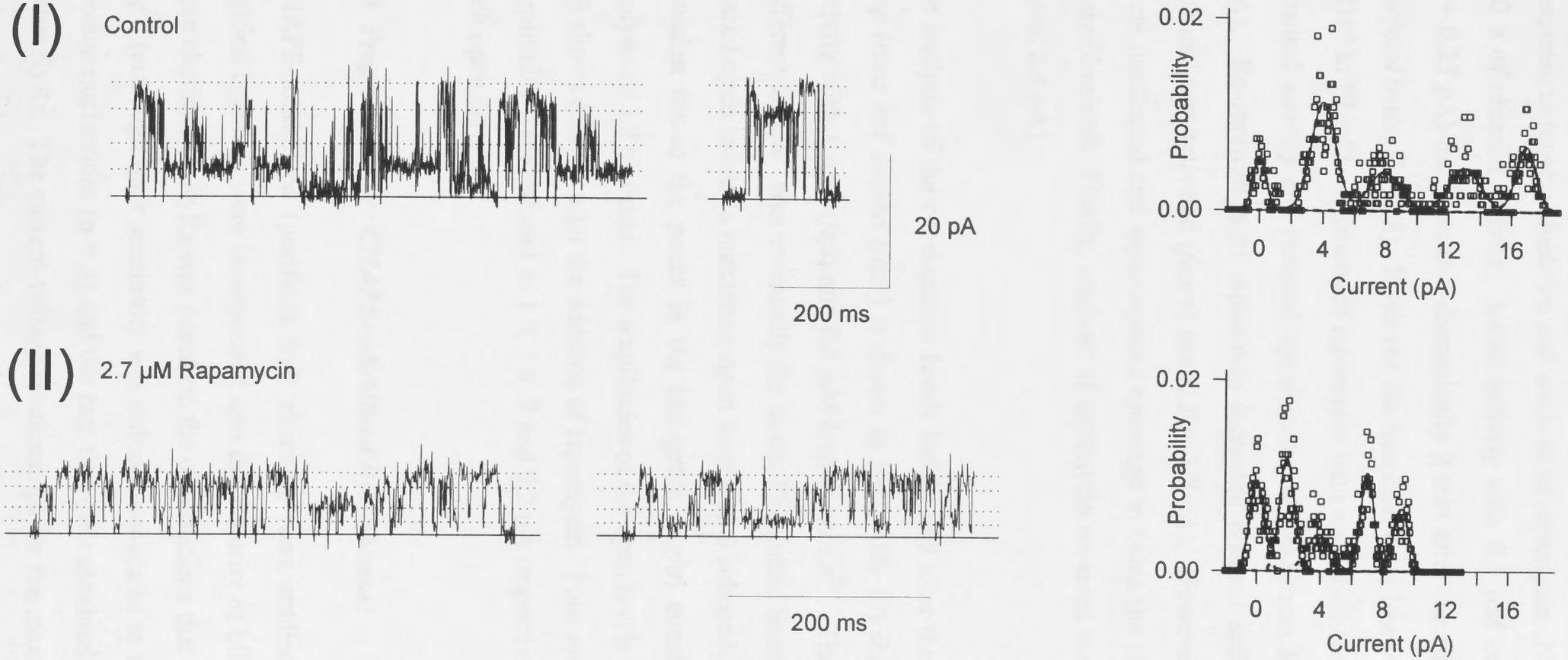

Fig. 6-6B. Parallel reduction in maximal conductance and subconductance levels by rapamycin in the FKBP12-stripped RyR shown in *Fig. 6-5A.* (I) Bursts of channel activity with 1 mM *cis* Ca^{2+}/ATP (*left*), 0.1 μM *cis* Ca^{2+} (*right*) showing four open levels (*dashed lines*) which are also seen in the histogram constructed from mean-variance analysis of 1.2 s of data. The amplitudes of the open levels derived from gaussian fits to the peaks in the histogram were 4.0, 7.9, 13.0 and 16.9 pA. (II) Current traces and histogram after the initial application of 2.7 μM rapamycin to the *cis* chamber show that the conductances of the four levels were similarly reduced. Current amplitudes were 1.9, 3.9, 7.0 and 9.2 pA. The histogram in II was constructed from 1.3 s of selected data.

response to repeated addition and washout of rapamycin. Note that each trace represents 60 s of channel activity. Initial activity with 0.1 μM *cis* Ca^{2+} was low (*top trace*, I'= 0.25 pA) but increased dramatically 2 min after the addition of 2.7 μM rapamycin (*second trace*, I' = 3.8). However, the maximal open level was reduced by ~ 50% (from "O1" to "Rap"). Washout of rapamycin with a solution containing 1 mM Ca^{2+} reduced channel activity and restored openings to the maximum level, O1 (third trace, I'=2.1 pA). Re-application of rapamycin increased channel activity and an additional RyR channel was activated (*fourth trace*, I' = 3.7 pA). However, the maximum open levels were unaffected and superimposed openings to twice the single channel amplitude (O_2) were observed. Finally, washout of rapamycin reversed the increase in activity (*bottom trace*, 2.4 pA)

An analysis of the conductance levels before and after the initial rapamycin treatment (*top trace* and *second trace*) is shown in *Fig. 6-6B*. (*I*) shows bursts of single channel activity with 1 mM (*left*) and 0.1 μM (*right*) *cis* Ca^{2+}. The maximum open level with different *cis* Ca^{2+} was essentially the same. The dotted lines indicate four nearly equally spaced open levels (a maximum open level and 3 subconductance states), derived from gaussian fits to the peaks in the histogram (*right*) constructed from mean-variance analysis of 1.2 s of data. The amplitudes of the open levels were 4, 7.9, 13 and 16.9 pA. (*II*) shows activity after the addition of rapamycin. Four open levels remained but their amplitudes were reduced to 1.9, 3.9, 7 and 9.2 pA respectively, a near 50% decrease for each open level.

6.4 *Properties of the CHAPS-solubilised RyR channel*

CHAPS-solubilised (purified) RyR channels were studied in 18 bilayers. Multiple purified channels were incorporated into the majority of bilayers. The identification of these channels as RyRs was based on the observations that they were sensitive to Ca^{2+}, Mg^{2+} (although their sensitivity was reduced compared to native channels, see below), adenine nucleotides (n = 3) and the fact that their maximal conductance was similar to native RyRs. The current-voltage relationships for the maximum open level of purified and native channels were almost identical (*Fig. 6-7B*). The reversal potential and slope

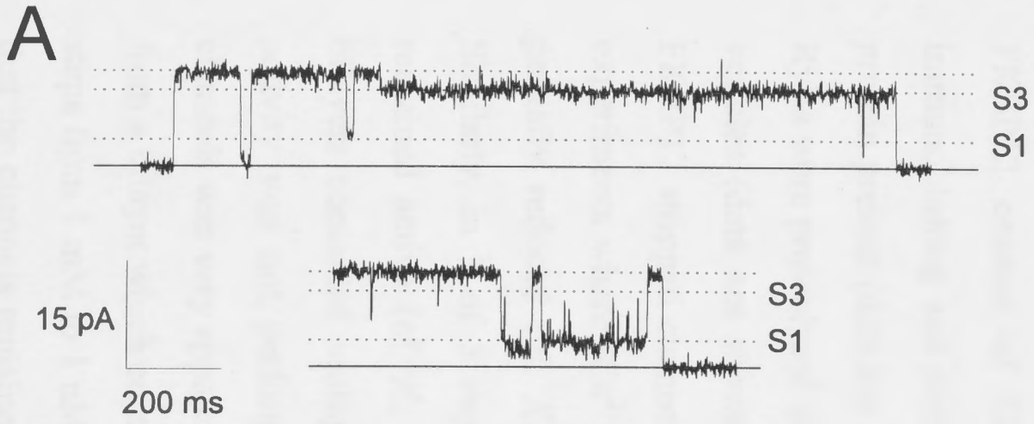

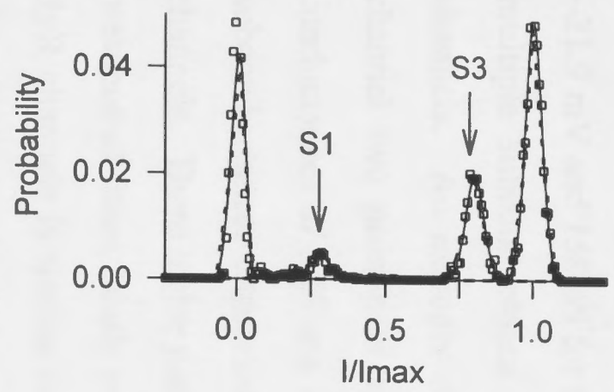

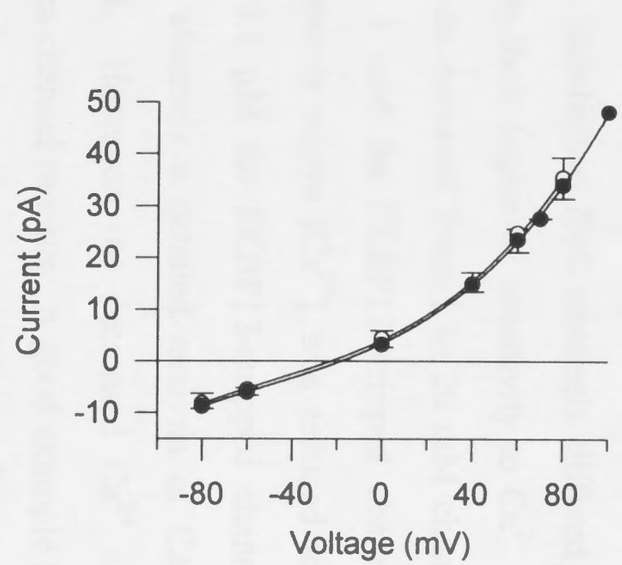

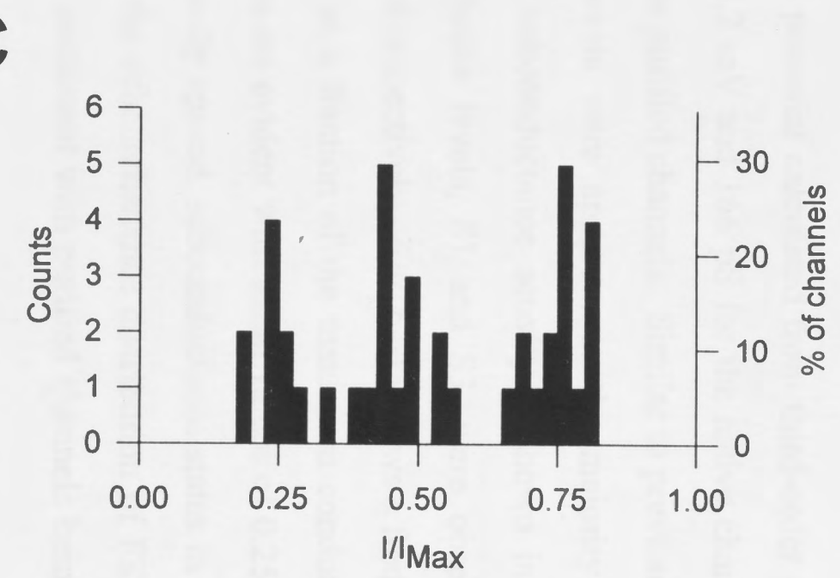

Fig. 6-7. Conductance properties of the CHAPS-solubilised RyR channel. (A) Current traces from a single RyR channel with 1 mM *cis* Ca^{2+}, bilayer potential +40 mV and a histogram constructed from mean-variance analysis of 4.6 s of data. Two prominent substates (S1and S3) are evident with fractional conductances of 0.28 and 0.8 respectively. (B) I-V relationship for the maximum open level of CHAPS-solubilised RyR channels (*open symbols*, n = 23) compared with native RyR channels (*closed symbols*, n = 8). Data are the mean ± SD and the lines are the best fit to a third-order polynomial function. The reversal potential and slope conductance at the reversal potential obtained from third-order polynomial fits to the data, were –18.2 mV and 166 pS for native channels and –21.9 mV and 158 pS for the purified channels. (C) Frequency distribution of subconductance states in CHAPS-solubilised RyR channels. Values were obtained from 17 channels, expressed as a fraction of the maximum conductance and binned in 0.025 intervals. Peaks (mean ± SD) were obtained at 0.25 + 0.04, 0.47 ± 0.05 and 0.75 ± 0.05

conductance at the reversal potential calculated from third-order polynomial functions fitted to the data, were −18.2 mV and 166 pS for the native channels, compared with −21.9 mV and 158 pS for the purified channels. Similar to previous reports (*Table 1-1*), multiple subconductance levels were apparent in the majority of solubilised RyR channels. An example of subconductance activity is shown in *Fig. 6-7A*. In this channel two prominent substate levels, S1 and S3, were observed with fractional conductances of 0.28 and 0.8 respectively. *Fig. 6-7C* shows a frequency distribution of subconductances expressed as a fraction of the maximum conductance in 17 purified channels. Three major peaks are evident with mean values of 0.25, 0.47 and 0.75. The presence of three, nearly equally spaced, subconductance states in detergent-solubilised RyR channels is similar to the subconductance distribution of FKBP12-stripped RyRs (*Fig. 5-18*) and is therefore consistent with purified channels being partially or wholly stripped of FKBP12.

FKBP12 content of CHAPS-solubilised RyR protein was detected by Western immunoblotting and estimated to be < 15% of that expected for the amount of RyR protein present (data not shown). SDS-PAGE also showed that a higher percentage of RyRs were proteolysed in the CHAPS solubilised preparation compared with native SR vesicles (data not shown). Solubilised RyR channels differed from the native and FKBP12 stripped channels in their degree of sensitivity to Ca^{2+} and Mg^{2+}. In 5 of 6 experiments where [Ca^{2+}] was increased from 1 to 20 mM channel activity was only partially reduced (cf. $K_I \sim 1$ mM for FKBP12-stripped channels, see Chapter 5). Similarly, in 3 of 5 experiments where [Ca^{2+}] was reduced to 1 nM the channels remained active (cf. $K_A \sim 0.1$ μM for FKBP12-stripped channels). Because most bilayers contained multiple channels a detailed analysis of Ca^{2+}-dependent channel activity was not performed. However, the decreased Ca^{2+} sensitivity of purified channels was very apparent in channel records. A good example is shown in *Fig. 6-8A* from a bilayer which contained at least three RyRs. *Cis* Ca^{2+} was decreased in 100-fold steps from 1 mM to 1 nM and then finally raised to 21 mM. It is clear from the traces that the channels remained robustly active with Ca^{2+} as low as 1 nM and as high as 20 mM. However, the kinetics were more rapid when Ca^{2+} was 1 or 20 mM.

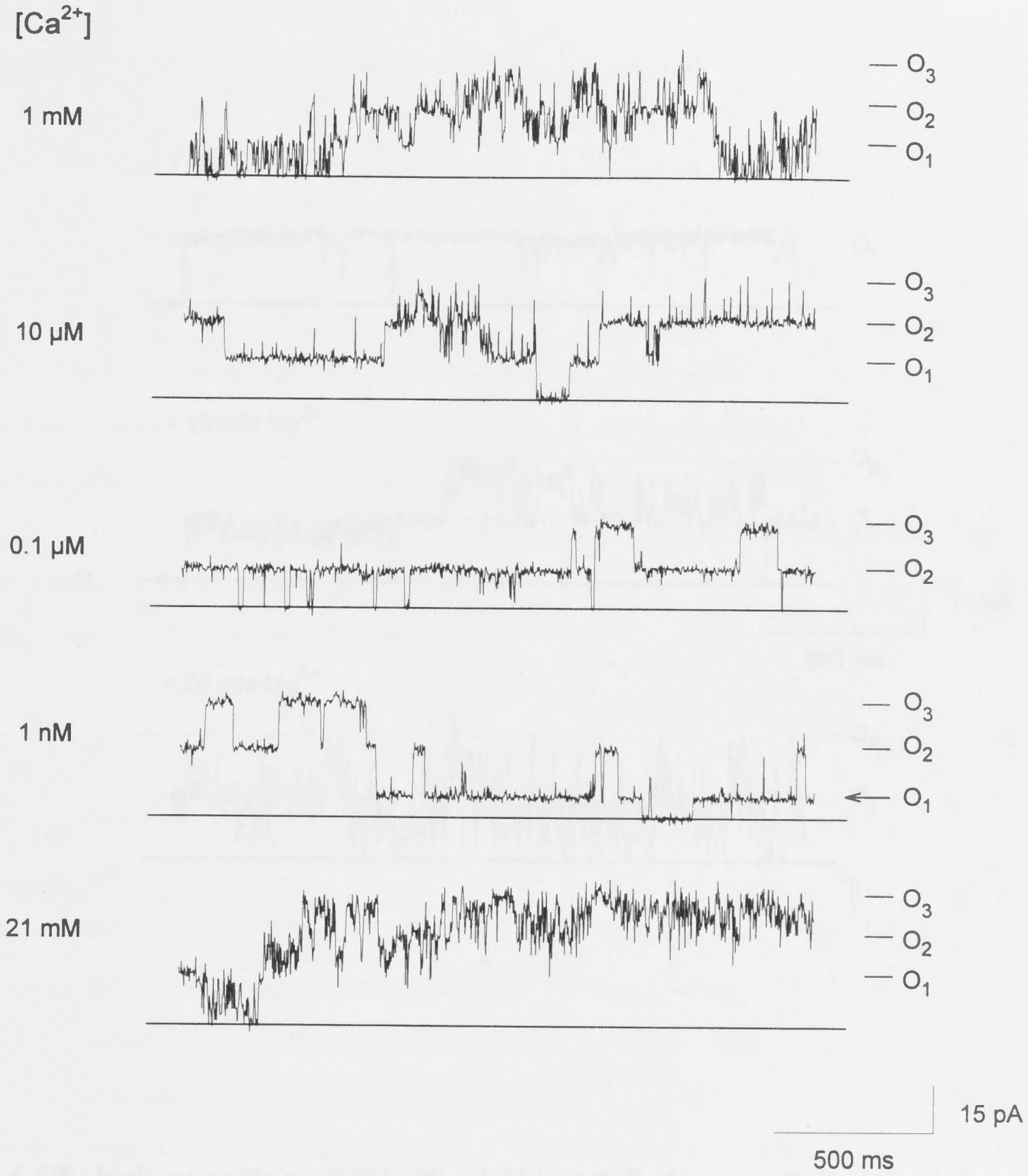

Fig. 6-8A. Ca^{2+} insensitivity of CHAPS-solubilised RyR channel. Current traces from a bilayer containing at least three RyR channels with fully open levels O_1-O_3. The bilayer potential was +40 mV. *Cis* [Ca^{2+}] was initially 1 mM and was sequentially adjusted by perfusion to indicated values. Activity of the channels was relatively independent of Ca^{2+} although the kinetics were faster in the millimolar range. Note the long-lived substate (*arrow*) at ~50 % of the main open level in one channel in the trace shown for 1 nM.

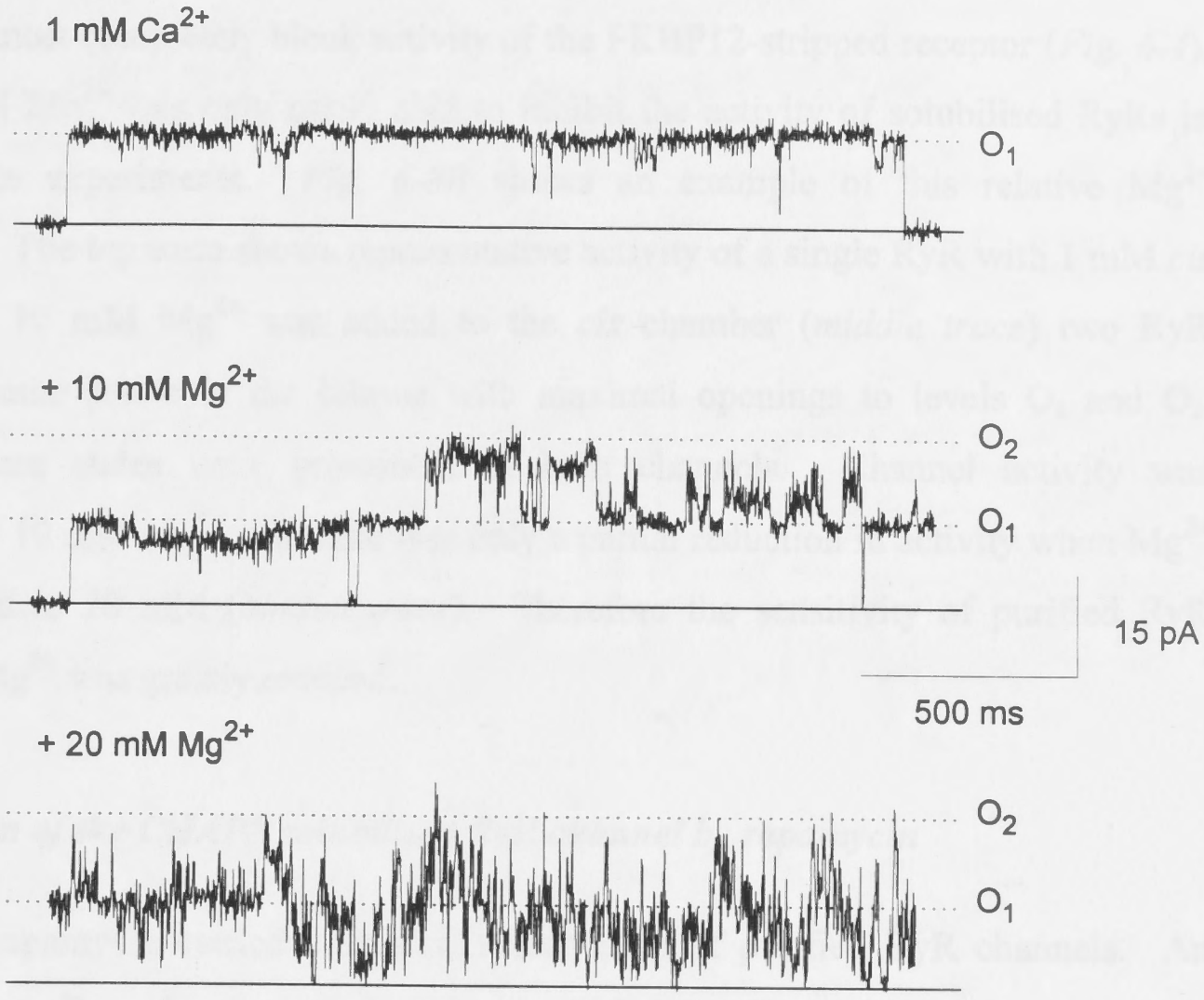

Fig. 6-8B. Mg^{2+} insensitivity of CHAPS-solubilised RyR channels. RyR channel activity from a single experiment with 1 mM *cis* Ca^{2+} (*top trace*), after addition of 10 mM Mg^{2+} (*middle trace*) and after a second addition of 10 mM Mg^{2+} (total $[Mg^{2+}]$ = 20 mM, *bottom trace*). Two channels were active in the bilayer after addition of 10 mM Mg^{2+} and the channels were only partially inhibited when the $[Mg^{2+}]$ was increased to 20 mM. Note the substates evident in both channels in the *top* and *middle traces*.

Likewise, the Mg^{2+} sensitivity of the purified RyR channel was also greatly reduced. Whereas 4 mM Mg^{2+} can totally inhibit channel activity of the native RyR (Smith *et al.*, 1986) and almost completely block activity of the FKBP12-stripped receptor (*Fig. 6-4*), up to 30 mM Mg^{2+} was only partly able to inhibit the activity of solubilised RyRs in three separate experiments. *Fig. 6-8B* shows an example of this relative Mg^{2+} insensitivity. The top trace shows representative activity of a single RyR with 1 mM *cis* Ca^{2+}. After 10 mM Mg^{2+} was added to the *cis* chamber (*middle trace*) two RyR channels became active in the bilayer with maximal openings to levels O_1 and O_2. Subconductance states were prominent in both channels. Channel activity was unaffected by 10 mM Mg^{2+} and there was only a partial reduction in activity when Mg^{2+} was increased to 20 mM (*bottom trace*). Therefore the sensitivity of purified RyR channels to Mg^{2+} was greatly reduced.

6.5 *Activation of the CHAPS solubilised RyR channel by rapamycin*

Addition of rapamycin caused a reversible activation of purified RyR channels. An example of the effect of rapamycin is shown in *Fig. 6-9*. (*A*) shows activity of a single channel under control conditions with 1 mM *cis* Ca^{2+}/0.3 mM AMP-PNP. The bilayer potential was +40 mV. (*B*) shows activity 60 s after the addition of 6 μM rapamycin to the *cis* chamber. Three channels became active in the bilayer (maximum open levels O_1 - O_3) and I' increased nearly seven-fold, from 2.1 to 13.8 pA. After washout of the *cis* chamber with 1 mM Ca^{2+} in (*C*), only 2 superimposed maximum open levels are observed (O_1 and O_2) and I' decreased to 2.5 pA. In summary, rapamycin increased the I' of purified RyR channels in 7 of 8 experiments. The average I' increased from 8.2 ± 3.1 pA to 15.1 ± 4.3 pA (mean ± sem, n = 8; $P<0.01$, paired t-test) with 6 - 13 μM rapamycin. In three experiments where the cis chamber was perfused with drug-free solutions, I' fell from 13.8 to 2.5 pA, 1.61 to 0.33 pA and 14.5 to 11.4 pA respectively. The average response was not significant.

In one purified channel, rapamycin induced a long-lived, open state with a reduced conductance (*Fig. 6-10*). The majority of openings in this channel under control conditions (1 mM Ca^{2+}, +40 mV) were to the maximal open level of 234 pS (*dashed*

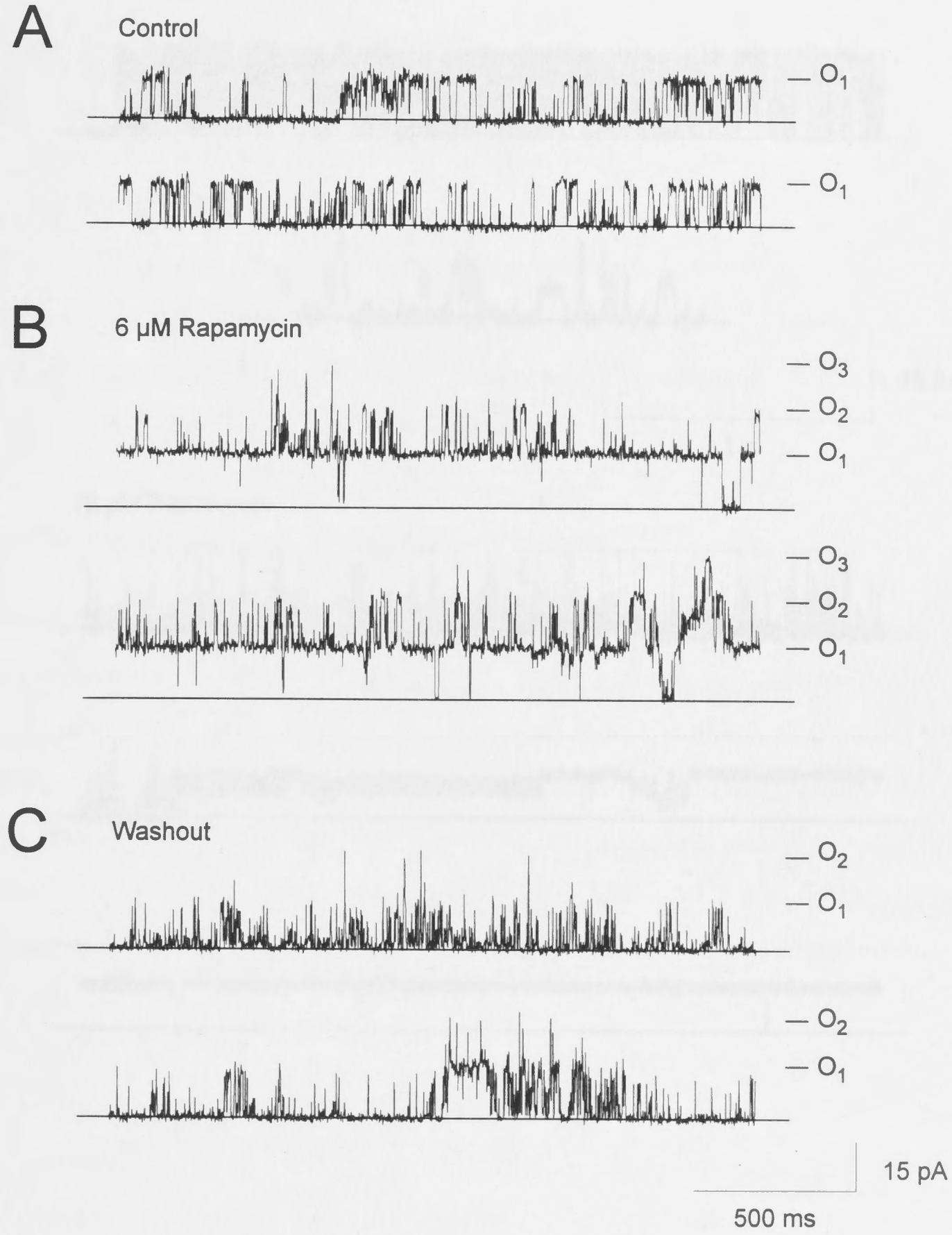

Fig. 6-9. Reversible activation of the CHAPS-solubilised RyR channel by rapamycin. (A) representative activity of a single channel recorded +40 mV, with 1 mM Ca^{2+} and 0.3 mM AMP-PNP in the *cis* chamber. "O_1" is the maximum open level. (B) Channel activity from the same experiment 60 s after the addition of 6 µM rapamycin to the *cis* chamber. Three channels are evident with superimposed openings to levels "O_1-O_3". (C) Channel activity after perfusion of the *cis* chamber with a solution containing 1 mM Ca^{2+}. Activity was reduced and only two open levels "O_1 and O_2" are evident.

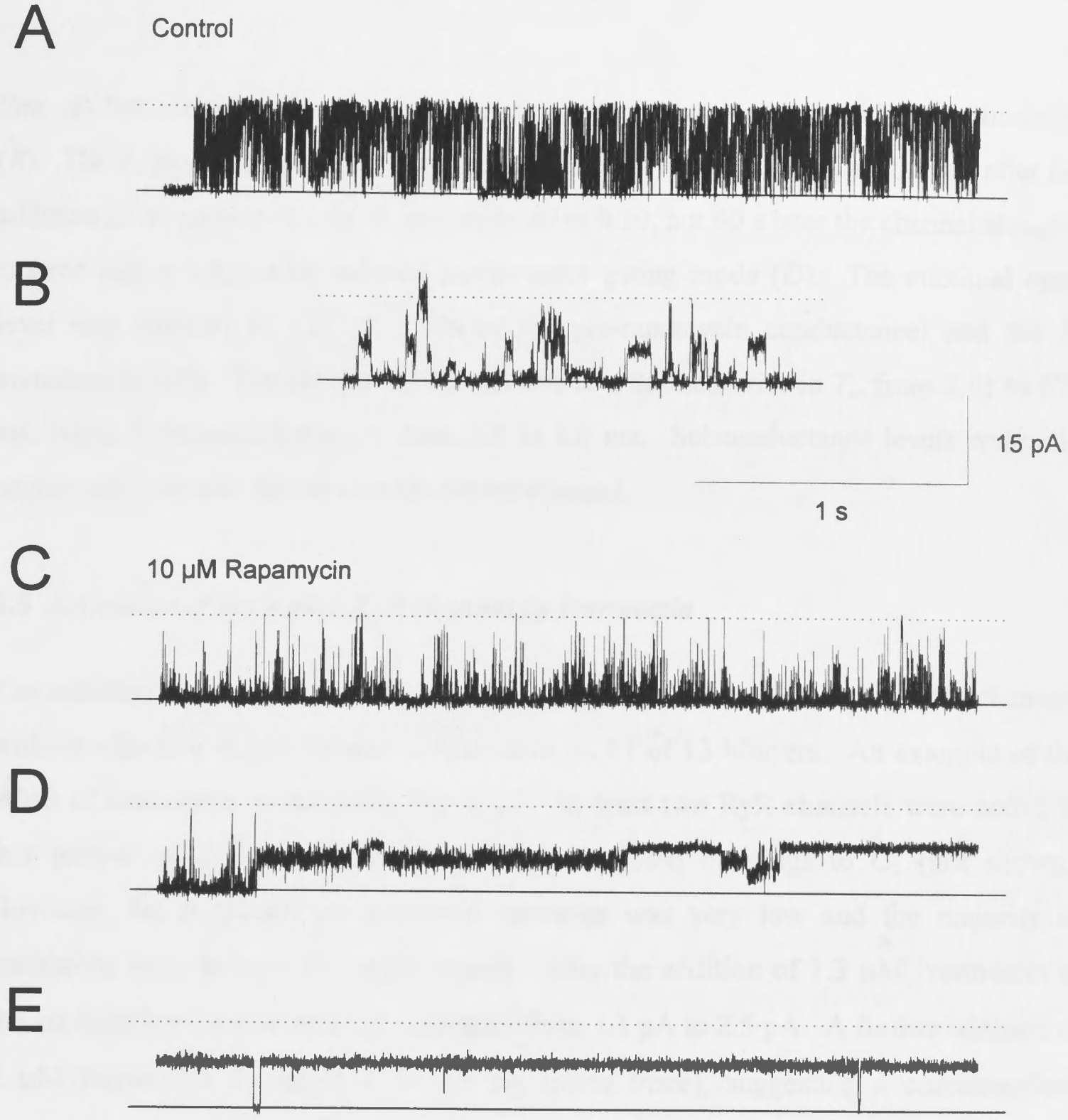

Fig. 6-10. A long-lived, low-conductance mode induced by rapamycin in a CHAPS-solubilised RyR channel. (A) Representative control channel activity with 1 mM *cis* Ca^{2+} shows transitions mainly between closed (*solid line*) and maximum open level (*dashed line*). The maximum channel conductance was 234 pS. (B) Example of subconductance states occasionally evident in the same channel. (C) Reduction in channel activity 60 s after addition of 10 μM rapamycin to the *cis* chamber. (D and E) Change in activity 60 s later, with the induction of an irreversible, long-lived, open state with a maximal conductance of 121 pS (52 % of the control).

line, A) but occasional bursts of submaximal openings were also evident as shown in (*B*). The P_o measured during 79 s of continuous activity was 0.42. One minute after the addition of rapamycin (*C*) the P_o was reduced to 0.19, but 60 s later the channel abruptly entered into a long-lived, reduced conductance gating mode (*D*). The maximal open level was reduced to 121 pS (52% of the pre-rapamycin conductance) and the P_o increased to 0.99. The increase in P_o was due to a dramatic rise in T_o, from 2.51 to 575 ms, while T_c increased slightly from 3.4 to 3.6 ms. Subconductance levels were still occasionally seen in this rapamycin altered channel.

6.6 *Activation of the native RyR channel by Ivermectin*

The anthelmintic macrolide, ivermectin, increased the P_o or I' of native RyR channels without affecting single channel conductance, in 11 of 13 bilayers. An example of the effect of ivermectin is shown in *Fig. 6-11*. At least two RyR channels were active in this bilayer as indicated by occasional superimposed openings to O_2 (not shown). However, the frequency of combined openings was very low and the majority of transitions were to level O_1 (*upper trace*). After the addition of 1.3 μM ivermectin to the *cis* chamber (*second trace*) I' increased from 1.1 pA to 2.5 pA. A further addition of 2 μM ivermectin increased I' to 6.9 pA (*third trace*), suggesting a concentration-dependent relationship between ivermectin and channel activation. Finally, 80 μM ruthenium red blocked all channel activity confirming that the channels were RyRs. *Fig. 6-12* summarises the effects of ivermectin on P_o, T_o and F_o in eight single channels mostly with 0.1 μM or 1 mM *cis* Ca^{2+}. (*A*) shows the P_o (measured from continuous activity of at least 60 s) of each channel before and after 0.66 - 4.0 μM ivermectin. In 6 of 8 channels ivermectin caused a large increase in P_o while in the other channels there was a small increase (30%) and a small decrease (17%) in P_o respectively. There was no apparent correlation between the magnitude of the response and the $[Ca^{2+}]$. Mean P_o increased from 0.015 ± 0.004 to 0.079 ± 0.019 ($P<0.01$). There was a moderate increase in T_o in all channels after ivermectin treatment (*Fig. 6-12B*) and average T_o increased from 0.71 ± 0.06 ms to 1.21 ± 0.22 ms ($P<0.05$). F_o increased in 7/8 channels (*Fig. 6-12C)* and decreased in the other. Average F_o increased from 21.2 ± 5.6 s^{-1} to 68.0 ± 10.2

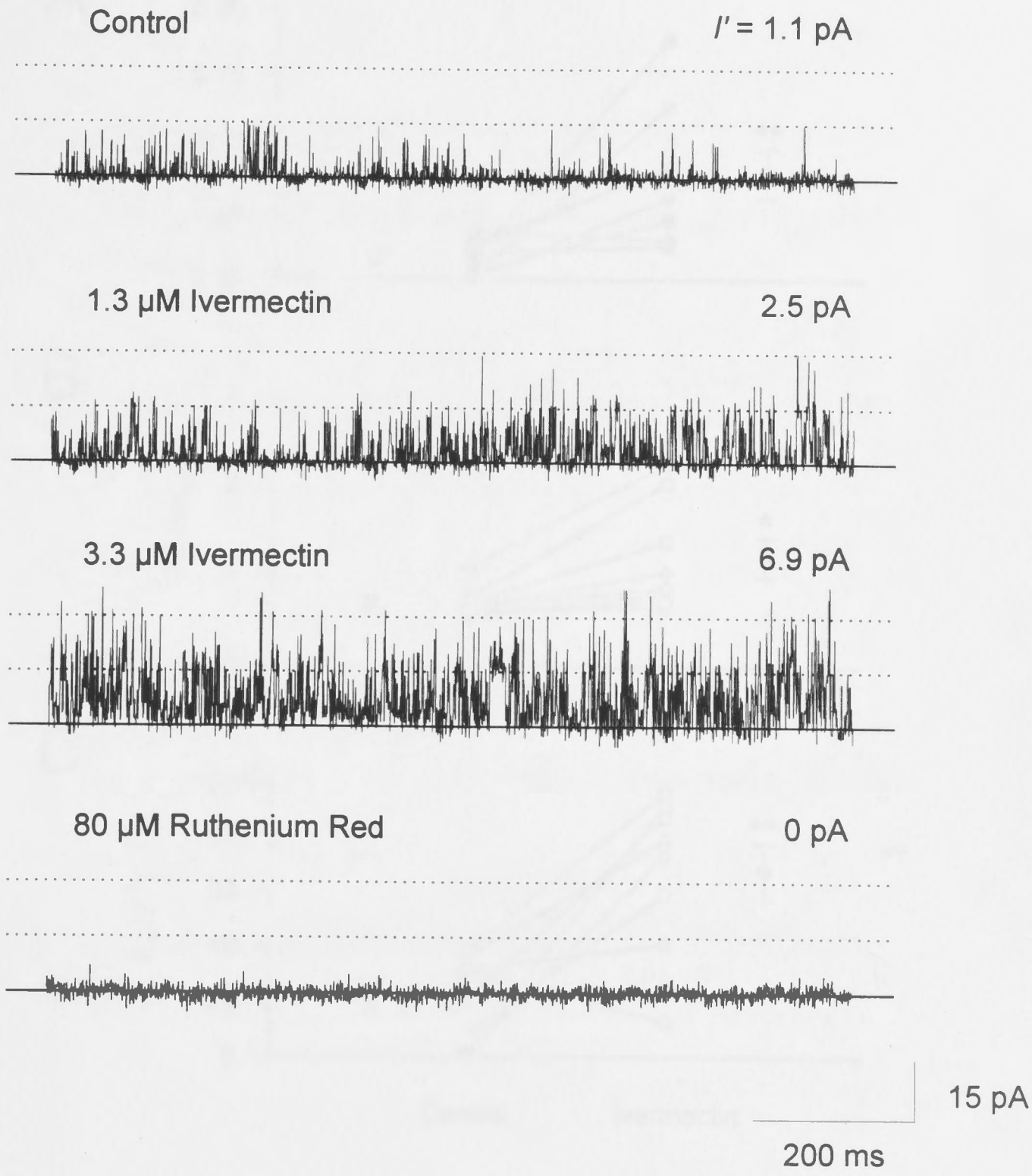

Fig. 6-11. Activation of the native RyR channel by ivermectin. Representative channel activity from a bilayer containing two RyR channels incorporated from B4 vesicles with 1 mM *cis* Ca^{2+} (control, *top trace*) and after the addition of 1.3 µM ivermectin (*second trace*) 3.3 µM ivermectin (*third trace*) and 80 µM ruthenium red (*bottom trace*). The dotted lines represent amplitudes drawn by eye for single and double channel openings. The mean current for each treatment (calculated from at least 60 s of activity) is indicated at the top right of each trace.

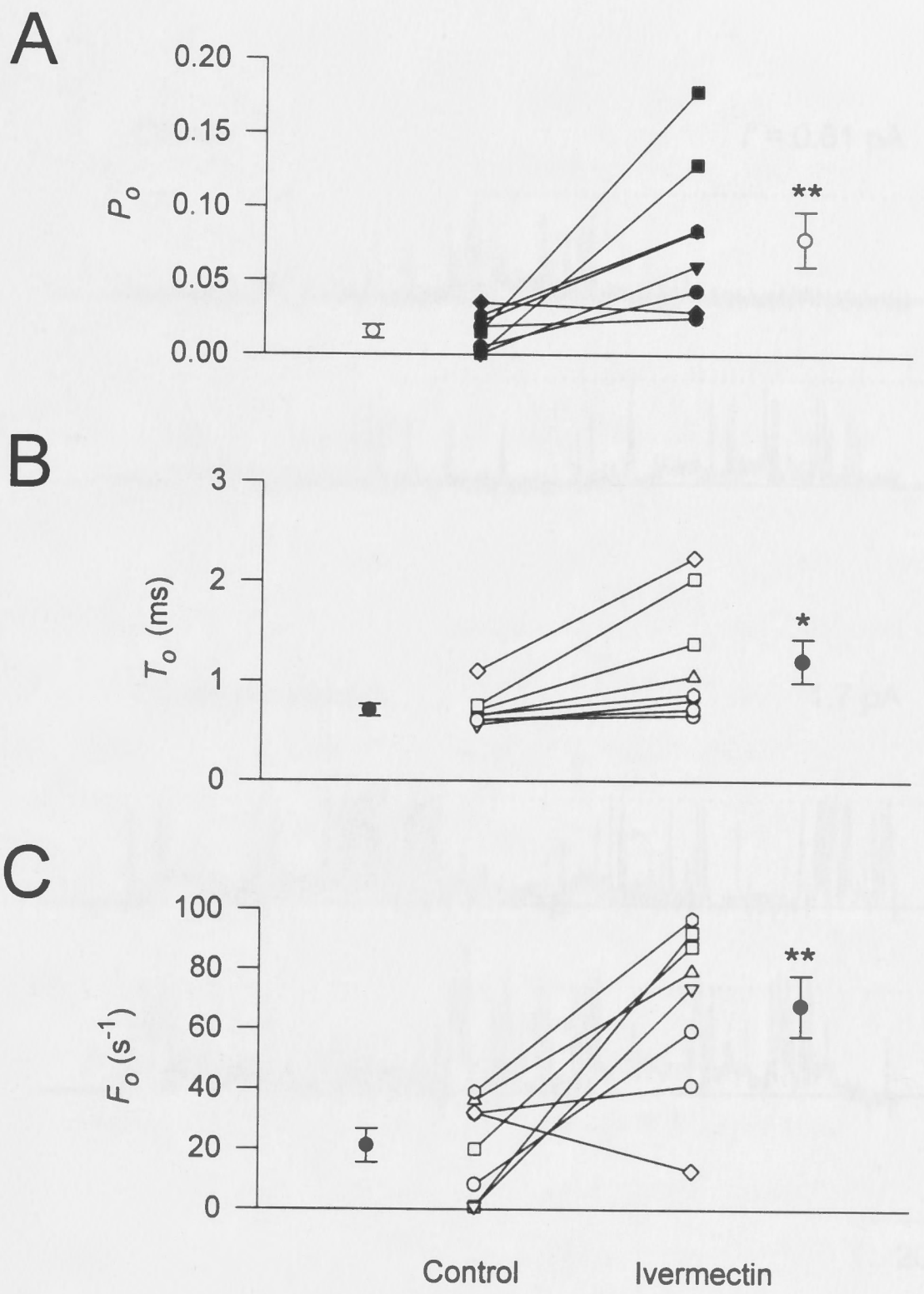

Fig. 6-12. Summary of effects of ivermectin on native RyR channel kinetics. (A) P_o (B) T_o and (C) F_o of 8 individual channels before and after treatment with 0.66 - 4.0 μM ivermectin. *Cis* Ca^{2+} was varied between 0.1 μM to 1 mM. Mean values (± sem) are plotted alongside the individual data. Differences between the means were evaluated using a paired t-test (* $P<0.05$, ** $P<0.01$).

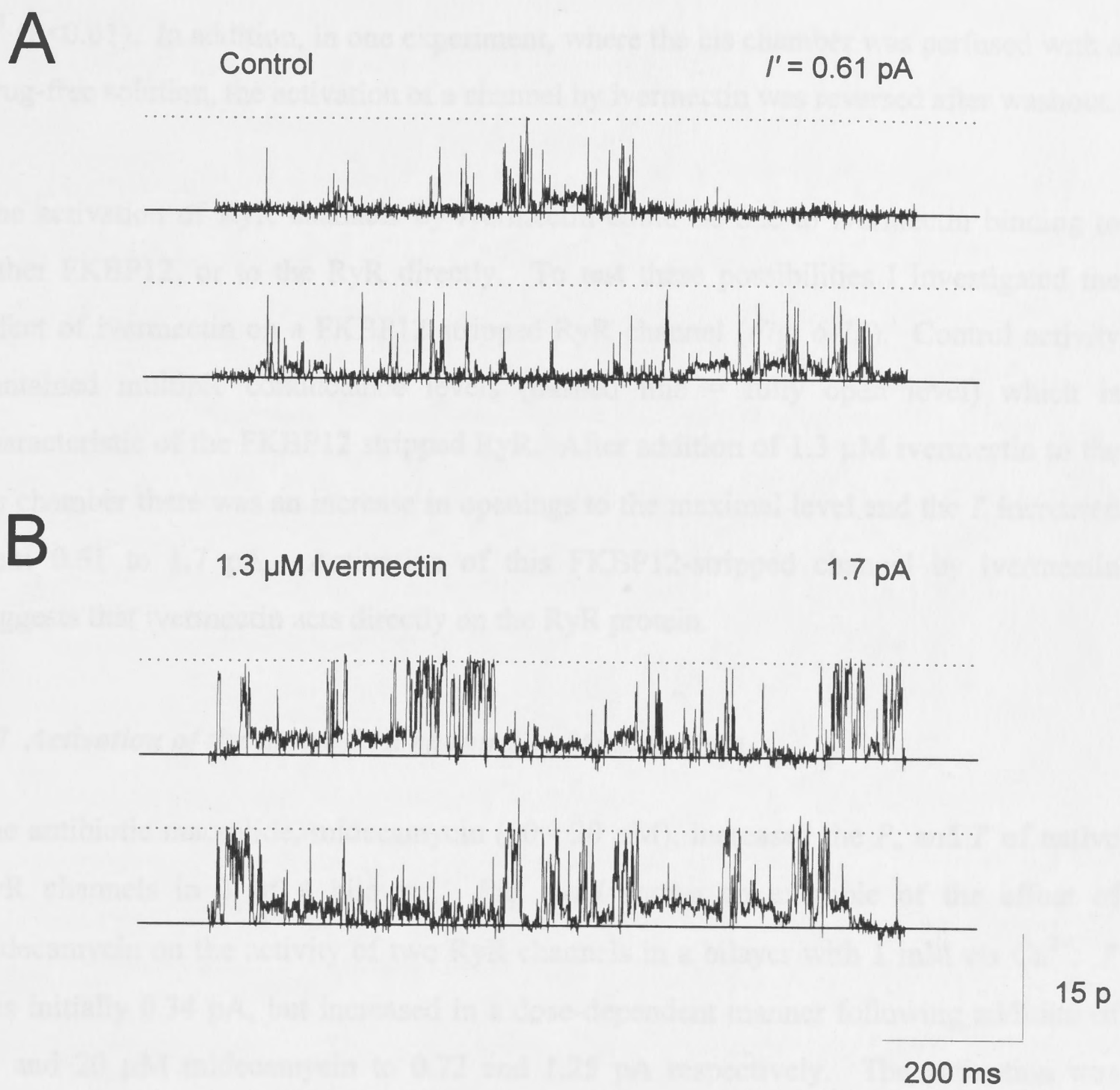

Fig. 6-13. Activation of a FKBP12-stripped RyR channel by ivermectin. (A) Representative channel activity of a RyR channel, incorporated from vesicles that were fully stripped of FKBP12 by pre-treatment with 10 µM rapamycin for 15 min at 37°C. *Cis* Ca^{2+} was 1 mM and the bilayer potential was +40 mV. The dashed line represents the fully open level drawn by eye. The prominent subconductance activity is characteristic of a FKBP12-stripped channel. (B) Activity from the same bilayer 30 s after addition of 1.3 µM ivermectin to the *cis* chamber. *I'* increased from 0.61 to 1.7 pA.

s^{-1} ($P<0.01$). In addition, in one experiment, where the cis chamber was perfused with a drug-free solution, the activation of a channel by ivermectin was reversed after washout.

The activation of RyR channels by ivermectin could be due to ivermectin binding to either FKBP12, or to the RyR directly. To test these possibilities I investigated the effect of ivermectin on a FKBP12 stripped RyR channel (*Fig. 6-13*). Control activity contained multiple conductance levels (dashed line = fully open level) which is characteristic of the FKBP12 stripped RyR. After addition of 1.3 μM ivermectin to the *cis* chamber there was an increase in openings to the maximal level and the I' increased from 0.61 to 1.7 pA. Activation of this FKBP12-stripped channel by ivermectin suggests that ivermectin acts directly on the RyR protein.

6.7 *Activation of the native RyR channel by Midecamycin*

The antibiotic macrolide, midecamycin (10 - 20 μM), increased the P_o and I' of native RyR channels in 3 of 4 bilayers. *Fig. 6-14* shows an example of the effect of midecamycin on the activity of two RyR channels in a bilayer with 1 mM *cis* Ca^{2+}. I' was initially 0.34 pA, but increased in a dose-dependent manner following addition of 10 and 20 μM midecamycin to 0.72 and 1.25 pA respectively. The activation was reversed upon washout of the *cis* chamber and the I' decreased to 0.45 pA. A second addition of 10 μM midecamycin produced a greater activation compared with the first treatment and I' increased to 2.01 pA. Finally, the addition of 13 μM ryanodine locked both channels into the characteristic ryanodine substate gating mode. In two other bilayers with single RyR channels (and 1 mM *cis* Ca^{2+}), midecamycin (10 and 16 μM) increased the P_o from 0.029 to 0.051 and 0.05 to 0.17 respectively. The increase in P_o was due to small increases in T_o, from 0.64 to 0.71 ms and 0.89 to 1.19 ms, and larger increases in F_o, from 44.3 to 71.8 s^{-1} and 56.7 to 142.3 s^{-1}.

6.8 *Activation of the native RyR channel by CsA*

CsA increased native RyR channel activity (P_o and I') in 22 of 28 bilayers with 1 μM - 1 mM *cis* Ca^{2+}. *Fig. 6-15* shows an example of the increase in activity with

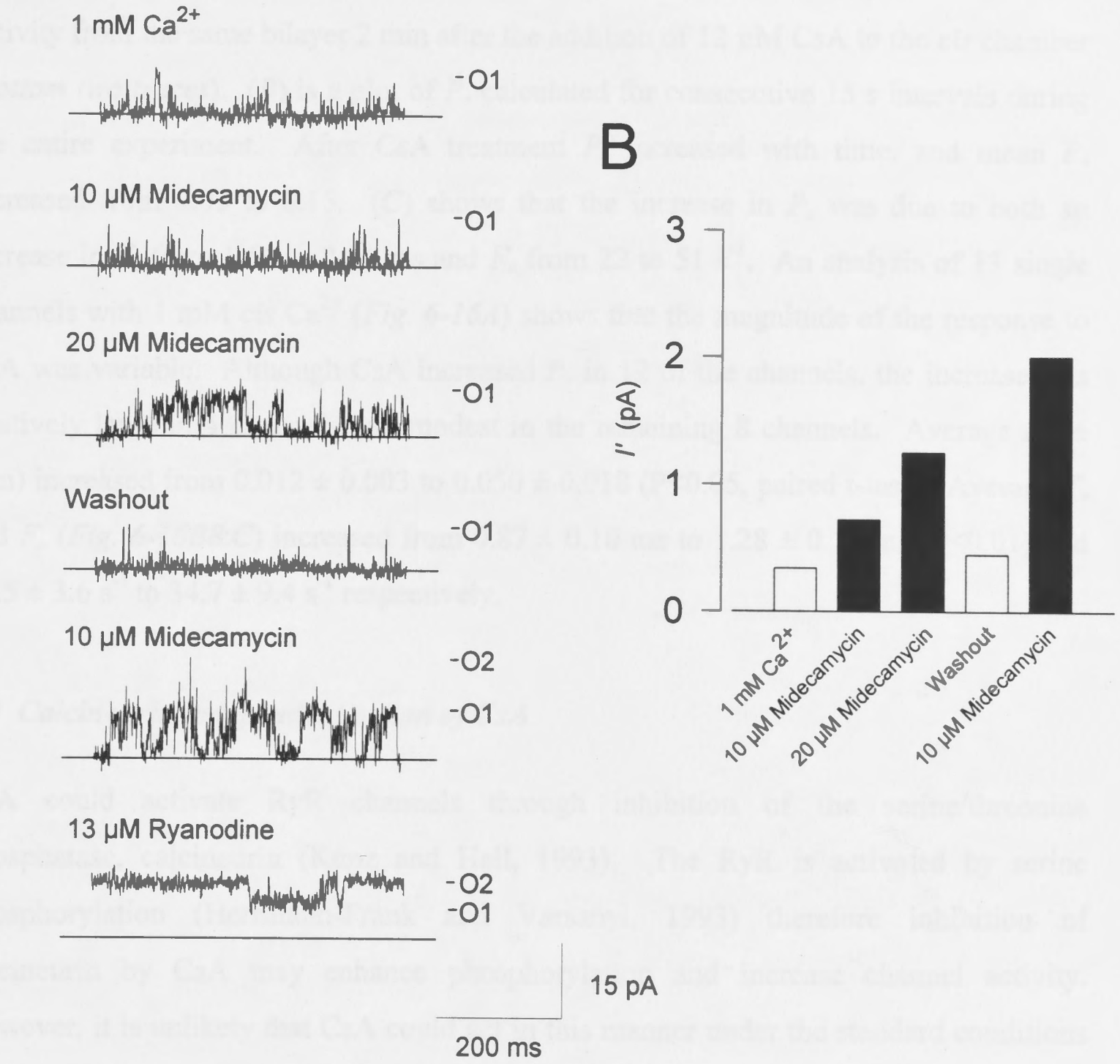

Fig. 6-14. Reversible activation of native RyR channels by midecamycin. (A) Representative channel activity from a bilayer containing at least two RyR channels. The *cis* chamber contained 1 mM Ca^{2+} (*top trace*) to which was added 10 µM midecamycin (*second trace*), 20 µM midecamycin (*third trace*), washout of *cis* chamber (*fourth trace*), re-addition of 10 µM midecamycin (*fifth trace*) and finally addition of 13 µM ryanodine (*bottom trace*). Activation of the RyRs was reversed upon washout of midecamycin. In the presence of ryanodine both channels were locked into characteristic, long-lived open states and the activity of one channel is shown superimposed on the other. (B) I' (calculated from >80 s for each condition) for the experiment shown in A.

CsA. (*A*) shows representative control activity with 1 mM *cis* Ca^{2+} (*top two traces*) and activity from the same bilayer 2 min after the addition of 12 μM CsA to the *cis* chamber (*bottom two traces*). (*B*) is a plot of P_o calculated for consecutive 15 s intervals during the entire experiment. After CsA treatment P_o increased with time, and mean P_o increased from 0.03 to 0.15. (*C*) shows that the increase in P_o was due to both an increase in T_o from 1.54 to 2.94 ms and F_o from 22 to 51 s^{-1}. An analysis of 13 single channels with 1 mM *cis* Ca^{2+} (*Fig. 6-16A*) shows that the magnitude of the response to CsA was variable. Although CsA increased P_o in 12 of the channels, the increase was relatively large in 4 channels and modest in the remaining 8 channels. Average P_o (± sem) increased from 0.012 ± 0.003 to 0.050 ± 0.018 ($P<0.05$, paired t-test). Average T_o and F_o (*Fig. 6-16B&C*) increased from 0.87 ± 0.10 ms to 1.28 ± 0.19 ms ($P<0.01$) and 13.5 ± 3.6 s^{-1} to 34.7 ± 9.4 s^{-1} respectively.

6.9 *Calcineurin independent action of CsA*

CsA could activate RyR channels through inhibition of the serine/threonine phosphatase, calcineurin (Kunz and Hall, 1993). The RyR is activated by serine phosphorylation (Herrmann-Frank and Varsanyi, 1993) therefore inhibition of calcineurin by CsA may enhance phosphorylation and increase channel activity. However, it is unlikely that CsA could act in this manner under the standard conditions of the artificial lipid bilayer. Firstly, the major cellular CsA receptor (CyP A) is a cytosolic protein and unlikely to associate with SR vesicles. Secondly, the experiments were performed without Mg^{2+} and ATP which are essential for phosphorylation. Nonetheless, to test for a possible calcineurin-dependent action of CsA the effects of a specific calcineurin inhibitor, deltamethrin (Enan and Matsumura, 1992), were investigated. In 3 of 3 bilayers, addition of 13 nM deltamethrin to the *cis* chamber and incubation for up to 7 minutes had little effect on RyR activity. Subsequent addition of CsA in 2/2 bilayers caused an increase in P_o. An example of these effects is shown in *Fig. 6-17*. In this bilayer the P_o during 3 mins of treatment with deltamethrin actually decreased from 0.0058 to 0.003. Subsequent addition of 3 and 16 μM CsA produced successive increases in P_o to 0.01 and 0.015 respectively.

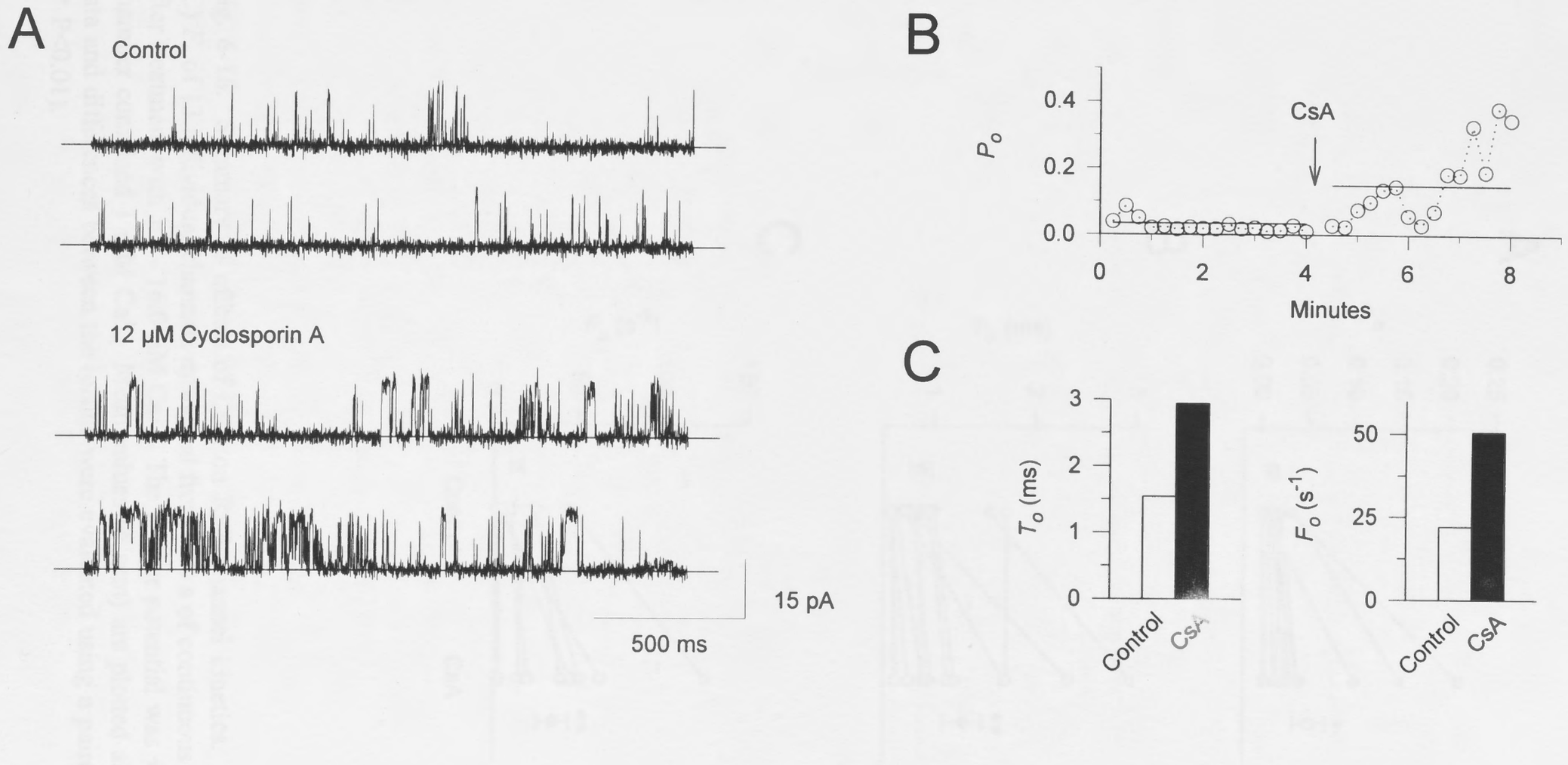

Fig. 6-15. Activation of the RyR by CsA. (A) Single channel records (opening upwards) of RyR activity under control conditions with 1 mM *cis* Ca^{2+} (*upper traces*) and after addition of 12 μM CsA (*lower traces*). (B) Plot of P_o measured over consecutive 15 s segments for the same experiment in A. Mean P_o (*solid lines*) increased from 0.03 (control) to 0.15 (CsA). (C) T_o and F_o in the same channel increased from 1.54 to 2.94 ms and 22 to 51 s^{-1} respectively after application of CsA.

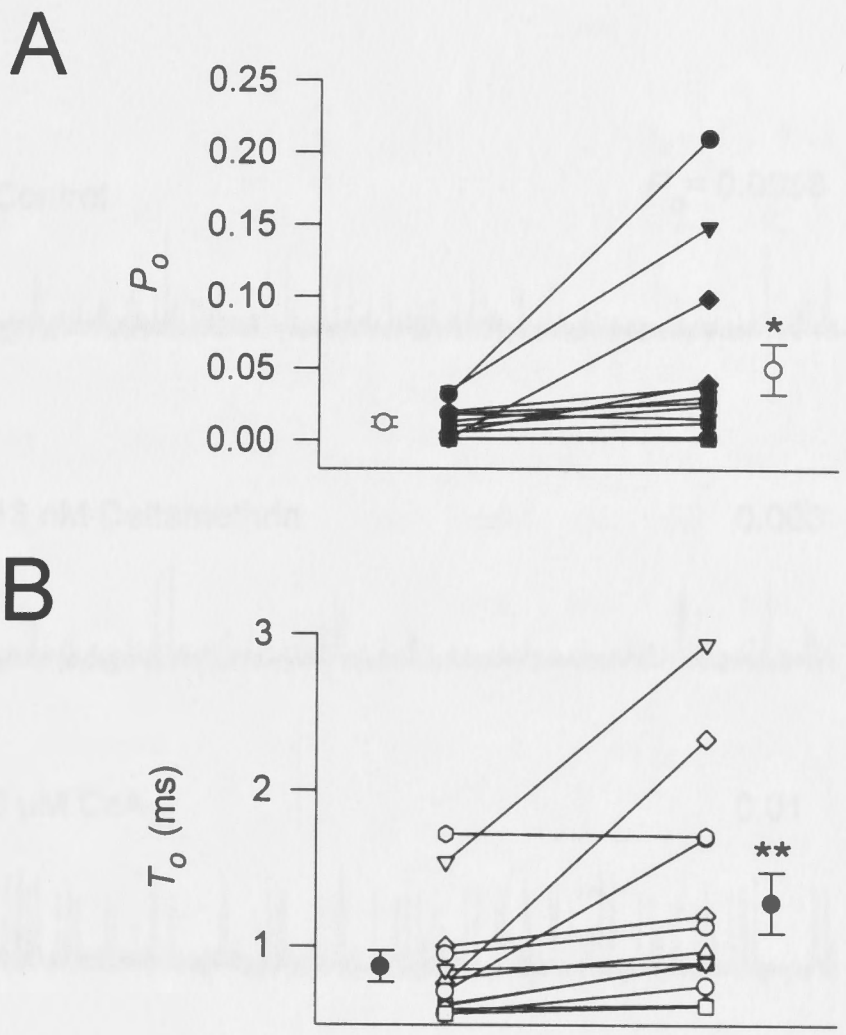

Fig. 6-16. Summary of effects of CsA on RyR channel kinetics. (A) P_o (B) T_o and (C) F_o of 13 individual channels measured from >60 s of continuous activity before and after treatment with 1.3 - 16.0 μM CsA. The bilayer potential was +40 mV and the *cis* chamber contained 1 mM Ca^{2+}. Mean values (± sem) are plotted alongside individual data and differences between the means were evaluated using a paired t-test (* $P<0.05$, ** $P<0.01$).

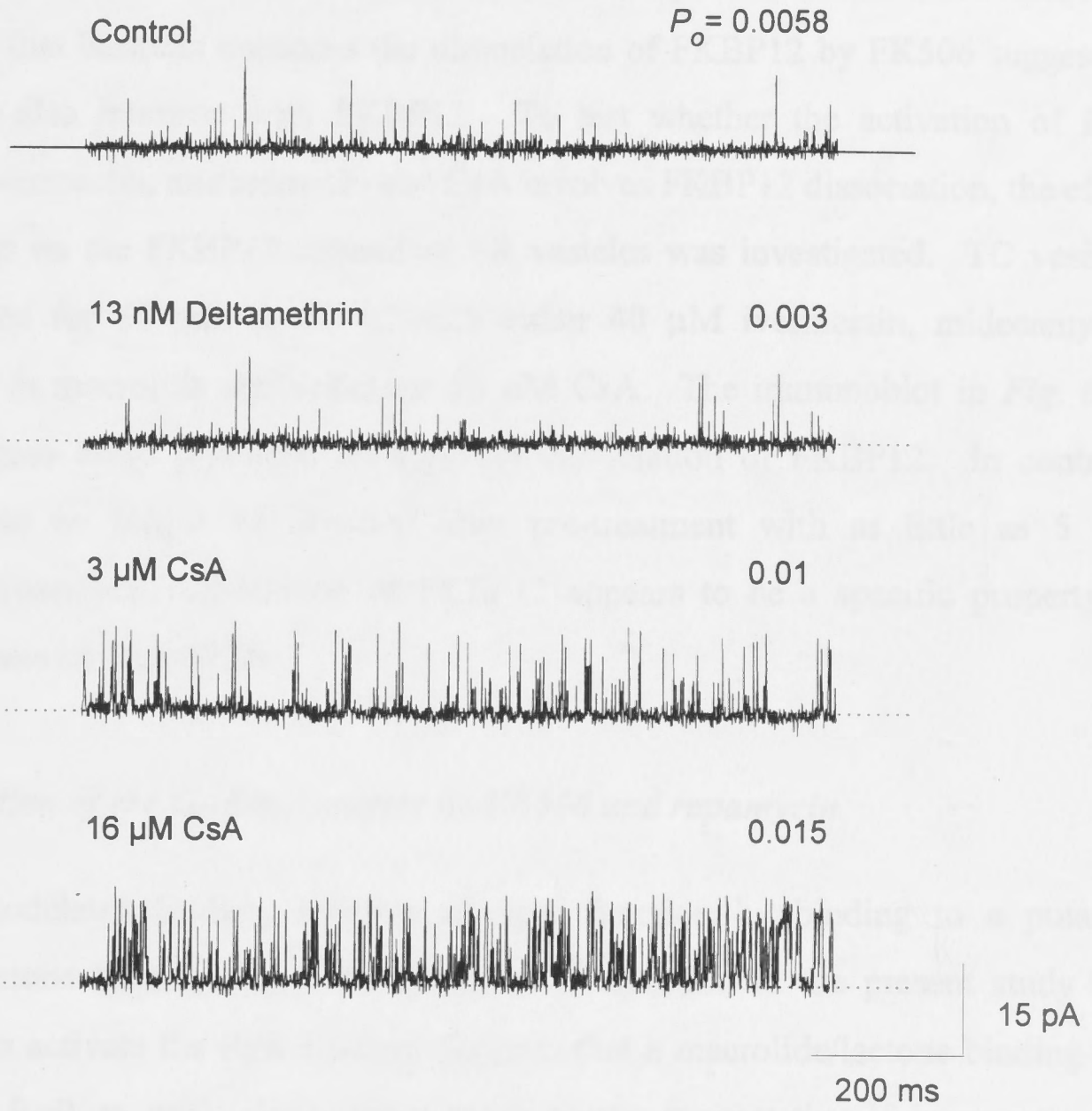

Fig. 6-17. Activation of the RyR by CsA is independent of calcineurin. Representative activity of a RyR channel with 1 mM *cis* Ca^{2+} (*top trace*) and after addition of 13 nM deltamethrin (a specific calcineurin antagonist, *second trace*), 3 µM CsA (*third trace*) and 16 µM CsA (*bottom trace*). P_o was measured from at least 120 s of continuous activity for each condition and is indicated at top right of each trace. Activation of the channel by CsA in the presence of a calcineurin antagonist and the absence of an effect by the calcineurin antagonist alone, suggests that CsA acts independently of calcineurin. Note that P_o increases with [CsA].

6.10 *Ivermectin, midecamycin and CsA do not induce FKBP12 dissociation*

Mack *et al.* (1994) have shown that the macrocyclic compound, bastadin, activates RyR channels and that bastadin enhances the dissociation of FKBP12 by FK506 suggesting that bastadin also interacts with FKBP12. To test whether the activation of RyR channels by ivermectin, midecamycin and CsA involves FKBP12 dissociation, the effect of these drugs on the FKBP12 content of SR vesicles was investigated. TC vesicles were incubated for 15 min at 37 °C with either 40 μM ivermectin, midecamycin, erythromycin (a macrolide antibiotic), or 20 μM CsA. The immunoblot in *Fig. 6-18* shows that these drugs produced no apparent dissociation of FKBP12. In contrast, FKBP12 could no longer be detected after pre-treatment with as little as 5 μM rapamycin. Therefore, dissociation of FKBP12 appears to be a specific property of immunosuppressant macrolides.

6.11 *Modulation of the $GABA_A$ receptor by FK506 and rapamycin*

Ivermectin modulates $GABA_A$ receptor channel function by binding to a putative avermectin/lactone binding site. Therefore the observation in the present study that ivermectin can activate the RyR channel suggests that a macrolide/lactone binding site exists on the RyR as well. In addition these results suggest that if ivermectin and FK506/rapamycin share a common macrolide binding site on the RyR then they may also share a common binding site on the $GABA_A$ receptor. It was therefore of interest to test whether FK506 or rapamycin could modulate $GABA_A$ receptor channel function.

The following experiments were performed in Professor Peter Gage's laboratory (JCSMR, Australian National University) with the assistance of Dr. Louis Premkumar. I am grateful also for the assistance of Dr. John Bekkers (Neurophysiology Group, JCSMR) who kindly provided the autaptic cultures.

Inhibitory synaptic currents mediated by $GABA_A$ receptors were recorded from cultured hippocampal pyramidal neurones which had been grown in isolation on microislands to form "autaptic" synapses (see methods). Superimposed autaptic inhibitory currents recorded before and during perfusion of the cell with 12 μM FK506 show that FK506

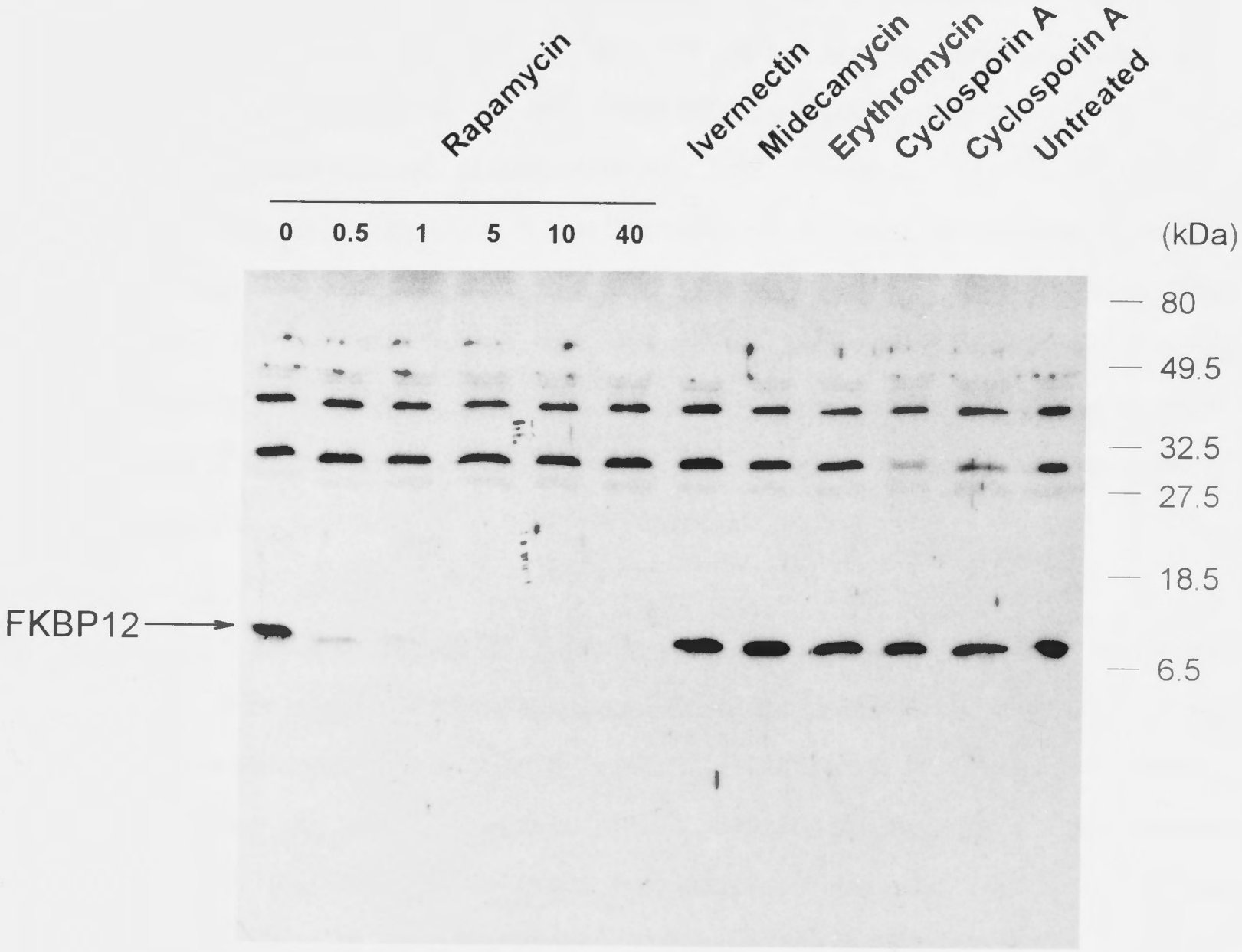

Fig. 6-18. Non-immunosuppressive macrolides and CsA do not induce FKBP12 dissociation from SR vesicles. Western analysis of FKBP12 in 10 μg of B4 SR vesicles probed with rabbit anti-peptide sera. SR vesicles were either untreated (*lane 12*), or incubated for 15 min at 37 °C with 0-40 μM rapamycin (*lanes 1-6*), 40 μM ivermectin (*lane 7*), 40 μM midecamycin, 40 uM erythromycin and 20 μM CsA (*lanes 10 & 11*). The blot was developed using an HRP-conjugated secondary antibody and the enhanced chemiluminescence detection system. The higher molecular weight bands are non-specific.

clearly prolonged the decay phase of the current with little effect (but see below) on the current amplitude (*Fig. 16-19A*). The time constant (τ) for the current decay derived from a single exponential fit to the data was increased from 69 to 143 ms. The effect of application of 20 μM diazepam to the same cell is shown in *Fig. 16-19B*. The current decay was prolonged (τ increased from 54 to 153 ms) but the amplitude was not affected by diazepam. The increase in the time course of the autaptic current in the presence of diazepam indicated that the current was specifically mediated by $GABA_A$ receptor channels. Diazepam, like other benzodiazepines, is believed to increase P_o of the $GABA_A$ receptor by facilitating re-binding of GABA (Study and Barker, 1981). The similarity of the FK506 and diazepam response suggests that FK506 also modulates ligand affinity for the $GABA_A$ receptor. In addition, the increased decay time constant seen with FK506 is consistent with the earlier finding that ivermectin potentiates whole cell GABA evoked currents and slows their desensitisation rate (Sigel and Baur, 1987).

Because FK506, when bound to FKBP12, is a potent inhibitor of the phosphatase calcineurin, it is possible that the prolongation of the $GABA_A$-inhibitory current was mediated by phosphorylation processes which are known to modulate the $GABA_A$ receptor (Stelzer and Shi, 1994; Stelzer, 1992). However, prolongation of the inhibitory current by FK506 was rapid in onset and completely reversible (*Fig. 6-20A*) and therefore unlikely to be the result of phosphorylation. In addition, a similar reversible increase in the time course of the inhibitory current was recorded with rapamycin (1 μM, *Fig. 6-20B*) which does not inhibit calcineurin.

In summary, a reversible prolongation of the inhibitory autaptic currents was seen in 3 of 3 cells with FK506 and 2 of 2 cells with rapamycin. Interestingly, in 2 cells repetitive application of either FK506 or rapamycin (>10 μM) decreased the amplitude of the current while prolonging the timecourse. An example of this effect is shown in *Fig. 6-21*. (*A*) shows that the first application of 12 μM FK506 not only increased the decay time constant but caused a slight reduction in current amplitude by 12%. However, after washout the amplitude recovered and overshot the control value by 32%. Thirty seconds later a second application of 12 μM FK506 produced an even greater decrease in the current amplitude of 57% (*Fig. 6-21B*), but the amplitude was restored to 2%

above the second control value after washout. The modulation of the current amplitude by FK506 was unlikely to be due to a presynaptic action, because applications of 3 μM FK506 had no effect on the fast excitatory current mediated by non-NMDA receptors (*Fig. 6-22*).

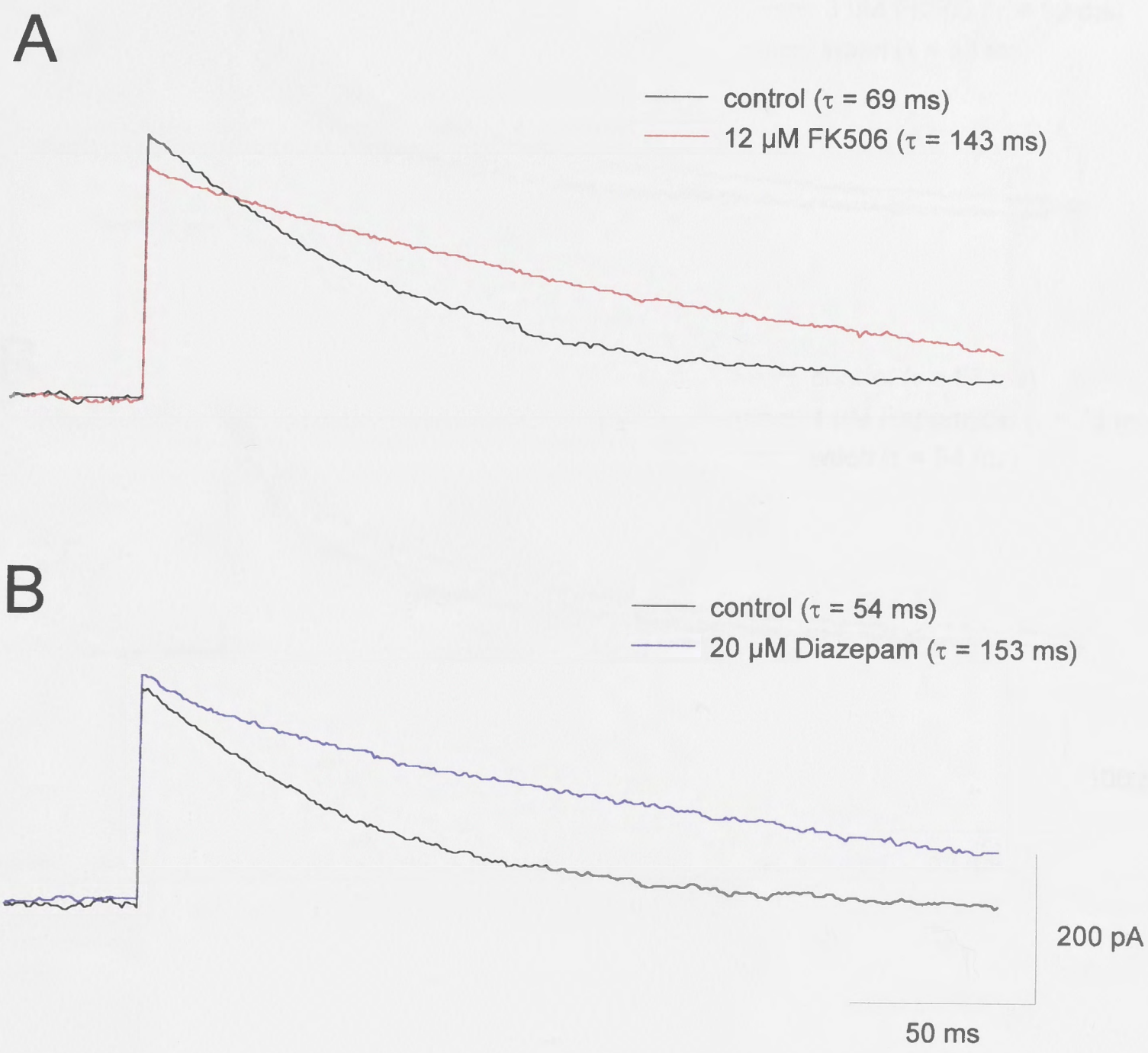

Fig. 6-19. Prolongation of the $GABA_A$ receptor-mediated inhibitory autaptic current by FK506 in a hippocampal neuron. Autaptic currents were stimulated by a 2 ms depolarisation from –40 mV to +40 mV. The currents shown are the averages of 4 sweeps at 0.2 s^{-1} and were recorded at –40 mV (see methods). (A) Superimposed inhibitory currents in control solution (*black*) and 5 s later during application of 12 μM FK506 (*red*). The decay phase of the current was prolonged and the time constant, (τ), derived from a single exponential fit to the data, was increased from 69 ms to 143 ms. (B) Superimposed inhibitory currents from the same cell as above, in control solution (*black*) and during application of 20 μM of the specific $GABA_A$ receptor agonist, diazepam (*blue*). Diazepam prolonged the decay phase of the current (τ increased from 54 ms to 153 ms) showing that the current was mediated by $GABA_A$ receptor channels.

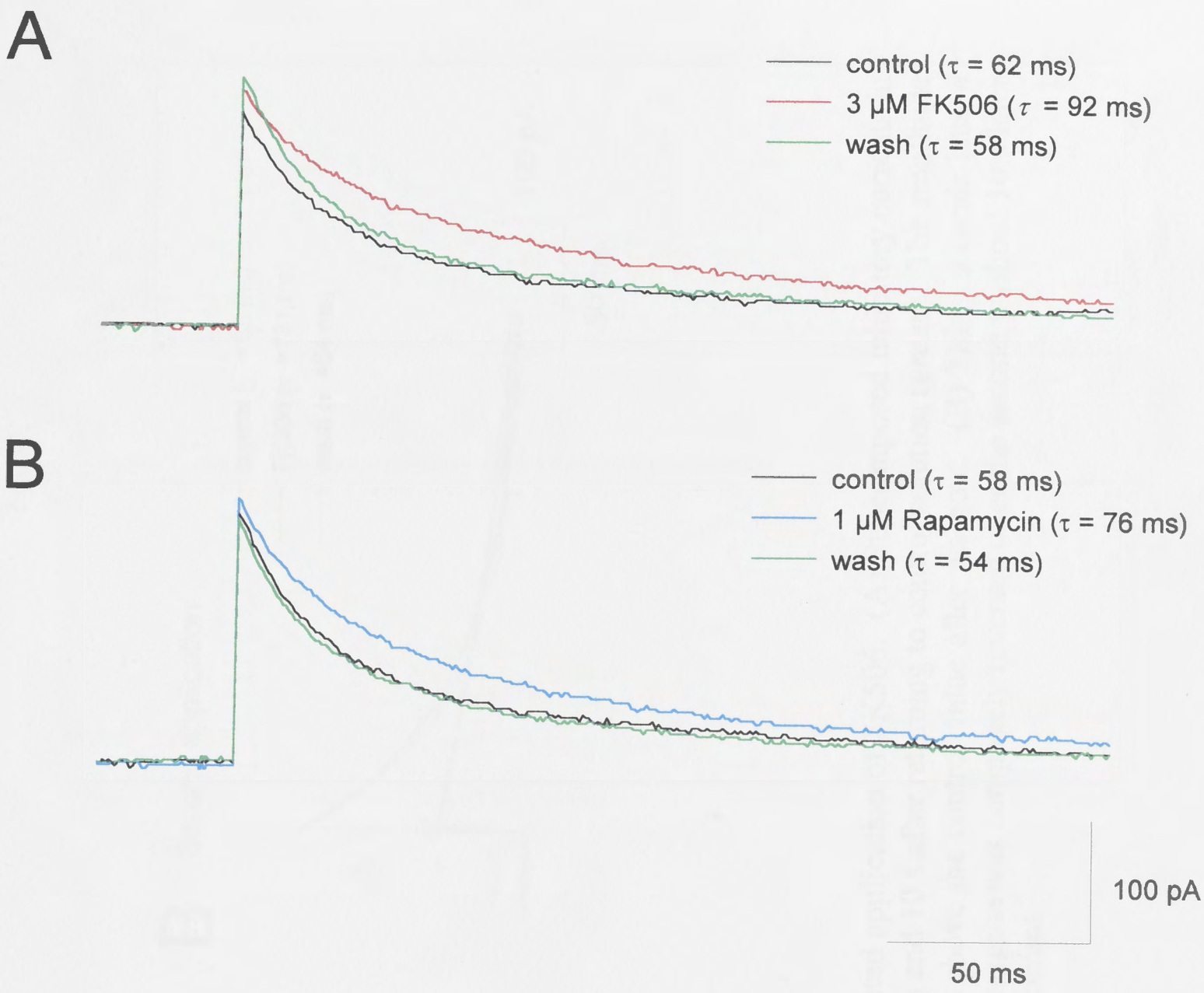

Fig. 6-20. Reversible prolongation of $GABA_A$ receptor-mediated inhibitory autaptic currents by FK506 and rapamycin. (A) Superimposed inhibitory currents in control solution (*black*), 5 s later during application of 3 μM FK506 (*red*) and 10 s after returning to control solution (*green*). FK506 reversibly prolonged the current. The time constant (τ) increased from 62 to 92 ms with FK506 application but decreased to 58 ms after returning to control solution. The currents were recorded at –40 mV. (B) Superimposed inhibitory currents from the same cell in A, in control solution (*black*), during application of 1 μM rapamycin (*blue*) and after returning to control solution (*green*). As with FK506, rapamycin produced a reversible prolongation of the inhibitory current (τ increased from 58 to 76 ms during application of rapamycin and decreased to 54 ms after washout), suggesting an action at a "macrolide" binding site on the $GABA_A$ receptor complex.

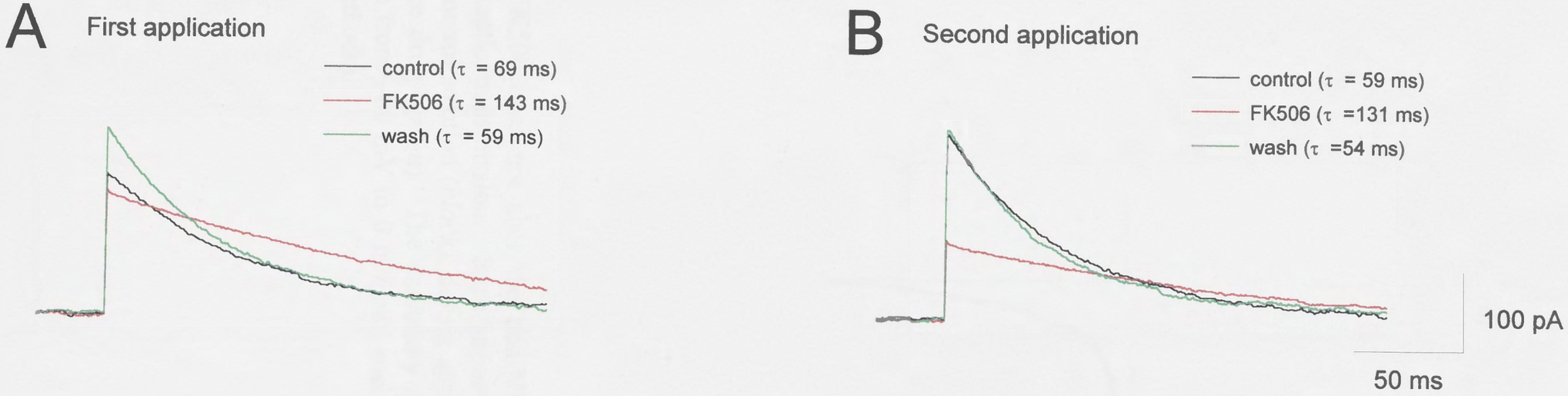

Fig. 6-21. The amplitude of the inhibitory autaptic current is reduced by repeated application of FK506. (A) Superimposed inhibitory currents in control solution (*black*), 5 s later during first application of 12 μM FK506 (*red*) and 10 s after returning to control solution (*green*). The amplitude of the current was initially depressed 12 % by FK506 but rebounded to 32 % above the control value after washout. (B) Thirty seconds later a second application of 12 μM FK506 reduced the amplitude by 57 % but this decrease was completely reversed after the second washout 10 s later without overshooting. Note that FK506 still prolonged the decay phase of the current.

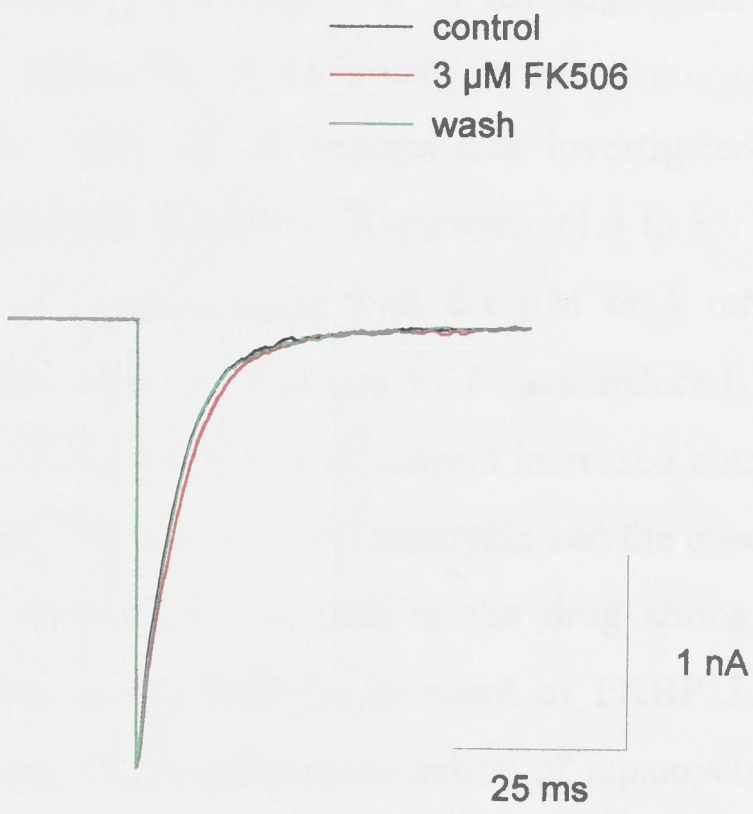

Fig. 6-22. FK506 does not alter the non-NMDA receptor-mediated component of excitatory autaptic transmission. Superimposed fast excitatory currents recorded at −60 mV, in control solution (*black*), during application of 3 µM FK506 (*red*) and after washout of the drug (*green*). The excitatory synaptic current was elicited by a 2 ms depolarisation from −80 mV to 0 mV and each trace is the average of four sweeps at 0.2 s^{-1} (see methods).

Discussion

6.12 *Rapamycin activation of the FKBP12-stripped RyR channel*

The experiments in this chapter were performed to investigate the possibility that rapamycin and FK506 can activate the RyR channel independently of their effect of dissociating FKBP12. The initial set of experiments investigated the effects of rapamycin on FKBP12-stripped RyR channels. Rapamycin (1.3 to 5.0 μM) produced a ~ 6-fold increase in the I' of stripped RyRs with 0.1 μM or 1 mM *cis* Ca^{2+} and, significantly, in 3 of 3 experiments the increase in I' was reduced by ~ 80% after washout. Single channel analysis showed that rapamycin increased both T_o and F_o. The activation of FKBP12-stripped RyR channels by rapamycin and the observation that this activation could be mostly reversed by washout of the drug strongly suggests that rapamycin has a direct action on the RyR independent of FKBP12. Although not investigated in detail, the apparent dose-dependent action of rapamycin (*Fig. 6-2*) also supports the presence of a direct binding site. The fact that the activation caused by rapamycin was not completely reversed after washout may be explained by one of two possibilities. The first is that a component of the activation is irreversible, for example, if one or more FKBP12 monomers were still associated to the channels then the removal of the FKBP12 by rapamycin may account for an irreversible increase in channel activity. However, the probability of encountering channels still bound by one or more FKBP12 monomers would be very slight using ~ 100% stripped vesicles and would be very unlikely to occur in all nine experiments. A more likely explanation is that rapamycin was not completely removed within the washout period. Rapamycin is highly lipophilic and residual amounts are likely to remain in the bilayer despite exchange of 4 - 8 volumes of the *cis* bath.

These results are consistent with the findings of Lamb and Stephenson (1996), which showed that rapamycin and FK506 reversibly potentiated contractile responses in rat, skeletal muscle; but not support the observations of Brillantes *et al.* (1994), that FK506 has no effect on channel activity of the FKBP12-deficient RyR expressed in insect cells. However, it is likely that the RyR expressed in insect cells differs from the RyR

expressed in muscle, in respect to post-translational protein modification and the presence of associated proteins other than FKBP12.

6.13 *Properties of CHAPS-solubilised RyR and activation by rapamycin*

The second set of experiments examined the properties of the CHAPS-solubilised (purified) RyR and tested whether activity of the purified channel was affected by rapamycin. Previous studies have reported prominent discrete conducting levels in purified RyRs at ~ 0.25, 0.5 and 0.75 of the maximal conductance (see *Table 1-1*). This subconductance pattern is similar to that of the FKBP12-stripped RyR, raising the possibility that detergent solubilisation causes dissociation of FKBP12. The maximum conductance and reversal potential of purified RyRs in this study were indistinguishable from those of the native RyR (*Fig. 6-7B*), but similar to previous reports, three major subconductance levels were observed which were nearly equally spaced at 0.25, 0.47 and 0.75 of the maximal conductance. Thus, the substate pattern of purified channels was consistent with the channels being stripped of FKBP12; the FKBP12 content was estimated to be <15%. However, the relative insensitivity of purified channels to both sub-activating (1 nM to 0.1 μM) and inhibiting Ca^{2+} (≥1 mM) and inhibiting Mg^{2+} (*Figs 7&8*) differs from the properties of both native and FKBP12-stripped RyRs. The gross difference in the Ca^{2+} and Mg^{2+} sensitivity of native/stripped RyRs and purified RyRs suggests that purified channels were severely altered in the purification process. One possibility is that degradation of RyR protein occurred during purification resulting in the loss or alteration of critical Ca^{2+}/Mg^{2+} binding sites. Indeed, there was a greater percentage of proteolysed RyR channels in the CHAPS-solubilised preparations. In addition, purification may have altered ligand sensitivity by removing proteins, other than FKBP12, which associate with the RyR and possibly regulate its activity, for example, triadin and calsequestrin (Guo and Campbell, 1995). Therefore, while the subconductance properties of the purified channel suggest they are deficient in FKBP12, their altered ligand sensitivity also suggests loss of other critical binding sites or associated proteins. I' of the purified channel was increased by rapamycin (6 to 13 μM) in 7 of 8 bilayers by ~ 2-fold and fully reversed in 2 of 3 bilayers. The reversible activation of the purified RyR by rapamycin is the same as the reversible activation of

FKBP12-stripped channels. Both observations support the hypothesis that rapamycin can activate the RyR independently of binding to FKBP12. However, the increase in I' produced by rapamycin in purified channels (~ 2 fold) was considerably less than that in FKBP12-stripped channels (~ 6 fold). The difference may be explained by the fact that the I' of purified channels prior to addition of rapamycin was considerably greater than that of FKBP12-stripped channels so there was less scope for an activation.

6.14 *Reduction in maximal RyR channel conductance by rapamycin*

In addition to channel activation, rapamycin also produced a long-lived (~ 50% reduced) maximal conductance in a stripped (*Fig. 6-6*) and a purified channel (*Fig. 6-10*). One might speculate that rapamycin induced selective openings of the 50% substate level (S2) in these channels, however, this possibility is ruled out by the observation that the four open levels present in the stripped channel were still observed after addition of rapamycin, albeit each with a ~ 50% reduced conductance. The implication therefore, is that rapamycin caused a uniform block of all the open levels in a similar manner to ryanodine. The altered kinetics of the reduced conductance state (in *Fig. 6-10*, T_o increased from 2.5 to 575 ms) are remarkably similar to that of the ryanodine-poisoned channel. The similarity of the effects of rapamycin in these channels to the well characterised ryanodine effects suggests that rapamycin might act at or near the ryanodine binding site. Such an action would be consistent with reports that FK506 decreases the ryanodine binding affinity in skeletal SR vesicles (Mack *et al.*, 1994) and that rapamycin and FK506 antagonise ryanodine binding in cardiac muscle (Kaftan *et al.*, 1995) and liver (Kraus-Friedmann and Feng, 1994) respectively.

6.15 *Activation of the native RyR channel by ivermectin and midecamycin*

The third set of experiments explored the possibility that there is a macrolide binding site on the RyR. Previous studies have shown that a macrocyclic compound, bastadin, which is structurally similar to FK506 and rapamycin, increases SR Ca^{2+} release and modifies single channel RyR activity (Mack *et al.*, 1994). In this study I investigated the effects of two non-immunosuppressive macrolides, ivermectin and midecamycin. Ivermectin is a 18 member-ring macrolide which has anthelmintic and insecticidal

properties which are believed to arise from binding to and modification of $GABA_A$ receptors at invertebrate neuromuscular junctions. Ivermectin produced a substantial increase (~ 5-fold) in the mean P_o of native RyR channels, due to an increase in T_o and F_o. It is interesting to note that side-effects of ivermectin treatment include muscle tremor, although this is believed to be neurogenic (Lovell, 1990; Hopkins *et al.*, 1990). The 16 member ring macrolide anti-biotic, midecamycin, produced a more modest increase in P_o (by ~ 1.6-fold, n = 2) and I' (~ 2.7-fold, n = 1) suggesting that the degree of activation produced by the macrolides might be related to the size of the lactone ring. The different potencies of the drugs may also be due to their relative lipophilicity as midecamycin is more water soluble compared with ivermectin and less likely to interact with hydrophobic regions in the RyR. The activation by midecamycin was reversed by washout in 2 of 2 bilayers and neither midecamycin nor ivermectin produced subconductance activity in the channels, or affected FKBP12 association with SR vesicles (*Fig. 6-18*), indicating that their action was unrelated to dissociation of FKBP12. Importantly, ivermectin produced a clear activation of a FKBP12-stripped RyR channel (*Fig. 6-13*), again suggesting that macrolide activation is independent of binding to FKBP12. Moreover, the kinetics of the activation produced by ivermectin and midecamyin were similar to the kinetic changes produced by rapamycin in FKBP12-stripped channels with all drugs producing an increase in T_o and F_o.

In contrast to the results shown here, Mack *et al.* (1994) reported that the macrocyclic compound, bastadin 5, slowed RyR channel kinetics and produced a large increase in both T_o and T_c without affecting P_o. Although bastadins are large macrocyclic compounds, they are structurally distinct from macrolides and this may account for the different responses. Another possibility is that RyR activation by bastadin or macrolides may be Ca^{2+} dependent as the experiments of Mack *et al.* were performed at maximal activating *cis* Ca^{2+} (10 μM) whereas, the majority of bilayers in this study used sub-activating or inhibiting Ca^{2+} (0.1 μM or 1 mM). A Ca^{2+}-dependent action by bastadin may explain the apparent inconsistency in the Mack *et al.* study, that bastadin produced no change in single channel P_o with 10 μM *cis* Ca^{2+}, even though it caused an 8-fold increase in Ca^{2+} release from SR vesicles with <0.1 μM extravesicular Ca^{2+}. Moreover,

Mack *et al.* reported that ^{3}H-ryanodine binding was enhanced by bastadin with >1 mM Ca^{2+} but not with 100 μM Ca^{2+}, which again is consistent with a Ca^{2+}-dependent action.

6.16 *Activation of the native RyR channel by CsA*

The effect of CsA was originally tested as a control for calcineurin specific effects of the FK506/FKBP12 complex on the RyR, because CsA when bound to its immunophilin receptor inhibits calcineurin (Kunz and Hall, 1993). Calcineurin associates with the RyR (Cameron *et al.*, 1995b) and may regulate the phosphorylation state of the channel. CsA produced an increase in P_o of variable magnitude in the majority of bilayers, suggesting that a calcineurin-sensitive pathway might influence RyR activity. However, the activation produced by CsA was not reproduced or affected by prior treatment with a calcineurin antagonist, deltamethrin, suggesting that the activation by CsA was independent of calcineurin. Irrespective of this result, it would be highly unlikely that CsA could act via a calcineurin sensitive phosphorylation pathway in the artificial lipid bilayer set-up, because the cytosolic CsA receptor (cyclophilin A) is unlikely to be present in the SR fractions and the bilayer solutions did not contain ATP and Mg^{2+} which are necessary for phosphorylation.

There are two alternative mechanisms which could explain the channel activation produced by CsA. The first, is that CsA acts non-specifically on hydrophobic regions either on the RyR, perhaps at the same site(s) involved in macrolide activation, or on a protein associated with the RyR. Although structurally different from the macrolides, CsA is large and non-polar, and may therefore partly mimic macrolide action. Indeed, the similarity between the average kinetic responses of ivermectin and CsA (cf. *Figs 6-13 & 6-17*) suggests that they may share a common mode of action. Other evidence in support of a direct binding action of CsA is the apparent concentration-dependence of CsA activation (*Fig. 6-17*). The second, less likely mechanism, is that CsA acts on an unidentified cyclophilin. Cyclophilins, like FKBPs, possess rotamase activity (Galat, 1993) and have been shown to associate with and regulate the function of the mitochondrial transition pore (Nicolli *et al.*, 1996) and also to regulate subunit association of the acetyl-choline and serotonin receptors when they are expressed in

Xenopus oocytes (Helekar *et al.*, 1994). There is no evidence for a cyclophilin-RyR association, however "s-cyclophilin", has been shown to associate with the Ca^{2+} binding proteins calreticulin and calsequestrin at the luminal face of the SR (Arber *et al.*, 1992). Calsequestrin, in turn, associates with triadin and the RyR (Guo and Campbell, 1995) and is thought to regulate RyR activity (Ikemoto *et al.*, 1989), so it is possible that CsA could modify RyR function by disrupting a s-cyclophilin/calsequestrin/RyR complex.

No previous studies have examined CsA effects on RyR single channel activity. However, Timerman *et al.* (1993) showed that, unlike FK506 and rapamycin, CsA did not affect the rate of Ca^{2+} uptake into SR vesicles, suggesting that CsA did not increase RyR activity. One explanation for the different results is that Timerman *et al.* recorded uptake in solutions containing 4 mM Mg^{2+} (to inhibit RyR activity) and it is possible that activation of the RyR by CsA is ineffective under those conditions. Time constraints prevented this possibility being tested here.

6.17 *FK506 and rapamycin modulate $GABA_A$ Receptor function: evidence for action at a macrolide binding site*

The ability of ivermectin, a macrolide lactone and a specific $GABA_A$ receptor agonist, to activate the RyR suggested the existence of a macrolide lactone binding site on the RyR. It was therefore of interest to investigate the corollary, whether FK506 and rapamycin could modulate $GABA_A$ receptor function.

$GABA_A$-mediated inhibitory synaptic currents were recorded from cultured, hippocampal neurones which had been grown in isolation to form synapses on themselves (autapses). The advantage of the autaptic system is the convenience of studying transmission in a single cell and the homogeneity of the synaptic response. Both FK506 and rapamycin reversibly prolonged the decay phase of inhibitory currents indicating a post-synaptic activation of $GABA_A$ receptors. The fact that both immunosuppressants had qualitatively similar effects indicates that their action is independent of calcineurin; rapamycin does not inhibit calcineurin. The rapid activation and reversibility of the current prolongation also suggests that FK506 and rapamycin do

not act via FKBP12 but bind directly to the $GABA_A$ receptor complex. Further evidence in support of direct binding was the dose-dependence and duality of FK506 action. At 12 μM FK506, not only was the prolongation enhanced (compared with 3 μM FK506), but there was also a marked reduction in current amplitude and a rebound effect after washout. These changes in the current amplitude were unlikely to result from pre-synaptic actions because the amplitudes of excitatory currents were unaffected. Previous studies have shown that ivermectin produces both an increase and a decrease in $GABA_A$-mediated Cl^- currents (Sigel and Baur, 1987; Duce and Scott, 1985). Similarly, butyro-lactones have been reported to both prolong and reduce the amplitude of $GABA_A$-mediated inhibitory post-synaptic currents and to potentiate GABA evoked currents (Holland *et al.*, 1991; Peterson *et al.*, 1994) while also producing a large "off" response, or current surge after washout (Holland *et al.*, 1995). The interpretation given for these results is that ivermectin and butyro-lactones have dual agonistic and antagonistic effects at the receptor. Therefore, a possible explanation for the dual effects of FK506 and rapamycin on inhibitory currents in this study is that they have similar mixed agonistic and antagonistic actions. This would account for an increase in amplitude and prolongation of the current at low concentrations and a decrease in current amplitude at high concentrations, as the number of functional channels is reduced. A low affinity blocking action of FK506/rapamycin may account for the rebound phenomena upon washout, since the channels will be rapidly unblocked and available to pass current again. Therefore, taken together, the results suggests that FK506 and rapamycin act directly on the $GABA_A$ receptor, possibly at the putative ivermectin/lactone binding sites.

6.18 *Summary*

The results in this chapter using four independent approaches present a persuasive case for an FKBP12 independent action of FK506 and rapamycin on the RyR. Firstly rapamycin reversibly activated the FKBP12-stripped RyR; secondly, rapamycin reversibly activated the CHAPS solubilised RyR (the CHAPS solubilised RyR showed characteristics consistent with it being stripped of FKBP12); thirdly, the macrolides ivermectin and midecamycin activated both the native and FKBP12-stripped RyR and

did not induce FKBP12 dissociation; lastly FK506 and rapamycin modulated the $GABA_A$ receptor in a similar manner to that described for ivermectin.

Chapter 7.

General Summary

General Summary

The single channel properties of the RyR were studied by fusion of TC vesicles into planar lipid bilayers (Chapter 3). Native RyR channels had a large conductance (~ 500 pS) and a linear I-V relationship in symmetric 250 mM Cs^+, and displayed characteristic sensitivity to *cis* [Ca^{2+}], adenine nucleotides, Mg^{2+}, ryanodine and ruthenium red. The RyR channel studied here was thus functionally the same as that described in a number of earlier studies.

The main aim of this study was to investigate the role of the immunophilin, FKBP12, in regulating RyR channel activity. In the experiments described in Chapter 4 a functional regulation of the RyR by FKBP12 was investigated by treating channels in the bilayer with the immunosuppressants, FK506 and rapamycin, which bind to FKBP12 and dissociate it from the RyR. FK506 and rapamycin increased the P_o of RyR channels over the *cis* Ca^{2+} range 10^{-9} - 10^{-3} M and stabilised subconductance states. Substates of similar magnitude were occasionally evident in channels prior to drug treatment but their frequency was greatly increased after treatment. Substates were found equally spaced at ~ 0.25, 0.5 and 0.75 (S1 - S3) of the full conductance, but were most frequently observed at the ~ 0.25 (S1) level. The actions of FK506 may have resulted from: (i) removal of FKBP12 from the RyR or (ii) an alteration in the phosphorylation state of the RyR, since the FK506/FKBP12 complex inhibits the serine/threonine phosphatase calcineurin and the RyR is activated by serine phosphorylation. However, as rapamycin had similar effects to FK506 it is unlikely that inhibition of calcineurin was responsible for the actions of FK506 (the rapamycin-FKBP12 complex does not interact with calcineurin). That the enhanced subconductance activity produced by FK506 and rapamycin was irreversible is consistent with the idea that both drugs acted by removing FKBP12, although channels were unlikely to be fully stripped of FKBP12 under bilayer conditions (~22 - 25°C).

It was also possible that FK506 and rapamycin acted directly on the RyR protein. In the experiments described in Chapter 5, TC vesicles were pre-treated with rapamycin at

37°C to remove FKBP12 prior to incorporation of vesicles into the bilayer. Using this technique, RyRs could be fully stripped of FKBP12 and the effects of removal of FKBP12 on RyR channel activity could be studied in the absence of the immunosuppressive drugs. FKBP12-stripped channels displayed pronounced subconductance activity with a similar amplitude distribution to channels treated with FK506/rapamycin in the bilayer, except that the probability of substates was greater in the stripped channels. This suggests that the probability of substates was correlated with the extent of FKBP12 removal, since channels treated with FK506/rapamycin in the bilayer were probably only partially stripped of FKBP12. These results are consistent with the findings of Brillantes *et al.* (1994), that FKBP12 stabilises the full conductance activity of the channel. However, the relative proportion of substate to maximal state activity was variable between channels derived from fully stripped vesicles, indicating that factors other than FKBP12 may also be involved in regulating the conductance states of the channel.

A significant and intriguing result was that substates at the same fraction of the maximal conductance were seen before and after ryanodine modification. Clearly, the unitary reduced conductance level commonly observed in ryanodine-modified channels is unrelated to intrinsic RyR substate activity. That ryanodine proportionally reduced the conductance of each open level implies that ryanodine has a homogenous action on the channel structure(s) responsible for the different conductance states.

The existence of four major RyR conductance levels has interesting implications in terms of channel structure. For example, the channel may be composed of four identical ion-conducting pores, a single pore with a variable diameter or a combination of both. Consideration of the results suggest that a combined structure may be more realistic.

An important finding of this study was that FKBP12-stripped channels displayed a ~ 10 -fold increase in their sensitivity to activation by Ca^{2+} and a 10-fold decrease in their sensitivity to Ca^{2+}-inhibition, compared with unstripped RyR channels. An increased sensitivity to Ca^{2+}-activation has previously been reported for FKBP12-stripped channels (Mayrleitner *et al.*, 1994), but a parallel decrease in the sensitivity to

Ca^{2+}-inhibition is a novel finding. The altered sensitivity of stripped RyRs to Ca^{2+} (reported here), caffeine and Mg^{2+} (reported by others) indicates that FKBP12 modulates the RyR protein at multiple sites, possibly through steric interactions, and is integral in regulating channel activity.

The Ca^{2+} dependence of P_o was different for FKBP12-stripped channels (Chapter 5) and channels treated with FK506/rapamycin in the bilayer (Chapter 4). The P_o of stripped channels was greater than control channels at sub-activating (0.1 μM) and inhibiting (1 mM) [Ca^{2+}] but not at maximal activating (10 μM) [Ca^{2+}]. In contrast, the P_o of channels treated with FK506/rapamycin in the bilayer was elevated over the entire Ca^{2+} range. An obvious implication of this result is that FK506 and rapamycin may directly activate RyRs independently of binding and dissociating FKBP12. To test for this possibility I investigated whether rapamycin altered the activity of FKBP12-stripped RyRs. That rapamycin was able to reversibly activate stripped channels suggests that it can directly interact with the RyR protein. Further evidence in support of this hypothesis were the observations that:

(i) rapamycin reversibly activated the CHAPS solubilised RyR (the CHAPS solubilised RyR showed characteristics consistent with it being stripped of FKBP12);

(ii) the macrolides, ivermectin and midecamycin activated both the native and FKBP12-stripped RyR and did not induce FKBP12 dissociation;

(iii) FK506 and rapamycin modulated the $GABA_A$ receptor (which possesses macrolide/lactone binding sites) in a similar manner to that described for ivermectin.

Taken together these results suggest the existence of a macrolide binding site on the RyR complex which is distinct from FKBP12. These results are consistent with the observations that FK506 and rapamycin reversibly potentiate depolarisation- and caffeine-induced tension responses in rat skeletal muscle .

In conclusion, the results in this study demonstrate that FKBP12 plays a fundamental role in regulating RyR channel activity, and they also suggest that the FKBP12 ligands, FK506 and rapamycin, have additional actions on the RyR protein. Questions that remained to be answered include whether the proline isomerase activity of FKBP12, or whether FKBP12 binding *per se*, is functionally important in RyR regulation; and whether FKBP12 plays a dynamic role in RyR activation eg. excitation-contraction coupling.

Bibliography

Bibliography

Abramson, J.J., Cronin, J.R., and Salama, G. (1988). Oxidation induced by phthalocyanine dyes causes rapid calcium release from sarcoplasmic reticulum vesicles. Arch. Biochem. Biophys. *263*, 245-255.

Ahern, G.P., Junankar, P.R., and Dulhunty, A.F. (1994). Single channel activity of the ryanodine receptor calcium release channel is modulated by FK-506. FEBS Lett. *352*, 369-374.

Anderson, K., Lai, F.A., Liu, Q.Y., Rousseau, E., Erickson, H.P., and Meissner, G. (1989). Structural and functional characterization of the purified cardiac ryanodine receptor-Ca^{2+} release channel complex. J. Biol. Chem. *264*, 1329-1335.

Arber, S., Krause, K.H., and Caroni, P. (1992). s-cyclophilin is retained intracellularly via a unique COOH-terminal sequence and colocalizes with the calcium storage protein calreticulin. J. Cell Biol. *116*, 113-125.

Armstrong, C.M., Bezanilla, F.M., and Horowicz, P. (1972). Twitches in the presence of ethylene glycol bis (-aminoethyl ether)-N,N'-tetracetic acid. Biochim. Biophys. Acta *267*, 605-608.

Ashley, R.H. and Williams, A.J. (1990). Divalent cation activation and inhibition of single calcium release channels from sheep cardiac sarcoplasmic reticulum. J. Gen. Physiol. *95*, 981-1005.

Bekkers, J.M. and Stevens, C.F. (1991). Excitatory and inhibitory autaptic currents in isolated hippocampal neurons maintained in cell culture. Proc. Natl. Acad. Sci. U. S. A. *88*, 7834-7838.

Berridge, M.J. (1993). Inositol trisphosphate and calcium signalling. Nature *361*, 315-325.

Blake, M.S., Johnston, K.H., Russell Jones, G.J., and Gotschlich, E.C. (1984). A rapid, sensitive method for detection of alkaline phosphatase-conjugated anti-antibody on Western blots. Anal. Biochem. *136*, 175-179.

Brandt, N.R., Caswell, A.H., Wen, S.R., and Talvenheimo, J.A. (1990). Molecular interactions of the junctional foot protein and dihydropyridine receptor in skeletal muscle triads. J. Membr. Biol. *113*, 237-251.

Brandt, N.R., Caswell, A.H., Brunschwig, J.P., Kang, J.J., Antoniu, B., and Ikemoto, N. (1992). Effects of anti-triadin antibody on Ca^{2+} release from sarcoplasmic reticulum. FEBS Lett. *299*, 57-59.

Brillantes, A.-M.B., Ondrias, K., Scott, A., Kobrinsky, E., Ondriasová, E., Moschella, M.C., Jayaraman, T., Landers, M., Ehrlich, B.E., and Marks, A.R. (1994). Stabilization of calcium release channel (ryanodine receptor) function by FK506-binding protein. Cell *77*, 513-523.

Brum, G., Stefani, E., and Rios, E. (1987). Simultaneous measurements of Ca^{2+} currents and intracellular Ca^{2+} concentrations in single skeletal muscle fibers of the frog. Can. J. Physiol. Pharmacol. *65*, 681-685.

Buck, E., Zimanyi, I., Abramson, J.J., and Pessah, I.N. (1992). Ryanodine stabilizes multiple conformational states of the skeletal muscle calcium release channel. J. Biol. Chem. *267*, 23560-23567.

Cameron, A.M., Steiner, J.P., Sabatini, D.M., Kaplin, A.I., Walensky, L.D., and Snyder, S.H. (1995a). Immunophilin FK506 binding protein associated with inositol 1,4,5-trisphosphate receptor modulates calcium flux. Proceedings of the National Academy of Sciences of the United States of America *92*, 1784-1788.

Cameron, A.M., Steiner, J.P., Roskams, A.J., Ali, S.M., Ronnett, G.V., and Snyder, S.H. (1995b). Calcineurin associated with the inositol 1,4,5-trisphosphate receptor-FKBP12 complex modulates Ca^{2+} flux. Cell *83*, 463-472.

Campbell, W.C., Fisher, M.H., Stapley, E.O., Albers-Schonberg, G., and Jacob, T.A. (1983). Ivermectin: a potent new antiparasitic agent. Science *221*, 823-828.

Cannell, M.B., Berlin, J.R., and Lederer, W.J. (1987). Effect of membrane potential changes on the calcium transient in single rat cardiac muscle cells. Science *238*, 1419-1423.

Chen, S.R., Vaughan, D.M., Airey, J.A., Coronado, R., and MacLennan, D.H. (1993). Functional expression of cDNA encoding the Ca^{2+} release channel (ryanodine receptor) of rabbit skeletal muscle sarcoplasmic reticulum in COS-1 cells. Biochemistry *32*, 3743-3753.

Chen, S.R.W., Zhang, L., and MacLennan, D.H. (1994). Asymmetrical blockade of the Ca^{2+} release channel (ryanodine receptor) by 12-kDa FK506 binding protein. Proceedings of the National Academy of Sciences of the United States of America *91*, 11953-11957.

Chu, A., Fill, M., Stefani, E., and Entman, M.L. (1993). Cytoplasmic Ca^{2+} does not inhibit the cardiac muscle sarcoplasmic reticulum ryanodine receptor Ca^{2+} channel, although $Ca(^{2+})$-induced Ca^{2+} inactivation of Ca^{2+} release is observed in native vesicles. J. Membr. Biol *135*, 49-59.

Collins, J.H. (1991). Sequence analysis of the ryanodine receptor: possible association with a 12K, FK506-binding immunophilin/protein kinase C inhibitor. Biochem. Biophys. Res. Commun. *178*, 1288-1290.

Colombini, M. (1987). Regulation of the mitochondrial outer membrane channel, VDAC. J. Bioenerg. Biomembr. *19*, 309-320.

Coronado, R., Rosenberg, R.L., and Miller, C. (1980). Ionic selectivity, saturation, and block in a K+-selective channel from sarcoplasmic reticulum. J. Gen. Physiol. *76*, 425-446.

Coronado, R., Morrissette, J., Sukhareva, M., and Vaughan, D.M. (1994). Structure and function of ryanodine receptors. Am. J. Physiol. *266*, C1485-C1504.

Csernoch, L., Jacquemond, V., and Schneider, M.F. (1993). Microinjection of strong calcium buffers suppresses the peak of calcium release during depolarization in frog skeletal muscle fibers. J. Gen. Physiol. *101*, 297-333.

Cully, D.F., Vassilatis, D.K., Liu, K.K., Paress, P.S., Van der Ploeg, L.H., Schaeffer, J.M., and Arena, J.P. (1994). Cloning of an avermectin-sensitive glutamate-gated chloride channel from Caenorhabditis elegans. Nature *371*, 707-711.

Damiani, E. and Margreth, A. (1991). Subcellular fractionation to junctional sarcoplasmic reticulum and biochemical characterization of 170 kDa Ca^{2+}- and low-density-lipoprotein-binding protein in rabbit skeletal muscle. Biochem. J. *277*, 825-832.

Diaz Munoz, M., Hamilton, S.L., Kaetzel, M.A., Hazarika, P., and Dedman, J.R. (1990). Modulation of Ca^{2+} release channel activity from sarcoplasmic reticulum by annexin VI (67-kDa calcimedin). J. Biol. Chem. *265*, 15894-15899.

Duce, I.R. and Scott, R.H. (1985). Actions of dihydroavermectin B1a on insect muscle. Br.J.Pharmacol. *85*, 395-401.

el-Hayek, R., Valdivia, C., Valdivia, H.H., Hogan, K., and Coronado, R. (1993). Activation of the Ca^{2+} release channel of skeletal muscle sarcoplasmic reticulum by palmitoyl carnitine. Biophys. J. *65*, 779-789.

Enan, E. and Matsumura, F. (1992). Specific inhibition of calcineurin by type II synthetic pyrethroid insecticides. Biochem. Pharmacol. *43*, 1777-1784.

Endo, M., Tanaka, M., and Ogawa, Y. (1970). Calcium induced release of calcium from the sarcoplasmic reticulum of skinned skeletal muscle fibres. Nature *228*, 34-36.

Fano, G., Marsili, V., Angelella, P., Aisa, M.C., Giambanco, I., and Donato, R. (1989). S-100a0 protein stimulates Ca^{2+}-induced Ca^{2+} release from isolated sarcoplasmic reticulum vesicles. FEBS Lett. *255*, 381-384.

Ficker, E., Taglialatela, M., Wible, B.A., Henley, C.M., and Brown, A.M. (1994). Spermine and spermidine as gating molecules for inward rectifier K+ channels. Science *266*, 1068-1072.

Fill, M., Coronado, R., Mickelson, J.R., Vilven, J., Ma, J.J., Jacobson, B.A., and Louis, C.F. (1990). Abnormal ryanodine receptor channels in malignant hyperthermia. Biophys. J. *57*, 471-475.

Fischer, G., Bang, H., and Mech, C. (1984). [Determination of enzymatic catalysis for the cis-trans-isomerization of peptide binding in proline-containing peptides]. Biomed. Biochim. Acta *43*, 1101-1111.

Fischer, G., Wittmann-Liebold, B., Lang, K., Kiefhaber, T., and Schmid, F.X. (1989). Cyclophilin and peptidyl-prolyl cis-trans isomerase are probably identical proteins [see comments]. Nature *337*, 476-478.

Ford, L.E. and Podolsky, R.J. (1970). Regenerative calcium release within muscle cells. Science *167*, 58-59.

Fritz, L.C., Wang, C.C., and Gorio, A. (1979). Avermectin B1a irreversibly blocks postsynaptic potentials at the lobster neuromuscular junction by reducing muscle membrane resistance. Proc. Natl. Acad. Sci. U. S. A. *76*, 2062-2066.

Fruen, B.R., Mickelson, J.R., Shomer, N.H., Roghair, T.J., and Louis, C.F. (1994). Regulation of the sarcoplasmic reticulum ryanodine receptor by inorganic phosphate. J. Biol. Chem. *269*, 192-198.

Galat, A. (1993). Peptidylproline cis-trans-isomerases: immunophilins. Eur. J. Biochem. *216*, 689-707.

Galat, A. and Metcalfe, S.M. (1995). Peptidylproline cis/trans isomerases. Prog. Biophys. Mol. Biol. *63*, 67-118.

Garber, S.S. and Miller, C. (1987). Single Na^+ channels activated by veratridine and batrachotoxin. J. Gen. Physiol. *89*, 459-480.

Giannini, G., Conti, A., Mammarella, S., Scrobogna, M., and Sorrentino, V. (1995). The ryanodine receptor/calcium channel genes are widely and differentially expressed in murine brain and peripheral tissues. J. Cell Biol. *128*, 893-904.

Green, N., Alexander, H., Olson, A., Alexander, S., Shinnick, T.M., Sutcliffe, J.G., and Lerner, R.A. (1982). Immunogenic structure of the influenza virus hemagglutinin. Cell *28*, 477-487.

Grunwald, R. and Meissner, G. (1995). Lumenal sites and C terminus accessibility of the skeletal muscle calcium release channel (ryanodine receptor). J. Biol. Chem. *270*, 11338-11347.

Guo, W. and Campbell, K.P. (1995). Association of triadin with the ryanodine receptor and calsequestrin in the lumen of the sarcoplasmic reticulum. J. Biol. Chem. *270*, 9027-9030.

Gyorke, S. and Fill, M. (1993). Ryanodine receptor adaptation: control mechanism of Ca^{2+}-induced Ca^{2+} release in heart [see comments]. Science *260*, 807-809.

Haendler, B., Hofer-Warbinek, R., and Hofer, E. (1987). Complementary DNA for human T-cell cyclophilin. EMBO J. *6*, 947-950.

Hakamata, Y., Nakai, J., Takeshima, H., and Imoto, K. (1992). Primary structure and distribution of a novel ryanodine receptor/calcium release channel from rabbit brain. FEBS Lett. *312*, 229-235.

Hakamata, Y., Nishimura, S., Nakai, J., Nakashima, Y., Kita, T., and Imoto, K. (1994). Involvement of the brain type of ryanodine receptor in T-cell proliferation. FEBS Lett. *352*, 206-210.

Handschumacher, R.E., Harding, M.W., Rice, J., Drugge, R.J., and Speicher, D.W. (1984). Cyclophilin: a specific cytosolic binding protein for cyclosporin A. Science *226*, 544-547.

Harding, M.W., Handschumacher, R.E., and Speicher, D.W. (1986). Isolation and amino acid sequence of cyclophilin. J. Biol. Chem. *261*, 8547-8555.

Harding, M.W., Galat, A., Uehling, D.E., and Schreiber, S.L. (1989). A receptor for the immunosuppressant FK506 is a cis-trans peptidyl-prolyl isomerase. Nature *341*, 758-760.

Hayano, T., Takahashi, N., Kato, S., Maki, N., and Suzuki, M. (1991). Two distinct forms of peptidylprolyl-cis-trans-isomerase are expressed separately in periplasmic and cytoplasmic compartments of Escherichia coli cells. Biochemistry *30*, 3041-3048.

Helekar, S.A., Char, D., Neff, S., and Patrick, J. (1994). Prolyl isomerase requirement for the expression of functional homo-oligomeric ligand-gated ion channels. Neuron *12*, 179-189.

Herrmann-Frank, A. and Varsanyi, M. (1993). Enhancement of Ca^{2+} release channel activity by phosphorylation of the skeletal muscle ryanodine receptor. FEBS Lett. *332*, 237-242.

Holland, K.D., Yoon, K.W., Ferrendelli, J.A., Covey, D.F., and Rothman, S.M. (1991). Gamma-butyrolactone antagonism of the picrotoxin receptor: comparison of a pure antagonist and a mixed antagonist/inverse agonist. Mol. Pharmacol. *39*, 79-84.

Holland, K.D., Mathews, G.C., Bolos-Sy, A.M., Tucker, J.B., Reddy, P.A., Covey, D.F., Ferrendelli, J.A., and Rothman, S.M. (1995). Dual modulation of the gamma-aminobutyric acid type A receptor/ionophore by alkyl-substituted gamma-butyrolactones. Mol. Pharmacol. *47*, 1217-1223.

Hopkins, K.D., Marcella, K.L., and Strecker, A.E. (1990). Ivermectin toxicosis in a dog. J. Am. Vet. Med. Assoc. *197*, 93-94.

Hunter, M. and Giebisch, G. (1987). Multi-barrelled K channels in renal tubules. Nature *327*, 522-524.

Hymel, L., Inui, M., Fleischer, S., and Schindler, H. (1988a). Purified ryanodine receptor of skeletal muscle sarcoplasmic reticulum forms Ca^{2+}-activated oligomeric Ca^{2+} channels in planar bilayers. Proc. Natl. Acad. Sci. U. S. A. *85*, 441-445.

Hymel, L., Schindler, H., Inui, M., and Fleischer, S. (1988b). Reconstitution of purified cardiac muscle calcium release channel (ryanodine receptor) in planar bilayers. Biochem. Biophys. Res. Commun. *152*, 308-314.

Ikemoto, N., Ronjat, M., Meszaros, L.G., and Koshita, M. (1989). Postulated role of calsequestrin in the regulation of calcium release from sarcoplasmic reticulum. Biochemistry *28*, 6764-6771.

Imagawa, T., Smith, J.S., Coronado, R., and Campbell, K.P. (1987). Purified ryanodine receptor from skeletal muscle sarcoplasmic reticulum is the Ca^{2+}-permeable pore of the calcium release channel. J. Biol Chem. *262*, 16636-16643.

Jahr, C.E. and Stevens, C.F. (1987). Glutamate activates multiple single channel conductances in hippocampal neurons. Nature *325*, 522-525.

Jayaraman, T., Brillantes, A.M., Timerman, A.P., Fleischer, S., Erdjument-Bromage, H., Tempst, P., and Marks, A.R. (1992). FK506 binding protein associated with the calcium release channel (ryanodine receptor). J. Biol Chem. *267*, 9474-9477.

Kaftan, E., Marks, A.R., and Ehrlich, B.E. (1995). Effects of rapamycin on ryanodine receptors from skeletal and cardiac muscle. Biophys. J. A373.

Kass, I.S., Wang, C.C., Walrond, J.P., and Stretton, A.O. (1980). Avermectin B1a, a paralyzing anthelmintic that affects interneurons and inhibitory motoneurons in Ascaris. Proc. Natl. Acad. Sci. U. S. A. *77*, 6211-6215.

Kim, K.C., Caswell, A.H., Talvenheimo, J.A., and Brandt, N.R. (1990). Isolation of a terminal cisterna protein which may link the dihydropyridine receptor to the junctional foot protein in skeletal muscle. Biochemistry *29*, 9281-9289.

Kirino, Y., Osakabe, M., and Shimizu, H. (1983). Ca^{2+}-induced Ca^{2+} release from fragmented sarcoplasmic reticulum: Ca^{2+}-dependent passive Ca^{2+} efflux. J. Biochem. Tokyo. *94*, 1111-1118.

Kourie, J.I., Laver, D.R., Junankar, P.R., Gage, P.W., and Dulhunty, A.F. (1996a). Characteristics of two types of chloride channel in sarcoplasmic reticulum vesicles from rabbit skeletal muscle. Biophys. J. *70*, 202-221.

Kourie, J.I., Laver, D.R., Ahern, G.P., and Dulhunty, A.F. (1996b). A calcium-activated chloride channel in sarcoplasmic reticulum vesicles from rabbit skeletal muscle. Am. J. Physiol. (*In Press*).

Kraus-Friedmann, N. and Feng, L. (1994). Reduction of ryanodine binding and cytosolic Ca^{2+} levels in liver by the immunosuppressant FK506. Biochem. Pharmacol. *48*, 2157-2162.

Krouse, M.E., Schneider, G.T., and Gage, P.W. (1986). A large anion-selective channel has seven conductance levels. Nature *319*, 58-60.

Kunz, J. and Hall, M.N. (1993). Cyclosporin A, FK506 and rapamycin: more than just immunosuppression. Trends. Biochem. Sci. *18*, 334-338.

Kurebayashi, N. and Ogawa, Y. (1986). Characterization of increased Ca^{2+} efflux by quercetin from the sarcoplasmic reticulum in frog skinned skeletal muscle fibres. J. Muscle Res. Cell Motil. *7*, 142-150.

Laemmli, U.K. (1970). Cleavage of structural proteins during the assembly of the head of bacteriophage T4. Nature *227*, 680-685.

Lai, F.A., Erickson, H.P., Rousseau, E., Liu, Q.Y., and Meissner, G. (1988). Purification and reconstitution of the calcium release channel from skeletal muscle. Nature *331*, 315-319.

Lai, F.A., Misra, M., Xu, L., Smith, H.A., and Meissner, G. (1989). The ryanodine receptor-Ca^{2+} release channel complex of skeletal muscle sarcoplasmic reticulum. Evidence for a cooperatively coupled, negatively charged homotetramer. J. Biol Chem. *264*, 16776-16785.

Lamb, G.D. and Stephenson, D.G. (1991). Effect of Mg^{2+} on the control of Ca^{2+} release in skeletal muscle fibres of the toad. J. Physiol. Lond. *434*, 507-528.

Lamb, G.D. and Stephenson, D.G. (1996). Effect of FK-506 and rapamycin on excitation-contraction coupling in skeletal muscle fibres of the rat. J. Physiol. Lond. (In Press).

Larini, F., Menegazzi, P., Baricordi, O., Zorzato, F., and Treves, S. (1995). A ryanodine receptor-like Ca^{2+} channel is expressed in nonexcitable cells. Mol. Pharmacol. *47*, 21-28.

Laver, D.R., Roden, L.D., Ahern, G.P., Eager, K.R., Junankar, P.R., and Dulhunty, A.F. (1995). Cytoplasmic Ca^{2+} inhibits the ryanodine receptor from cardiac muscle. J. Membr. Biol *147*, 7-22.

Lee, H.C. (1993). Potentiation of calcium- and caffeine-induced calcium release by cyclic ADP-ribose. J. Biol. Chem. *268*, 293-299.

Lindsay, A.R., Tinker, A., and Williams, A.J. (1994). How does ryanodine modify ion handling in the sheep cardiac sarcoplasmic reticulum Ca^{2+}-release channel? J. Gen. Physiol. *104*, 425-447.

Lindsay, A.R. and Williams, A.J. (1991). Functional characterisation of the ryanodine receptor purified from sheep cardiac muscle sarcoplasmic reticulum. Biochim. Biophys. Acta *1064*, 89-102.

Liu, G. and Pessah, I.N. (1994). Molecular interaction between ryanodine receptor and glycoprotein triadin involves redox cycling of functionally important hyperreactive sulfhydryls. J. Biol. Chem. *269*, 33028-33034.

Liu, J., Farmer, J.D.J., Lane, W.S., Friedman, J., Weissman, I., and Schreiber, S.L. (1991). Calcineurin is a common target of cyclophilin-cyclosporin A and FKBP-FK506 complexes. Cell *66*, 807-815.

Liu, Q.Y., Lai, F.A., Rousseau, E., Jones, R.V., and Meissner, G. (1989). Multiple conductance states of the purified calcium release channel complex from skeletal sarcoplasmic reticulum. Biophys. J. *55*, 415-424.

Lopatin, A.N., Makhina, E.N., and Nichols, C.G. (1994). Potassium channel block by cytoplasmic polyamines as the mechanism of intrinsic rectification. Nature *372*, 366-369.

Lovell, R.A. (1990). Ivermectin and piperazine toxicoses in dogs and cats. Vet. Clin. North Am. Small. Anim. Pract. *20*, 453-468.

Lowry, O.H., Rosebrough, N.J., Farr, A.L., and Randall, R.J. (1951). Protein measurement with the Folin reagent. J. Biol. Chem. *193*, 265-275.

Lu, X., Xu, L., and Meissner, G. (1994). Activation of the skeletal muscle calcium release channel by a cytoplasmic loop of the dihydropyridine receptor. J. Biol. Chem. *269*, 6511-6516.

Lucchesi, K.J. and Moczydlowski, E. (1991). On the interaction of bovine pancreatic trypsin inhibitor with maxi $Ca^{(2+)}$-activated K+ channels. A model system for analysis of peptide-induced subconductance states. J. Gen. Physiol. *97*, 1295-1319.

McCaffrey, P.G., Perrino, B.A., Soderling, T.R., and Rao, A. (1993). NF-ATp, a T lymphocyte DNA-binding protein that is a target for calcineurin and immunosuppressive drugs. J. Biol. Chem. *268*, 3747-3752.

Ma, J., Fill, M., Knudson, C.M., Campbell, K.P., and Coronado, R. (1988). Ryanodine receptor of skeletal muscle is a gap junction-type channel. Science *242*, 99-102.

Ma, J. (1993). Block by ruthenium red of the ryanodine-activated calcium release channel of skeletal muscle. Journal of General Physiology *102*, 1031-1056.

Ma, J. (1995). Desensitization of the skeletal muscle ryanodine receptor: Evidence for heterogeneity of calcium release channels. Biophysical Journal *68*, 893-899.

Ma, J., Bhat, M.B., and Zhao, J. (1995). Rectification of skeletal muscle ryanodine receptor mediated by FK506 binding protein. Biophys. J. *69*, 2398-2404.

Ma, J. and Zhao, J. (1994). Highly cooperative and hysteretic response of the skeletal muscle ryanodine receptor to changes in proton concentrations. Biophys. J. *67*, 626-633.

Mack, M.M., Molinski, T.F., Buck, E.D., and Pessah, I.N. (1994). Novel modulators of skeletal muscle FKBP12/calcium channel complex from *Ianthella basta*. Role of FKBP12 in channel gating. J. Biol. Chem. *269*, 23236-23249.

Marks, A.R., Tempst, P., Hwang, K.S., Taubman, M.B., Inui, M., Chadwick, C., Fleischer, S., and Nadal-Ginard, B. (1989). Molecular cloning and characterization of the ryanodine receptor/junctional channel complex cDNA from skeletal muscle sarcoplasmic reticulum. Proc. Natl. Acad. Sci. U. S. A. *86*, 8683-8687.

Marks, A.R., Fleischer, S., and Tempst, P. (1990). Surface topography analysis of the ryanodine receptor/junctional channel complex based on proteolysis sensitivity mapping. J. Biol. Chem. *265*, 13143-13149.

Marsili, V., Mancinelli, L., Menchetti, G., Fulle, S., Baldoni, F., and Fano, G. (1992). S-100ab increases Ca^{2+} release in purified sarcoplasmic reticulum vesicles of frog skeletal muscle. J. Muscle Res. Cell Motil. *13*, 511-515.

Marty, I., Robert, M., Villaz, M., De Jongh, K., Lai, Y., Catterall, W.A., and Ronjat, M. (1994). Biochemical evidence for a complex involving dihydropyridine receptor and ryanodine receptor in triad junctions of skeletal muscle. Proc. Natl. Acad. Sci. U. S. A. *91*, 2270-2274.

Matsuda, H. (1991). Effects of external and internal K+ ions on magnesium block of inwardly rectifying K+ channels in guinea-pig heart cells. J. Physiol. Lond. *435*, 83-99.

Mayrleitner, M., Timerman, A.P., Wiederrecht, G., and Fleischer, S. (1994). The calcium release channel of sarcoplasmic reticulum is modulated by FK-506 binding protein: Effect of FKBP-12 on single channel activity of the skeletal muscle ryanodine receptor. Cell Calcium *15*, 99-108.

Meissner, G. (1984). Adenine nucleotide stimulation of Ca^{2+}-induced Ca^{2+} release in sarcoplasmic reticulum. J. Biol. Chem. *259*, 2365-2374.

Meissner, G. (1986). Ryanodine activation and inhibition of the Ca^{2+} release channel of sarcoplasmic reticulum. J. Biol. Chem. *261*, 6300-6306.

Meissner, G., Darling, E., and Eveleth, J. (1986). Kinetics of rapid Ca^{2+} release by sarcoplasmic reticulum. Effects of Ca^{2+}, Mg^{2+}, and adenine nucleotides. Biochemistry *25*, 236-244.

Meissner, G. (1994). Ryanodine receptor/Ca^{2+} release channels and their regulation by endogenous effectors. Ann. Rev. Physiol. *56*, 485-508.

Meissner, G. and el-Hashem, A. (1992). Ryanodine as a functional probe of the skeletal muscle sarcoplasmic reticulum Ca^{2+} release channel. Mol. Cell Biochem. *114*, 119-123.

Mellin, T.N., Busch, R.D., and Wang, C.C. (1983). Postsynaptic inhibition of invertebrate neuromuscular transmission by avermectin B1a. Neuropharmacology *22*, 89-96.

Meszaros, L.G., Bak, J., and Chu, A. (1993). Cyclic ADP-ribose as an endogenous regulator of the non-skeletal type ryanodine receptor Ca^{2+} channel. Nature *364*, 76-79.

Miller, C. and Racker, E. (1976). Ca^{++}-induced fusion of fragmented sarcoplasmic reticulum with artificial planar bilayers. Cell *9*, 283-300.

Miller, C. and White, M.M. (1984). Dimeric structure of single chloride channels from Torpedo electroplax. Proc. Natl. Acad. Sci. U. S. A. *81*, 2772-2775.

Moczydlowski, E., Garber, S.S., and Miller, C. (1984). Batrachotoxin-activated Na+ channels in planar lipid bilayers. Competition of tetrodotoxin block by Na+. J. Gen. Physiol. *84*, 665-686.

Moore, C.L. (1971). Specific inhibition of mitochondrial Ca^{++} transport by ruthenium red. Biochem. Biophys. Res. Commun. *42*, 298-305.

Nabauer, M., Callewaert, G., Cleemann, L., and Morad, M. (1989). Regulation of calcium release is gated by calcium current, not gating charge, in cardiac myocytes Science *244*, 800-803.

Nagasaki, K. and Fleischer, S. (1988). Ryanodine sensitivity of the calcium release channel of sarcoplasmic reticulum. Cell Calcium *9*, 1-7.

Nagasaki, K. and Kasai, M. (1984). Channel selectivity and gating specificity of calcium-induced calcium release channel in isolated sarcoplasmic reticulum. J. Biochem. Tokyo. *96*, 1769-1775.

Nakai, J., Imagawa, T., Hakamat, Y., Shigekawa, M., Takeshima, H., and Numa, S. (1990). Primary structure and functional expression from cDNA of the cardiac ryanodine receptor/calcium release channel. FEBS Lett. *271*, 169-177.

Nicolli, A., Basso, E., Petronilli, V., Wenger, R.M., and Bernardi, P. (1996). Interactions of cyclophilin with the mitochondrial inner membrane and regulation of the permeability transition pore, a cyclosporin A-sensitive channel. J. Biol. Chem. *271*, 2185-2192.

Ogawa, Y. (1994). Role of ryanodine receptors. Crit. Rev. Biochem. Mol. Biol. *29*, 229-274.

Ogawa, Y. and Ebashi, S. (1976). Ca-releasing action of beta, gamma-methylene adenosine triphosphate on fragmented sarcoplasmic reticulum. J. Biochem. Tokyo. *80*, 1149-1157.

Ohnishi, S.T. (1979). Calcium-induced calcium release from fragmented sarcoplasmic reticulum. J. Biochem. Tokyo. *86*, 1147-1150.

Otsu, K., Willard, H.F., Khanna, V.K., Zorzato, F., Green, N.M., and MacLennan, D.H. (1990). Molecular cloning of cDNA encoding the Ca^{2+} release channel (ryanodine receptor) of rabbit cardiac muscle sarcoplasmic reticulum. J. Biol. Chem. *265*, 13472-13483.

Patlak, J.B. (1988). Sodium channel subconductance levels measured with a new variance-mean analysis. J. Gen. Physiol. *92*, 413-430.

Pessah, I.N., Francini, A.O., Scales, D.J., Waterhouse, A.L., and Casida, J.E. (1986). Calcium-ryanodine receptor complex. Solubilization and partial characterization from skeletal muscle junctional sarcoplasmic reticulum vesicles. J. Biol. Chem. *261*, 8643-8648.

Pessah, I.N., Stambuk, R.A., and Casida, J.E. (1987). Ca^{2+}-activated ryanodine binding: mechanisms of sensitivity and intensity modulation by Mg^{2+}, caffeine, and adenine nucleotides. Mol. Pharmacol. *31*, 232-238.

Peterson, E.M., Xu, K., Holland, K.D., McKeon, A.C., Rothman, S.M., Ferrendelli, J.A., and Covey, D.F. (1994). Alpha-spirocyclopentyl- and alpha-spirocyclopropyl-gamma-butyrolactones: conformationally constrained derivatives of anticonvulsant and convulsant alpha,alpha-disubstituted gamma-butyrolactones. J. Med. Chem. *37*, 275-286.

Petronilli, V., Nicolli, A., Costantini, P., Colonna, R., and Bernardi, P. (1994). Regulation of the permeability transition pore, a voltage-dependent mitochondrial channel inhibited by cyclosporin A. Biochim. Biophys. Acta *1187*, 255-259.

Pong, S.S., DeHaven, R., and Wang, C.C. (1982). A comparative study of avermectin B1a and other modulators of the gamma-aminobutyric acid receptor chloride ion channel complex. J. Neurosci. *2*, 966-971.

Radermacher, M., Rao, V., Grassucci, R., Frank, J., Timerman, A.P., Fleischer, S., and Wagenknecht, T. (1994). Cryo-electron microscopy and three-dimensional reconstruction of the calcium release channel/ryanodine receptor from skeletal muscle. J. Cell Biol. *127*, 411-423.

Rardon, D.P., Cefali, D.C., Mitchell, R.D., Seiler, S.M., Hathaway, D.R., and Jones, L.R. (1990). Digestion of cardiac and skeletal muscle junctional sarcoplasmic reticulum vesicles with calpain II. Effects on the Ca^{2+} release channel. Circ. Res. *67*, 84-96.

Rios, E. and Brum, G. (1987). Involvement of dihydropyridine receptors in excitation-contraction coupling in skeletal muscle. Nature *325*, 717-720.

Ritucci, N.A. and Corbett, A.M. (1995). Effect of Mg^{2+} and ATP on depolarization-induced Ca^{2+} release in isolated triads. Am. J. Physiol. *269*, C85-95.

Rousseau, E., Smith, J.S., and Meissner, G. (1987). Ryanodine modifies conductance and gating behavior of single Ca^{2+} release channel. Am. J. Physiol. *253*, C364-8.

Rousseau, E. (1989). Single chloride-selective channel from cardiac sarcoplasmic reticulum studied in planar lipid bilayers. J. Membr. Biol. *110*, 39-47.

Rousseau, E. and Meissner, G. (1989). Single cardiac sarcoplasmic reticulum Ca^{2+}-release channel: activation by caffeine. Am. J. Physiol. *256*, H328-33.

Sabatini, D.M., Pierchala, B.A., Barrow, R.K., Schell, M.J., and Snyder, S.H. (1995). The rapamycin and FKBP12 target (RAFT) displays phosphatidylinositol 4-kinase activity. J. Biol. Chem. *270*, 20875-20878.

Saito, A., Seiler, S., Chu, A., and Fleischer, S. (1984). Preparation and morphology of sarcoplasmic reticulum terminal cisternae from rabbit skeletal muscle. J. Cell Biol. *99*, 875-885.

Schreiber, S.L. (1991). Chemistry and biology of the immunophilins and their immunosuppressive ligands. Science *251*, 283-287.

Seiler, S., Wegener, A.D., Whang, D.D., Hathaway, D.R., and Jones, L.R. (1984). High molecular weight proteins in cardiac and skeletal muscle junctional sarcoplasmic reticulum vesicles bind calmodulin, are phosphorylated, and are degraded by Ca^{2+}-activated protease. J. Biol. Chem. *259*, 8550-8557.

Sigel, E. and Baur, R. (1987). Effect of avermectin B1a on chick neuronal gamma-aminobutyrate receptor channels expressed in Xenopus oocytes. Mol. Pharmacol. *32*, 749-752.

Sigworth, F.J. and Sine, S.M. (1987). Data transformations for improved display and fitting of of single-channel dwell time histograms. Biophys. J. *52*, 1047-1054.

Sitsapesan, R., Montgomery, R.A., and Williams, A.J. (1995). New insights into the gating mechanisms of cardiac ryanodine receptors revealed by rapid changes in ligand concentration. Circ. Res. *77*, 765-772.

Sitsapesan, R. and Williams, A.J. (1995). Cyclic ADP-ribose and related compounds activate sheep skeletal sarcoplasmic reticulum Ca^{2+} release channel. Am. J. Physiol. *268*, C1235-40.

Smith, J.S., Coronado, R., and Meissner, G. (1985). Sarcoplasmic reticulum contains adenine nucleotide-activated calcium channels. Nature *316*, 446-449.

Smith, J.S., Coronado, R., and Meissner, G. (1986). Single channel measurements of the calcium release channel from skeletal muscle sarcoplasmic reticulum. Activation by Ca^{2+} and ATP and modulation by Mg^{2+}. J. Gen. Physiol *88*, 573-588.

Smith, J.S., Imagawa, T., Ma, J., Fill, M., Campbell, K.P., and Coronado, R. (1988). Purified ryanodine receptor from rabbit skeletal muscle is the calcium-release channel of sarcoplasmic reticulum. J. Gen. Physiol *92*, 1-26.

Smith, J.S., Rousseau, E., and Meissner, G. (1989). Calmodulin modulation of single sarcoplasmic reticulum Ca^{2+}-release channels from cardiac and skeletal muscle. Circ. Res. *64*, 352-359.

Stelzer, A. (1992). Intracellular regulation of GABAA-receptor function. Ion. Channels *3*, 83-136.

Stelzer, A. and Shi, H. (1994). Impairment of GABAA receptor function by N-methyl-D-aspartate-mediated calcium influx in isolated CA1 pyramidal cells. Neuroscience *62*, 813-828.

Study, R.E. and Barker, J.L. (1981). Diazepam and (--)-pentobarbital: fluctuation analysis reveals different mechanisms for potentiation of gamma-aminobutyric acid responses in cultured central neurons. Proc. Natl. Acad. Sci. U. S. A. *78*, 7180-7184.

Takahashi, N., Hayano, T., and Suzuki, M. (1989). Peptidyl-prolyl cis-trans isomerase is the cyclosporin A-binding protein cyclophilin. Nature *337*, 473-475.

Takasago, T., Imagawa, T., Furukawa, K., Ogurusu, T., and Shigekawa, M. (1991). Regulation of the cardiac ryanodine receptor by protein kinase-dependent phosphorylation. J. Biochem. Tokyo. *109*, 163-170.

Takeda, K. and Trautmann, A. (1984). A patch-clamp study of the partial agonist actions of tubocurarine on rat myotubes. J. Physiol. Lond. *349*, 353-374.

Takekura, H., Bennett, L., Tanabe, T., Beam, K.G., and Franzini Armstrong, C. (1994). Restoration of junctional tetrads in dysgenic myotubes by dihydropyridine receptor cDNA. Biophys. J. *67*, 793-803.

Takeshima, H., Nishimura, S., Matsumoto, T., Ishida, H., Kangawa, K., Minamino, N., Matsuo, H., Ueda, M., Hanaoka, M., Hirose, T., and et-al (1989). Primary structure and expression from complementary DNA of skeletal muscle ryanodine receptor. Nature *339*, 439-445.

Tanabe, T., Beam, K.G., Powell, J.A., and Numa, S. (1988). Restoration of excitation-contraction coupling and slow calcium current in dysgenic muscle by dihydropyridine receptor complementary DNA. Nature *336*, 134-139.

Tanifuji, M., Sokabe, M., and Kasai, M. (1987). An anion channel of sarcoplasmic reticulum incorporated into planar lipid bilayers: single-channel behavior and conductance properties. J. Membr. Biol. *99*, 103-111.

Tedeschi, H., Mannella, C.A., and Bowman, C.L. (1987). Patch clamping the outer mitochondrial membrane. J. Membr. Biol. *97*, 21-29.

Timerman, A.P., Ogunbumni, E., Freund, E., Wiederrecht, G., Marks, A.R., and Fleischer, S. (1993). The calcium release channel of sarcoplasmic reticulum is modulated by FK-506-binding protein. Dissociation and reconstitution of FKBP-12 to

the calcium release channel of skeletal muscle sarcoplasmic reticulum. J. Biol. Chem. *268*, 22992-22999.

Timerman, A.P., Jayaraman, T., Wiederrecht, G., Onoue, H., Marks, A.R., and Fleischer, S. (1994). The ryanodine receptor from canine heart sarcoplasmic reticulum is associated with a novel FK-506 binding protein. Biochemical and Biophysical Research Communications *198*, 701-706.

Timerman, A.P., Wiederrecht, G., Marcy, A., and Fleischer, S. (1995). Characterization of an exchange reaction between soluble FKBP-12 and the FKBP×ryanodine receptor complex. Modulation by FKBP mutants deficient in peptidyl-prolyl isomerase activity. J. Biol. Chem. *270*, 2451-2459.

Tinker, A., Lindsay, A.R., and Williams, A.J. (1992b). Large tetraalkyl ammonium cations produce a reduced conductance state in the sheep cardiac sarcoplasmic reticulum $Ca(^{2+})$-release channel. Biophys. J. *61*, 1122-1132.

Tinker, A., Lindsay, A.R., and Williams, A.J. (1992a). A model for ionic conduction in the ryanodine receptor channel of sheep cardiac muscle sarcoplasmic reticulum. J. Gen. Physiol. *100*, 495-517.

Tinker, A. and Williams, A.J. (1993). Charged local anesthetics block ionic conduction in the sheep cardiac sarcoplasmic reticulum calcium release channel. Biophys. J. *65*, 852-864.

Tripathy, A., Xu, L., Mann, G., and Meissner, G. (1995). Calmodulin activation and inhibition of skeletal muscle Ca^{2+} release channel (ryanodine receptor). Biophys. J. *69*, 106-119.

Tu, Q., Velez, P., Brodwick, M., and Fill, M. (1994). Streaming potentials reveal a short ryanodine-sensitive selectivity filter in cardiac Ca^{2+} release channel. Biophys. J. *67*, 2280-2285.

Tyerman, S.D., Terry, B.R., and Findlay, G.P. (1992). Multiple conductances in the large K+ channel from Chara corallina shown by a transient analysis method. Biophys. J. *61*, 736-749.

Valdivia, H.H., Kaplan, J.H., Ellis-Davies, G.C.R., and Lederer, W.J. (1995). Rapid adaptation of cardiac ryanodine receptors: Modulation by Mg^{2+} and phosphorylation. Science *267*, 1997-2000.

Wagenknecht, T., Berkowitz, J., Grassucci, R., Timerman, A.P., and Fleischer, S. (1994). Localization of calmodulin binding sites on the ryanodine receptor from skeletal muscle by electron microscopy. Biophysical Journal *67*, 2286-2295.

Wagenknecht, T. and Radermacher, M. (1995). Three-dimensional architecture of the skeletal muscle ryanodine receptor. FEBS Lett. *369*, 43-46.

Wang, J. and Best, P.M. (1992). Inactivation of the sarcoplasmic reticulum calcium channel by protein kinase. Nature *359*, 739-741.

Weber, A. (1968). The mechanism of the action of caffeine on sarcoplasmic reticulum. J. Gen. Physiol. *52*, 760-772.

Weber, A. and Herz, R. (1968). The relationship between caffeine contracture of intact muscle and the effect of caffeine on reticulum. J. Gen. Physiol. *52*, 750-759.

Williams, A.J. (1992). Ion conduction and discrimination in the sarcoplasmic reticulum ryanodine receptor/calcium-release channel. J. Muscle Res. Cell Motil. *13*, 7-26.

Witcher, D.R., Kovacs, R.J., Schulman, H., Cefali, D.C., and Jones, L.R. (1991). Unique phosphorylation site on the cardiac ryanodine receptor regulates calcium channel activity. J. Biol. Chem. *266*, 11144-11152.

Yano, M., el Hayek, R., and Ikemoto, N. (1995a). Conformational changes in the junctional foot protein/Ca^{2+} release channel mediate depolarization-induced Ca^{2+} release from sarcoplasmic reticulum. J. Biol. Chem. *270*, 3017-3021.

Yano, M., el Hayek, R., and Ikemoto, N. (1995b). Role of calcium feedback in excitation-contraction coupling in isolated triads. J. Biol. Chem. *270*, 19936-19942.

Zahradnikova, A. and Palade, P. (1993). Procaine effects on single sarcoplasmic reticulum Ca^{2+} release channels. Biophys. J. *64*, 991-1003.

Zorzato, F., Fujii, J., Otsu, K., Phillips, M., Green, N.M., Lai, F.A., Meissner, G., and MacLennan, D.H. (1990). Molecular cloning of cDNA encoding human and rabbit forms of the Ca^{2+} release channel (ryanodine receptor) of skeletal muscle sarcoplasmic reticulum. J. Biol. Chem. *265*, 2244-2256.